



HAL
open science

Biodiversity, Cretaceous-Palaeogene crisis survival and phylogeny of Metasuchia (Crocodyliformes, Pseudosuchia)

Paul Aubier

► **To cite this version:**

Paul Aubier. Biodiversity, Cretaceous-Palaeogene crisis survival and phylogeny of Metasuchia (Crocodyliformes, Pseudosuchia). Paleontology. Sorbonne Université, 2023. English. NNT : 2023SORUS619 . tel-04581016

HAL Id: tel-04581016

<https://theses.hal.science/tel-04581016>

Submitted on 21 May 2024

HAL is a multi-disciplinary open access archive for the deposit and dissemination of scientific research documents, whether they are published or not. The documents may come from teaching and research institutions in France or abroad, or from public or private research centers.

L'archive ouverte pluridisciplinaire **HAL**, est destinée au dépôt et à la diffusion de documents scientifiques de niveau recherche, publiés ou non, émanant des établissements d'enseignement et de recherche français ou étrangers, des laboratoires publics ou privés.

Sorbonne Université

École doctorale Géosciences, Ressources Naturelle et Environnement(398)

Centre de recherche en paléontologie-Paris/Équipe phylogénie des Métazoaires

Biodiversity, Cretaceous-Palaeogene crisis survival and phylogeny of Metasuchia (Crocodyliformes, Pseudosuchia)

Par Paul Aubier

Thèse de doctorat de Biogéosciences

Dirigée par Jorge Cubo, Stéphane Jouve, Johann Schnyder et Valentin Rineau

Présentée et soutenue publiquement le 8 décembre 2023

Devant un jury composé de :

Mario de Pinna	Professeur à l'Université de São Paulo	Rapporteur
David Williams	Principal Researcher au Natural History Muséum (Londres)	Rapporteur
Yves Desdevises	Professeur à Sorbonne Université	Président
Pedro Godoy	Docteur à l'Université de São Paulo	Examineur
Michael Benton	Professeur à l'Université de Bristol	Invité
Guillaume Lecointre	Professeur au Muséum National d'Histoire Naturelle	Invité
Jorge Cubo	Professeur à Sorbonne Université	Directeur de thèse
Stéphane Jouve	Docteur à Sorbonne Université	Co-encadrant de thèse
Johann Schnyder	Maître de conférence à Sorbonne Université	Co-encadrant de thèse
Valentin Rineau	Maître de conférence à Sorbonne Université	Co-encadrant de thèse

À ma mamie.

Remerciements

J'écris ces lignes alors que la soutenance de cette thèse s'est déjà (bien) déroulée. Étant fidèle à ma personne, j'ai finalisée la rédaction du présent manuscrit dans une certaine urgence dont j'estimais alors qu'elle ne me permettait pas de donner aux personnes envers qui je suis redevable la pleine place qui devait leur être dédiée ici. J'ai donc repoussé la rédaction de ces remerciements (restant au passage fidèle à ma religieuse procrastination). Mais voilà qu'est venu ce moment au cours duquel je dois me refaire le film de ces trois années de travail, d'explorations, de découvertes et – à bien des égards – de batailles. L'image du doctorant, harnaché à son bureau, pinte de café d'un côté, carnet de l'autre, luttant seul à démêler d'épineuses et touffues questions pourrait sembler à certains et certaines adéquate. Cette section vise à montrer l'inverse. Car si c'est bien moi qui suis à même de revendiquer la paternité du manuscrit qui suit, je suis loin, très loin d'être le seul à y avoir participé. Ce manuscrit est un produit collectif. Mais ici m'est donnée l'occasion d'explicitier le rôle de toutes les personnes qui m'ont, tout au long de ces trois années, corrigé, guidé, conseillé, accompagné, aidé, entouré. Sans elles, ce travail ne serait pas.

Je remercie tout d'abord les institutions qui m'ont accueilli et m'ont permis de réaliser cette recherche, l'école doctorale Géosciences, Ressources Naturelles et Environnement (GRNE, ED398), Sorbonne Université et le Centre de Recherche en Paléontologie – Paris (CR2P).

J'adresse également mes remerciements aux membres de mon jury. Mario de Pinna et David Williams : vos deux noms ont habités très tôt ma bibliographie. Vous avoir eu comme rapporteurs a été pour moi un honneur. Yves Desdevises et Pedro Godoy : vos retours ont témoigné de votre expertise et je les ai pris avec reconnaissance pour leur valeur et leur pertinence. Je remercie également les deux membres invités, Mike Benton et Guillaume Lecointre : vos remarques, propositions et critiques ont été bienvenues.

Votre participation à cette thèse en a marqué la conclusion. Merci d'avoir pris le temps de lire ce manuscrit, de m'avoir écouté le présenter et d'avoir fait de la soutenance un moment de discussions enrichissantes et d'échanges fournis.

Mes profonds remerciements s'adressent au directeur de ce projet de thèse, Jorge Cubo. Je ne saurais assez faire ressortir dans ces quelques lignes l'énormité de ce que ce travail te doit ; de ce que tu m'as

offert comme développements, tant sur le plan scientifique que personnel. Les errements, obstacles, incompréhensions et doutes inhérents à la réalisation d'une thèse ont été nombreux aux cours de ces trois années. C'est en grande partie grâce à la confiance totale que tu as eu en moi que ce projet a pu arriver à son terme. Tu as su proposer une issue à chaque impasse et trouver un rebondissement fécond à chaque égarement. Mais surtout, tu m'as laissé une grande liberté de travail. Si cette latitude a pu trouver mauvais ménage avec ma nature procrastinatrice, c'est grâce à elle que j'ai pu m'approprier pleinement cette thèse et reconnaître comme miens les travaux réalisés au cours de cette dernière. Cette thèse, je l'ai commencé comme un novice, un intrus chanceux qui, perdu dans un nouveau monde doit courir après les événements pour paraître en maîtrise, en confiance et donner l'impression qu'il mérite d'être là où il est. C'est ta direction qui m'a peu à peu mué en scientifique, heureux de pouvoir jouer sa part au sein d'une communauté qui le dépasse mais dont il se sent dorénavant faire partie. Je n'aurais pu espérer meilleur directeur. Merci de m'avoir accompagné et guidé toutes ces années.

Cette thèse a été co-encadrée par Stéphane Jouve, Johann Schnyder et Valentin Rineau.

Je suis redevable au premier de son insondable expertise du groupe d'étude. J'ai encore le souvenir hautement désagréable de l'une de nos premières rencontres lors de mon stage de Master 2 au cours de laquelle j'ai pris conscience du gouffre qui nous séparait sur ce sujet. Et chaque réunion, chaque entrevue était pour moi une occasion de refaire l'expérience de ce gouffre dont j'observais cependant avec satisfaction qu'il semblait peu à peu se combler (certes, avec une exaspérante lenteur, mais il faut se satisfaire de ce que l'on a). Ainsi, tout au long de cette thèse, tu as joué à mes yeux un rôle double. Un premier, collectif : celui d'un 'contrôleur du possible', m'informant et me corrigeant sur la plausibilité et la pertinence tant des résultats produits que des méthodes utilisées pour les produire. Un second, plus personnel : celui d'un horizon scientifique vers lequel se diriger ; une motivation, celle d'être un jour aussi compétent et capable que toi sur cette portion de réel que constitue une diversité.

Johann a été le 'réfèrent géosciences' de ce projet de thèse. Ton encadrement n'a pas été facilité par ma réticence à m'aventurer dans des eaux qui me semblaient alors peu accueillantes (il est temps pour moi de l'admettre) : celles de la sédimentologie, stratigraphie et paléoclimatologie. J'étais alors principalement intéressé par les statistiques et la phylogénie et j'aurais sans regret laissé les géosciences à celles et à ceux qui les font. Il n'a tenu qu'à ta motivation et ta constance que ces rives aient été abordées

dans cette thèse et composent la majeure partie du premier chapitre de ce manuscrit, ta persévérance et ta positivité ayant finalement achevé de me convaincre de m'atteler à cette tâche. J'ai ainsi fréquenté un domaine scientifique duquel je m'étais jusqu'alors poliment tenu à l'écart. J'y ai découvert une littérature et une méthode de recherche dont la compréhension naissante, force est de le reconnaître, s'est révélée très précieuse pour moi et m'a ouvert de nombreuses portes que nous allons continuer à explorer. Pour m'avoir poussé à sortir de ma zone de confort, et sans oublier tes nombreux conseils prodigués tout au long de ces trois années, je te remercie.

Valentin a rejoint l'équipe en cours de route, alors que nous achevions la publication de l'étude qui compose le second chapitre de ce manuscrit. Ton arrivée dans l'encadrement de cette thèse s'est faite lors d'un point pivot de cette dernière : nous allions – enfin – laisser derrière nous ce premier article sur lequel j'étais focalisé depuis près d'un an et demi, que j'avais écrit, réécrit, lu, corrigé, relu, recorrecté, modifié, augmenté, étoffé, guyoté, raccourci et abrégé, une fois, deux fois, trois fois...; cet article dont je commençais sérieusement à m'exaspérer de le voir encore et toujours prendre toute mon attention allait enfin laisser place au projet suivant dont je savais depuis le début qu'il me serait le plus excitant, la phylogénie. Dans la mise en place de ce projet, tu as été la personne centrale ; dans sa réalisation, la pierre angulaire. Je connaissais déjà ton expertise méthodologique en la matière et ta facilité à proposer une solution à chaque accroc, à chaque obstacle n'a fait que confirmer cela. Mais l'évidence avec laquelle tu as pris en charge une problématique phylogénétique dont tu n'avais jusqu'alors jamais entendu parlé et la justesse de tes remarques lors de nos réunions ont forcé mon admiration. Tu as pris mes idées au sérieux, dédié le temps nécessaire pour les rendre effectives, applicables et productives tant en créant les outils qu'elles nécessitaient qu'en les amendant pour les améliorer. Ton encadrement a achevé de me convaincre que j'avais ma place dans le monde de la recherche, qu'il était possible que mes quelques idées puissent amener à des productions qui pourraient, à leur échelle, contribuer à la compréhension du réel.

Je n'ai pas passé ces trois années seul face à mes questions et mon ordinateur. Je l'ai passé au sein d'un bureau que j'ai partagé. D'abord avec Mathieu Faure-Brac (cet « illustre prédécesseur »). Ainsi, c'est à tes côtés que j'ai commencé ma thèse et c'est aux miens que tu as terminé la tienne. Merci pour m'avoir aidé à prendre mes marques et répondu à mes incessantes questions de petit nouveau. Puis ce fut avec Marianna Valéria de Araújo Sena. C'est avec toi que j'ai partagé la majeure partie des journées qui

ont composées ma thèse. Je t'ai vu débarquer après avoir passé plusieurs mois seul dans ce bureau que je m'étais mis à considérer comme le mien. Au départ soupçonneux de cette personne avec qui j'allais devoir de nouveau le partager, je n'ai pu que me rendre à l'évidence : t'avoir comme co-bureau a été une immense chance. Tu m'as supporté tout au long de ce périple, et avoir à mes côtés ta bienveillance et ta joie de vivre ont été pour moi un motif constant de motivation. Merci d'avoir fait de l'exercice de ma thèse, par nos discussions (au cours desquelles, performance, j'ai même pu m'initier aux ragottages), une histoire humaine.

Les bornes d'un bureau sont poreuses et l'importance de la vie qui anime ce couloir 46-56, au 5ème étage ne saurait être minimisée ici. J'ai eu la chance d'évoluer au sein de cette petite communauté qui n'a jamais été dans la retenue quand il s'agissait de fournir aide et conseils. Mais, et c'est peut-être le plus important, j'ai eu la chance d'évoluer au sein d'une équipe qui n'était pas non plus dans la retenue quand il s'agissait d'être festif et heureux. Je pense à tous ces « pots » qui, que ce soit pour célébrer le succès de l'une, le départ d'un autre, ou simplement pour se retrouver, ont rythmé la vie au sein de ce couloir d'épisodes légers et l'ont teinté d'une douce entente. Je pense notamment ici aux membres de la « Cubo Team », Marianna Valéria de Araújo Sena, Romain Pellarin, Tom Forêt, Hugo Bert, Manon Sicard et Cassandra Cheyron, mais également aux jeunes du labo, Allison Rowe, Guillaume Houée, Elvis Guillam, Béatrice Below, Isabelle Deregnaucourt, Laura Bento Da Costa, Vincent Decuyper et Antoine Logghe. Sans oublier celles et ceux déjà en place au premier rang desquels Jérémie Bardin, Loïc Villier, Isabelle Kruta, Dominique Gommery, Sylvia Gardin, Franck Senegas, Isabelle Rouget et Delphine Desmares.

Dans le registres des âmes festives, je ne pourrais oublier ici deux personnages, Michaël Hermoso et Fabrice Minoletti, à qui je ne dois pas tout (contrairement à ce qu'ils vous raconteront), mais néanmoins beaucoup (probablement plus qu'il ne l'admettront).

Mon premier travail de recherche, lors du stage de Master 1, s'est réalisé sous la direction de René Zaragüeta. Il m'a laissé le souvenir des nœuds au cerveau et du pataugeage difficile au sein d'une littérature absconse et hirsute, passionnée et opaque, au cours duquel j'ai vu mes questions se multiplier et mes incompréhensions s'ammonceler. Me poussant à tout problématiser, nos discussions, loin d'éclaircir mes interrogations, les ont d'abord emmêlées (je me rappelle notamment de cette fois où, répondant

à une question méthodologique que je t'avais posé tu m'avais dit « Mais Paul, la connaissance au final, c'est quoi ? », me laissant ainsi dubitatif face à une question autrement plus profonde à laquelle je n'avais évidemment aucun début de réponse, et qui surtout n'avait à mes yeux aucun rapport avec mes préoccupations). Arriva cependant ce moment où le premier verrou a sauté, suivi d'un autre, puis d'un suivant, jusqu'à ce que l'ensemble fasse sens et que la collection de tes réponses incompréhensibles devinrent soudain intelligibles. C'est durant ce travail que j'ai pour la première fois fait l'expérience de ce sentiment profond, de cette satisfaction intense qui survient lorsque la pensée se reforme face à une idée dont on a bataillé pour la saisir. Cette expérience, qui m'a convaincu d'emprunter la direction de la recherche et qui m'a poussé à persévérer dans ce sens à été pour moi fondatrice. Je suis ainsi redevable à René, sans ce travail, sans sa direction, ce manuscrit n'existerait probablement pas.

Je tiens ici également à remercier Frank Alvarez-Pereyre pour m'avoir laissé participer au séminaire doctoral qu'il anime. J'y ai fréquenté une méthode de pensée, de réflexion et d'analyse qui, en tranchant d'avec celle qui m'était familière, m'a enrichi. J'y ai également trouvé un lieu d'une constante sollicitude, d'une attention particulière et d'une sincère gentillesse, propice à la survenue d'une parole libre, toujours prise comme matière à pensée.

Bien heureusement, cette thèse fut aussi partagée avec des amis. En premier lieu celles et ceux qui, rencontrés avant ou pendant ces trois années, ont vécu ou vivent encore la même expérience. Le premier d'entre tous, Dr. Vincent Haÿ, le C⁴ : copain, coloc, collègue et cuisinier (rien ne sert de le nier, je ne sais pas me nourrir). Mais les autres, Dr. Christopher Smith, Dr. Thomas Laville, Hugo Potier, Dr. Léa Poli, Louise Abot et Jérôme Isle de Beauchaine. Sans les bières, les jérémiades collectives, les discussions sérieuses, les bières, les discussions moins sérieuses, les cafés et les bières, cette thèse aurait été triste...et sèche. Je remercie également mes amis de longue date et d'autres cercles : Pierre-Emmanuel Faux, Gaspard Vrielinck, Dr. Timothée Chabot, Axel Lambert, Léo Héloire, Aymeric Imbert, Paul de Marliave et Sophie Delorme. Je vous suis redevable d'avoir été présents, de m'avoir entouré et permis de déconnecter d'avec la thèse, de sortir la tête et d'apercevoir ce qui m'a semblé pendant 3 ans être un autre monde, distant, celui dans lequel on chill, on profite, on grimpe, on discute, et où l'on se tient bien

éloigné des préoccupations metasuchiennes.

J'ai un merci particulier à formuler à Lucile Jourdain-Fievet. C'est avec toi que j'ai commencé à réfléchir. Cette thèse est la continuation d'une aventure intellectuelle que nous avons commencé ensemble (et je repense avec une nostalgie versée de fierté à cette année suivant notre Master) et que nous continuerons. Merci d'avoir été à la source de ma curiosité intellectuelle et de continuer à en être une pièce centrale tout en étant, excusez du peu, une amie hors-pair.

Mes derniers remerciements collectifs s'adressent évidemment à ma famille, mes Parents, mon frère, Baptiste, et mes sœurs, Sophie et Clémence, mes cousines et cousins, mes oncles et tantes, ma Grand-Mère. Plus le temps s'avance et plus je réalise l'in vraisemblable chance que j'ai de vous avoir eu et de continuer à vous avoir. Dire que sans vous cette thèse n'existerait pas serait un truisme. Je ne vous dois pas cette thèse, je ne vous dois pas ce travail, je vous dois tout. J'ai finalisé ce manuscrit et préparé sa soutenance en vous ayant en tête et en voulant vous rendre aussi fier que je le suis de vous avoir à mes côtés. Jérémy, Laura et Blaise, je ne vous oublie bien évidemment pas.

J'ai gardé jusqu'ici mes derniers remerciements. Ils s'adressent à Salomé Strauch. Notre histoire à commencé, peu ou prou, en même temps que celle de ma thèse. Mais il en est une que je suis satisfait de voir se terminer et une autre dont je fait le vœu qu'elle dure. Me contenter ici de dire que ces trois années n'ont pas été traversées en solitaire serait une litote. Ce fut trois années à échanger, à discuter, à débattre, à s'enrichir. Merci pour ton soutien, pour avoir partagé mes doutes et m'avoir aidé à les surmonter, merci pour ton écoute, ta confiance, ta bienveillance et ton amour. Tu as été l'ancre à laquelle j'ai toujours pu me raccrocher.

Résumé Étendu

La diversité actuelle des Metasuchia correspond aux Crocodylia. Ce groupe contient moins de 30 espèces réparties dans trois grands clades, les Alligatoroidea, les Crocodyloidea et les Gavialoidea. Cette diversité actuelle, peu fournie numériquement parlant, est relativement homogène d'un point de vue morphologique et écologique : les espèces qui la composent sont toutes semi-aquatiques, carnivores généralistes, à posture semi-érigée et possédant un corps recouvert d'ostéodermes. Cette faible diversité numérique et disparité morphologique tranchent avec la diversité de leur plus proches parents actuels, les oiseaux, qui comportent plus de 10 000 espèces présentant une grande variété de morphologies et d'écologies. Mais si la diversité actuelle des Metasuchia est relativement faible, le registre fossile du groupe comprend des organismes aux morphologies très différentes les unes des autres, indiquant une grande variété d'écologies et suggérant ainsi une haute diversité passée du groupe. Ce contraste entre la faible diversité actuelle et l'importante diversité passée pose la question de l'effondrement de la seconde pour en arriver à la première. Éclaircir les causes pouvant expliquer cet important déclin de la paléobiodiversité des Metasuchia est la problématique générale au sein de laquelle cette thèse s'inscrit.

Le premier chapitre de ce manuscrit s'attache à dresser un portrait général des Metasuchia. Ce chapitre présente :

(1) les principales controverses phylogénétiques du groupe et indique le cadre phylogénétique suivi dans ce manuscrit. Dans ce dernier, le groupe des Metasuchia est composé de deux clades : les Neosuchia et les Notosuchia. Une problématique majeure concerne la position phylogénétique des Thalattosuchia. Ce groupe de Crocodyliformes adapté à un mode de vie complètement marin a pu être retrouvé soit à l'extérieur des Metasuchia, soit à l'intérieur, inclus dans les Neosuchia. Nous avons choisi ici de suivre la première hypothèse, nous reposant sur le fait qu'elle correspond à la définition originelle du groupe des Metasuchia. Nous discutons également dans cette section des différentes hypothèses phylogénétiques concernant les sous-groupes inclus dans les Neosuchia et Metasuchia.

(2) l'évolution numérique et taxique de la diversité du groupe du Jurassique au présent. Pour ce faire, nous nous sommes basés sur les données de la PaleoBiology Database (PBDB). Nous avons ensuite représenté l'extension stratigraphique de chaque espèce de Metasuchia et produit une courbe de diversité. Nous montrons que si le groupe apparaît durant le Jurassique Moyen et Supérieur, sa diversité reste faible

durant cette période. C'est au cours du Crétacé que la diversité du groupe explose, atteignant un pic au Crétacé Supérieur durant lequel tous les groupes majeurs coexistent. Cette radiation évolutive est déclenchée par les diversifications conjointes des Notosuchia et, au sein des Neosuchia, des Crocodylia. La crise Crétacé-Paléogène (K-Pg) marque un arrêt brutal à cette diversification, la majeure partie des groupes de Metasuchia s'éteignant lors de celle-ci. Les Neosuchia sont cependant moins impactés par cette crise que les Notosuchia, les Crocodylia (qui composent dès la fin du Crétacé la majeure partie de la diversité des Neosuchia) la traversant avec succès. Durant le Cénozoïque, la diversité des Metasuchia adopte peu à peu sa structure moderne, avec l'extinction des derniers néosuchiens non crocodiliens (Dyrosauroida) durant l'Éocène et celle des derniers notosuchiens (Sebecidae) au cours du Miocène.

(3) la diversité des paléoenvironnements occupés par la paléobiodiversité du groupe. Toujours en nous basant sur les données de la PBDB, nous avons pu récolter les informations relatives aux formations géologiques au sein desquelles les spécimens fossiles de métasuchiens ont été retrouvés. Nous montrons que la grande majorité des occurrences fossiles (70%) sont retrouvées dans des dépôts d'eau douce, souvent fluviaux, le reste (30%) correspondant à des dépôts marins. Cette proportion n'implique cependant pas que 70% des spécimens fossiles avaient un mode de vie semi-aquatique car les métasuchiens dont la terrestrialité est non-équivoque (*e.g.* Sebecosuchia) sont également retrouvés dans ce type de dépôts. Elle indique cependant que même quand il ne sont pas semi-aquatiques, les métasuchiens restent fortement associés à ces environnements d'eau douce. Il a été récemment montré qu'au cours de l'histoire évolutive des Crocodylomorpha (un groupe plus inclusif qui inclut les Metasuchia), presque tous les types de transition de milieu de vie (semi-aquatique d'eau douce, terrestre et marin) ont eu lieu au moins une fois. Ainsi, cette prédominance des milieux d'eau douce témoigne à la fois de la spécialisation du groupe à cet environnement mais également du rôle pivot que ces milieux ont joué dans les différents événements de transition de milieu de vie.

(4) l'évolution des préférences paléoclimatiques du groupe du Jurassique au présent. En utilisant les paléocoordonnées des occurrences fossiles fournies par la PBDB et des cartes paléogéographiques indiquant la distribution géographique des zones paléoclimatiques, nous avons pu associer un climat à chaque occurrence fossile. En ce qui concerne les occurrences actuelles, nous avons utilisé les données issues de la Global Biodiversity Information Facility (GBIF) et la classification Köppen-Geiger des climats. Nous mettons en évidence trois tendances. Premièrement, la proportion d'occurrences situées

sous des climats tropicaux est très faible avant, et augmente considérablement après le Maastrichtien. Deuxièmement, la proportion d'occurrences situées sous des climats arides suit une tendance inverse, élevée durant le Crétacé Inférieur puis diminuant. Troisièmement, la proportion d'occurrences situées sous des climats tempérés chaud est presque toujours la plus importante et n'est dépassée par la proportion d'occurrences situées sous des climats tropicaux que durant l'Oligocène. Ces résultats montrent que les *Metasuchia* ont exploré différents biomes au cours de leur histoire évolutive. Cette variation des préférences climatiques, tant à l'échelle du groupe au cours du temps qu'entre les différents sous-groupes rend délicate la recherche de patrons évolutifs généraux valides à l'échelle du groupe dans son entièreté.

En résumé, nous montrons dans ce chapitre que la diversité actuelle des *Metasuchia* est peu représentative de la diversité globale du groupe. Elle n'en représente en effet qu'une petite fraction, tant sur le plan taxonomique que sur les plans morphologique et écologique. De plus, étant donné l'importante diversité fossile des *Metasuchia*, notamment du point de vue écologique, nous mettons en évidence l'importance de réaliser des études plus fines, phylogénétiquement et temporellement, pour mettre en évidence des patrons macroévolutifs.

Suivant la conclusion du premier chapitre, le second présente une étude (publié dans le journal *Palaeontology* en Janvier 2023) focalisée sur la survie différentielle des *Notosuchia* (l'un des deux groupes composant les *Metasuchia*) lors de la crise K-Pg. De nombreuses études réalisées à grande échelle (taxonomique et temporelle) ont produit des résultats ambigus voir contradictoires, motivant ainsi la focale plus fine de l'étude composant ce chapitre. Les *Notosuchia* sont relativement homogènes du point de vue du milieu de vie, la plupart d'entre eux étant terrestres. De plus, la crise K-Pg semble avoir joué un rôle pivot dans la restructuration de la diversité des *Metasuchia*. Cet étude se propose ainsi de mettre en lumière les patrons macroévolutifs à l'œuvre au sein de ce groupe lors de cet épisode.

Cette étude repose sur l'utilisation des Méthodes Phylogénétiques Comparatives (PCMs). Ces méthodes statistiques sont capables de prendre en compte les relations de parenté entre espèces ainsi que les temps de coévolution, contournant ainsi la non-indépendance statistique des observations inhérente aux données issues d'une diversité interspécifique. Nous avons dans un premier temps compilé un super-arbre incluant 43 espèces de *Notosuchia*. Deux topologies, en compétition dans la littérature, ont été produites afin de prendre en compte l'effet de cette incertitude phylogénétique. Afin de prendre en

charge l'incertitude temporelle, liée à la mauvaise précision des datations des espèces fossiles, nous avons produit, pour chaque topologie, 200 super-arbres. Chaque arbre représentant une datation possible (tant des nœuds internes que terminaux), l'ensemble des 200 arbres constitue un éventail représentatif de toutes les datations possibles. En réalisant les analyses statistiques sur l'ensemble de ces super-arbres, l'incertitude temporelle a été prise en compte.

Dans un premier temps, nous avons mesuré la structure phylogénétique de l'extinction/survie. Nos analyses montrent que, indépendamment de l'hypothèse phylogénétique suivie, l'extinction/survie n'est pas aléatoire vis-à-vis de la phylogénie. Ce résultat suggère qu'il existe un ou plusieurs facteur(s), ayant un fort signal phylogénétique, pouvant expliquer cette survie différentielle.

Dans un second temps, nous avons utilisé la Régression Logistique Phylogénétique (PLR) pour tester l'effet de la paléotempérature locale et de la taille corporelle (utilisation la longueur crânienne comme proxy) sur la extinction/survie. La PLR est une PCM dont la variable réponse est binaire. Son usage est donc particulièrement pertinent pour investiguer les facteurs explicatifs de la extinction/survie et cette étude est la première dans laquelle cette méthode est utilisée dans un cadre macroévolutif. D'après nos analyses, la paléotempérature locale n'a pas joué de rôle dans l'extinction/survie des *Notosuchia* lors de la crise K-Pg. Nous expliquons ce résultat par le fait que la distribution géographique des espèces de ce groupe est fortement contrainte par le climat. Par conséquent, à un temps donné, toutes les espèces vivent sous des climats (et donc des paléotempératures locales) similaires. La taille, en revanche, explique significativement l'extinction/survie : plus les notosuchiens étaient grands, plus ils avaient de chance de survivre. Une explication proposée de cette relation positive est l'avantage compétitif. Cependant, étant donné que toutes les espèces qui ont survécu sont carnivores et que la majorité de celles qui se sont éteintes sont omnivores, cette explication n'est pas pertinente dans notre cas. Afin d'expliquer cette relation taille survie, nous avons exploré plus en détail l'histoire évolutive de ce facteur chez les *Notosuchia*.

En utilisant les Moindres Carrés Généralisés Phylogénétiques (PGLS), une PCM dont la variable réponse est continue, nous avons testé la relation taille temps. Nous avons pu montrer que les espèces de *Notosuchia* les plus récentes étaient significativement plus grandes que les plus anciennes, mettant ainsi en évidence une tendance macroévolutive à l'augmentation de la taille corporelle chez ce groupe. Cependant cette tendance disparaît lorsque les espèces carnivores sont retirées de l'échantillon, suggérant

une relation taille régime alimentaire. En utilisant la méthode des PGLS, nous avons pu montrer que le régime alimentaire expliquait significativement les variations de tailles corporelles, les espèces carnivores étant significativement plus grandes que les espèces omnivores. Nous reposant sur le fait que le régime alimentaire carnivore généraliste est ancestral pour le groupe et que les espèces carnivores spécialistes apparaissent au sein d'un groupe omnivore, nous suggérons que cette tendance à l'augmentation de la taille est associée à un shift d'un régime alimentaire omnivore vers un régime alimentaire carnivore spécialiste. La taille corporelle expliquerait ainsi la survie différentielle des *Notosuchia* lors de la crise K-Pg parce qu'elle approxime le régime alimentaire.

En conclusion, cette étude est la première à utiliser la PLR pour tester des hypothèses macroévolutives. Nous avons pu montrer que l'extinction qui intervient lors de la crise K-Pg chez les *Notosuchia* n'est pas aléatoire vis-à-vis de la phylogénie et qu'elle est expliquée par la taille corporelle. De plus, la taille corporelle est liée au régime alimentaire et son augmentation au cours du temps semble associée à un shift d'un régime alimentaire omnivore à un régime carnivore spécialiste. Cette diversité de régime alimentaire, et donc d'écologie, expliquerait donc la survie différentielle des *Notosuchia*.

L'étude présentée en Chapitre 3 repose très largement sur l'utilisation des PCMs. Disposer de phylogénies fiables constitue un prérequis à l'utilisation de telles méthodes. Dans le cas d'une diversité dont les relations phylogénétiques sont largement controversées, il est ainsi nécessaire de résoudre les contradictions avant de pouvoir les utiliser. Le Chapitre 3 de ce manuscrit présente une nouvelle méthode pour mesurer précisément le soutien phylogénétique contenu dans une matrice phylogénétique et aider ainsi à la résolution de conflits phylogénétiques. Nous prenons l'exemple des *Crocodylia*. Ce groupe est composé de trois clades : les *Alligatoroidea*, les *Crocodyloidea* et les *Gavialoidea*. Il existe deux hypothèses contradictoires quand aux relations phylogénétiques entre ces trois groupes : (1) l'hypothèse *Brevirostres*, classiquement retrouvée par les études morpho-anatomiques, dans laquelle les *Crocodyloidea* et *Alligatoroidea* sont groupes frères, formant le clade des *Brevirostres* duquel les *Gavialoidea* sont exclus ; (2) l'hypothèse *Longirostres*, systématiquement retrouvée par les études moléculaires, dans laquelle les *Crocodyloidea* et *Gavialoidea* sont groupes frères, formant le clade des *Longirostres* duquel les *Alligatoroidea* sont exclus. Les *Tomistominae*, un sous-groupe d'une dizaine d'espèces, se retrouvent alternativement inclus dans les *Crocodyloidea* dans la première hypothèse et dans les *Gavialoidea* dans la

seconde. Ce conflit persiste dans la littérature depuis son apparition dans les années 80. Récemment, une étude phylogénétique morpho-anatomique a retrouvé l'hypothèse Longirostres. L'étude présentée dans le Chapitre 3 de ce manuscrit se propose de mesurer précisément les soutiens aux hypothèses Brevirostres et Longirostres contenu dans cette nouvelle matrice.

La parcimonie, méthode de reconstruction phylogénétique très majoritairement utilisée pour traiter les caractères morpho-anatomiques, ne permet pas de mesurer précisément le soutien d'une hypothèse phylogénétique directement dans la matrice. En effet, parce que cette méthode recherche l'arbre optimal par optimisation des changements d'états de caractères, les regroupements soutenus par un caractère au sein de la matrice peuvent différer de ceux soutenus par ce même caractère sur l'arbre optimal retrouvé. Ainsi, le soutien contenu dans la matrice est en partie déconnecté du résultat topologique de l'analyse et sa mesure est donc incapable d'éclairer le rôle de chaque caractère et taxon dans l'obtention de ce résultat. Nous avons ainsi utilisé une méthode alternative, l'Analyse à Trois-Éléments (3ia). La 3ia décompose les hypothèses de caractères en hypothèses minimales de relations à trois taxons (3ts) parmi lesquels deux sont plus apparentés entre eux qu'au troisième. La recherche de l'arbre optimal se fait via la recherche du plus grand ensemble de 3ts non-contradictaires (i.e. la max-clique). Les 3ts non-inclus dans cet ensemble sont réfutés et ne participent pas à la construction de l'arbre optimal. Ainsi, parce les soutiens contenus dans la matrice sont soit retrouvés tel quel dans l'arbre optimal (si les 3ts sont inclus dans la max-clique) soit absents de ce dernier (si les 3ts ne sont pas inclus dans la max-clique). Conséquemment, quantifier les soutiens phylogénétiques directement dans la matrice permet d'expliquer l'obtention du résultat de l'analyse. Nous proposons un nouvel indice, l'Indice de Contradiction (IC) capable de mesurer en 3ia le soutien d'une hypothèse phylogénétique relativement à une autre. Les bornes de cet indice (0 et 1) correspondent aux cas de figure dans lesquels il existe du soutien pour une seule des deux hypothèses. Une valeur de 0.5 indique un soutien strictement égal aux deux hypothèses.

Après avoir « converti » les caractères de la matrice récemment publiée en caractères analysables en 3ia, nous avons réalisé des analyses phylogénétiques en utilisant la parcimonie et la 3ia qui ont toutes deux retrouvé un arbre optimal compatible avec l'hypothèse Longirostres. Nous avons ensuite analysé le contenu de la matrice de 3ts. Nos quantifications montrent que l'hypothèse Longirostres est plus soutenue que l'hypothèse Brevirostres. Elle reste cependant très contredite, n'étant que 1.6 fois plus soutenue ($IC \approx 0.62$).

Nous avons ensuite quantifié les soutiens fournis par les espèces de Tomistominae et montré que de ce groupe est issue la majorité ($\approx 63\%$) du soutien à l'hypothèse Longirostres de toute la matrice. Ainsi, retirer ce groupe de l'échantillonnage taxonomique suffit à faire basculer l'arbre optimal retrouvé lors des analyses en parcimonie et 3ia de l'hypothèse Longirostres à l'hypothèse Brevirostres. En quantifiant le soutien fourni par chaque caractère, nous avons également pu montrer que les caractères corrélés à la longirostrie, bien qu'apportant plus de soutien à l'hypothèse Longirostres qu'à l'hypothèse Brevirostres, ne jouent pas un rôle majeur à l'échelle de la matrice totale ($\approx 22\%$).

Cette étude présente ainsi une nouvelle méthodologie pour mesurer le soutien phylogénétique. Nous avons pu montrer que le résultat fourni par la matrice analysée était hautement dépendant de l'inclusion d'un groupe, les Tomistominae, dans l'échantillonnage taxonomique. Cette nouvelle méthodologie permet de quantifier précisément le rôle joué par chaque taxon et caractère dans l'obtention de l'arbre optimal permettant de cibler les taxons/caractères ayant un impact particulièrement important. Comparer le contenu de différentes matrices soutenant des hypothèses contradictoires permettrait dès lors d'identifier les éventuelles différences expliquant la contradiction. Cette méthode constitue ainsi un nouvel outil pour comprendre et résoudre des conflits phylogénétiques.

La problématique générale au sein de laquelle cette thèse s'est inscrite était d'investiguer les raisons expliquant l'important déclin en diversité du groupe des Metasuchia. Le premier travail de recherche a permis de mettre en lumière le rôle joué par le régime alimentaire dans la survie différentielle des Notosuchia lors de la crise K-Pg. Ce travail a montré l'intérêt et la pertinence des études macroévolutives à fine échelle. Elle a aussi montré la puissance des PCMs dans la recherche de patrons macroévolutifs. Le second travail de recherche présenté dans ce manuscrit propose ainsi une nouvelle méthodologie pour aider à la résolution des conflits phylogénétiques, nécessaire à l'utilisation des PCMs.

Thesis Abstract

Metasuchia appeared during the Jurassic. At the Cretaceous, its diversity included semi-aquatic (*e.g.* Eusuchia) as well as marine (Tethysuchia) and terrestrial (Notosuchia) organisms. During its evolutionary history, it crossed two major crisis events, the OAE2 and the K/Pg boundary. The response of Metasuchia to each was different as the first one produced a global decrease in diversity, contrary to the second one. Large-scale studies, both temporally and phylogenetically speaking, yielded contrasted results regarding the main drivers of Metasuchian diversification, pleading for more refined studies. The second chapter of this manuscript was focused on the differential survival of the Notosuchia at the K/Pg crisis. This group radiated during the Upper Cretaceous but was strongly affected by this crisis and the Sebecidae is the sole clade to have survived it. Investigating the reasons explaining this survival, we showed that the extinction/survival that occurred in this clade during this event was not randomly distributed with respect to the phylogeny, therefore suggesting that there were specific factors, with a strong phylogenetic signal, that may explain it. Using PLR analysis, we showed that large notosuchians were significantly less prone to become extinct than smaller ones. Using PGLS, we were able to show that body size was associated with diet in this group, with larger species being carnivorous and smaller species being omnivorous. This led us to hypothesize that their hypercarnivorous diet explains the survival of the Sebecidae. According to our analyses, palaeotemperature did not play a significant role in the differential survival of the Notosuchia at the K/Pg crisis. The small time scale of our study explains this. Indeed, this variable was probably a major driver of notosuchian diversity as the radiations of this group seem to correlate with palaeoclimatic variations. The work presented in this chapter corroborates the value of smaller-scaled evolutionary studies. Furthermore, it highlights the importance and usefulness of the PCMs in such studies. However, such methods require a strong phylogenetic framework. Multiple controversies exist regarding the phylogeny of the Metasuchia. Regarding the Crocodylia, the conflict between the Longirostres and Brevirostres hypotheses not only concerns the topology but also the dating of the nodes which could strongly affect PCM analyses. Thus, treating this phylogenetic controversy the same way we treated that of the Notosuchia would probably yield strongly contradicting results depending on the phylogenetic hypothesis, impairing their discussion. The third chapter of this manuscript investigates this Longirostres/Brevirostres conflict. We used the 3ta to develop a new method of phylogenetic support assessment. Because of character optimization

in parsimony, the link between the characters as hypothesized in the matrix and as optimized on the optimal tree is lost. Because this is not the case in 3ta, phylogenetic support measured directly from the matrix can provide explanations regarding the yielded topology of the optimal tree. We present the Contradictory Index, a metric that computes the support of a relationship hypothesis relative to a second, contradicting one. We analysed the most recently published morphological matrix. We showed that despite the Longirostres hypothesis being the most supported, it is highly contradicted in the matrix. We were able to quantitatively target the Tomistominae as the main providers of support to the Longirostres hypothesis. Furthermore, we showed that characters considered by previous studies to be correlated to longirostry were not those that support the most the Longirostres hypothesis. Finally, our results suggest that resolving conflict between characters describing the skull will be more helpful in the resolution of the Longirostres/Brevirostres conflict than the description of new postcranial ones.

Contents

0.1	General Foreword	25
1	Overview of Metasuchia	29
1.1	Introduction	31
1.2	Phylogenetic Framework	34
1.2.1	<i>The Thalattosuchian Problem</i>	34
1.2.2	<i>Neosuchia</i>	35
1.3	Stratigraphic Distribution of Metasuchia	37
1.3.1	<i>Jurassic</i>	37
1.3.2	<i>Cretaceous</i>	39
1.3.3	<i>Palaeogene</i>	41
1.3.4	<i>Neogene to Present Time</i>	42
1.3.5	<i>Conclusions</i>	42
1.4	Palaeoenvironments of Metasuchian-Bearing Beds	44
1.4.1	<i>Limits in Identifying Precisely the Facies Using Database Collections</i>	44
1.4.2	<i>Depositional Environments: Predominance of Fluvial/Freshwater Habitats</i>	46
1.4.3	<i>Conclusions</i>	50
1.5	Evolution in Palaeoclimatic Preferences of Metasuchia	52
1.5.1	<i>Extant Diversity</i>	52
1.5.2	<i>Jurassic</i>	55
1.5.3	<i>Cretaceous</i>	55
1.5.4	<i>Cenozoic</i>	60
1.5.5	<i>Conclusions</i>	61

1.6	Further Considerations Regarding the Climatic Drivers of Notosuchian Diversification . . .	66
1.7	Chapter Conclusions	68
1.8	References	71
2	Survival of Notosuchia at the Cretaceous-Palaeogene crisis	85
2.1	Foreword	87
2.2	Abstract	89
2.3	Introduction	90
2.4	Materials and Methods	93
2.4.1	<i>Supertrees</i>	93
2.4.2	<i>Phylogenetic logistic regression</i>	95
2.4.3	<i>Phylogenetic selectivity using D-statistic</i>	96
2.4.4	<i>Phylogenetic generalized least squares testing for skull length evolution</i>	97
2.4.5	<i>Phylogenetic generalized least squares testing for skull length evolution</i>	98
2.4.6	<i>Phylogenetic generalized least squares testing for the skull length \tilde{d}iet relationship</i> .	99
2.5	Results	100
2.5.1	<i>K-Pg crisis: phylogenetic structure of the extinction and biotic factors explaining survivals</i>	100
2.5.2	<i>Evolution of body size in Notosuchia and relationship with diet</i>	102
2.6	Discussion	106
2.6.1	<i>K-Pg crisis: Phylogenetic structure of extinction and biotic factors explaining survivals</i>	106
2.6.2	<i>Evolution of body size in Notosuchia and relationship with diet</i>	107
2.6.3	<i>Effects of phylogenetic and stratigraphic uncertainty</i>	108
2.7	Conclusions	110
2.8	Acknowledgments	110
2.9	Author Contribution	110
2.10	References	112
3	Phylogeny of Crocodylia	121

3.1	Foreword	123
3.2	Abstract	124
3.3	Introduction	126
3.4	Materials and Methods	130
3.4.1	<i>Three-taxon analysis(3ta)</i>	130
3.4.2	<i>Characters in 3ta</i>	130
3.4.3	<i>Three-taxon statements (3ts)</i>	131
3.4.4	<i>Fractional weighting</i>	132
3.4.5	<i>Measuring support in 3ta</i>	132
3.4.6	<i>Phylogenetic dataset</i>	134
3.4.7	<i>Phylogenetic analyses</i>	135
3.4.8	<i>Measuring the overall support from the matrix</i>	136
3.4.9	<i>Measuring the effect of 'Tomistominae'</i>	137
3.4.10	<i>Disparity in support among characters</i>	137
3.4.11	<i>Assessing the effect of 'Longirostrine' characters</i>	138
3.5	Results	139
3.5.1	<i>3ta and parsimony phylogenetic analyses</i>	139
3.5.2	<i>Overall Support from the Matrix</i>	139
3.5.3	<i>Assessing the effect of 'Tomistominae'</i>	141
3.5.4	<i>Disparity in Support Between Anatomical Categories</i>	142
3.5.5	<i>Assessing the effect of 'Longirostrine' characters</i>	145
3.6	Discussion	147
3.7	Conclusions	153
3.8	References	154
4	General Conclusions	161
4.1	References	170

0.1 General Foreword

Crocodylians are the sole extant representatives of Pseudosuchia. There are between 24 and 27 recognized species. If looking at the extant biodiversity, their closest relatives are the birds and there are $\approx 11,000$ species of them (IUCN, <https://www.iucnredlist.org/>). Here are two observations that struck me as soon as I started to work on this group. Because extant diversity results from past evolution, the fact that any crocodylian is more closely related to a robin than to any non-crocodylian animal is the promise of a complex, rich, intricate evolutionary history. Indeed, to explain this kinship between such different organisms, a lot had to have happened in their respective history. Furthermore, the extant diversity of both of these groups is dramatically different. One of them is represented by thousands of species, distributed all around the globe (even Antarctica!) under all climates and displaying a huge morphological range of adaptations, from the cursorial Struthioniformes (ostriches and their close relatives) and the aquatic Sphenisciformes (penguins) to the large gliding Andean condor and the tiny hummingbirds. The other group is represented by less than 30 species whose morphological and ecological diversity pales when compared to that of the former: they are restricted to tropical to warm temperate climates and all of them are semi-aquatic, sprawling, armor-bodied ambush predators.

The evolutionary history of birds has been heavily investigated for at least the past century. This is to the point that almost everyone knows about the dinosaurs from childhood. Even the person least interested in natural history knows what a *Tyrannosaurus* looked like and that it became extinct after an asteroid collided with the Earth. Dinosaurs are part of the popular culture and despite them being often misrepresented, the mere fact that they are part of it means that millions of people know about them. Everybody knows about crocodylians. Most people know that crocodiles, alligators, caimans, and gharials are different kinds of crocodylians. But who knows about Pseudosuchia, and who knows what *Simosuchus* looked like? I recently had an appointment with someone from the French administration and as she was surprised that I worked on fossil crocodylians, she asked me, intrigued, if I worked on the ‘whole species’. Palaeontology was not her field of expertise. However, had I told her that I worked on fossil birds, she probably would have known that there are multiple species of them. And for most of the people I have met who don’t even know what palaeontology is, the mere mention of dinosaurs sheds light and I have been often introduced as someone working on dinosaurs, even though I never did. These anecdotes show that for the general public, crocodylians do not really have a history. They are

here today as they have always been, sprawling creatures that hide underwater. And this view was not uncommon among researchers until fairly recently. Crocodylians were often referred to as ‘living fossils’, the genus *Crocodylia*, which includes numerous extant species, was attributed to Cretaceous specimens. The overall representation of crocodylian natural history was then the consistent reproduction of the same forms throughout millions of years, with notable but negligible exceptions. The evolutionary promise made by the kinship of crocodylians and birds was almost entirely fulfilled by the latter.

This view has now changed. The discovery of numerous new bizarre fossils uncovered an unsuspected disparity in the diversity of crocodylian extinct relatives. Most notably, the recent advances in the knowledge of a particular group, the Notosuchia, revealed a surprising diversity. It included organisms fit to inhabit terrestrial environments, with an erect posture and some even probably having cursorial habits. The diversity in teeth morphology, especially, turned out to be impressive with some being even more complex than those found in mammals. It allowed to infer that if some species were carnivorous, others were omnivorous and even herbivorous, leading to ecological niche partitions no longer existing today. This new diversity refuted the representation of the history of crocodylians as the monotonous persistence of modern-like-looking forms. The extinct cousins of the modern representatives did ‘explore’ ecological niches today deserted by them. Pseudosuchian evolutionary history was richer and more complex than previously thought. Thus, the small extant diversity, ecologically and morphologically speaking, of the crocodylians could no longer be explained by the fact that it had always been that way. This newly discovered extinct diversity has consequently raised the question of its decline. Maybe, the evolutionary promise made by the kinship between crocodylians and birds could also be fulfilled by the history of the former, after all.

This sets the context of my PhD research and the overarching question it pretends to be a part of. Because studying the whole group of Pseudosuchia would have been impossible, my research was focused on a less inclusive one, the Metasuchia. This group is composed of two clades, the Neosuchia and the Metasuchia.

This manuscript begins with an introductory chapter. This chapter mainly consists of a review of the literature and it aims to provide the reader a general picture of the studied group. I briefly present the main phylogenetic controversies and specify the phylogenetic framework followed here. I then describe

the evolution in diversity of the main metasuchian clades from the Jurassic to the present time. The last two parts of this chapter are focused on characterizing the palaeoenvironments and palaeoclimates in which metasuchian have been found.

The second chapter mainly consists of a study published during my PhD. It is focused on the clade Notosuchia. In this study, we used phylogenetic comparative methods to investigate the response of this group when it faced the K/Pg crisis. We used the Phylogenetic Logistic Regression (PLR) to test whether the effect of body size and palaeotemperature significantly explained the differential survival and the Phylogenetic Generalized Least Squares (PGLS) to investigate the relationship between notosuchian body size and diet.

The use of phylogenetic comparative methods requires a robust phylogeny. This is not the case for the clade Neosuchia because the phylogeny of the Crocodylia, the crown group of extant metasuchians, which account for a large part of the neosuchian diversity, is still highly debated with two contradicting topologies having been consistently found. In the third and final chapter of this manuscript, we investigate this phylogenetic controversy. We propose a new method to assess phylogenetic support directly from the matrix. Following this method, we investigate and quantify the contribution of particular taxa and characters in the support they provide to each topology hypothesis.

Chapter 1

Overview of Metasuchia

1.1 Introduction

The extant diversity of Metasuchia is composed of 24 to 27 species (Grigg & Kirshner, 2015). Several were only recently recognized, with advances in molecular studies (see the review from Brochu & Sumrall, 2020) and this amount will probably get higher in the next few years (Grigg & Kirshner, 2015; Brochu & Sumrall, 2020). Still, all of them belong to the clade Crocodylia, being distributed in three less inclusive ones: Alligatoroidea (alligators and caimans), Crocodyloidea (crocodiles), and Gavialoidea (the gharial). For a long time, the Metasuchia clade was considered to have evolved slowly, having it long been recognized that their morphology was very conservative (Lydekker, 1886; Sill, 1968; Tarsitano *et al.*, 1989; Densmore & Owen, 1989). This was reflected in the taxonomy of the group with, for instance, the *Crocodylus* genus that was considered to have originated 97 My ago (Markwick, 1998) and it even led some to consider crocodylians as ‘living fossils’ (*e.g.* Meyer, 1984). However, this view has been challenged. Indeed, it is now acknowledged that the origin of the metasuchian diversity as it is known today only occurred recently (Oaks, 2011; Scheyer *et al.*, 2013; Roberto *et al.*, 2020; Pan *et al.*, 2021). Present time diversity is only a fraction of that of the past, and a poorly representative one. As previously stated, extant metasuchians are all included in a single clade, Crocodylia. However, this clade, although it has long been a major one of the Metasuchia, is far from being the only one. Looking at the past diversity, Metasuchia is composed of two major clades: Neosuchia and Notosuchia (see First Part of this chapter). The former includes mostly semi-aquatic (freshwater) and marine organisms distributed in several subgroups among which: Atoposauridae, Goniopholididae, Tethysuchia, and Eusuchia (which includes Crocodylia). In some phylogenetic hypotheses, it also includes a group of semi-aquatic to fully marine organisms, Thalattosuchia. In such cases, the group that includes Neosuchia and Notosuchia is referred to as Mesoeucrocodylia. Notosuchia, on the other hand, includes mostly fully terrestrial organisms (*e.g.* Uruguaysuchidae and Ziphosuchia), whereas most semi-aquatic organisms are found in the Peirosauridae clade. This chapter mostly relies on a review of the literature. To illustrate and quantify the points I discuss, I downloaded all fossil metasuchian occurrences from the Paleobiology Database (PBDB, taxonomic resolution: species; regular taxa only; latest identification; accepted names only; downloaded in June 2023). All the figures and data from this chapter either come from the literature or this PBDB dataset (Supplementary File S1.1).

The first part of this chapter aims at specifying the phylogenetic framework in which my PhD was performed. The second part is focused on the stratigraphic distribution of Metasuchia. The fossil record of the group starts in the Lower Jurassic and lasts until the present time without temporal gaps. However, during its history, the composition of its diversity (*i.e.* the clades by which it is represented) varied a lot. To account for this variation in terms of taxonomic representation, I described the diversity during the Jurassic, Cretaceous, Palaeogene, and Neogene to the present time. I also computed a diversity curve using the shareholder quorum subsampling (SQS, Alroy, 2010, quorum fixed at 0.4) as a correction method for the uneven sampling of the fossil record. I used the script provided by Tennant *et al.* (2016) to compute confidence intervals using Bootstrap with 1,000 repetitions (see complete results of the SQS analysis in Supplementary File S1.2). Extant metasuchians (Crocodylia) all share similar living environments and lifestyles, all of them being semi-aquatic and inhabiting freshwater to brackish, fluvial, and lacustrine environments (Grigg & Kirshner, 2015). In the third part of this chapter, I present the various depositional environments in which metasuchian fossils have been found. Despite the PBDB providing a depositional environment for all fossil collections, I preferred to collect primary sources in the literature to assign them more confidently. Because reviewing this literature is time-consuming, I focused on geological formations that included at least three metasuchian occurrences. I was able to assign a depositional environment for 98 formations accounting for 783 fossil occurrences and 241 species, out of the 1,352 and 471 (respectively) downloaded from the PBDB (Supplementary File S1.1). The fourth and last part of this chapter is focused on the palaeoclimates under which metasuchian representatives lived. To assess the variety of climates under which extant metasuchians live, I gathered the recorded human observations of extant crocodylians from the Global Biodiversity Information Facility (GBIF, <https://doi.org/10.15468/dl.s59h72>, 8 September 2023, see Supplementary File S1.3, n = 107,222) and I assigned a Koeppen-Geiger (KG) climatic zone (Kottek *et al.*, 2006) to each of them using the ‘LookupCZ’ function from the ‘kgc’ R package (Bryant *et al.*, 2017) to each one. I was thus able to assess the diversity of climates under which extant metasuchians are found and I used the ‘ggplot2’ (Wickham, 2016), ‘sf’ (Pebesma, 2016), ‘rnaturalearth’ (Massicotte & South, 2023), ‘rnaturalearthdata’ (South, 2017) and ‘maps’ (Becker *et al.*, 2021) R packages to represent their geographical distribution on a map displaying the main KG climatic zones. Regarding extinct metasuchians, I used the PBDB dataset (Supplementary File S1.1) and various sources to plot the fossil occurrences on palaeomaps displaying palaeoclimatic

zones. I used the palaeomaps from Rees *et al.* (2000) for the Jurassic (Lower, Middle, and Upper), those from Chumakov *et al.* (1995), available in Hay & Floegel (2012), for the Cretaceous (Aptian, Albian, Cenomanian, Santonian and Maastrichtian) and those from Scotese (2005) for the Cenozoic (Paleocene, Early Eocene, Late Eocene, Oligocene and Miocene). I manually placed the fossil occurrences on the Jurassic and Cenozoic palaeomaps, relying on their present time coordinates. Regarding the Cretaceous, I used palaeomaps already displaying metasuchian geographical distributions for each five stages produced by F. Fluteau (IPGP, Paris) as part of an ongoing collaboration (see Conclusions of this chapter). As a result, I produced palaeomaps displaying both the palaeoclimatic zones and the metasuchians distribution for the Jurassic, Cretaceous, and Cenozoic. When an occurrence fell out of a climatic region, I considered the closest one (from a latitudinal point of view) to be the one it was under. Finally, this allowed me to assess the variations in frequency of each climate throughout time.

1.2 Phylogenetic Framework

Metasuchia is included in the Pseudosuchia clade, which forms with Avemetatarsalia the Archosauria clade (Nesbitt, 2011). Several phylogenetic uncertainties remain regarding the phylogeny of the group. In this section, I specify the phylogenetic framework of the manuscript.

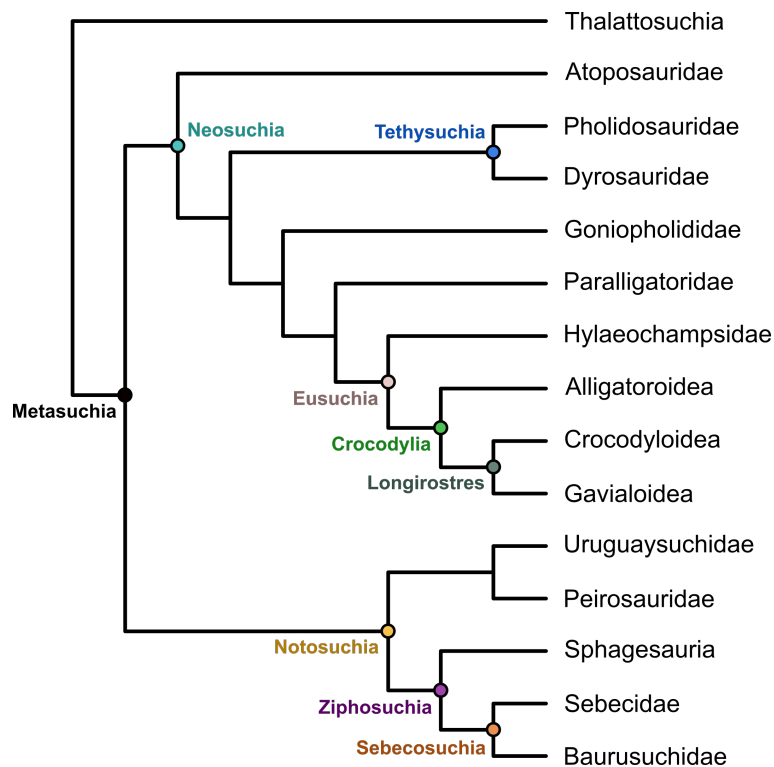


Figure 1.1: Phylogenetic framework of this manuscript.

1.2.1 The Thalattosuchian Problem

This group has been retrieved in various positions within Crocodylomorpha (Clark, 1994; Jouve *et al.*, 2006; Jouve, 2009; Pol & Gasparini, 2009; Montefeltro *et al.*, 2013; Wilberg, 2017; Wilberg *et al.*, 2019). This issue is dependent on the outgroup sampling (Wilberg, 2015) as well as characters that are correlated with longirostry (*i.e.* elongated rostrum), a feature known to have been acquired multiple times, independently in the Crocodylomorpha (Clark, 1994; Buckley & Brochu, 1999; Brochu, 2001; Jouve *et al.*, 2006; Hastings *et al.*, 2015; Ballell *et al.*, 2019). Investigating this controversial phylogenetic placement of the Thalattosuchia is out of the scope of this PhD and we chose to follow the hypothesis from Wilberg *et al.* (2019) that places this group in a basal position outside of the Crocodyliformes,

and thus outside of the Metasuchia. This matches with Benton & Clark (1988) who erected the name Metasuchia for the group “*comprised of non-thalattosuchians mesoeucrocodylians*” (p.320, but note that if Thalattosuchia is considered to be placed outside of the Mesoeucrocodylia, the latter is synonymous with Metasuchia).

1.2.2 *Neosuchia*

Following Wilberg *et al.* (2019), Metasuchia includes two clades, Neosuchia and Notosuchia. The former was erected by Benton & Clark (1988) to name the group that includes Atoposauridae, Goniopholididae, Pholidosauridae, Dyrosauridae, *Bernissartia*, Shamosuchus, and Eusuchia (which includes, among others, the Crocodylia clade). New groups have since been recognized and included in Neosuchia, each of which has its phylogenetic controversies. We followed the definition of Eusuchia from Brochu (1999) who defined it as the group that includes Hylaeochampsidae and Crocodylia. Another group, Paralligatoridae, was found to be inside Eusuchia by Wilberg (2015). However, they were retrieved as the sister group to all other eusuchians in Wilberg *et al.* (2019). In a more recent analysis (Rummy *et al.*, 2022), they were again retrieved as part of Eusuchia. However, the matrix used in this last study is based on that from Turner (2015) which contradicts that of Wilberg *et al.* (2019) on the issue of Thalattosuchia. As we chose to follow the latter, we considered Paralligatoridae to be the sister group of Eusuchia. The Crocodylia clade is also subject to phylogenetic controversies. Almost all phylogenetic analyses based on morphological characters have consistently retrieved Alligatoroidea and Crocodyloidea as sister groups, forming the Brevirostres clade, which Gavialoidea are excluded of (e.g. Norell, 1989; Brochu, 1997a; Brochu, 1997b; Salisbury *et al.*, 2006; Jouve *et al.*, 2015). On the other hand, molecular-based analyses have pleaded for the grouping of Crocodyloidea and Gavialoidea (forming the Longirostres clade) against Alligatoroidea (e.g. Densmore, 1983; Densmore & Owen, 1989; Harshman *et al.*, 2003; Pan *et al.*, 2021). The phylogenetic placement of a less inclusive group, Tomistominae, changes depending on the hypothesis: in the first one (Brevirostres), it is considered as a basal subgroup of Crocodyloidea while in the second one (Longirostres) they are basal gavialoids. Furthermore, the molecular hypothesis regarding the dating of the Gavialoidea clade (including Tomistominae) is incongruous with the fossil record because the oldest known gavialoids are much older than the age given by molecular dating. To tackle this incompatibility, multiple studies have proposed that the Late Cretaceous to Early Palaeo-

gene gavialoids belonged to a distinct non-crocodylian group (thoracosaur) and are wrongly included in Gavialoidea because of convergent evolution (Gatesy *et al.*, 2003; Harshman *et al.*, 2003; Vélez-Juarbe *et al.*, 2007; Lee & Yates, 2018; Ristevski *et al.*, 2020, 2023; Sookias, 2020). This hypothesis, however, was only retrieved by Lee & Yates (2018), using a Tip Dating method. However, a recent study retrieved topologies congruent with the Longirostres hypothesis using morphological characters (Rio & Mannion, 2021). Thus, in this chapter, we considered both the Tomistominae and the thoracosaur to be included in the Gavialoidea clade. The phylogenetic controversies regarding the Longirostres/Brevirostres conflict will be investigated in the third chapter of this manuscript.

1.3 Stratigraphic Distribution of Metasuchia

1.3.1 *Jurassic*

The apparition of Metasuchia in the Jurassic is the continuation of the initial diversification that Crocodyliformes initiated during the Late Triassic-Early Jurassic interval, triggered by the Triassic-Jurassic extinction (Bronzati *et al.*, 2015). The fossil record of Metasuchia is rather scarce during the Jurassic (Figure 1.2). Neosuchia is the only clade to diversify during this period. The first occurrence belongs to Goniopholididae (*Calsoyasuchus valliceps*, Tykoski *et al.*, 2002), in the Lower Jurassic. The rest of Goniopholididae, however, did not diversify until the Middle to Upper Jurassic. Furthermore, despite having been classically considered as included in Goniopholididae, *C. valliceps* was retrieved outside of Metasuchia by Wilberg *et al.* (2019), suggesting that the fossil record of the group may not be older than the Middle to Upper Jurassic. Similarly, Atoposauridae emerged during the Upper Jurassic where they reached their maximum diversity, contributing to the first notable increase in metasuchian diversity during this time (Figure 1.3). This clade has been retrieved as the basal-most member of Neosuchia (*e.g.* Adams, 2013; Sertich & O'Connor, 2014), but the fragmentary nature of most of the specimens makes this phylogenetic placement uncertain. Despite this group having very little species-level consensus, its rapid and intense diversification is probably not a taxonomic artefact and is genuine (Tennant & Mannion, 2014). The first Pholidosauridae were also recorded during the Middle to Upper Jurassic (Owen, 1884). A single occurrence of Gavialoidea is recorded during the Jurassic, long before its diversification during the Upper Cretaceous (Fig. 1.2). This occurrence belongs to *Gavialium rhodani*, named by Jourdan in 1892. I could not find the initial work from Jourdan. However, this specimen is described by Lortet (1982). He assigned it to the Gavialidae family but recognizes the fragility of this attribution given its fragmentary nature and the temporal gap separating it from the first following gavialids. Given the specimen's age and rostral morphology, it is most probably a thalattosuchian. Another puzzling occurrence is the notosuchian one (Fig. 1.2). It belongs to *Razanandrongobe sakalavae*, described by Maganuco *et al.* (2006) based on a fragmentary maxilla. Additional material led Dal Sasso *et al.* (2017) to consider this species as a Sebecosuchia and Martins *et al.* (2023) recovered it close to Baurusuchidae. However, the new material described (almost complete right maxilla, rostral half of a left dentary and a tooth crown) is still very fragmentary. Given the temporal gap between *R. sakalavae* from the

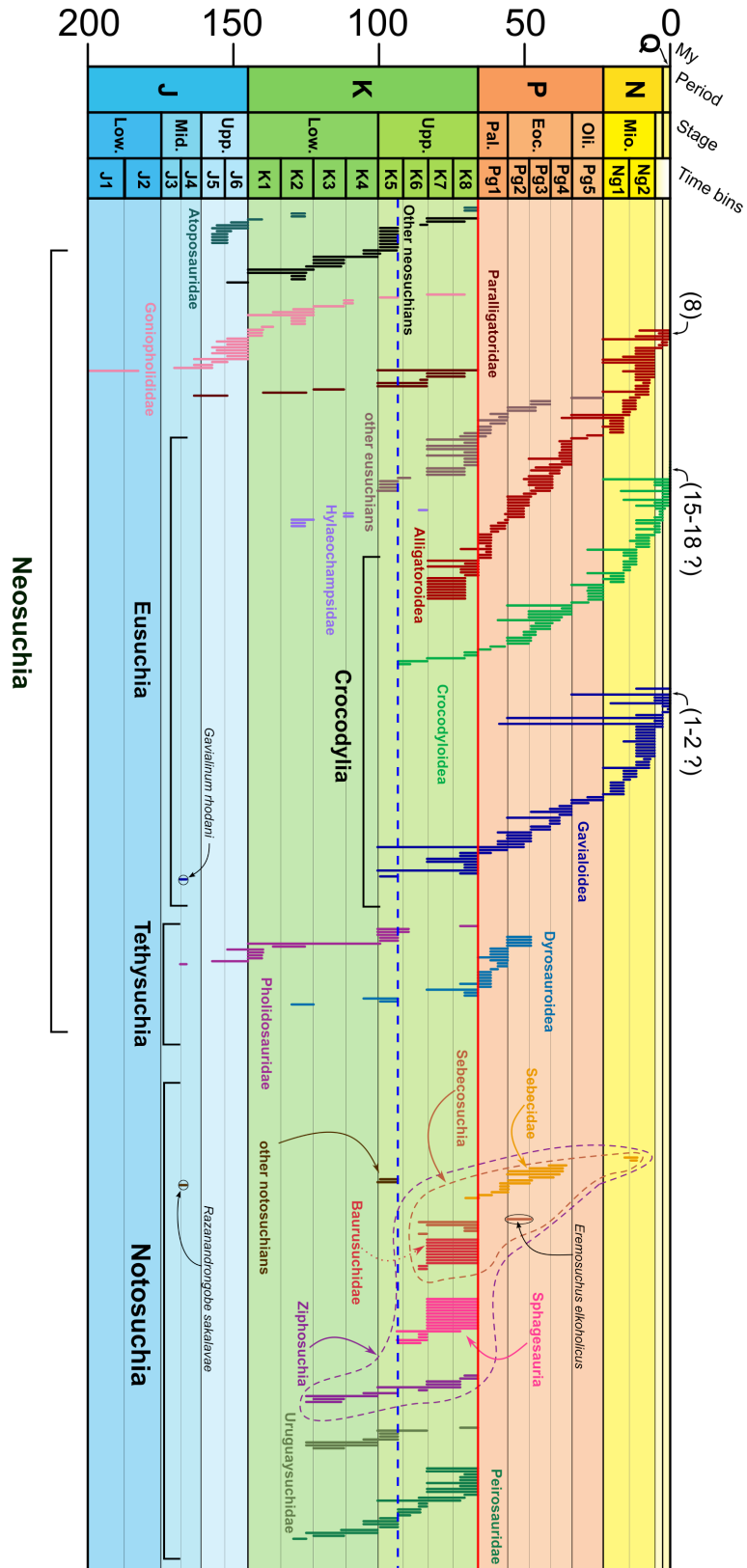


Figure 1.2: Stratigraphic extensions of Metasuchia (PBDB, see Supplementary File S1.1). Each colored bar represents a species. Colors differentiate the clades. Black brackets represent major metasuchian subgroups. Species individually discussed in the main text are specified. Red line: K-Pg boundary. Blue dotted line: Cenomanian-Turonian boundary. Numbers in brackets indicate the number of extant species according to Grigg & Kirshner (2015). Times bins corresponds to that of the diversity curve 1.3

following sebecosuchian, caution is advised regarding its attribution to Notosuchia. To sum it up, metasuchian diversity is very low during the Jurassic. Except for the Atoposauridae, and to some extent Goniopholididae, all the groups present during this period will reach a higher diversity in the following one. Overall, the Middle Jurassic marks the apparition of Metasuchia which diversity steadily increased during the Upper Jurassic (Figure 1.3) due to the diversification of atoposaurids and goniopholidids.

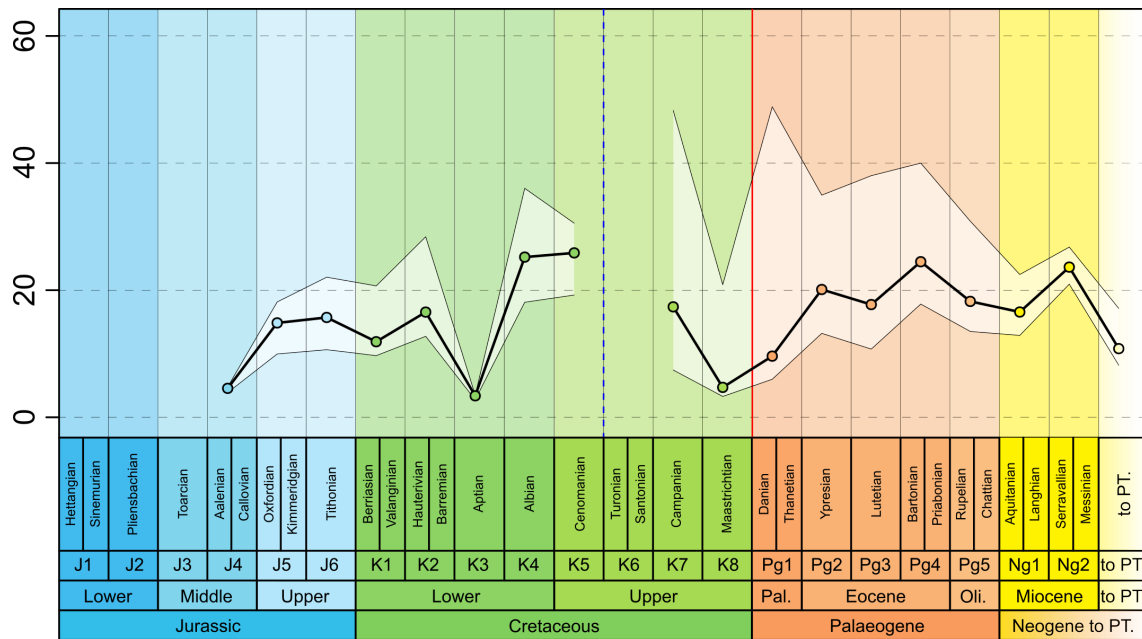


Figure 1.3: Diversity curve in species number of Metasuchia. Geological stages have been combined into time bins to even out the time intervals (mean = 9.08 My, sd = 2.08 My). Diversity values have been computed using SQS, with a quorum of 0.4 and 1,000 repetitions for each time bin. Circles corresponds to the median and the white area represents the 95% confidence interval. Blue dotted line: Cenomanian-Turonian boundary. Red line: K/Pg boundary. PT: Present Time.

1.3.2 Cretaceous

The Cretaceous is a period during which Metasuchia underwent a massive radiation, both numerically and ecologically speaking (Bronzati *et al.*, 2015; Mannion *et al.*, 2015; Melstrom & Irmis, 2019; Wilberg *et al.*, 2019). However, diversity evolution during this period is complex. The beginning of the Cretaceous is marked by a slight decrease in diversity compared to that of the uppermost Jurassic reaching its lowermost level during the Aptian (K3, Fig. 1.3). Both the diversity of Atoposauridae and Goniopholididae strongly decreases following the Jurassic-Cretaceous boundary, probably explaining this decrease in biodiversity. The diversity of Metasuchia bounces back at the end of the Lower Cretaceous (Fig.

1.3). The increase is mostly attributable to Notosuchia. Indeed, the three main groups that it includes (Ziphosuchia, Uruguaysuchidae and Peirosauridae, following Pol *et al.*, 2014 phylogenetic hypothesis) appeared during this time period (Fig. 1.2). The Cenomanian-Turonian boundary (blue dotted line, Fig. 1.2) seems to have affected multiple metasuchian clades. Following this boundary, Dyrosauroidea became the main representative of Tethysuchia, replacing Pholidosauridae. Foret *et al.* (*in review*, see Appendix of this manuscript) explored this faunal change and linked it with the second oceanic anoxic event (OAE 2) that occurred during the beginning of the Upper Cretaceous, at the Cenomanian-Turonian boundary (Selby *et al.*, 2009). But, following Figure 1.2, this event also seems to have impacted the diversity of non-crocodylian eusuchians, although they recovered well during the Upper Cretaceous, as well as Uruguaysuchidae which diversity drastically decreased after the Cenomanian-Turonian boundary. Following the OAE2 is the only gap in reconstructed diversity (Fig. 1.3). The fact that the SQS method we used to compute this diversity curve is not able to quantify the diversity during the Turonian to Santonian time period (K6, Fig. 1.3) testifies of this impact of the OAE2 on metasuchian diversity. This lack of computed diversity at that time is probably also impacted by the fact that most species present are singletons (*i.e.* represented by a single specimen), which are discarded by the SQS method. Indeed, according to the stratigraphic distributions (Fig. 1.2), Crocodylia radiated, becoming a major part of the eusuchian and neosuchian diversity during the late Upper Cretaceous. Bronzati *et al.* (2015) however, dated this radiation earlier, during the Cenomanian-Santonian interval. Similarly, Notosuchia also radiated during the Upper Cretaceous (except Uruguaysuchidae), especially Ziphosuchia which diversifies into two main groups. First, Sphagesauria (Pinheiro *et al.*, 2021), which is comprised of small- to medium-sized omnivorous to herbivorous organisms (see Aubier *et al.*, 2023 for diet inferences references). Second, Sebecosuchia (Colbert, 1946), which includes mostly large-sized carnivorous organisms, with theropodomorph-like teeth (*i.e.* ziphodont). This increase in notosuchian diversity highly contributed to the high Cretaceous diversity of Metasuchia (Bronzati *et al.*, 2015). During the Upper Cretaceous, the diversity of Sebecosuchia is almost entirely represented by the Baurusuchidae. Indeed, there is only one Cretaceous sebecid, the very small-sized *Ogresuchus furatus* (Sellés *et al.*, 2021). This result corroborates those from Bronzati *et al.* (2015) who observed a notosuchian diversification from the Aptian onward. However, this increase in diversity is not retrieved in the diversity curve controlling for the uneven sampling of the fossil record (Fig. 1.3). On the contrary, following the diversity curve,

the diversity of Metasuchia strongly decreased during the late Upper Cretaceous almost reaching the lowermost value of the Aptian at the Maastrichtian (Fig. 1.3, K8). Here again, the large proportion of singleton species probably explain this result. This would also explain the wideness of the confidence intervals at that time period.

1.3.3 Palaeogene

Overall, metasuchians seem to have benefited from the K/Pg crisis given that their diversity increased in the Palaeogene compared to the Maastrichtian (Fig. 1.3). However, this global increase in diversity masks an uneven effect of this crisis among metasuchians clades. Regarding Neosuchia, only eusuchians and tethysuchians survived it (Fig. 1.2). The former already composed most of the neosuchian diversity during the Cretaceous and they kept on diversifying. Indeed, while non-crocodylian eusuchians diversity slowly diminished throughout the Palaeogene, Crocodylia underwent a massive radiation during the Paleocene and Ypresian, especially regarding the Alligatoroidea clade (Bronzati *et al.*, 2015; Celis *et al.*, 2020) recorded in the diversity curve (Fig. 1.3, Pg1 and Pg2). Tethysuchia, the other surviving neosuchian group, also radiated right after the K/Pg boundary (Fig. 1.2). Their diversity is only represented by Dyrosauroidae which probably took advantage of the ecological niches left vacant by the extinction of Mosasauridae (Jouve *et al.*, 2008; Jouve, 2021; Foret *et al.*, *in review*). However, the fossil record of Dyrosauroidae stops in the middle of the Eocene, and the diversity of Tethysuchia with it. On the other hand, the effect of the K/Pg crisis was much more pronounced on Notosuchia. All groups, except Sebecosuchia, became extinct. Within the latter, the main Cretaceous representatives (Baurusuchidae) also disappeared and were replaced by the Sebecidae that diversified during this time period, therefore producing the last notosuchian diversification (Bronzati *et al.*, 2015). As such, almost all the Cretaceous notosuchian diversity collapsed. The only non-sebecid sebecosuchian found in the Palaeogene in this dataset is *Eremosuchus elkoholicus* (Fig. 1.2), described by Buffetaut (1989). Its phylogenetic affinities are still unclear, given the fragmentary nature of the material (Montefeltro *et al.*, 2011). However, it is probable that if it belongs to Sebecosuchia, it is a sebecid. The reasons why only the sebecids survived are still debated and are the focus of the second chapter of the manuscript.

1.3.4 *Neogene to Present Time*

From the Neogene onwards, crocodylians are the sole representatives of the Neosuchia. Alligatoroidea, Gavialoidea and Crocodyloidea intensely diversify (Fig. 1.3, Ng1 to Ng2). The only other clade represented is Sebecidae, with its last remnants occurring during the Miocene (Langston, 1965; Paolillo & Linares, 2007). The middle-late Miocene maximum in diversity is caused by the diversification of Alligatoroidea, Gavialoidea and Crocodyloidea (Celis *et al.*, 2020). Following the Miocene, the diversity of the first two groups decreased during the Pliocene whereas that of the latter increased, leading to an overall decrease of metasuchian diversity following the middle-late Miocene (Fig. 1.3). This increase in crocodyloid diversity is caused by the rapid and recent radiation of *Crocodylus* genus, during the Pliocene (Oaks, 2011). This comes to the extant diversity with Crocodylia as the only metasuchian representative. The exact number of species is still not fixed, as new molecular studies showed that there might be cryptic species (Grigg & Kirshner, 2015). Still, Crocodyloidea is today the most diverse clade, with fifteen to eighteen species, while Alligatoroidea and Gavialoidea only account for eight and a single to two species, respectively. Whether Gavialoidea is represented by one or two (*Gavialis gangeticus*, *Tomistoma schlegelii*) species is an issue related to the phylogenetic relationships between the three crocodylian clades and is the focus of the third chapter.

1.3.5 *Conclusions*

The evolutionary history of the group begins during the Middle to Upper Jurassic with Atoposauridae and Goniopholididae as main representatives. The Cretaceous is a contrasted period. The Lower Cretaceous is marked both by an overall increase in diversity with the apparition of Notosuchia and by the lowermost recorded diversity value during the Aptian. The OAE2 seems to have had a strong negative impact on Metasuchia as a whole. Following this event, Metasuchia diversified, according to the stratigraphic distribution of its species. It is during this time period that the first representatives of the modern and one of most successful metasuchians (Crocodylia) appeared. Concomitantly, Notosuchia also radiated with the diversification of Ziphosuchia and the apparition of Sphagesauria and Sebecosuchia. During the Upper Cretaceous, semi-aquatic, marine and terrestrial metasuchians coexisted. However, the assessment of this increase in diversity is impaired by the large number of singleton species. The Palaeogene contrasts with the Cretaceous in that the neosuchian and notosuchian diversities did not evolve similarly. While the

former continued its diversification, crocodylians steadily imposing themselves as main and eventually sole representatives of the group, the diversity of Notosuchia dramatically decreased and was reduced to a few species of Sebecidae. Both of these trends (diversification of Crocodylia and decrease of the notosuchian diversity) kept on going during the Neogene during which the last representatives of Notosuchia were found. Finally, it is during the Pliocene and the Quaternary that the structure of the crocodylian diversity changes, with Crocodyloidea becoming the most diverse super-family while the diversity of both Alligatoidea and Gavialoidea diminished compared to the Miocene.

1.4 Palaeoenvironments of Metasuchian-Bearing Beds

Based on the depositional environment gathered from the literature, I could compile them in a pie diagram (Figure 1.4). It displays the distribution of the main types of depositional environments. Reviewing the literature however, I could find numerous instances of classical biases that I wish to present before discussing the distribution of the metasuchian-bearing palaeoenvironments.

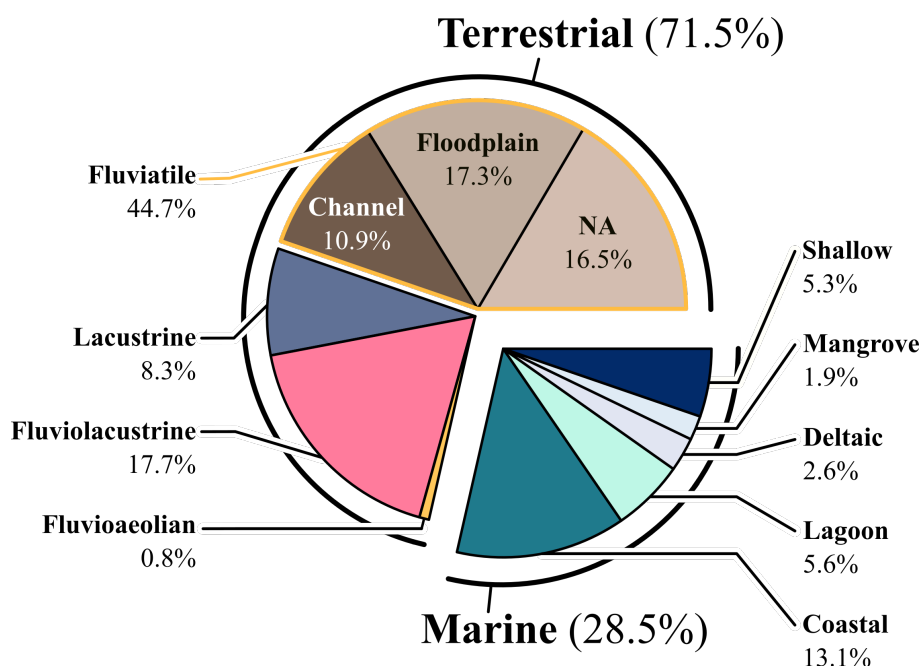


Figure 1.4: Pie diagram displaying the distribution of depositional environments in which metasuchians species have been found (see main text for detail on the data set). Orange bounded parts correspond to fluvatile deposits, the 'NA' part corresponds to the fluvatile occurrences that could not be specified further (*i.e.* 'Channel' or 'Floodplain').

1.4.1 Limits in Identifying Precisely the Facies Using Database Collections

Attributing a corresponding precise environment to fossil specimen occurrences documented in the PBDB to investigate the living environments of those extinct species has some limits. The main one I encountered was the accuracy of the stratigraphic location of the fossil specimen in the database. This is important, because facies and environmental deposits may evolve rapidly vertically and/or laterally in a given section or at a given fossil site. In that sense, the accuracy of living environments we inferred for metasuchians using the PBDB relies on the preciseness of the stratigraphical position of the specimen, as indicated in the database. As stated above (see Introduction of this chapter), I checked the primary

literature for the geological formations that included three or more metasuchian specimens. However, even when doing so, the precise stratigraphic position of a specimen with respect to the vertical/lateral facies distributions in the geological sites is not easily accessible, if accessible at all. Thus, unfortunately, a very precise stratigraphic location for fossils is not reached for most of the occurrences of this dataset and this can lower the confidence in the palaeoenvironmental inferences. However, for some geological formations, this is not an issue. Indeed, some geological formations are inferred to have been deposited in their entirety in the same environment, which has been precisely inferred. For instance, specimens of crocodylians and a sebecid were retrieved in the Messel Formation (Germany). This formation is considered to have been deposited in a maar lake (Lenz *et al.*, 2007, Moshayedi *et al.*, 2020). Despite lacking precise information regarding the stratigraphic location of the fossil specimens, we can confidently infer the depositional environment of the sediments in which they have been found because it is stable throughout the whole formation. However, most of the time, formations and fossil-bearing sites record multiple depositional environments. The Koobi Fora Formation (Kenya), for instance, has yielded several specimens of neosuchians. Cohen (1982) described four different facies corresponding to environments ranging from continental to marine, including coastal ones. Because no precise information is available regarding the precise stratigraphic location of the fossil specimens, they were all considered to have been deposited in a coastal environment in this dataset. This explains why the majority of marine metasuchian-bearing formations fall into the ‘coastal’ category (Fig. 1.4). Similarly to the Koobi Fora Fm, when a formation included marine as well as coastal and/or fluvial ‘phases’, the fossil specimen(s) included were considered to have been fossilized in a coastal depositional environment if no precise stratigraphic location(s) were available. This means that the coastal category (Fig. 1.4) is probably over-estimated, as an example of this kind of difficulties. Furthermore, because these marginal marine environments can rapidly shift throughout time, it is often complicated to precisely decipher the temporal series of changing environments. Thus, 56% of the species occurrences from the ‘coastal’ category were not specified further.

Another classical problem in using metasuchian-bearing beds as living environment indicators for Metasuchia is the transport of fossil material out of its original living environment. Fossil specimens can be allochthonous, meaning that the material was transported after the death of the animal and buried in a different location. Fluvial systems, for instance, are highly efficient in an eventually long-

distance upstream-to-downstream transport of a load charge (which can include entire carcasses or parts of animals). In such cases, using the depositional environment of the deposit to infer the precise living environment of the organism would be an error. However, Kidwell & Flessa (1995), based on the work from Behrensmeyer (1975) among others, found that “*with the exception of a few circumstances, usually recognizable by independent criteria, transport out of the original life habitat affects few individuals*” (p.269). Indeed, Voorhies (1969, cited in Behrensmeyer, 1975) experimentally showed that different fossil assemblages were formed depending on the type of transport. Therefore, taphonomic features can not only indicate if the fossil material was transported but also by which means. For example, Adams *et al.* (2017), describing a neosuchian, relied on the variety of preservation modes displayed by the meso- and microvertebrates in the deposit to consider the fossil community to be allochthonous. On the contrary, Sellés *et al.* (2020) considered the material they described to be autochthonous, based on the orientation of eggshell fragments and the work from Hayward *et al.* (2011). To sum it up, despite the transport of fossils out of their original living habitats being possible, the fact that such a phenomenon produces recognisable taphonomic features prevents it from being an insurmountable obstacle, and in general, reliable palaeoenvironmental life information can be deciphered from metasuchian-bearing beds.

Despite these shortcomings, several general lines arise from our study regarding the inferred life environments of the Metasuchia, as shown below.

1.4.2 Depositional Environments: Predominance of Fluvial Freshwater Habitats

One of the most striking observations from Figure 1.4 is the dominance of continental deposits (71.5%) compared to marine ones (28.5%). Among the former, only two species (*Sebecus icaeorhinus* and *Eo-caiman cavernensis*) have been retrieved in deposits inferred to have had an aeolian influence (Sarmiento Formation, Argentina, see Bellosi, 2010). The rest is distributed between fluvial (44.7%), fluvio-lacustrine (17.7%) and lacustrine (8.3%) deposits. Within fluvial deposits, the amount of species occurrences found in floodplain deposits (17.3%) is almost twice that of those found in channels (10.9%). Specimens from 76 species originate from sediments inferred to have been deposited in a marine environment (28.5%). But most of them correspond to coastal ones (13.1%), only 14 of them corresponding to

more distal, yet shallow, environments. To sum it up, 71.5% of the occurrences of metasuchian species from this dataset are associated with freshwater deposits, and almost 45% with fluviatile ones. Marine deposits only include $\approx 29\%$ of them, most of which belong to coastal environments, which are at the interface between fresh- and saltwater. From these data, three main points emerge: (1) continental species occurrences are much more abundant than marine ones; (2) among continental occurrences, freshwater fluviatile floodplain deposits are the most frequent; (3) concerning marine occurrences, coastal deposits are dominant over more distal ones. In the following sections, I will propose lines of explanation for each of these points. As we will see, some of them may shed light on the actual environmental preferences of the metasuchians while others may merely reflect biases commonly encountered in the fossil record.

Fluviatile sediments are deposited either within the stream channel or on the floodplain, during flooding events (Reading, 1996). Meade *et al.* (1990) analysed the storage of sediments from two present-day rivers in Pennsylvania and California in the USA during multiple decades. They showed that the majority of the sediment that was transported by these rivers was so during small time intervals, restricted to a few specific flooding events (Figure 1.5, after Meade *et al.*, 1990). Indeed, according to their data, on average, around half of the total sediment transported by rivers during a whole year is recorded during 1% of that year, and almost 90% during a bit more than a month. Furthermore, at a larger time scale, sediment transportation varies a lot and a few events account for most of the total (see year 1970 for Juniata River in Pennsylvania, Fig. 1.5a and year 1965 for Eel River in California, Fig. 1.5b). As a consequence, most of the volume of fluviatile deposits corresponds to flooding events, and those deposits are both the most intermittent and with one of the highest rates of sedimentation among the various environmental settings (Figure 1.6, after Schindel, 1980). And because in a river-floodplain system the surface covered by rivers is generally small compared to that of the floodplain (with the exception, however, of braided-river systems), fluviatile deposits are large-scale snapshots of their lateral environmental settings.

This geographically large-scaled and temporally restrained (intermittent) fluviatile sedimentation can provide explanations regarding the dominance of this kind of metasuchian bearing deposits in this dataset compared to that of other continental ones. Indeed, because intense flooding events are spatially large, the sediment deposition they cause can bury specimens of species that lived (or at least died) farther from the channels. Thus, terrestrial metasuchians are most often retrieved in fluviatile sediments deposited

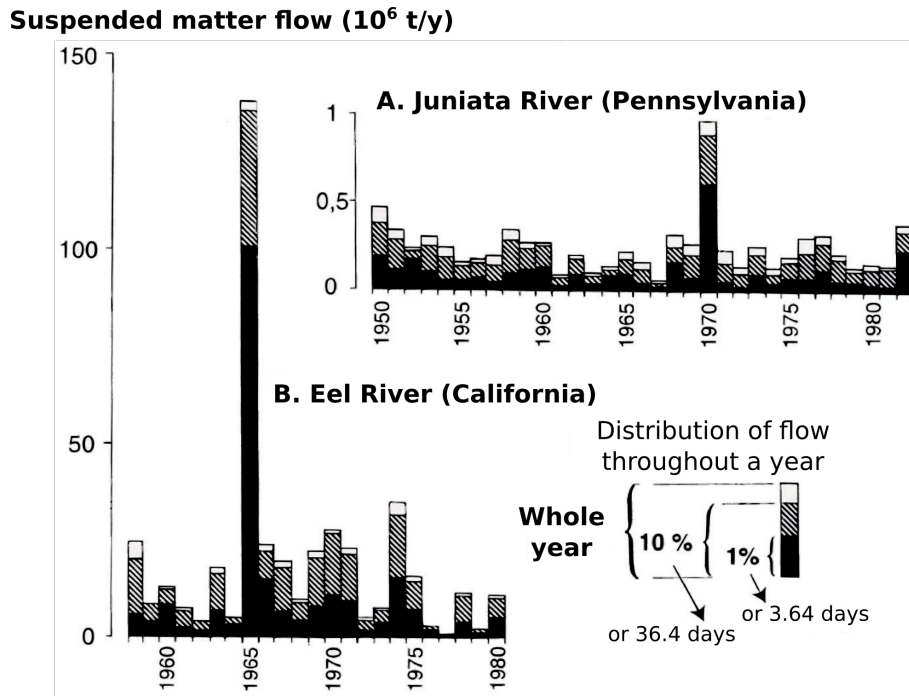


Figure 1.5: Suspended matter flow by year in the Juniata (A) and Eel river (B). After Meade *et al.* (1990).

on a floodplain. *Sebecus querejazus*, for instance, a terrestrial Sebecidae (Buffetaut & Marshall, 1991) was found in the fluvial deposits of the Santa Lucía Formation (Bolivia), in a floodplain environment (Rouchy *et al.*, 1993; Deconinck *et al.*, 2000).

The Adamantina Formation also provides a great example of this rule, being the most prolific terrestrial metasuchian bearing formation and corresponding to a fluvial system in an endoreic basin (Fernandes & Ribeiro, 2015; Basilici *et al.*, 2016; Batezelli *et al.*, 2019). On the other hand, the intermittent characteristic of fluvial deposits is well illustrated by the Maevarano Formation (Madagascar). Rogers *et al.* (2001) divided this formation into three members. These are (from base to top) the Masorobe Member, the Anembalemba Member and the Miadana Member (Figure 1.7). A fourth member, the Lake Kinkony Member, intercalated between the Anembalemba and the Miadana Members was described later (Rogers *et al.*, 2013). The Masorobe Member (green, Fig. 1.7) was interpreted as a well-drained floodplain while the Anembalemba Member (blue) was interpreted to have been deposited in shallow alluvial channels (Krause *et al.*, 2010; Rogers *et al.*, 2013). Numerous specimens of *Simosuchus clarki* ($n = 20$) and *Mahajangasuchus insignis* ($n = 5$) have been retrieved in the Anembalemba Member, the latter having also been found in the underlying Masorobe Member (Fig. 1.7). The fact numerous fossil specimens of *S. clarki*, a terrestrial species (Buckley *et al.*, 2000; Kley *et al.*, 2010), were found in

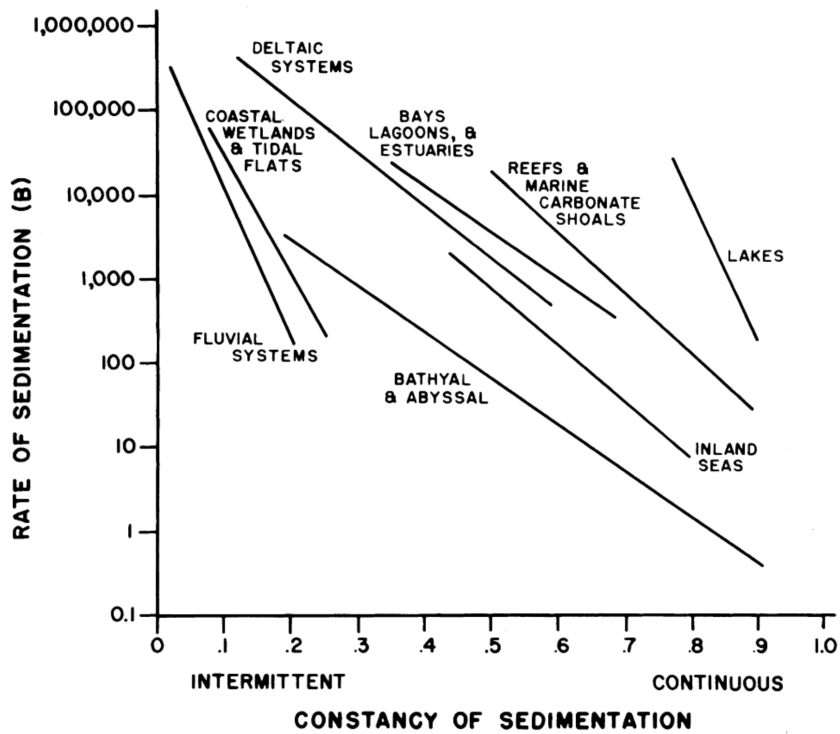


Figure 1.6: Rate and constancy of sedimentation of various depositional environments, after Schindel (1980). Fluvial systems are the most intermittent ones.

channels testifies this intermittent characteristic of fluvial deposits. Indeed, deposition in these channels has been considered to reflect strong seasonality, with episodes of intense rainfalls leading to mass flooding alternating with long periods of drought (Krause *et al.*, 2010; Rogers *et al.*, 2013). Such rapid and intense sediment deposition can lead to ‘ecological snapshots’ which provide a temporal resolution of minutes to years (Kidwell & Flessa, 1995). The biological communities included in these snapshots may not be accurate reflections of the actual community of the time (in our case, the over-representation of *S. clarki* compared to *M. insignis* in the channels). However, according to Kidwell & Flessa (1995), they approximate it.

However, the intense and intermittent nature of fluvial deposits does not fully explain the dominance of these environments in the metazoan fossil record, especially regarding terrestrial species. Bandeira *et al.* (2018) made a literature survey of all published Baurusuchidae (terrestrial notosuchians), Theropoda and Titanosauria (mainly terrestrial Dinosauria) specimens from the Bauru Group (which includes the Adamantina Formation). They showed that the remains of the former were better preserved than that of the latter and suggested that Baurusuchidae were more prone to live close to

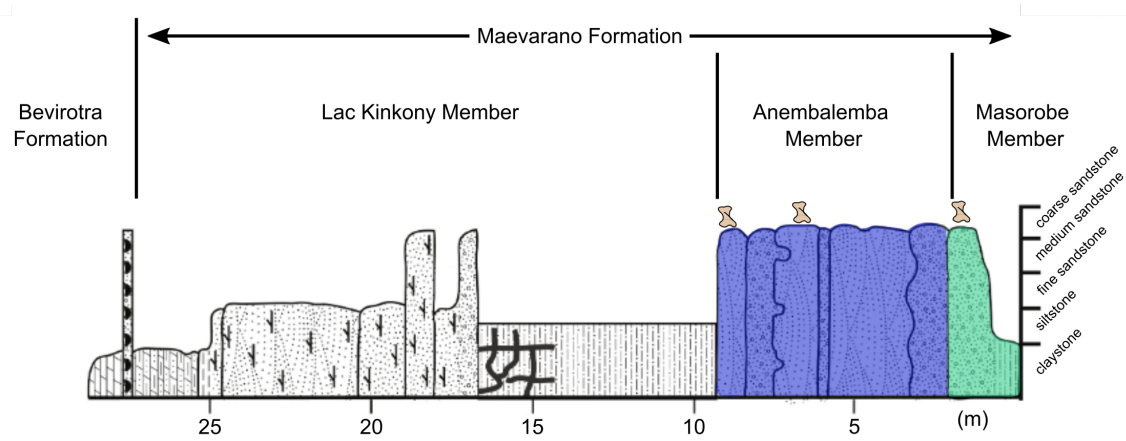


Figure 1.7: Rate and constancy of sedimentation of various depositional environments, after Schindel (1980). Fluvial systems are the most intermittent ones.

floodplains than Theropoda or Titanosauria. Thus, the dominance of fluvial environments in the metasuchian fossil record is also explained by the ecological preferences of the terrestrial species.

1.4.3 Conclusions

In this dataset, 71% of the metasuchian species occurrences were found in freshwater deposits, often fluvial ones. However, this does not imply that the same proportion were semi-aquatic species with a somewhat similar lifestyle to that of their extant representatives. Indeed, fluvial sediments are mainly deposited during flooding events that can cover large areas. Sediments carried during these events can therefore include organisms that did not live adjacently to the channels. Furthermore, flooding events are occasional (especially large ones). Thus, the biological community represented in the resulting deposits may not truthfully depict the actual one, mixing both transient and persistent species. As a consequence of these characteristics, fluvial deposits can include a variety of species that exceed that of semi-aquatic ones. Hence, terrestrial metasuchians are most often retrieved in them. This is all the more accentuated by the fact that aeolian sediment deposition rates are much lower. Fortunately, the lifestyle of an extinct crocodyliform can be inferred independently from the deposit in which it was found, using a wide range of cranial and post-cranial anatomical features (Wu & Sues, 1996; Gomani, 1997; Pol, 2005; Turner, 2006; Sereno & Larsson, 2009; Nascimento & Zaher, 2010; Riff & Kellner, 2011; Godoy *et al.*, 2016; Sena *et al.*, 2022). Regarding the 30% of marine occurrences, the over-dominance of coastal inferred ones is probably the result of the poor accuracy in fossil stratigraphic locations. Indeed, out of the coastal occurrences ($n = 62$, 23% of the total), less than half ($n = 27$) were specified further. The rest ($n =$

35) correspond to occurrences originating from formations that were not described further or (more frequently) from formations that recorded multiple environments, including coastal ones. Therefore, even if this distribution might have truly occurred in the extinct diversity, it is highly biased by the lack of accuracy in this dataset.

We have seen how sedimentation processes can explain (or sometimes bias) the more refined inferred environments of extinct metasuchians. However, regarding the broadest categorization, it is clear that continental environments are preferred by extinct metasuchians over marine ones. In this respect, the extinct diversity of this group is similar to the extant ones (see next section). At first sight, this preferred lifestyle may seem unexpected given that the past diversity includes organisms that occupied niches today deserted by the extant diversity. Putting aside the terrestrial notosuchians (for which we explained why they were retrieved in the same environments as semi-aquatic metasuchians), there were still the tethysuchians which were more adapted to marine environments than any modern crocodylians. The dominance of continental environments seems to show that, despite this increased ecological diversity, metasuchians' environmental preferences remained stable throughout their evolutionary history. Metasuchians, in the bulk of their diversity, were and still are specialized in inhabiting continental, freshwater environments. However, Wilberg *et al.* (2019) tempered this view. They showed evidence against the idea that the apparition of taxa adapted to terrestrial or marine environments occurred by diverging from a "freshwater semiaquatic phylogenetic core" (p.1). Contrary to a single shift model, where the colonization of terrestrial and marine environments occurred via the divergence of specific clades from this 'semiaquatic phylogenetic core', Wilberg *et al.* (2019) showed that these environmental shifts occurred multiple times within almost all major clades. Therefore, the dominance of freshwater habitats throughout the evolutionary history of the Crocodylomorpha (including metasuchians) does not so much testify to the stability of their environmental preferences as their capability to vary around a consistent one. The presence of fully terrestrial (Notosuchia) as well as more marine (Tethysuchia) metasuchians can be considered variations on a persistent, semi-aquatic theme.

1.5 Evolution in Palaeoclimatic Preferences of Metasuchia

1.5.1 *Extant Diversity*

Before describing the data available regarding the diversity of climates under which extinct metasuchians lived, I will briefly present the different climates under which the extant species thrive. Figure 1.8 shows that almost all the observations of crocodylians occur within the 30° to -30° latitude boundaries or just at around them. They seem to live under three main Koeppen-Geiger climate zones: equatorial (mean temperature of the coldest month $T_{min} > 18^{\circ}\text{C}$, red, Fig. 1.8), arid (annual precipitation $P_{ann} < 10 P_{th}$, yellow, see Kottek *et al.*, 2006 for explanations) and warm temperate ($-3^{\circ}\text{C} < T_{min} < 18^{\circ}\text{C}$, see Kottek *et al.*, 2006 for detailed criteria). However, each one of these main climate types includes quite different varied local climatic conditions. For instance, the temperature criterion for ‘warm temperate’ sensu Koeppen-Geiger is very large. Thus, despite both western North America and western Europe being classified as warm temperate, each corresponds to very different climatic conditions. Figure 1.9a displays the precise inferred climates from the Koeppen-Geiger classification (*i.e.* including the humidity and temperature variables) for each extant metasuchian occurrence. 67% of them are located under equatorial/tropical climates (‘A’ climates, Fig. 1.9a), the large majority of which (84%) correspond to seasonally dry ones (Aw + As). The rest of the ‘equatorial/tropical occurrences’ correspond to a monsoonal (Am = 9%) and a fully humid (Af = 7%) climate. These equatorial climates, dominated by seasonally dry winter ones (Aw), represent 67% of the total occurrences. The arid climates, in comparison, do not represent much of them (3%, ‘B’ climates). Almost all of these (90%) correspond to the steppe-like and hot climate (Bsh). The warm temperate climates are the second most frequent ones (29%) under which occurrences are located. This category is over-dominated (96%) by the fully humid and hot summer climate (Cfa). Following these results, it seems that the main climatic driver of crocodylian distribution is humidity. Indeed, they are the most numerous under humid climates (Aw and Cfa, Fig. 1.9a). On the other hand, they are not often found in arid climates, and when they are so, they prefer a steppe climate (BS) rather than a desertic one (BW).

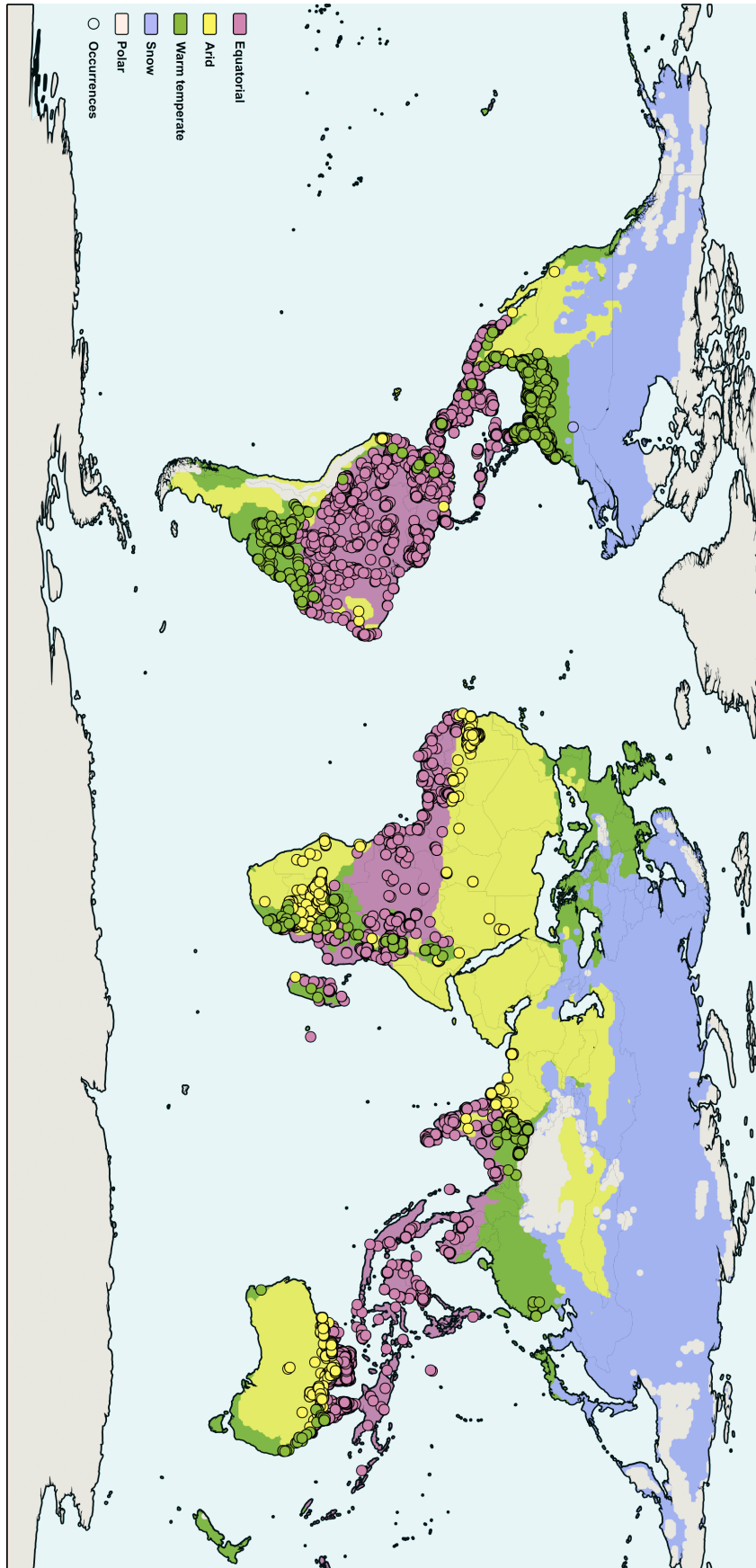


Figure 1.8: Geographic distribution and inferred climates of extant metasuchian (Crocodylia) occurrences. Colours indicate the main climates as defined in the Koeppen-Geiger classification.

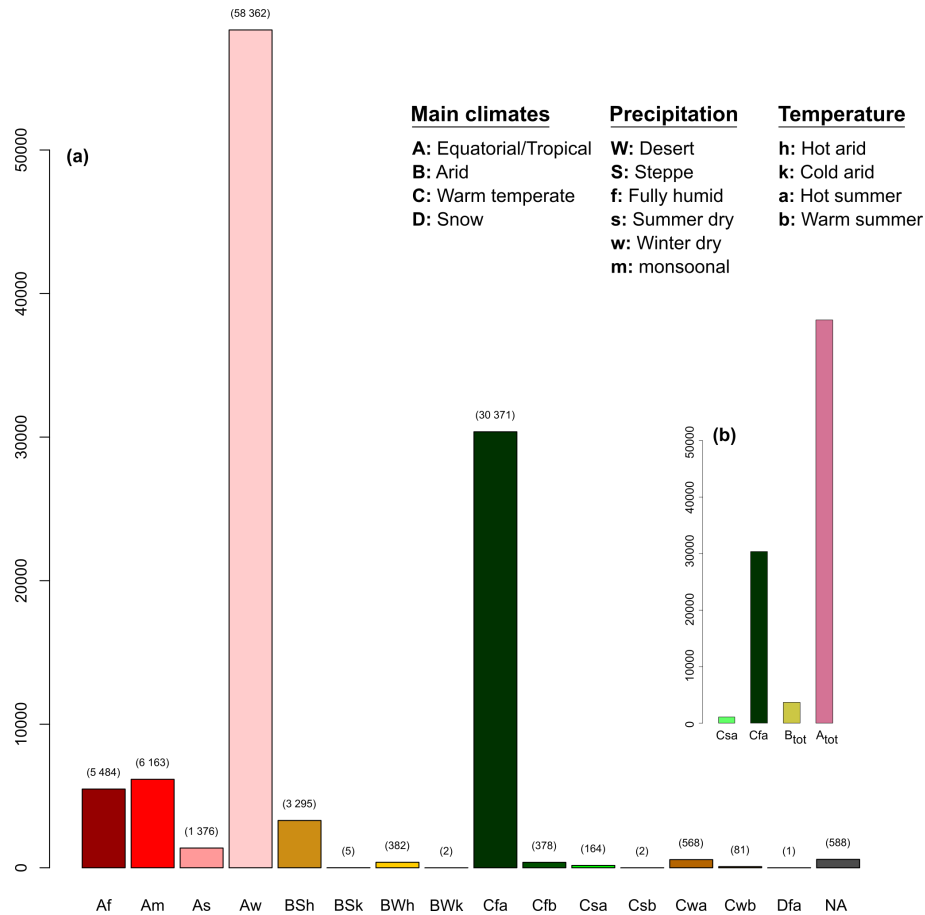


Figure 1.9: Inferred climates of extant metasuchian (Crocodylia) occurrences. Colours indicate the main climates as defined in the Koeppen-Geiger classification.

The second climatic driver seems to be the temperature. They are not found in snowy climates (maximal temperature of the warmest month $T_{max} < 10^{\circ}\text{C}$, Kottek *et al.*, 2006). Furthermore, when found in arid climates, they are rarely found in cold ones (BSk and Bwk, Fig. 1.9a, $n = 5$). Figure 1.9b is a simpler version of Figure 1.9a in that it just differentiates the four different main climates: temperate (light green, Cfb to Cwb from Fig. 1.9a), warm humid temperate (dark green, Cfa), arid (yellow, BSh to Bwk) and equatorial (red, As to Aw). It clearly shows that the latter is the most frequent climate under which extant metasuchians are retrieved, followed by the warm temperate one. Both the arid and temperate climates are negligible. Figure 1.9b uses a simplified climate classification (differentiating only the main KG climates). This simplified version will be helpful for the comparison with the extinct diversity, for which detailed climatic assessment (Fig. 1.9a) is not possible.

1.5.2 *Jurassic*

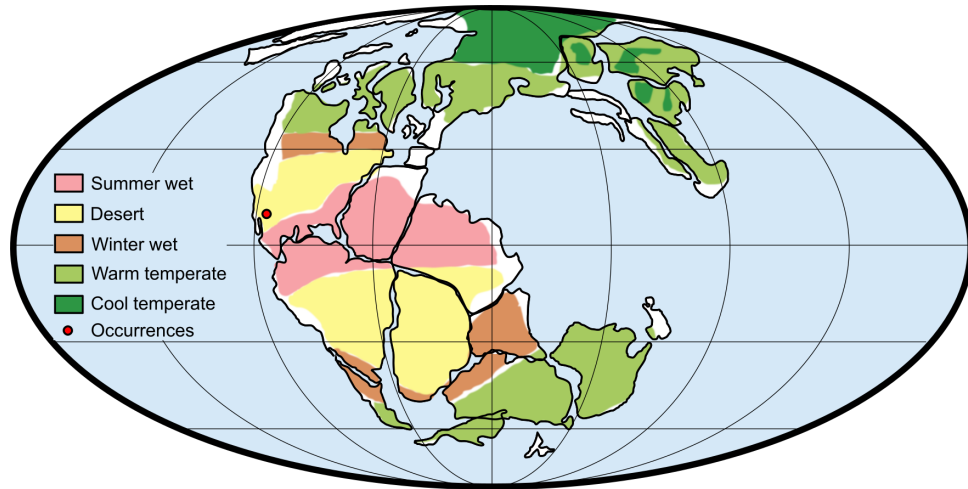
Table 1.1 summarises the climatic distribution of the Jurassic metasuchians according to their geographical distributions (Fig. 1.9). The diversity is very limited during both the Early and Middle Jurassic with respectively only one and five occurrences. The former is located under a desert climate while the latter are distributed under both ‘winter wet’ (n=3) and desert climate (n=2). The Late Jurassic includes more occurrences (n=31). Most of them are located under two climates: ‘winter wet’ (n = 14) and desert (n = 11). The rest of the occurrences are found in the warm temperate belt (n=4) and close to the equator, in the “summer wet’ belt (n=1). Because of the very few number of occurrences in the Early and Late Jurassic, the overall Jurassic climate distribution is very similar to that of the Late Jurassic. Nonetheless, during this period, metasuchians were never found in cool temperate climates.

Table 1.1: Number of metasuchian occurrences located in each climate category for the Lower, Middle and Upper Jurassic.

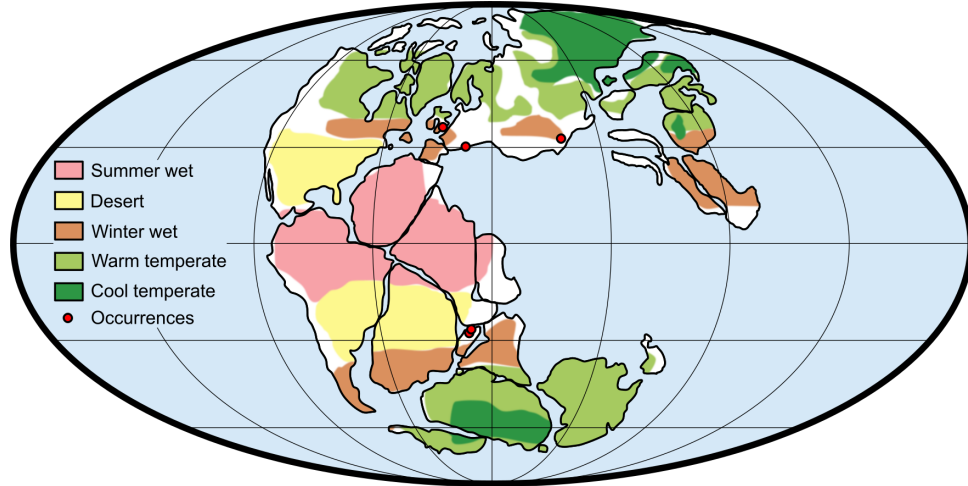
	Summer wet	Desert	Winter wet	Warm temperate	Cool temperate
Lower Jurassic	0	1	0	0	0
Middle Jurassic	0	2	3	0	0
Upper Jurassic	1	11	14	4	0
Total	1	14	17	4	0

1.5.3 *Cretaceous*

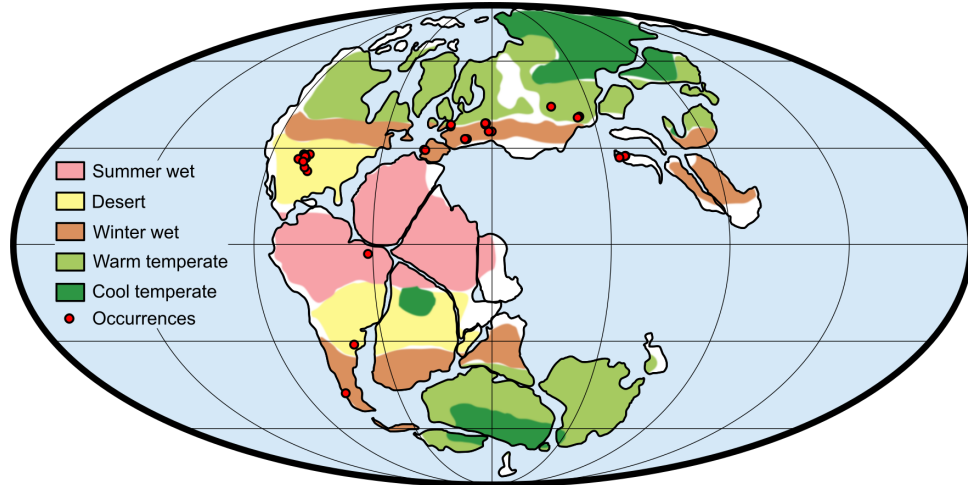
During the Cretaceous, the most frequent climate under which metasuchians lived was the warm humid temperate one (Table 1.2, Total). The second most frequent one is the arid climate, followed by the temperate one. The equatorial climate is the least frequent one. This contrasts with the extant diversity, for which this climate is the preferred one (Fig. 1.9b). This may be explained by the fact that the equatorial climatic belt is much more reduced during the Cretaceous than today. Indeed, this belt is even completely absent during the Aptian (Figure 1.10a). However, the number of ‘equatorial occurrences’ is the highest in the Albian, when this belt was thinnest, compared to the following Cretaceous stages (Fig. 1.10b). However, a large number of these occurrences during the Albian are located very close to the limit between the equatorial and arid palaeoclimatic zones. These limits as they are



(a) Lower Jurassic

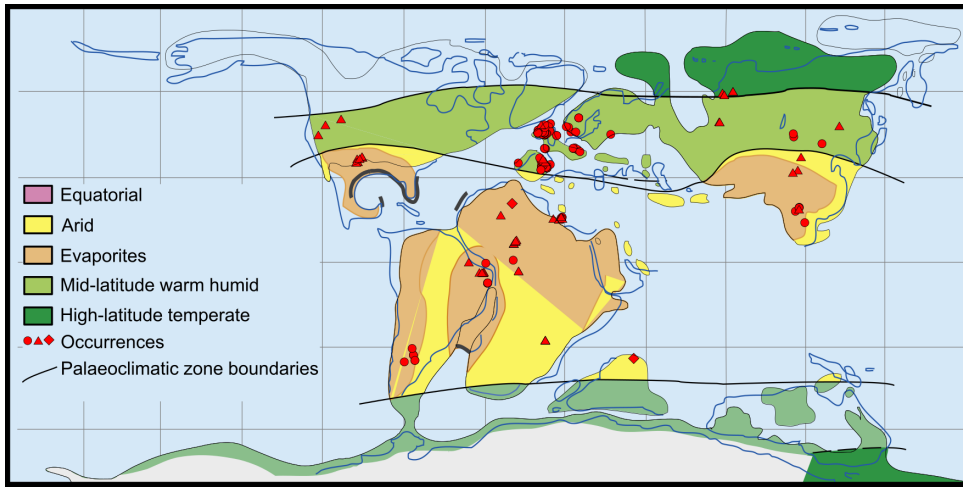


(b) Middle Jurassic

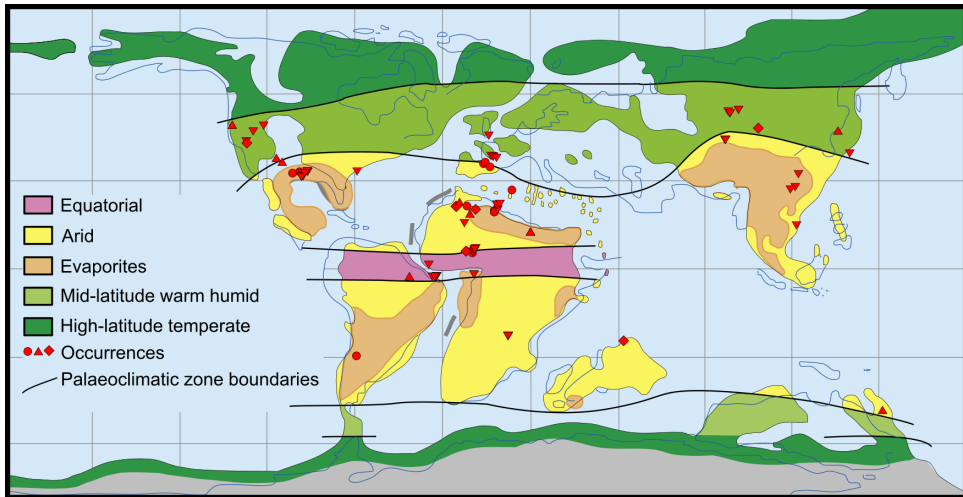


(c) Upper Jurassic

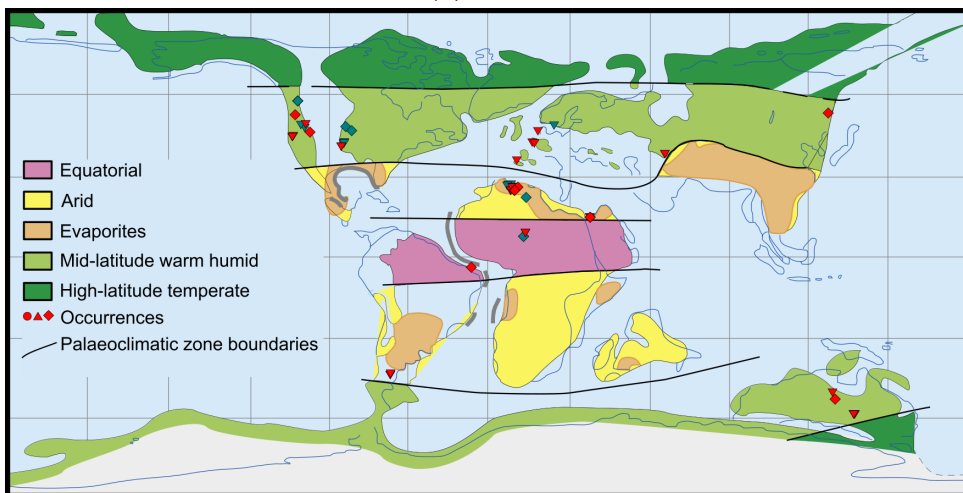
Figure 1.10: Geographic distribution of metasuchian occurrences and palaeoclimatic zones at the Lower (a), Middle (b) and Upper (c) Jurassic. Palaeomaps modified from Rees *et al.* (2000). See Introduction for details.



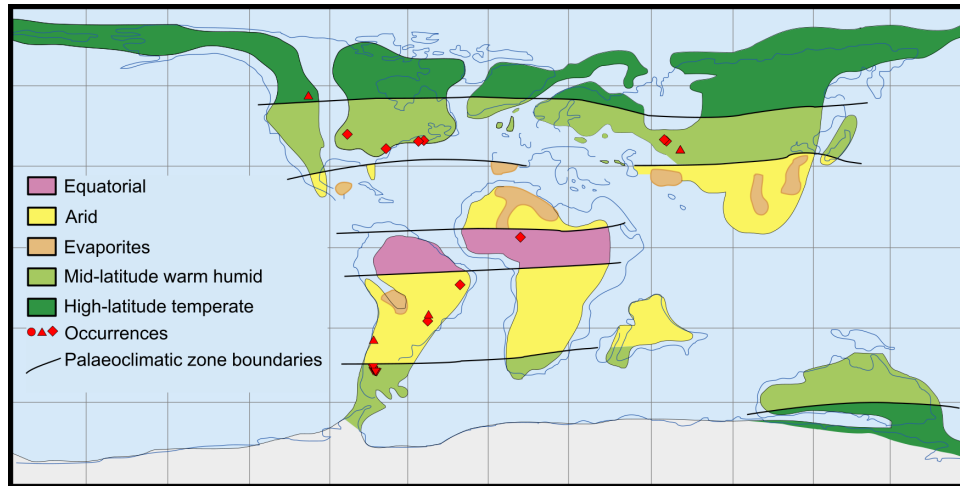
(a) Aptian



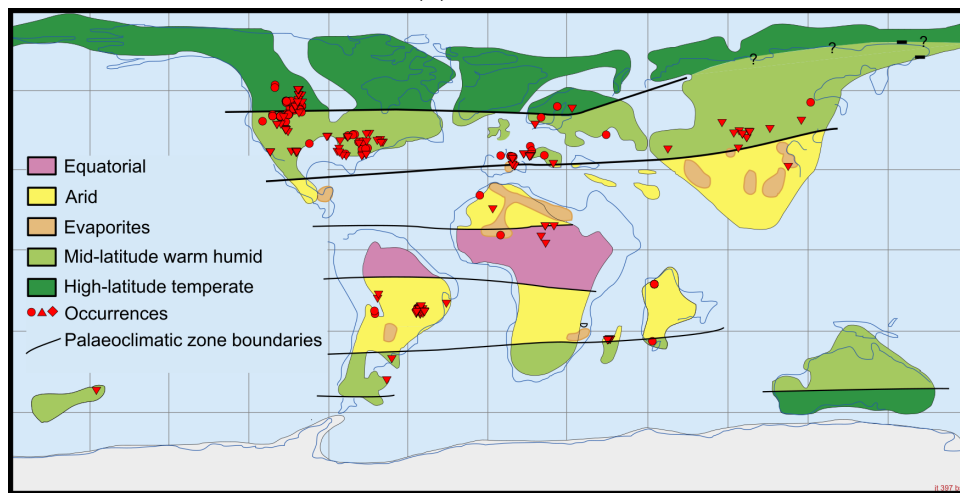
(b) Albian



(c) Cenomanian



(d) Santonian



(e) Maastrichtian

Figure 1.11: Geographic distribution of metasuchian occurrences and palaeoclimatic zones at the Aptian (a), Albian (b), Cenomanian (c) Santonian (d) and Maastrichtian (e). Palaeomaps modified from Chumakov *et al.* (1995). See Introduction for details.

represented on the palaeomaps are snapshots of boundaries that are known for changing regularly at more refined time scales. Milankovitch's cycles, for instance, are known to have a great effect on the earth's climate and they have common periods ranging from tens to hundreds of thousands of years. Some other climatic-related events, such as the OAE2 mentioned above, can occur in time frames of a few hundred thousand years as well. These high-frequency climatic cycles and changes, and eventually, the palaeogeographic shifting climatic boundaries they certainly implied, are out of the scope of commonly used palaeogeographic/palaeoclimatic maps, that at best, refer to geological stage resolution (e.g., the Albian lasted for 13 My). Therefore, caution is advised regarding the climatic inferences for occurrences located close to palaeoclimatic zone limits when using palaeogeographic/palaeoclimatic map

reconstructions. The Albian is also the only stage for which the warm-humid temperate climate is not the most frequent one regarding the locations of the occurrences. On the contrary, during the Albian, the arid climate is the one under which the occurrences are the most frequently situated. As for the equatorial occurrences, some occurrences located in the arid zone are close to the limit of the warm humid temperate palaeoclimatic zone; the same caution is thus advised here. Similarly, the Maastrichtian is the only stage where numerous occurrences are found within the temperate climatic belt (Fig. 1.10e), however, they all are located close to the limit of the warm humid temperate palaeoclimatic zone. Almost all of the occurrences located within this climatic belt for the whole Cretaceous come from this stage (Table 1.2, Total). From these palaeomaps can be drawn three main points: (1) very few extinct metasuchians lived under equatorial climates during the Cretaceous, contrary to extant ones; (2) proportionally, extinct Cretaceous metasuchians lived more frequently under arid climates than extant ones; and (3) the preferred climates for Cretaceous metasuchians are warm and humid, which matches the two main climatic drivers of the extant ones (humidity and temperature). Even though the third point is justified by the dominance of the warm-humid temperate climates, the first two points can temper it. Indeed, the near absence of occurrences located within the equatorial climatic belt shows that the high humidity was not as 'attractive' to Cretaceous metasuchians as it is for their extant counterparts. This is furthermore corroborated by the proportion of occurrences located within the arid climatic belts, proportionally much more important for Cretaceous metasuchians (Table 1.2, Total) than for extant ones (Fig. 1.9b). This may show that during the Cretaceous, humidity was not as much of a constraint to geographic distribution as it is today. The diversity in morphology and lifestyle could explain this. Indeed, modern metasuchians are all semi-aquatic, ambush predators. As such, water streams, lakes or ponds are necessary for them to inhabit an environment. Indeed, they not only depend on water to effectively ambush prey, but they also heavily rely on it for thermoregulation (Grigg & Kirshner, 2015; Grigg *et al.*, 2022). However, the diversity of extinct metasuchians includes fully terrestrial organisms like the Notosuchia. Multiple evidences have pointed out their ability to dig burrows and authors have suggested that they may have used this for thermoregulation (Gomani, 1997; Carvalho *et al.*, 2005; Vasconcellos & Carvalho, 2010). This would mean that they were less dependent on water and may have been able to wander off farther from them or inhabit environments with only temporary water places. This is the case, for instance, for the Anembalemba Member of the Maevarano Formation (Madagascar)

that has been interpreted as having been deposited under semiarid conditions with a strong seasonality alternating between long periods of droughts and mass flooding events (Krause *et al.*, 2010; Rogers *et al.*, 2013). On the other hand, the high number of occurrences located under an arid climate may be misleading. Indeed, extant metasuchians found under arid climatic conditions are most often associated with small habitats where water is permanently present (Brito *et al.*, 2011). Therefore, inhabiting an arid environment may not necessarily mean being less dependent on water places. Nonetheless, the fact that so few Cretaceous occurrences are located under an equatorial climate testifies that the metasuchians of this period had different climatic constraints than those of extant ones. However, the fine time-scale palaeoclimatic limits variations would need to be assessed to draw a definite answer.

Table 1.2: Number of metasuchian occurrences located in each climate category for the Aptian, Albian, Cenomanian, Santonian and Maastrichtian.

	Equatorial	Arid	Warm Humid	Temperate
Aptian	0	60	135	0
Albian	17	48	20	0
Cenomanian	5	25	38	0
Santonian	1	4	22	1
Maastrichtian	3	108	206	182
Total	26	245	421	183

1.5.4 *Cenozoic*

The Cenozoic occurrences are most frequently located under a warm temperate climate (40%, Table 1.3, Total, Figure 1.11). However, contrary to the Cretaceous, the second most frequent climate is not the arid one (20%) but the tropical one (36%). This result is highly driven by the distribution of Miocene occurrences. In fact, during the Paleocene to Oligocene, the arid climate is the second most represented one, after the warm temperate one. During these stages, the number of occurrences found under a tropical climate varies between 1 and 8 (Table 1.3). This contrasts with the 169 occurrences of the Miocene (Table 1.3). Most of the occurrences located in the arid climatic belt during the Paleocene to Oligocene correspond to dyrosaurids and sebecids. If the latter are terrestrial, the former are considered to be

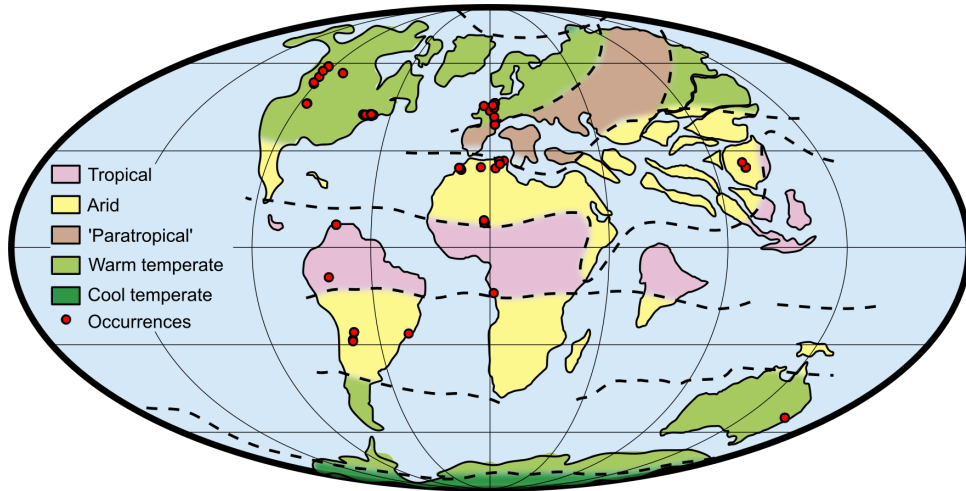
semi-aquatic (Andrade & Sayão, 2014). It is only during the Oligocene that the occurrences located under an arid climate correspond to eusuchians. This shows that regarding the Paleocene to Oligocene time period, differences in lifestyle (*i.e.* terrestrial *vs* semi-aquatic) do not explain the high proportion of metasuchians living under an arid climate. The rise in the number of ‘tropical occurrences’ during the Miocene may be linked to the establishment of large continental basins. Indeed, the formation of the Amazonian basin started during the Middle Miocene (Méndez-Camacho *et al.*, 2021) and it hosted a diverse community of crocodylians (Salas-Gismondi *et al.*, 2015). In the same way, the East African Rift started to open during the Miocene. The majority of ‘tropical occurrences’ were located in these areas during the Miocene (Fig. 1.11e). This would suggest that the main environmental constraint for metasuchians is the presence of water places rather than climatic variables.

Table 1.3: Number of metasuchian occurrences located in each climate category for the Paleocene, Early Eocene, Late Eocene, Oligocene and Miocene.

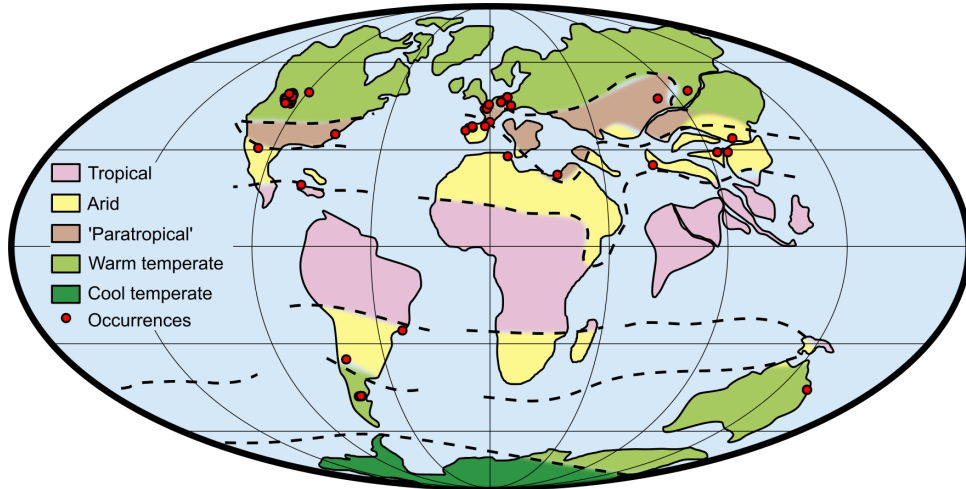
	Tropical	'Paratropical'	Arid	Warm temperate	Cool temperate
Paleocene	8	5	34	56	0
Early Eocene	1	7	19	52	0
Late Eocene	4	9	7	12	0
Oligocene	3	4	13	19	0
Miocene	169	0	30	66	0
Total	185	25	103	205	0

1.5.5 *Conclusions*

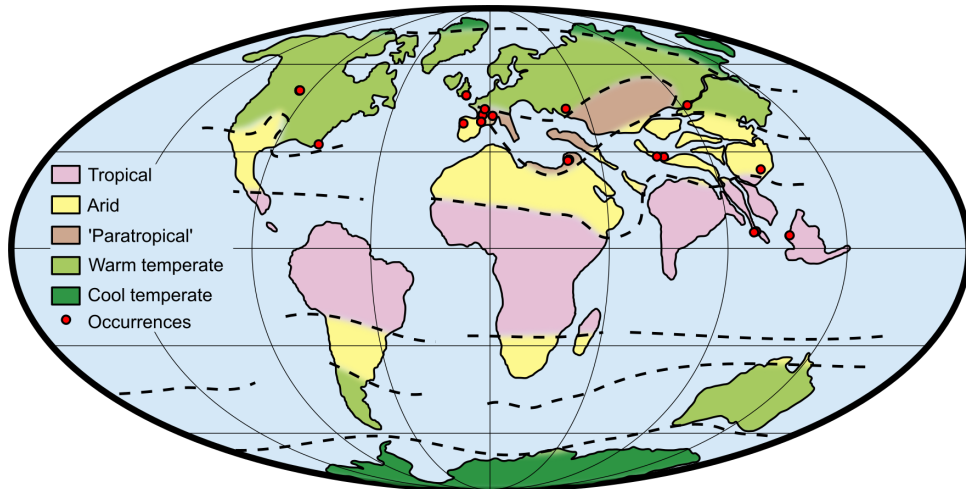
The climate classifications used by Rees *et al.* (2000), Chumakov *et al.* (1995) and Scotese (2005) do not perfectly fit with the Koeppen-Geiger one. Table 1.4 shows the correspondence of each with the five climatic types I distinguished in Figure 1.13. This figure illustrates the variations of the proportions in the climates under which metasuchian occurrences have been retrieved from the Early Jurassic to the present. As stated above, the very low record from the Early and Middle Jurassic renders the values for these time periods poorly representative. However, despite this issue, three patterns seem to emerge. First, the proportion of occurrences located under a tropical climate is very low before and rises after the



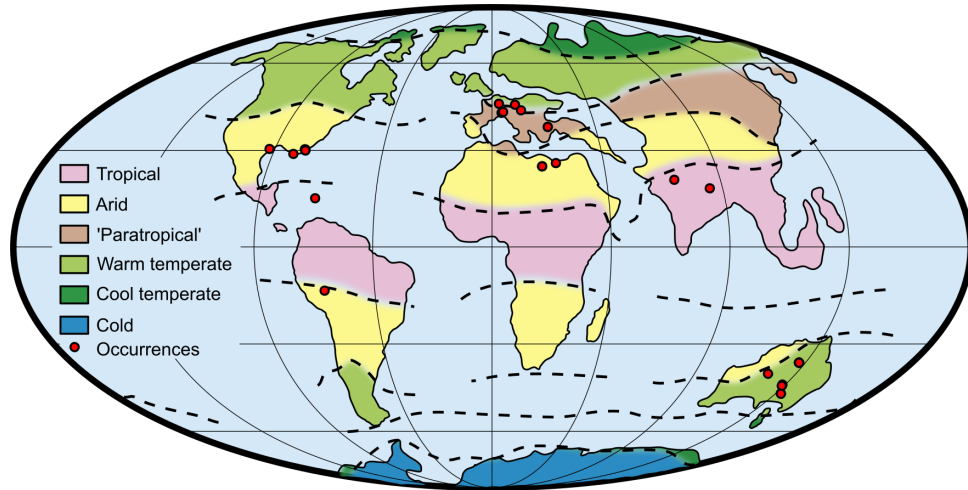
(a) Paleocene



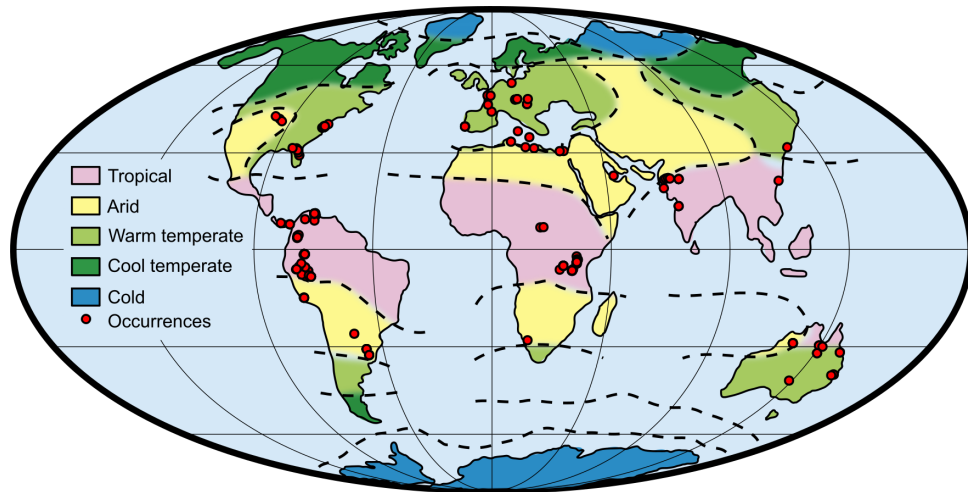
(b) Early Eocene



(c) Late Eocene



(d) Oligocene



(e) Miocene

Figure 1.12: Geographic distribution of metasuchian occurrences and palaeoclimatic zones at the Paleocene (a), Early Eocene (b), Late Eocene (c) Oligocene (d) and Miocene (e). Palaeomaps modified from Scotese (2005). See Introduction for details.

Maastrichtian. Second, the proportion of occurrences located under an arid climate follows an opposite curve, high in the past, and decreasing toward the present. Third, the proportion of extinct occurrences located under a warm temperate climate is almost always the highest and only crosses the curve of ‘tropical occurrences’ during the Oligocene. Two geological stages stand out in front of these patterns. First, the Albian during which the proportion of ‘tropical occurrences’ rises to 20%. This rise in ‘tropical occurrences’ is matched with a corresponding strong decrease in ‘warm temperate’ ones. Second, the Maastrichtian stage is the only time interval where the proportion of ‘cool temperate occurrences’ is high (36%). This rise is also matched with a decrease in ‘warm temperate occurrences’. However, as discussed above, these ‘outliers’ might result from more refined time-scale palaeoclimatic zone limit vari-

ations. Anyhow, the reasons behind those trends are out of the scope of this PhD. Still, they show that during their evolutionary history, metasuchians explored multiple biomes and thrived under different ones than their extant counterparts. Furthermore, the climatic preferences seem to vary depending on the taxa under consideration. Indeed, the Cretaceous metasuchian diversity is characterised by a high number of notosuchian species whereas they are rare during the Cenozoic. This might explain, at least partly, the differences in climate preferences. Multiple studies have focused on the impact of climatic variables on the biodiversity and different body variables of Metasuchia or of more or less inclusive nodes (e.g. Martin *et al.*, 2014; Mannion *et al.*, 2015; Godoy *et al.*, 2019; Stockdale & Benton, 2021). However, the changes in climate preferences throughout time, as well as the variations in metasuchians subgroups with different climatic tolerances make it complicated to draw general rules regarding the climatic constraints of the whole group. This highlights the need for more precise studies: because of the variations in the relationship to the environment of the group through time and between subgroups, studies focused on the diversification/extinction patterns should be restricted to specific subgroups, during particular time intervals (Bronzati *et al.*, 2015).

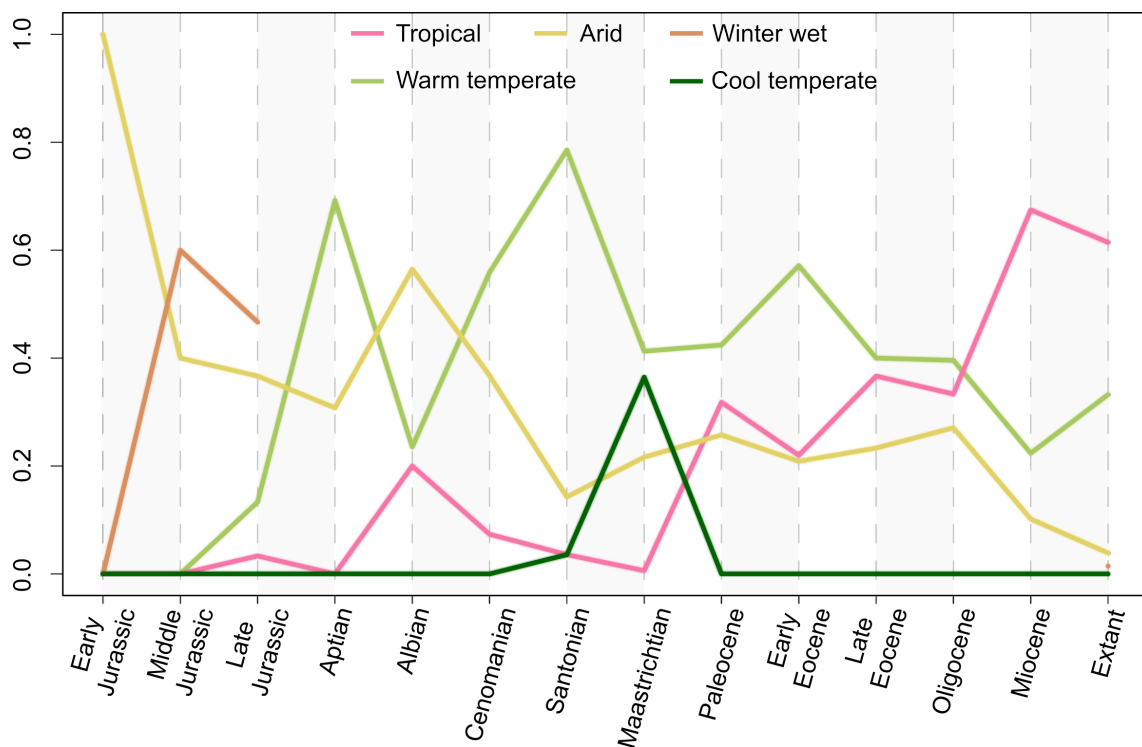


Figure 1.13: Climate distribution in metasuchian occurrences from the Lower Jurassic to the present time. See main text for details.

Table 1.4: Correspondences between the climate classifications from the sources used for the Palaeomaps with the classification used in Figure 1.13.

Rees <i>et al.</i> (1999)	Chumakov <i>et al.</i> (1995)	Scotese (2005)	Koeppen-Geiger	Fig. 1.13
Summer wet	Equatorial	Tropical 'Paratropical'	Aw	Tropical
Desert	Arid	Arid	BSh, BSk, BWh	Arid
Winter wet	-	-	As	Winter wet
Warm temperate	Mid-latitude warm humid	Warm temperate	Cfa, Cfb, Csa, Csb, Cwa, Cwb	Warm temperate
Cool temperate	High-latitude temperate	Cool Temperate	Dfa	Cool temperate

1.6 Further Considerations Regarding the Climatic Drivers of Notosuchian Diversification

As an example of more focused studies linking metasuchian subgroups distribution through time and at particular time intervals, the Notosuchia seems to be marked by two episodes of diversification. First, during the Barremian-Aptian, during which the group appears (discarding *Rukwasuchus saklavae*) with the first representatives of Ziphosuchia, Uruguaysuchidae and Peirosauridae (Figure 1.14a, blue lines). The second one was during the Coniacian-Santonian where Ziphosuchia radiated with the sudden and intense diversification of the Sphagesauria and the apparition of Sebecosuchia (Fig. 1.14a). Interestingly, both of these diversification episodes occur during arid and cool or cooling time periods, associated with marine regressions (Fig. 1.14b, after Price, 1999 in Deconinck, 2006). This suggests that aridity and low temperature might have been the main drivers of notosuchian diversification. This corroborates part of the climatic preferences described in Chapter 1, Part 3. Indeed, both the Aptian and the Santonian are followed by an increase in the proportion of metasuchian fossils found under arid palaeoclimates (Fig. 1.13). On the other hand, the warmest and most humid period of the Cretaceous, during the Cenomanian is marked by a strong decrease in the proportion of occurrences located under arid climates (Fig. 1.13). This link between aridity and diversification had already been noted for the Cretaceous terrestrial Crocodyliformes by Carvalho *et al.* (2010), based on palaeomaps. Solorzano *et al.* (2020) proposed that crocodylian diversification was positively linked to the size of the warm temperate climatic belt. This might also be the case for Notosuchia as the two diversification events suggested by our data occur at time periods during which the number of ‘warm temperate’ metasuchian occurrences peaked (Fig. 1.13). They also proposed that the speciation rate slows down when the diversity is high. This also matches the results from the diversity curve where both diversification (Fig. 1.3, K3 to K4 and K8 to Pg1) are followed by a relative stasis. Studying notosuchian diversification would allow us to assess whether the climatic drivers suggested for Crocodylia also drive the diversity of this group composed of organisms radically different from their extant relatives. To investigate further these relationships between diversity variations and climatic variables, we started a collaboration with a climate modeller from the Institut de Physique du Globe de Paris (IPGP), F. Fluteau. This project is aimed at characterizing the climate with a high spatial resolution (3.6° in longitude, 1.8° in latitude) during chosen Cretaceous stages to

assess the precise climate in which notosuchians lived. We chose to focus on the Aptian, Cenomanian and Santonian. By doing so, we will be able to assess the climatic variations between two cool and dry stages (Aptian and Santonian) with a warm and humid one in between (Cenomanian). First, this will allow us to correlate diversity patterns with local climatic variables, and not global ones. Second, this will provide us with insights regarding the magnitude of latitudinal variations of the palaeoclimatic zone limits (see Chapter 1, Part 3). Unfortunately, the palaeoclimatic models need to run for a long time before reaching an equilibrium and due to the availability of the supercomputer, it was not possible to complete those tests before the final writing of this manuscript.

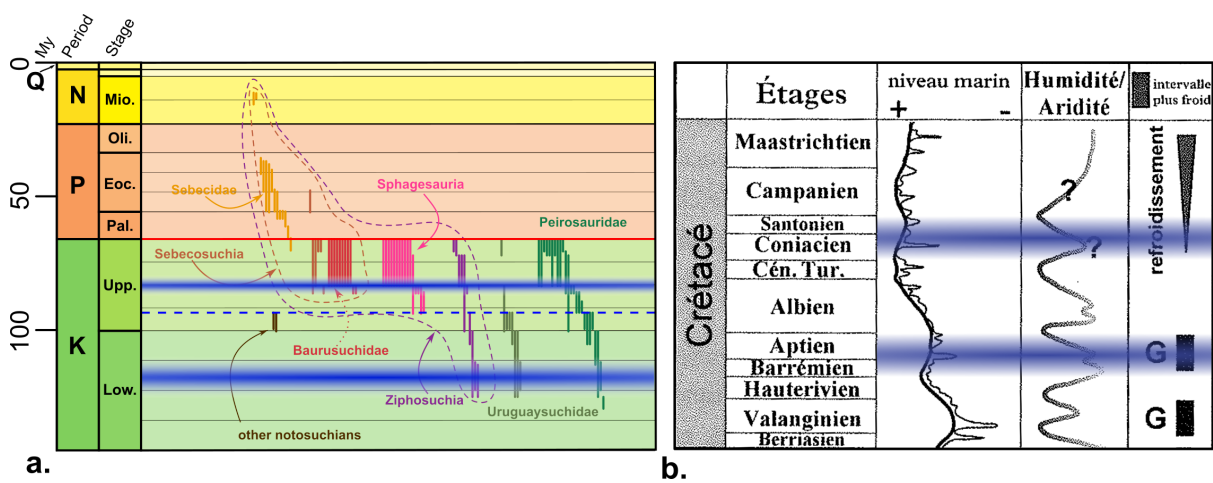


Figure 1.14: a) Stratigraphic distribution of Notosuchia. b) Variations of the eustatic level, aridity and temperature during the Cretaceous, after Price, 1999.

1.7 Chapter Conclusions

In this chapter, we reviewed the stratigraphy of Metasuchia. They appeared during the Jurassic, though their diversity at that time was low, mostly reduced to Atoposauridae and Goniopholididae. The Cretaceous seems to have been the ‘golden age’ of the group. This is especially true for the Upper Cretaceous, during which the major groups of both Neosuchia and Notosuchia radiated with the diversification of Crocodylia and Ziphosuchia, respectively. However, this Upper Cretaceous diversity is mostly represented by singleton species, thus impairing its precise assessment. The Palaeogene and Neogene may be seen as a transition from this ‘Cretaceous diversity’ to the modern one. Non-crocodylian metasuchians still existed throughout the Palaeogene. However, their diversity steadily decreased during that time so at the Neogene, almost all of it had disappeared. Finally, it is only during the Pliocene and the Quaternary that the structure of the diversity of Crocodylia began to match that of the present time, with a recent radiation of Crocodyloidea and a decrease of both Alligatoidea and Gavialoidea. During its evolutionary history, Metasuchia encountered two major crises that impacted its diversity: the OAE 2 and the K-Pg crisis. However, the group reacted differently to each one. Indeed the former seems to have had a strong negative impact on almost all metasuchian groups, except the Peirosauridae. On the other hand, the impact of the K-Pg crisis differed greatly depending on the groups. Crocodylia was only slightly affected by it. For Dyrosauroidae, this crisis was followed by an intense diversification. Finally, its impact on Notosuchia was dramatic as the whole group except Sebecidae became extinct. This shows that the impact of global biological crises not only varies greatly between the groups, but also between the crises as this variability between groups is great for the K-Pg crisis, but seems rather low for the OAE 2.

We also reviewed the depositional environments in which metasuchian remains have been found. From these results, it seems that throughout their history, Metasuchia remained a predominantly continental group with $\sim 70\%$ of the fossil species found in freshwater, mostly fluvial deposits and only $\sim 30\%$ in marine ones. The fact the terrestrial deposits are almost not represented results both from the facts that these environments have very low sedimentation rates compared to that of fluvial environments and that terrestrial metasuchians lived near water places. As a result, most of them are found in freshwater fluvial deposits, like semi-aquatic metasuchians. Similarly, these results do not imply that 30% of the species from the dataset used were marine. Indeed, most of these occurrences fell into the ‘coastal’

category which includes a variety of environments with a large range of salinity. However, these results show that freshwater fluviatile environments were the pivoting ones for the metasuchians throughout their evolutionary history. In that sense, Metasuchia has remained stable until modern times.

Finally, we also reviewed the climatic preferences of the group throughout its history. We showed that these preferences, contrary to the depositional environments, varied through time. Today, most metasuchians thrive under a tropical climate, but this has not always been the case. Indeed, the number of fossil occurrences located under such a climate was low during the Jurassic and Cretaceous. It only started to increase after the Maastrichtian and did so throughout the Palaeogene and Neogene. This is matched by the opposite evolution of the number of occurrences found under an arid climate. This number steadily decreased throughout the Cretaceous and the Cenozoic. Values for the Jurassic are also very high, however, this is biased by the very low number of occurrences. On the other hand, the number of occurrences located under a warm temperate climate got high during the Cretaceous and remained so until modern times, despite high variations. Modern climatic preferences led us to infer that the main climatic drivers for extant metasuchians were humidity and temperature. Past ones suggest that humidity may not have been a strong driver since the beginning of the group's history. These results rely on the palaeolocations of the occurrences and the palaeoclimatic zone limits. However, we pointed out that because climate variations often occur at higher frequency time scales than the geological stage one, the approach may lead to wrong climatic attribution, especially regarding occurrences located close to palaeoclimatic zone limits. This may, for instance, explain why both the Albian and Maastrichtian stand out in front of the trends discussed above. But it also tempers the confidence we may have regarding these trends.

To summarize, Metasuchia as it is known today is poorly representative of its past diversity. Taxonomically speaking, it is only a fraction of the past as only the nested clade Crocodylia has survived until now. This is also true ecologically and morphologically speaking: all present-day species share a similar shape and inhabit similar environments. The more marine and fully terrestrial ones became fully extinct during the Cenozoic and with them most of the morphological diversity of the group. This loss in ecological diversity translates into variation regarding climatic preferences. Despite those of Crocodylia probably having been consistent throughout time, this was not the case at the scale of the whole group. Thus, the fact that the climatic preferences of extant metasuchians were set up during the Cenozoic is

probably due to the extinction of non-crocodylian metasuchians during this time, and with them their climatic preferences. The depositional environments study, on the other hand, shows that the dependence of the group on freshwater places remained stable throughout their history. Despite the existence of a significant amount of terrestrial and marine species, Metasuchia is and has consistently been a group associated with these environments.

1.8 References

Adams T.L. 2013. A new neosuchian crocodyliform from the Lower Cretaceous (late Aptian) Twin Mountains Formation of North-Central Texas. *Journal of Vertebrate Paleontology*. 33:85–101.

Adams T.L., Noto C.R., Drumheller S. 2017. A large neosuchian crocodyliform from the Upper Cretaceous (Cenomanian) Woodbine Formation of North Texas. *Journal of Vertebrate Paleontology*. 37:e1349776.

Alroy J. 2010. The Shifting Balance of Diversity Among Major Marine Animal Groups. *Science*. 329:1191–1194.

Andrade R.C.L.P. de, Sayão J.M. 2014. Paleohistology and Lifestyle Inferences of a Dyrosaurid (Archosauria: Crocodylomorpha) from Paraíba Basin (Northeastern Brazil). *PLoS ONE*. 9:e102189.

Aubier P., Jouve S., Schnyder J., Cubo J. 2023. Phylogenetic structure of the extinction and biotic factors explaining differential survival of terrestrial notosuchians at the Cretaceous–Palaeogene crisis. *Palaeontology*. 66.

Ballell A., Moon B.C., Porro L.B., Benton M.J., Rayfield E.J. 2019. Convergence and functional evolution of longirostry in crocodylomorphs. *Palaeontology*. 62:867–887.

Basilici G., Bo P.F.D., de Oliveira E.F. 2016. Distribution of palaeosols and deposits in the temporal evolution of a semiarid fluvial distributary system (Bauru Group, Upper Cretaceous, SE Brazil). *Sedimentary Geology*. 341:245–264.

Batezelli A., Ladeira F.S.B., Nascimento D.L.D., Da Silva M.L. 2019. Facies and palaeosol analysis in a progradational distributive fluvial system from the Campanian-Maastrichtian Bauru Group, Brazil. *Sedimentology*. 66:699–735.

Becker O.S. code by R.A., Minka A.R.W.R. version by R.B.E. by T.P., Deckmyn A. 2021. maps: Draw Geographical Maps.

Behrensmeyer A.K. 1975. The taphonomy and paleoecology of Plio-Pleistocene vertebrate assemblages east of Lake Rudolf, Kenya. *Bulletin of the Museum of Comparative Zoology at Harvard College*. 146:473–578.

Belloso E. 2010. Loessic and fluvial sedimentation in Sarmiento Formation pyroclastics, middle Cenozoic of central Patagonia. p. 278–292.

Benton M.J., Clark J.M. 1988. Archosaur phylogeny and the relationships of the Crocodylia. In: Benton M., editor. Amphibians, Reptiles, Birds. Oxford: Clarendon Press. p. 295–338.

Brito J.C., Martínez-Freiría F., Sierra P., Sillero N., Tarroso P. 2011. Crocodiles in the Sahara Desert: An Update of Distribution, Habitats and Population Status for Conservation Planning in Mauritania. PLoS ONE. 6:e14734.

Brochu C.A. 1997a. A review of “*Leidyosuchus*” (Crocodyliformes, Eusuchia) from the Cretaceous through Eocene of North America. Journal of Vertebrate Paleontology. 17:679–697.

Brochu C.A. 1997b. Morphology, Fossils, Divergence Timing, and the Phylogenetic Relationships of *Gavialis*. Systematic Biology. 46:479–522.

Brochu C.A. 1999. Phylogenetics, Taxonomy, and Historical Biogeography of Alligatoroidea. Journal of Vertebrate Paleontology. 19:9–100.

Brochu C.A. 2001. Crocodylian Snouts in Space and Time: Phylogenetic Approaches Toward Adaptive Radiation. Am Zool. 41:564–585.

Brochu C.A., Sumrall C.D. 2020. Modern cryptic species and crocodylian diversity in the fossil record. Zoological Journal of the Linnean Society. 189:700–711.

Bronzati M., Montefeltro F.C., Langer M.C. 2015. Diversification events and the effects of mass extinctions on Crocodyliformes evolutionary history. R. Soc. open sci. 2:140385.

Bryant C., Wheeler N.R., Rubel F., French R.H. 2017. kgc: Koeppen-Geiger Climatic Zones.

Buckley G.A., Brochu C.A. 1999. An enigmatic new crocodile from the Upper Cretaceous of Madagascar. Cretaceous Fossil Vertebrates. 60:149–175.

Buckley G.A., Brochu C.A., Krause D.W., Pol D. 2000. A pug-nosed crocodyliform from the Late Cretaceous of Madagascar. Nature. 405:941–944.

Buffetaut E. 1989. A New ziphodont mesosuchian crocodile from the Eocene of Algeria. *Paleontologica Abt.* 208.

Buffetaut E., Marshall L.G. 1991. A new crocodylian, *Sebecus querejazus*, nov. sp. (Mesosuchia, Sebecidae) from the Santa Lucia Formation (early Paleocene) at Vila Vila, southcentral Bolivia. *Fósiles y Facies de Bolivia, Vertebrados*. Santa Cruz: Revista Técnica de YPF. p. 545–557.

Carvalho I. de S., Arruda Campos A. de C., Nobre P.H. 2005. *Baurusuchus salgadoensis*, a New Crocodylomorpha from the Bauru Basin (Cretaceous), Brazil. *Gondwana Research*. 8:11–30.

Carvalho I. de S., de Gasparini Z.B., Salgado L., de Vasconcellos F.M., Marinho T. da S. 2010. Climate's role in the distribution of the Cretaceous terrestrial Crocodyliformes throughout Gondwana. *Palaeogeography, Palaeoclimatology, Palaeoecology*. 297:252–262.

Celis A.D., Narváez I., Ortega F. 2020. Spatiotemporal palaeodiversity patterns of modern crocodiles (Crocodyliformes: Eusuchia). *Zoological Journal of the Linnean Society*. 189:635–656.

Chumakov N.M., Zharkov M.A., Herman A.B., Doludenko M.P., Kalandadze N.N., Lebedev E.L., Ponomarenko A.G., Rautian A.S. 1995. Climatic Belts of the Mid-Cretaceous Time. *Stratigraphy, Stratigraphy and Geological Correlation*. 3:42–63.

Clark J.M. 1994. Patterns of Evolution in Mesozoic Crocodyliformes. In: Fraser N.C., Sues H.-D., editors. *In the Shadow of the Dinosaurs*. Cambridge: Harvard University Press. p. 83–97.

Cohen A.S. 1982. Paleoenvironments of Root Casts from the Koobi Fora Formation, Kenya. *SEPM JSR*. 52:401–414.

Dal Sasso C., Pasini G., Fleury G., Maganuco S. 2017. *Razanandrongobe sakalavae*, a gigantic mesoeucrocodylian from the Middle Jurassic of Madagascar, is the oldest known notosuchian. *PeerJ*. 5:e3481.

Deconinck J.F. 2006. Paléoclimats, l'enregistrement des variations climatiques. *Vuibert*.

Deconinck J.F., Blanc-Valleron M.M., Rouchy J.M., Camoin G., Badaut-Trauth D. 2000. Palaeoenvironmental and diagenetic control of the mineralogy of Upper Cretaceous–Lower Tertiary deposits of the Central Palaeo–Andean basin of Bolivia (Potosi area). *Sedimentary Geology*. 132:263–278.

Densmore L.D. 1983. Biochemical and Immunological Systematics of the Order Crocodylia. In: Hecht M.K., Wallace B., Prance G.T., editors. *Evolutionary Biology*. Boston, MA: Springer US. p. 397–465.

Densmore L.D., Owen R.D. 1989. Molecular Systematics of the Order Crocodylia. *Am Zool.* 29:831-841.

Fernandes L.A., Ribeiro C.M.M. 2015. Evolution and palaeoenvironment of the Bauru Basin (Upper Cretaceous, Brazil). *Journal of South American Earth Sciences.* 61:71–90.

Foret T., Aubier P., Jouve S., Cubo J. *Accepted (Paleobiology)*. Biotic and abiotic factors and the phylogenetic structure of extinction in the evolution of Tethyuchia.

Gasparini Z. 1971. Los Notosuchia des Cretacico de America del sur como un nuevo infraorden de los Mesosuchia (Crocodylia). *Ameghiniana.* 8:83–103.

Gatesy J., Amato G., Norell M. 2003. Combined Support for Wholesale Taxic Atavism in Gavialine Crocodylians. *Systematic Biology.* 52.

Geroto C.F.C., Bertini R.J. 2019. New material of *Pepesuchus* (Crocodyliformes; Mesoeucrocodylia) from the Bauru Group: implications about its phylogeny and the age of the Adamantina Formation. *Zoological Journal of the Linnean Society.* 185:312–334.

Godoy P.L., Benson R.B.J., Bronzati M., Butler R.J. 2019. The multi-peak adaptive landscape of crocodylomorph body size evolution. *BMC Evol Biol.* 19:167.

Godoy P.L., Bronzati M., Eltink E., Marsola J.C. de A., Cidade G.M., Langer M.C., Montefeltro F.C. 2016. Postcranial anatomy of *Pissarrachampsia sera* (Crocodyliformes, Baurusuchidae) from the Late Cretaceous of Brazil: insights on lifestyle and phylogenetic significance. *PeerJ.* 4:e2075.

Gomani E.M. 1997. A crocodyliform from the Early Cretaceous Dinosaur Beds, northern Malawi. *Journal of Vertebrate Paleontology.* 17:280–294.

Grigg G., Kirshner D. 2015. *Biology and Evolution of Crocodylians*. Melbourne: CSIRO Publishing.

Grigg G., Nowack J., Bicudo J.E.P.W., Bal N.C., Woodward H.N., Seymour R.S. 2022. Whole-body endothermy: ancient, homologous and widespread among the ancestors of mammals, birds and crocodylians. *Biological Reviews*. 97:766–801.

Harshman J., Huddleston C.J., Bollback J.P., Parsons T.J., Braun M.J. 2003. True and False Gharials: A Nuclear Gene Phylogeny of Crocodylia. *Systematic Biology*. 52:386–402.

Hastings A.K., Bloch J.I., Jaramillo C.A. 2015. A new blunt-snouted dyrosaurid, *Anthracosuchus balrogus* gen. et sp. nov. (Crocodylomorpha, Mesoeucrocodylia), from the Palaeocene of Colombia. *Historical Biology*. 27:998–1020.

Hay W.W., Floegel S. 2012. New thoughts about the Cretaceous climate and oceans. *Earth-Science Reviews*. 115:262–272.

Hayward J.L., Dickson K.M., Gamble S.R., Owen A.W., Owen K.C. 2011. Eggshell taphonomy: environmental effects on fragment orientation. *Historical Biology*. 23:5–13.

Jouve S. 2009. The skull of *Teleosaurus cadomensis* (Crocodylomorpha; Thalattosuchia), and phylogenetic analysis of Thalattosuchia. *Journal of Vertebrate Paleontology*. 29:88–102.

Jouve S. 2021. Differential diversification through the K-Pg boundary, and post-crisis opportunism in longirostrine crocodyliforms. *Gondwana Research*. 99:110–130.

Jouve S., Bardet N., Jalil N.-E., Suberbiola X.P., Bouya B., Amaghazaz M. 2008. The oldest African crocodylian: phylogeny, paleobiogeography, and differential survivorship of marine reptiles through the Cretaceous-Tertiary boundary. *Journal of Vertebrate Paleontology*. 28:409–421.

Jouve S., Bouya B., Amaghazaz M., Meslouh S. 2015. *Maroccosuchus zennaroi* (Crocodylia: Tomistominae) from the Eocene of Morocco: phylogenetic and palaeobiogeographical implications of the basalmost tomistomine. *Journal of Systematic Palaeontology*. 13:421–445.

Jouve S., Iarochène M., Bouya B., Amaghazaz M. 2006. A new species of *Dyrosaurus* (Crocodylomorpha, Dyrosauridae) from the early Eocene of Morocco: phylogenetic implications. *Zoological Journal of the Linnean Society*. 148:603–656.

- Kidwell S.M., Flessa K.W. 1995. The quality of the fossil record: populations, species, and communities. *Annual Review of Ecology and Systematics*. 26:269–299.
- Kley N.J., Sertich J.J.W., Turner A.H., Krause D.W., O'Connor P.M., Georgi J.A. 2010. Craniofacial morphology of *Simosuchus clarki* (Crocodyliformes: Notosuchia) from the Late Cretaceous of Madagascar. *Journal of Vertebrate Paleontology*. 30:13–98.
- Kottek M., Grieser J., Beck C., Rudolf B., Rubel F. 2006. World Map of the Köppen-Geiger climate classification updated. *metz*. 15:259–263.
- Krause D.W., Sertich J.J.W., Rogers R.R., Kast S.C., Rasoamiaramanana A.H., Buckley G.A. 2010. Overview of the discovery, distribution, and geological context of *Simosuchus clarki* (Crocodyliformes: Notosuchia) from the Late Cretaceous of Madagascar. *Journal of Vertebrate Paleontology*. 30:4–12.
- Langston W. 1965. Fossil crocodylians from Colombia and the Cenozoic history of the Crocodylia in South America. University of California Press.
- Larsson H.C.E., Sues H.-D. 2007. Cranial osteology and phylogenetic relationships of *Hamadasuchus rebouli* (Crocodyliformes: Mesoeucrocodylia) from the Cretaceous of Morocco. *Zoological Journal of the Linnean Society*. 149:533–567.
- Lee M.S.Y., Yates A.M. 2018. Tip-dating and homoplasy: reconciling the shallow molecular divergences of modern gharials with their long fossil record. *Proc. R. Soc. B*. 285:20181071.
- Lenz O.K., Wilde V., Riegel W. 2007. Recolonization of a Middle Eocene volcanic site: quantitative palynology of the initial phase of the maar lake of Messel (Germany). *Review of Palaeobotany and Palynology*. 145:217–242.
- Lortet L.C.E. 1892. Les reptiles fossiles du bassin du Rhône. *mhnly*. 5:3–63.
- Lydekker R. 1886. Indian tertiary and post-tertiary vertebrata: Siwalik Crocodylia, Lactertilia, & Ophidia. *Paleontologica Indica*. 3:209–240.
- Maganuco S., Dal Sasso C., Pasini G. 2006. A new large predatory archosaur from the Middle Jurassic (Bathonian) of Madagascar. *Atti della Società Italiana di Scienze Naturali e del Museo Civico di Storia Naturale di Milano*. 147:19–51.

Mannion P.D., Benson R.B.J., Carrano M.T., Tennant J.P., Judd J., Butler R.J. 2015. Climate constrains the evolutionary history and biodiversity of crocodylians. *Nat Commun.* 6:8438.

Markwick P.J. 1998. Crocodylian diversity in space and time: the role of climate in paleoecology and its implication for understanding K/T extinctions. *Paleobiology.* 24:470–497.

Martin J.E., Amiot R., Lécuyer C., Benton M.J. 2014. Sea surface temperature contributes to marine crocodylomorph evolution. *Nat Commun.* 5:4658.

Massicotte P., South A. 2023. *rnaturalearth: World Map Data from Natural Earth.*

Meade R.H., Yuzyk T.R., Day T.J. 1990. Movement and storage of sediment in rivers of the United States and Canada. In: Wolman M.G., Riggs H.C., editors. *Surface Water Hydrology.* U.S.A: Geological Society of America. p. 255–280.

Melstrom K.M., Irmis R.B. 2019. Repeated Evolution of Herbivorous Crocodyliforms during the Age of Dinosaurs. *Current Biology.* 29:2389-2395.e3.

Méndez-Camacho K., Leon-Alvarado O., Miranda-Esquivel D.R. 2021. Biogeographic evidence supports the Old Amazon hypothesis for the formation of the Amazon fluvial system. *PeerJ.* 9:e12533.

Meyer E.R. 1984. Crocodylians as Living Fossils. In: Eldredge N., Stanley S.M., editors. *Living Fossils.* New York, NY: Springer New York. p. 105–131.

Montefeltro F.C., Larsson H.C.E., de França M.A.G., Langer M.C. 2013. A new neosuchian with Asian affinities from the Jurassic of northeastern Brazil. *Naturwissenschaften.* 100:835–841.

Montefeltro F.C., Larsson H.C.E., Langer M.C. 2011. A New Baurusuchid (Crocodyliformes, Mesoeucrocodylia) from the Late Cretaceous of Brazil and the Phylogeny of Baurusuchidae. *PLoS ONE.* 6:e21916.

Moshayedi M., Lenz O.K., Wilde V., Hinderer M. 2020. The recolonisation of volcanically disturbed Eocene habitats of Central Europe: the maar lakes of Messel and Offenthal (SW Germany) compared. *Palaeobio Palaeoenv.* 100:951–973.

Nascimento P.M., Zaher H. 2010. A new species of *Baurusuchus* (Crocodyliformes, Mesoeucrocodylia) from the Upper Cretaceous of Brazil, with the first complete postcranial skeleton described for the family Baurusuchidae. *Pap. Avulsos Zool. (São Paulo)*. 50:323–361.

Nesbitt S.J. 2011. The Early Evolution of Archosaurs: Relationships and the Origin of Major Clades. *Bulletin of the American Museum of Natural History*. 352:1–292.

Norell M.A. 1989. The Higher Level Relationships of the Extant Crocodylia. *Journal of Herpetology*. 23:325.

Oaks J.R. 2011. A time-calibrated species tree of Crocodylia reveals a recent radiation of the true crocodiles. *Evolution*. 65:3285–3297.

Owen R. 1884. *A History of British Fossil Reptiles*. London: Cassell & Company Ltd.

Pan T., Miao J.-S., Zhang H.-B., Yan P., Lee P.-S., Jiang X.-Y., Ouyang J.-H., Deng Y.-P., Zhang B.-W., Wu X.-B. 2021. Near-complete phylogeny of extant Crocodylia (Reptilia) using mitogenome-based data. *Zoological Journal of the Linnean Society*. 191:1075–1089.

Paolillo A., Linares O.J. 2007. Nuevos cocodrilos Sebecosuchia del Cenozoico sudamericano (Mesosuchia: Crocodylia). *Paleobiologia Neotropical*. 3:1–25.

Pebesma E. 2018. Simple Features for R: Standardized Support for Spatial Vector Data. *The R Journal*. 10:439–446.

Pinheiro A.E., Pereira P.V.L.G. da C., de Souza R.G., Brum A.S., Lopes R.T., Machado A.S., Bergqvist L.P., Simbras F.M. 2018. Reassessment of the enigmatic crocodyliform “*Goniopholis paulistanus* Roxo, 1936: Historical approach, systematic, and description by new materials. *PLoS ONE*. 13:e0199984.

Pinheiro A.E.P., Souza L.G.D., Bandeira K.L.N., Brum A.S., Pereira P.V.L.G.C., Castro L.O.R.D., Ramos R.R.C., Simbras F.M. 2021. The first notosuchian crocodyliform from the Araçatuba Formation (Bauru Group, Paraná Basin), and diversification of sphagesaurians. *An. Acad. Bras. Ciênc.* 93:e20201591.

Pol D. 2005. Postcranial remains of *Notosuchus terrestris* Woodward (Archosauria: Crocodyliformes) from the upper Cretaceous of Patagonia, Argentina. *Ameghiniana*. 42:21–38.

Pol D., Gasparini Z. 2009. Skull anatomy of *Dakosaurus andiniensis* (Thalattosuchia: Crocodylomorpha) and the phylogenetic position of Thalattosuchia. *Journal of Systematic Palaeontology*. 7:163–197.

Pol D., Nascimento P.M., Carvalho A.B., Riccomini C., Pires-Domingues R.A., Zaher H. 2014. A New Notosuchian from the Late Cretaceous of Brazil and the Phylogeny of Advanced Notosuchians. *PLoS ONE*. 9:e93105.

Price G. 1999. The evidence and implications of polar ice during the Mesozoic. *Earth-Science Reviews*. 48:183–210.

Reading H.G., editor. 1996. *Sedimentary Environments: Processes, Facies and Stratigraphy*. Oxford: Blackwell Publishing.

Rees P.M.C.A., Ziegler A.M., Valdes P.J. 2000. Jurassic phytogeography and climates: new data and model comparisons. In: Huber B.T., Macleod K.G., Wing S.L., editors. *Warm Climates in Earth History*. Cambridge: Cambridge University Press. p. 197–318.

Riff D., Kellner A.W.A. 2011. Baurusuchid crocodyliforms as theropod mimics: clues from the skull and appendicular morphology of *Stratiotosuchus maxhechti* (Upper Cretaceous of Brazil). *Zoological Journal of the Linnean Society*. 163:S37–S56.

Rio J.P., Mannion P.D. 2021. Phylogenetic analysis of a new morphological dataset elucidates the evolutionary history of Crocodylia and resolves the long-standing gharial problem. *PeerJ*. 9:e12094.

Ristevski J., Weisbecker V., Scanlon J.D., Price G.J., Salisbury S.W. 2023. Cranial anatomy of the mekosuchine crocodylian *Trilophosuchus rackhami* Willis, 1993. *The Anatomical Record*. 306:239–297.

Ristevski J., Yates A.M., Price G.J., Molnar R.E., Weisbecker V., Salisbury S.W. 2020. Australia's prehistoric 'swamp king': revision of the Plio-Pleistocene crocodylian genus *Pallimnarchus* de Vis, 1886. *PeerJ*. 8:e10466.

Roberto I.J., Bittencourt P.S., Muniz F.L., Hernández-Rangel S.M., Nóbrega Y.C., Ávila R.W., Souza B.C., Alvarez G., Miranda-Chumacero G., Campos Z., Farias I.P., Hrbek T. 2020. Unexpected but unsurprising lineage diversity within the most widespread Neotropical crocodylian genus *Caiman* (Crocodylia, Alligatoridae). *Systematics and Biodiversity*. 18:377–395.

Rogers R.R., Hartman J.H., Krause D.W. 2001. Stratigraphic Analysis of Upper Cretaceous Rocks in the Mahajanga Basin, Northwestern Madagascar: Implications for Ancient and Modern Faunas: A Reply. *The Journal of Geology*. 109:674–676.

Rogers R.R., Krause D.W., Kast S.C., Marshall M.S., Rahantarisoa L., Robins C.R., Sertich J.J.W. 2013. A new, richly fossiliferous member comprised of tidal deposits in the Upper Cretaceous Maevarano Formation, northwestern Madagascar. *Cretaceous Research*. 44:12–29.

Rouchy J.M., Camoin G., Casanova J., Deconinck J.F. 1993. The central palaeo-Andean basin of Bolivia (Potosi area) during the late Cretaceous and early Tertiary: reconstruction of ancient saline lakes using sedimentological, paleoecological and stable isotope records. *Palaeogeography, Palaeoclimatology, Palaeoecology*. 105:179–198.

Ruiz J.V., Bronzati M., Ferreira G.S., Martins K.C., Queiroz M.V., Langer M.C., Montefeltro F.C. 2021. A new species of *Caipirasuchus* (Notosuchia, Sphagesauridae) from the Late Cretaceous of Brazil and the evolutionary history of Sphagesauria. *Journal of Systematic Palaeontology*. 19:1–23.

Rummy P., Wu X.-C., Clark J.M., Zhao Q., Jin C.-Z., Shibata M., Jin F., Xu X. 2022. A new paralligatorid (Crocodyliformes, Neosuchia) from the mid-Cretaceous of Jilin Province, northeastern China. *Cretaceous Research*. 129:105018.

Salas-Gismondi R., Flynn J.J., Baby P., Tejada-Lara J.V., Wesselingh F.P., Antoine P.-O. 2015. A Miocene hyperdiverse crocodylian community reveals peculiar trophic dynamics in proto-Amazonian mega-wetlands. *Proc. R. Soc. B*. 282:20142490.

Salisbury S.W., Molnar R.E., Frey E., Willis P.M.A. 2006. The origin of modern crocodyliforms: new evidence from the Cretaceous of Australia. *Proc. R. Soc. B*. 273:2439–2448.

Scheyer T.M., Aguilera O.A., Delfino M., Fortier D.C., Carlini A.A., Sánchez R., Carrillo-Briceño J.D., Quiroz L., Sánchez-Villagra M.R. 2013. Crocodylian diversity peak and extinction in the late Cenozoic of the northern Neotropics. *Nat Commun.* 4:1907.

Schindel D.E. 1980. Microstratigraphic sampling and the limits of paleontologic resolution. *Paleobiology.* 6:408–426.

Scotese C.R. 2005. Paleomap project. <http://www.scotese.com>.

Selby D., Mutterlose J., Condon D.J. 2009. U–Pb and Re–Os geochronology of the Aptian/Albian and Cenomanian/Turonian stage boundaries: Implications for timescale calibration, osmium isotope seawater composition and Re–Os systematics in organic-rich sediments. *Chemical Geology.* 265:394–409.

Sellés A.G., Blanco A., Vila B., Marmi J., López-Soriano F.J., Llácer S., Frigola J., Canals M., Galobart À. 2020. A small Cretaceous crocodyliform in a dinosaur nesting ground and the origin of sebecids. *Scientific Reports.* 10:1–11.

Sena M.V. de A., Marinho T. da S., Montefeltro F.C., Langer M.C., Fachini T.S., Nava W.R., Pinheiro A.E.P., Araújo E.V. de, Aubier P., Andrade R.C.L.P. de, Sayão J.M., Oliveira G.R. de, Cubo J. 2022. Osteohistological characterization of notosuchian osteoderms: evidence for an overlying thick leathery layer of skin. *Journal of Morphology.*:jmor.21536.

Sereno P., Larsson H. 2009. Cretaceous Crocodyliforms from the Sahara. *ZK.* 28:1–143.

Sereno P.C., Sidor C.A., Larsson H.C.E., Gado B. 2003. A new notosuchian from the Early Cretaceous of Niger. *Journal of Vertebrate Paleontology.* 23:477–482.

Sertich J.J.W., O'Connor P.M. 2014. A new crocodyliform from the middle Cretaceous Galula Formation, southwestern Tanzania. *Journal of Vertebrate Paleontology.* 34:576–596.

Sill W.D. 1968. The Zoogeography of the Crocodylia. *Copeia.* 1968:76.

Solórzano A., Nuñez-Flores M., Inostroza-Michael O., Hernández C. 2020. Biotic and abiotic factors driving the diversification dynamics of Crocodylia. *Palaeontology.* 63:1–15.

Sookias R.B. 2020. Exploring the effects of character construction and choice, outgroups and analytical method on phylogenetic inference from discrete characters in extant crocodylians. *Zoological Journal of the Linnean Society*. 189:670–699.

South A. 2017. `rnatuarearthdata`: World Vector Map Data from Natural Earth Used in “`rnatuarearth`.”

Stockdale M.T., Benton M.J. 2021. Environmental drivers of body size evolution in crocodile-line archosaurs. *Commun Biol*. 4:38.

Tarsitano S.F., Frey E., Riess J. 1989. The Evolution of the Crocodylia: A Conflict Between Morphological and Biochemical Data. *Am Zool*. 29:843–856.

Tennant J.P., Mannion P.D. 2014. Revision of the Late Jurassic crocodyliform *Alligatorellus*, and evidence for allopatric speciation driving high diversity in western European atoposaurids. *PeerJ*. 2:e599.

Tennant J.P., Mannion P.D., Upchurch P. 2016. Sea level regulated tetrapod diversity dynamics through the Jurassic/Cretaceous interval. *Nat Commun*. 7:12737.

Turner A.H. 2006. Osteology and phylogeny of a new species of *Araripesuchus* (Crocodyliformes: Mesoeucrocodylia) from the Late Cretaceous of Madagascar. *Historical Biology*. 18:255–369.

Turner A.H. 2015. A Review of *Shamosuchus* and *Paralligator* (Crocodyliformes, Neosuchia) from the Cretaceous of Asia. *PLoS ONE*. 10:e0118116.

Tykoski R.S., Rowe T.B., Ketcham R.A., Colbert M.W. 2002. *Calsoyasuchus valliceps*, a new crocodyliform from the Early Jurassic Kayenta Formation of Arizona. *Journal of Vertebrate Paleontology*. 22:593–611.

Vasconcellos F.M., Carvalho I.D.S. 2010. Paleoichnological assemblage associated with *Baurusuchus salgadoensis* remains, a Baurusuchidae Mesoeucrocodylia from the Bauru Basin, Brazil (Late Cretaceous). *Bulletin of the New Mexico Museum of Natural History and Science*. 51:227–237.

Vélez-Juarbe J., Brochu C.A., Santos H. 2007. A gharial from the Oligocene of Puerto Rico: transoceanic dispersal in the history of a non-marine reptile. *Proc. R. Soc. B*. 274:1245–1254.

Wickham H. 2016. ggplot2: Elegant Graphics for Data Analysis. Springer-Verlag New York.

Wilberg E.W. 2015. What's in an Outgroup? The Impact of Outgroup Choice on the Phylogenetic Position of Thalattosuchia (Crocodylomorpha) and the Origin of Crocodyliformes. *Systematic Biology*. 64:621–637.

Wilberg E.W. 2017. Investigating patterns of crocodyliform cranial disparity through the Mesozoic and Cenozoic. *Zoological Journal of the Linnean Society*. 181:189–208.

Wilberg E.W., Turner A.H., Brochu C.A. 2019. Evolutionary structure and timing of major habitat shifts in Crocodylomorpha. *Sci Rep*. 9:10.

Wu X.-C., Sues H.-D. 1996. Anatomy and phylogenetic relationships of *Chimaerasuchus paradoxus*, an unusual crocodyliform reptile from the Lower Cretaceous of Hubei, China. *Journal of Vertebrate Paleontology*. 16:688–702.

Chapter 2

Survival of Notosuchia at the Cretaceous-Palaeogene crisis

2.1 Foreword

The work presented in this chapter was the first task of my PhD. The final form of this work was submitted to the *Palaeontology* journal and published in January 2023. Before presenting this work, I wanted to give some context regarding its production. The project aimed to use, for the first time, the Phylogenetic Logistic Regression (PLR) to analyse the evolution of palaeodiversity. The PLR is a phylogenetic comparative method (PCM), that is, a phylogenetically informed statistical analysis. Including the phylogenetic relationships between the species of a group on which statistical analyses are performed allows us to circumvent the issue of the non-independence of observations. Indeed, the closer two species are, phylogenetically speaking, the more recently they have diverged from one another and the higher the probabilities are that they will look alike. Therefore, biological interspecific observations are not independent. The use of PCMs thus allows to test whether one or several explanatory variable(s) significantly explain a response variable, given the phylogenetic relationships and divergence times. The PLR distinguishes itself from other PCMs in that its response variable is binary. This characteristic allowed us to consider survival/extinction as the binary response variable and test which explanatory variable(s) significantly explained it. This method had never been used before to analyse the evolution of biodiversity so a large part of the work was to investigate what was possible and what was not. Initially, the project aimed at performing such a test at all the stage boundaries crossed by the Notosuchia. However, it rapidly became evident to us that both the paucity and the poor stratigraphic precision of the fossil record would not allow such an exhaustive approach. We thus chose to focus ourselves solely on the Cretaceous-Palaeogene boundary. Furthermore, we initially planned to code each species that crossed the boundary as ‘survivors’ and each one that did not as ‘extinct’. Only, here again, the scarcity of the fossil record prevented us from doing so, as no notosuchian species had its fossil record present both in the Maastrichtian and in the Danian. To circumvent this issue, we decided to code as ‘survivors’ the species that had been found in post-Cretaceous deposits. It is important to explicitly state that, by doing so, we considered that the post-Cretaceous fauna is representative of the notosuchian diversity that survived the K-Pg crisis. This might look like a weakening working hypothesis because it is a strong, unsupported assumption. However, I will elaborate in the conclusions of this manuscript that it is not. The first draft of this study was submitted in February of 2022. The main criticism of the reviewers dealt with the fact that we initially used a single tree topology and method of node and taxa

dating. Following the reviewer's recommendations, we included another topology illustrating a second phylogenetic hypothesis and used different dating methods. It took me until July of the same year to submit a second manuscript, given these substantial modifications. The second round of reviews was minor and a third version of the manuscript was accepted on the 24th of October 2022. Thus, this study was the main task of my PhD for the first two years.

Phylogenetic Structure of the of the Extinction and Biotic Factors explaining Differential Survival of Terrestrial Notosuchians at the Cretaceous-Palaeogene Crisis

Paul Aubier¹, Stéphane Jouve¹, Johann Schnyder² & Jorge Cubo¹

¹ Sorbonne Université, Muséum national d'Histoire naturelle, CNRS, Centre de Recherche en Paléontologie de Paris (CR2P), 4 place Jussieu, 75005 Paris;

² Sorbonne Université, Institut des Sciences de la Terre de Paris (ISTeP), 4 place Jussieu, 75005 Paris

2.2 Abstract

Although the clade Crocodylomorpha is represented by a few extant species (Crocodylia), it has a rich fossil record. Hundreds of species adapted to terrestrial, semi-aquatic and marine environments, have existed over more than 200 million years. Numerous studies have attempted to characterize the factors driving the diversification and extinction events of Crocodylomorpha, resulting in ambiguous and even contradictory conclusions, which points to the need for phylogenetically and temporally smaller-scaled studies. Here, we focus on differential survival at the Cretaceous-Palaeogene crisis of Notosuchia, a diverse clade of mostly terrestrial Crocodylomorpha that achieved great diversity during the Cretaceous. More precisely, we tested the effect of body size and palaeotemperatures on notosuchian survival probability during the K-Pg crisis as well as the effect of diet on the evolution of their body size. We find that Notosuchia showed an evolutionary trend towards larger body sizes through time, associated with a shift from an omnivorous to a carnivorous diet. This may explain why sebecids were the only notosuchians to survive the K-Pg crisis. We also corroborate the conclusions of previous studies that detected a Lagerstätten effect occurring in the Adamantina Formation (Upper Cretaceous, Brazil, Bauru Group). This work confirms the value of more finely scaled macroevolutionary studies for understanding the history of a rich and complex group such as Crocodylomorpha.

Keywords: Notosuchia, Cretaceous-Palaeogene crisis, phylogenetic comparative method, Crocodylomorpha, Adamantina Formation, phylogenetic selectivity.

2.3 Introduction

The extant diversity of crocodylians includes 24 species (Grigg & Kirshner, 2015) and is, based on morphological phylogenetic analyses, structured in three clades: Gavialoidea, Alligatoroidea and Crocodyloidea. They share a similar overall morphology characterized by an armoured body with a sprawling posture, and an amphibious, generalist carnivore ecology (Grigg & Kirshner, 2015). Yet, the apparent ‘uniformity’ of this extant diversity fades when compared to that of related fossil taxa. Crocodylia belongs to the Crocodylomorpha, which has a rich and complex evolutionary history. Two major clades within this group are Neosuchia (including extant Crocodylia) and the extinct Notosuchia. Crocodylomorphs diversified during the Mesozoic Era and survived multiple extinction events, notably in the Late Triassic, at the Jurassic-Cretaceous boundary, and at the Cretaceous-Palaeogene (K-Pg) boundary (Mannion *et al.*, 2015). During its evolution, Crocodylomorpha occupied various environments. The basal ‘sphenosuchians’ were terrestrial (Wilberg *et al.*, 2019), characterized by an erect stance and long and gracile limbs. During the Early Jurassic, crocodylomorphs such as protosuchians colonized shallow freshwater biomes, and metriorhynchoids and thalattosuchians evolved into marine pelagic swimmers. These shifts among marine, freshwater and terrestrial environments, occurred repeatedly within Mesozoic Crocodylomorpha (Wilberg *et al.*, 2019). Several studies have tried to characterize the extrinsic factors that may have driven the palaeobiodiversity and morphological evolution of this group and have pointed out the importance of climatic variables. Martin *et al.* (2014) suggested that sea surface palaeotemperature variations were strongly correlated with the evolution of the diversity of marine crocodylomorphs: diversification events were associated with warm periods, and extinctions with cold ones. Mannion *et al.* (2015) also found that diversification patterns tracked climatic changes. Stockdale & Benton (2021) demonstrated that size transitions during the Neogene were associated with the Miocene Climate Optimum suggesting that environmental factors were the principal drivers. However, other authors challenged those views. Godoy *et al.* (2019) did not find strong correlations between abiotic factors and body size evolution in Crocodylomorpha, Jouve *et al.* (2017) suggested that several biases may have affected the reliability of Martin *et al.*’s (2014) results and the results of Stockdale & Benton (2021) might be flawed by the use of non-logged measurement data as demonstrated by a reply to that article (Benson *et al.*, 2022). It has been repeatedly shown that crocodylomorph cranial morphology disparity changed through time, attaining the highest value at the Cretaceous and declining during the Cenozoic

(Wilberg, 2017; Godoy, 2020; Stubbs *et al.*, 2021). Nevertheless, studies have failed to detect a clear common evolutionary trend at a large phylogenetic scale and rather found that evolution occurred through rapid diversification events that were restricted to small groups at specific time intervals (Bronzati *et al.*, 2015; Celis *et al.*, 2020; Godoy *et al.*, 2019; Jouve, 2021; Stockdale & Benton, 2021; Stubbs *et al.*, 2021). These diversification/extinction events were driven by different factors depending on the clade under consideration. Jouve (2021) suggested that the evolution of each crocodylomorph group should be considered separately because the driving factors could differ from one group to another. Indeed, local environmental conditions could also have affected crocodylomorph evolution, and these factors are often missing in global approaches (Jouve, 2021). It has been proposed that ecological specialization might explain the survivorship of crocodylomorphs during extinction events such as the K-Pg crisis. Because freshwater vertebrate communities were much less affected by this crisis than terrestrial and marine ones, Buffetaut (1990) proposed that one of the factors that might explain the survival of vertebrates during the K-Pg crisis is the food chain to which a group belongs. Within Notosuchia, Kellner *et al.* (2014) noted that the sebecids, which survived the K-Pg crisis, were less specialized hypercarnivores than the baurusuchids, which became extinct. The aim of our study is to test the effect of potential factors driving the evolution of the diversity of a group of crocodylomorphs, Notosuchia, at the K-Pg crisis because it is the main crisis that this group faced. Notosuchians were probably ectothermic (Cubo *et al.*, 2020, 2022). Almost all of them were adapted to a terrestrial environment (Wu & Sues, 1996; Gomani, 1997; Pol, 2005; Turner, 2006; Sereno & Larsson, 2009; Nascimento & Zaher, 2010; Riff & Kellner, 2011; Godoy *et al.*, 2016), a legacy of the ancestral crocodylomorph terrestriality (Wilberg *et al.*, 2019). Notosuchian phylogenetic relationships are still debated. According to Pol *et al.* (2014), this group is composed of four clades: Uruguaysuchidae, Peirosauridae, advanced notosuchians (including Sphagesauridae) and Sebecosuchia (including Baurusuchidae and Sebecidae), which diversified through two major radiation events, in the Lower and the Upper Cretaceous (Carvalho *et al.*, 2010; Pol *et al.*, 2014), and persisted until the Miocene (*Barinasuchus arveloi* Paolillo & Linares, 2007). Other hypotheses have been proposed, notably that the Peirosauridae and Sebecidae are not notosuchians (Sereno *et al.*, 2003; Geroto & Bertini, 2019) and that they form the sister clade (Sebecia) of Neosuchia (Larsson & Sues, 2007; Pinheiro *et al.*, 2018). Sebecidae has also recently been recovered as the sister group of Peirosauridae but still within the Notosuchia (Ruiz *et al.*, 2021). The diversity of Notosuchia declined drastically during the

Late Upper Cretaceous (Pol & Leardi, 2015): all taxa except Sebecidae became extinct after the K-Pg crisis. Notosuchia shows great diversity in terms of diet and food processing specialization (Melstrom & Irmis, 2019). Some species retained the ancestral generalist carnivorous diet (e.g. Peirosauridae), but there were also omnivorous (e.g. Sphagesauridae), herbivorous (*Chimaerasuchus paradoxus* Wu *et al.*, 1995; *Simosuchus clarki* Buckley *et al.*, 2000), and hypercarnivorous lineages (Sebecosuchia). Despite this diversity, few studies have tried to elucidate the drivers of notosuchian evolution (Carvalho *et al.*, 2010) or to characterize their diversification pattern (Ősi, 2014) and fewer have used quantitative approaches (Pol & Leardi, 2015, Celis *et al.*, 2020). Here we examined the phylogenetic structure of the extinction in terrestrial Notosuchia at the K-Pg crisis and tested the possible effects of climate (an extrinsic factor), body size, and diet (intrinsic/endogenous factors) on the differential survival of notosuchians at the K-Pg crisis. We expect body size to be significantly correlated with the survival of Notosuchians because this parameter has long been considered to affect the survival of species during extinction crises (McKinney, 1997). Yet, to test the effect of body size on survival is difficult, because it largely depends on the taxa and on the phylogenetic scale considered (McKinney, 1997). Concerning the effect of palaeotemperatures on survival, Carvalho *et al.* (2010) showed that climate, and particularly temperature, highly constrained the distribution of notosuchians, which is expected for ectothermic organisms. Notosuchia are found in nearly identical (semi-arid to arid) climatic regions (Carvalho *et al.*, 2010) with relatively similar palaeotemperatures. Thus, this variable is not expected to be associated with survival because it is a constant for Notosuchia. We performed further analyses to test the effect of several factors on notosuchian body size evolution and investigated whether there are evolutionary trends. Godoy *et al.* (2019) and Stockdale & Benton (2021) suggested that Cope's Rule (multi-lineage trend of directional evolution towards larger body sizes, Stanley 1973) did not apply to Crocodylomorpha as a whole nor to Notosuchia. Finally, we tested whether body size evolution was associated with diet. Notosuchia presents an array of cranial features that accounted for a large part of crocodylomorph peak cranial disparity during the Cretaceous (Stubbs *et al.*, 2021). Furthermore, it has been shown that skull shapes are linked to ecological niche and diet in Crocodylia (Busbey, 1995; McHenry *et al.*, 2006; Pierce *et al.*, 2008; Drumheller & Wilberg, 2020; Godoy, 2020; Stubbs *et al.*, 2021) and in Notosuchia (Ősi, 2014; Montefeltro *et al.*, 2020; Nieto *et al.*, 2021). Therefore, it is possible that the diversity of diets found in Notosuchia drove the evolution of their body size to some extent.

2.4 Materials and Methods

2.4.1 *Supertrees*

To take into consideration the phylogenetic relationships and divergence ages, we constructed supertrees of Notosuchia using the phylogeny published by Nicholl *et al.* (2021) as a reference topology. 18 species were manually added to the sample of Nicholl *et al.* (2021) to construct our topology, following taxonomic and phylogenetic evidence published in the literature (see Supplementary File S2.1.1). We included phylogenetic hypotheses that were not contradictory to those expressed in the topology of Nicholl *et al.* (2021). When for a given species only contradictory relationships were published, or when no phylogeny including it had been published, this species was added as a polytomy into the most inclusive node according to its taxonomy. The Nicholl *et al.* (2021) topology recovers the phylogenetic hypothesis in which the Sebecidae and the Baurusuchidae are sister taxa (Sebecosuchia). However, alternative hypotheses for the phylogenetic placement of the Sebecidae exist. A recent study recovered the Sebecidae as the sister group of the Peirosauridae (Ruiz *et al.*, 2021). In both of these hypotheses, the Sebecidae is the only notosuchian clade to survive the K-Pg crisis and its phylogenetic placement may affect the results of the analyses. To test the effect of this alternative phylogenetic position of the Sebecidae, we constructed an “alternative” topology using the one we produced based on Nicholl *et al.* (2021) but placing the Sebecidae as the sister group of the Peirosauridae. In doing so, the phylogenetic relationships among species inside the clades were kept unchanged. Thus, differences in the analytical results between the two topologies can be attributed strictly to the placement of Sebecidae. See Supplementary File S2.1.2 for the topologies. The timePaleoPhy function from the ‘Paleotree’ (v.3.3.25) R package (Bapst, 2012) was used to time-calibrate the two topologies. The choice of the time-scaling method has been shown to affect comparative phylogenetic analyses (Lloyd *et al.*, 2016; Bapst *et al.*, 2016; Bapst & Hopkins, 2017). Therefore, two different methods to time-calibrate the internal nodes were used for each topology, using the ‘type’ argument of the timePaleoPhy function. First was the “equal” method, which works by adjusting zero-length branches to distribute the time on early branches equally on the later branches. Second was the “mbl” method which dates internal nodes by the oldest species they include and gives the possibility to assign a minimum branch length (which we set as 1 My using the ‘vartime’ argument) to avoid the many zero-length branches this dating method inevitably produces.

The age of the root was constrained as the age of the lower bound of the Aptian because it is the geological stage that includes the oldest species included in our sample. In order to assign an age for the species in our sample, a stratigraphic range for each was defined using data downloaded from the Paleobiology Database (PBDB, www.paleobiodb.org). For the species with occurrences from geological formations of different ages, we took the shortest stratigraphic interval that included all of them in order to minimize the stratigraphic uncertainty. For species that had occurrence(s) restricted to a single geological formation, the stratigraphic range was bounded by the lower and upper ages of the formation. Given that the majority of the species we included in our analyses are represented by a single specimen or by several belonging to the same geological formation, we considered the species stratigraphic ranges as minimum and maximum possible ages (i.e. as a range of uncertainty) and not as intervals of presence. This could be done using the 'minMax' value for the 'dateTreatment' argument of the timePaleoPhy function which assigns an age for a species by randomly picking a value in its stratigraphic range. In order to account for this stratigraphic uncertainty, we produced 100 different supertrees for each topology and each method of internal nodes calibration, for a total of 400 trees (200 for each topology). One of the supertrees is illustrated in Figure 2.1. All the supertrees can be found in Supplementary Files S2.1.3 and S2.1.4 (for the Nicholl *et al.*, 2021 topology and 'alternate' topology, respectively) and the age ranges for each species in Supplementary File S2.1.5. Two taxa included in Nicholl *et al.* (2021) were removed before the time-calibration of the topologies: the 'Lumbrera form' because it has no published description, and *Razanandrongobe sakalavae* Maganuco *et al.*, 2006 based on the fragmentary nature of the specimens and the considerable temporal gap separating it from the first following notosuchians (at least 41 My). The time-calibrated trees thus included 77 species. The tips of the supertrees then had to match exactly the species included in the datasets used in the following analyses. We thus also removed several species after the time-calibration stage of the supertree production so that the temporal information they carry is not lost. Because the following analyses use the skull length as a variable (see following sections), we removed from the time-calibrated supertrees 26 species with unknown skull length, keeping only species for which skull length has either been estimated by other authors or was measured by us (from the tip of the snout to the posterior edge of the skull table) on available illustrations in the literature (see Supplementary File S2.1.1). Additionally, we removed *Stolokrosuchus lapparenti* Larsson & Gado, 2000, *Mahajangasuchus insignis* Buckley & Brochu, 1999, *Pepesuchus deiseae* Campos *et al.*,

2011 and *Barreirosuchus franciscoi* Iori & Garcia, 2012 because they have been considered freshwater species (Larsson & Gado, 2000; Turner & Buckley, 2008, Sena *et al.*, 2018) and this study focuses on terrestrial notosuchians. We also removed *Kaprosuchus saharicus* Sereno & Larsson, 2009 which was originally considered a terrestrial species (Sereno & Larsson, 2009), but the platyrostral shape of the skull and the dorsally facing external nares led Wilberg *et al.* (2019) to consider it as a freshwater animal. The removal of non-terrestrial species allows us to reduce the bias in the relationship between cranial length and body size induced by adaptations to different environments. Finally, we removed *Pakasuchus kapilimai* O'Connor *et al.*, 2010 and *Ogresuchus furatus* Sellés *et al.*, 2020 because they were outliers and caused the non-normality of the residuals of the PGLS analyses (see last Material & Method section). The final 400 supertrees include 43 species (See Supplementary File S2.1.6). According to the PBDB, the age of the Adamantina Formation (Upper Cretaceous, Brazil, Bauru basin) is Campanian-Maastrichtian, following Gobbo-Rodrigues *et al.* (1999) and Batezelli (2017). However, this age is still debated: some authors propose an older Santonian-Turonian age (*e.g.* Dias-Britto *et al.*, 2001). Castro *et al.* (2018) established a post-Turonian (≤ 87.8 My) maximal age for this formation using high-precision U-Pb geochronology. We thus considered the age of the Adamantina Formation to be Santonian-Maastrichtian (86.6-66 My). However, we ran sensitivity analyses, assigning the Adamantina Formation to different epochs (see section below). Indeed, Celis *et al.* (2020) suggested that this formation, due to the high number of notosuchian species it yielded (18 in our sample), caused a Lagerstätten effect that distorts palaeobiodiversity estimates. Thus, the age of the Adamantina formation might profoundly change the results of our analyses.

2.4.2 Phylogenetic logistic regression

We used the Phylogenetic Logistic Regression (PLR) (Ives & Garland 2010), using the `phylglm` function of the ‘`phylolm`’ R package (Ho & Ane, 2014), to test whether body size and/or palaeotemperatures explain the survival of notosuchians at the K-Pg crisis. We used log-transformed skull lengths obtained from the literature (see Supplementary File S2.1.1) as a proxy for body size. Based on the palaeolatitudes gathered from PBDB, we used the latitudinal temperature gradient proposed by Amiot *et al.* (2004) for the Upper Campanian-Middle Maastrichtian, based on the $\delta^{18}\text{O}$ of continental vertebrates. When several occurrences were available for a given species, we took the occurrence with the highest

palaeolatitude (in absolute value) to perform analyses on the maximum latitudinal range. PLR allows the production of predictive models for a binary dependent variable (here, survival versus extinction) using a set of explanatory variables and the phylogeny. Phylogenetic relationships and divergence times were included because observations (at the species level) are not independent among them (Felsenstein, 1985; Harvey & Pagel, 1991). Traditionally, PLR is used to infer the probability of occurrence of values of the response variable. Here we constructed models and tested whether the explanatory variables (log-transformed skull length and palaeotemperature) significantly explain the response variable (the probability of survival). Thus, this method allows us to test if and to what extent each variable explains the survival probability of the notosuchians. Because the response variable is the survival/extinction of species at the Cretaceous-Palaeogene crisis (K-Pg crisis), we excluded from these analyses all species that became extinct before the Maastrichtian. Because most notosuchian species were described from a single specimen, or a set of specimens all coming from the same geological formation, our sample of species contained none that had a duration long enough to be unambiguously interpreted as crossing two distinct geological stages. As a consequence, none of the notosuchian species included in this analysis was codable as ‘1’ (survival) based solely on the fossil record. Sebecidae is the only clade, in the two phylogenetic hypotheses we test here, that appeared before the K-Pg crisis (*Ogresuchus furatus*, Sellés *et al.*, 2020) and survived this crisis, so we considered that all sebecids survived the crisis and we coded them accordingly.

Finally, we ran two sets of analyses for each variable to assess the effect of the stratigraphic interval uncertainty of the Adamantina Formation. First, we included all the species belonging to this formation and assigned a Late Upper Cretaceous Campanian-Maastrichtian age to it. Second, we included only the species of this formation with a Maastrichtian age (72.1-66 My). We performed 8 analyses in total, which are summarized in Table 2.1. See Supplementary Files S2.2.1 and S2.2.2 for the dataset and detailed results.

2.4.3 Phylogenetic selectivity using *D*-statistic

Phylogenetic clustering of extinction was tested for Notosuchia at the K-Pg crisis using the *D*-statistic of Fritz & Purvis (2010). This statistic considers the extinction/survival as a binary variable and observes

Table 2.1: Summary of the different sets of PLR analyses conducted. The "Alternate" topology corresponds to the alternate position of the Sebecidae as the sister group of the Peirosauridae. The species belonging to the Adamantina Fm are either all included or included only if they are dated in the Maastrichtian.

Analysis	Response variable	Topology	Adamantina Fm treatment
A	log(Skull length)	Nicholl <i>et al.</i> (2021)	All included
B	log(Skull length)	Nicholl <i>et al.</i> (2021)	Only Maast. sp.
C	log(Skull length)	Alternate	All included
D	log(Skull length)	Alternate	Only Maast. sp.
E	Palaeotemperature	Nicholl <i>et al.</i> (2021)	All included
F	Palaeotemperature	Nicholl <i>et al.</i> (2021)	Only Maast. sp.
G	Palaeotemperature	Alternate	All included
H	Palaeotemperature	Alternate	Only Maast. sp.

its distribution on the phylogeny. The D values are calculated by comparing the observed distribution of extinction/survival events across the tips of the phylogeny with two simulated distributions, one made under a Brownian model and the other made with a randomisation method. D is equal to 1 if the survival/extinction has a phylogenetically random distribution across the tips of the phylogeny and to 0 if it is clustered on the phylogeny as it would be if it followed a Brownian motion (*i.e.* strong phylogenetic signal). Still, D values can fall outside this range. We used the `phylo.d` function from the ‘caper’ R package (Orme *et al.*, 2018) with 1000 permutations as recommended by Fritz & Purvis (2010). This function calculates the D value, the probability of obtaining this D value if the survival/extinction is randomly distributed and the probability of obtaining this value if it follows a Brownian motion. Survival/extinction was coded as detailed above (see PLR section). We also performed two sets of analyses to assess the stratigraphic interval uncertainty of the Adamantina Formation, first including all the species belonging to this formation and second including only those from the Maastrichtian (see PLR section). See Supplementary File S2.3.1 for detailed results.

2.4.4 *Phylogenetic generalized least squares testing for skull length evolution*

We tested whether more recent notosuchian species were significantly larger than older ones using log-transformed skull length as a surrogate for body size. We used the Phylogenetic Generalized Least

Squares (PGLS) and the `pgls` function from the ‘`caper`’ R package (Orme *et al.*, 2018). We tested the relationship between log-transformed skull length and age for *Notosuchia* as a whole and also excluding hypercarnivores, generalist carnivores and all carnivores to assess the impact of the diet. We finally tested this relationship for the hypercarnivores only. The age of a given species was defined as the difference between the age of the root and the stratigraphic age of the species. We tested the normality of the residuals using the Shapiro-Wilk test. To differentiate whether a significant change in skull length was due to an overall directional shift or simply to an increase in skull length variance (Jablonski, 1987; Gould, 1988), we tested whether the latter significantly changed throughout time. Following Bokma *et al.* (2016), who associated the increase in body size with cladogenesis, we compared the variance in body size of notosuchians from clades originating in the first radiation during the Lower Cretaceous (Uruguaysuchidae, Peirosauridae and Ziphosuchia, Pol *et al.* 2014) with that of the notosuchians belonging to clades originating in the second radiation during the Upper Cretaceous (advanced notosuchians, Baurusuchidae and Sebecidae, Pol *et al.* 2014). We also performed the tests after separating the sebecids from the species originating in the Late Cretaceous group to see whether there was a significant difference between the survivors of the crisis and the other notosuchians. Because the skull lengths are not normally distributed, we used the Fligner-Killeen test to check the homogeneity of the variances for the log-transformed skull lengths, because this test is the most robust against departure from normality (Conover *et al.* 1981). See Supplementary Files S2.4.1 and S2.4.2 for the species lists used in each analysis and detailed results.

2.4.5 *Phylogenetic generalized least squares testing for skull length evolution*

We tested three evolutionary models: Brownian motion (BM), Ornstein-Uhlenbeck (OU) and Early Burst (EB) for skull length. We used the `fitContinuous` function from the ‘`geiger`’ R package (Pennell *et al.*, 2014) to calculate AICc values for each model for each supertree. We then performed a Tukey (HSD) test to compare the means of AICc values of the three evolutionary models to test if one of the three models had significantly lower AICc values. The `fitContinuous` function requires the trees to be binary (*i.e.* without polytomies). We thus performed these model-fitting analyses on supertrees produced following the same methodology presented above but using the TRUE value for the ‘`randres`’ argument of the `timePaleoPhy` function, which randomly resolves polytomies. See detailed results in Supplementary Files S2.5.1 and S2.5.2.

2.4.6 *Phylogenetic generalized least squares testing for the skull length $\tilde{\text{diet}}$ relationship*

We coded the diet into two categories (omnivorous and carnivorous), according to the literature (see Supplementary File S2.6.1). We log-transformed the skull length before performing the analyses using the `pgls` function ('caper' R package, Orme *et al.*, 2018). We tested the normality of the residuals controlling for the phylogeny using the Shapiro-Wilk test and the homoscedasticity using the Bartlett test. This normality was never respected when two species with really small skulls for their diet (*Pakasuchus kapilimai* and *Ogresuchus furatus*) were included. We thus removed them from the sample. See Supplementary Files S2.6.2–S2.6.4 for data and detailed results. The R script used for all analyses can be found in Supplementary File S2.7.

2.5 Results

2.5.1 *K-Pg crisis: phylogenetic structure of the extinction and biotic factors explaining survivals*

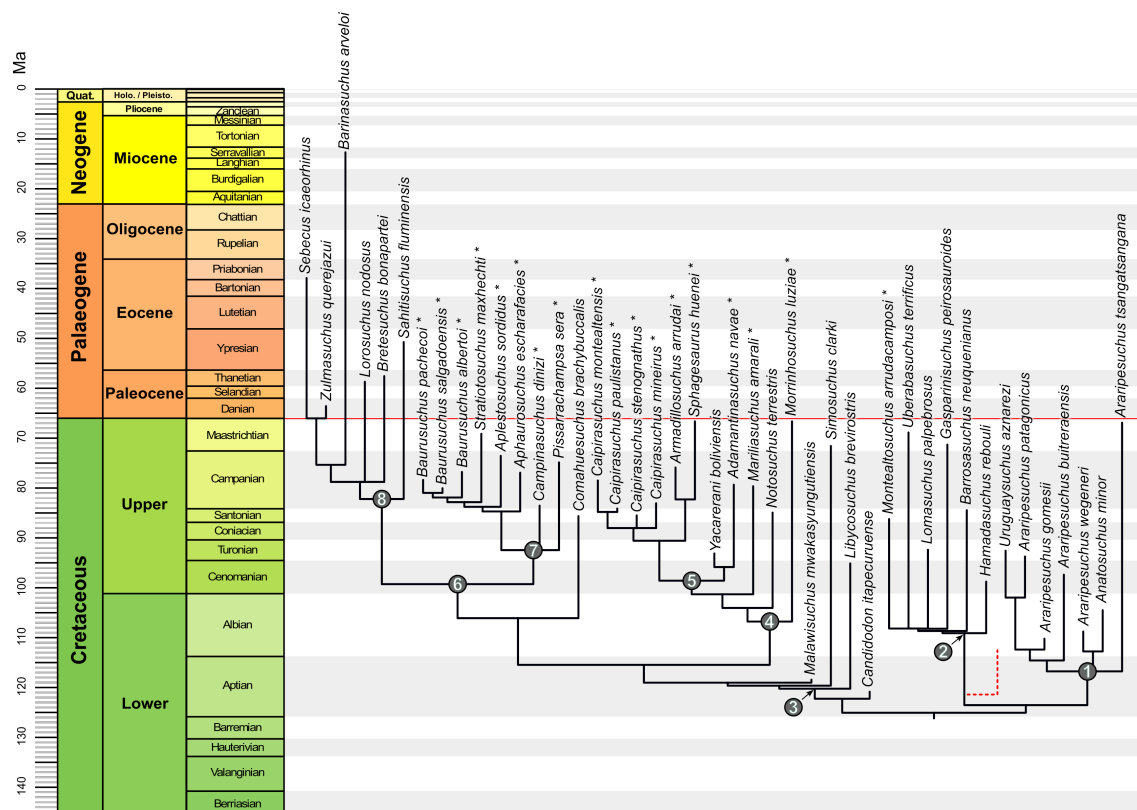


Figure 2.1: One of the 400 supertrees of Notosuchia used in this study. 1, Uruguaysuchidae; 2, Peirosauridae; 3, Ziphosuchia; 4, Advanced notosuchians; 5, Sphagesauridae; 6, Sebecosuchia; 7, Baurusuchidae; 8, Sebecidae. The red-dotted branch indicates the position of the Sebecidae in the ‘alternate’ topology. The red line indicates the Maastrichtian–Danian boundary. Species belonging to the Adamantina Formation are indicated with a star. References for the topology and the dating of the species are cited in the main text and available in Aubier *et al.*(2023, data 2.1.1 and 2.1.5).

The D-statistic analyses show that regardless of the topology used or whether all the species of the Adamantina Formation are included or only those from the Maastrichtian, the extinction during the K-Pg crisis is not randomly distributed across the phylogeny of the Notosuchia (Table 2.2). However, there are differences between the analyses. First, the D values are lower for the ‘alternate’ topology in which Sebecidae is the sister group of Peirosauridae. This may be because, in this ‘alternate’ topology, the Sebecidae are more deeply nested in the phylogeny compared to the Nicholl *et al.* (2021) hypothesis. A second difference is observed for both topologies between the analysis including all the species from the Adamantina Formation and the one including only the Maastrichtian species. The lower values observed

for the latter (and the higher standard deviation associated) are probably due to the variability of taxa included in these analyses. Indeed, because the ages of the species are randomly assigned (see supertrees section), the sample of species coming from the Adamantina Formation is not the same in all the trees, and so the results are more variable.

Table 2.2: Results of the D-statistics analyses.

Topology	Adamantina Fm. treatment	D value (sd)	P.random (sd)	P.brownian (sd)
Nicholl <i>et al.</i> (2021)	All included	-2.319 (0.260)	0* (0)	0.996* (0.004)
Nicholl <i>et al.</i> (2021)	Only Maast. sp.	-3.494 (0.934)	0* (0)	0.984* (0.017)
Alternate	log(Skull length)	-1.773 (0.184)	0* (0)	0.978* (0.014)
Alternate	log(Skull length)	-2.261 (0.542)	<1.10 ⁻³ * (0.001)	0.954* (0.028)

Table 2.3: Results of the PLR analyses. Values for the Estimates, StdErr, z.value and p.values are the rounded means of the values obtained for each 200 trees in each analysis with the standard deviation in brackets. Last column: percentage of significant analyses. Significant p.values are indicated with an asterisk.

Analysis	Estimate (sd)	StdErr (sd)	z.value (sd)	p.value (sd)	%
A	2.959 (0.145)	1.409 (0.069)	2.100 (0.054)	0.036* (0.005)	100
B	2.929 (0.557)	1.640 (0.320)	1.790 (0.121)	0.076 (0.020)	9.5
C	3.040 (0.176)	1.528 (0.093)	1.990 (0.046)	0.047* (0.005)	78.5
D	2.833 (0.563)	1.573 (0.313)	1.802 (0.096)	0.073 (0.016)	2.5
E	-0.027 (0.008)	0.095 (0.005)	-0.285 (0.088)	0.776 (0.068)	0
F	-0.028 (0.008)	0.111 (0.012)	-0.249 (0.065)	0.804 (0.050)	0
G	-0.025 (0.004)	0.079 (0.004)	-0.315 (0.038)	0.753 (0.029)	0
H	-0.021 (0.006)	0.088 (0.007)	-0.239 (0.060)	0.811 (0.046)	0

The PLR analyses show that palaeotemperature never explains the survival of the Notosuchia at the K-Pg crisis (Table 2.3, analyses E-H). Contrasting results occur regarding the skull length. This variable explains the survival in all the trees (Table 2.3, analysis A) or in the majority of them (Table 2.3, 78.5%, analysis C) depending on the topology (Nicholl *et al.*, 2021 or ‘alternate’, respectively) when all the species belonging to the Adamantina Formation are included. The positive effect associated with skull

length when it is significant indicates that this variable is positively correlated with survival (Figure 2.2). This means that the longer the skull, used here as a proxy for body size, the higher the survival probability. When the species from the Adamantina Formation are included only if they are from the Maastrichtian, skull length explains survival in only a minority of trees in both topologies (9.5% and 2.5%, respectively) Nonetheless, in the trees of these analyses (Table 2.3, B and D), a large number of the species belonging to the Adamantina Formation are excluded from the PLR analysis, thus drastically reducing the number of species considered to become extinct at the K-Pg crisis when compared to the analyses including all the species from this formation (from $n = 21$ when all the species from the Adamantina Formation are included to a mean of $n = 8.37$ when only those from the Maastrichtian are). As a consequence, the results of these two analyses may not be robust.

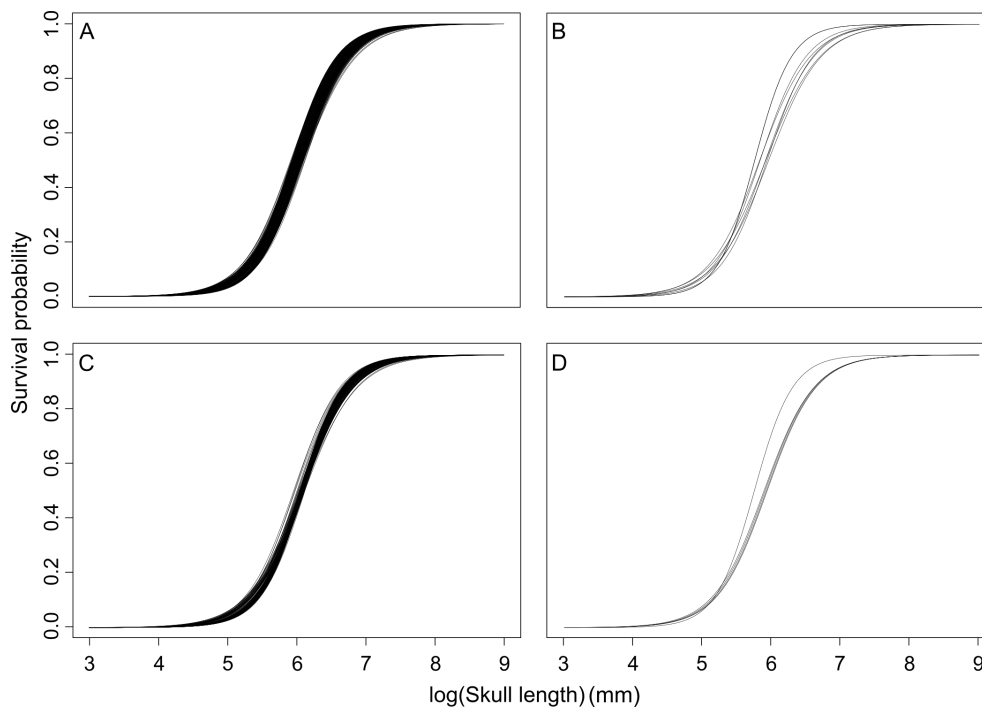


Figure 2.2: Distribution of the survival probability for Notosuchia at the K/Pg crisis. Each curve represents one significant model. A–B, topology based on Nicholl *et al.* (2021). C–D, ‘alternate’ topology. A and C include all species from the Adamantina Formation; B and D include only Maastrichtian species from the Adamantina Formation.

2.5.2 Evolution of body size in Notosuchia and relationship with diet

For both topologies, the results of the analyses are similar (Table 2.4) regarding the relationship between the log-transformed skull lengths and the ages of the species. Body size in Notosuchia seems to have

increased over time, with a positive correlation between skull length and the age of the species. This positive relationship is also observed when hypercarnivores or generalist carnivores are excluded from the sample. However, the relationship is not significant when all carnivores are excluded, nor when only hypercarnivores are considered. All residuals were normally distributed (Table 2.4). We failed to detect any significant change in the variance of skull lengths between the species that originated during the Lower Cretaceous radiation and the species that originated during the Late Cretaceous one, regardless of the inclusion ($p = 0.2354$) or not ($p = 0.5406$) of the Sebecidae in the Late Cretaceous originating species group. As a consequence, the size increase is not attributable to an increase in variance over geological time. Unfortunately, the model fitting analyses did not allow us to associate this body size increase to a specific evolutionary model (Figure 2.3). Indeed, none of the three models tested (BM, OU and EB) had significantly lower AICc values than the two others, regardless of the topology tested (ANOVA p-values = 0.112 and 0.107 with the topology from Nicholl *et al.*, 2021 and the ‘alternate’ topology, respectively).

Table 2.4: Results of the PGLS analyses testing the relationship between skull length and geological age. Values for the estimates, StdErr, z, $\Pr(>|t|)$, and the p-value of the normality test, are the rounded means of the values obtained for every 100 trees in each analysis with the standard deviation in brackets. Significant p-values are indicated with an asterisk.

Topology	Estimate (sd)	StdErr (sd)	t.value (sd)	Pr(> t) (sd)	Normality test p.value (sd)
Notosuchia					
Nicholl <i>et al.</i> (2021)	0.014 (0.002)	0.005 (<0.001)	3.210 (0.622)	0.009* (0.022)	0.542 (0.279)
Alternate	0.015 (0.002)	0.004 (<0.001)	3.416 (0.665)	0.005* (0.0132)	0.475 (0.296)
Notosuchia excluding hypercarnivores					
Nicholl <i>et al.</i> (2021)	0.013 (0.002)	0.005 (<0.001)	2.422 (0.541)	0.039* (0.045)	0.421 (0.294)
Alternate	0.012 (0.003)	0.005 (<0.001)	2.444 (0.645)	0.044* (0.062)	0.382 (0.299)
Notosuchia excluding generalist carnivores					
Nicholl <i>et al.</i> (2021)	0.012 (0.003)	<0.001 (<0.001)	2.629 (0.703)	0.0378* (0.068)	0.588 (0.283)
Alternate	0.014 (0.002)	0.005 (<0.001)	3.120 (0.699)	0.013* (0.029)	0.544 (0.287)
Notosuchia excluding all carnivores					
Nicholl <i>et al.</i> (2021)	0.007 (0.002)	0.004 (<0.001)	1.991 (0.868)	0.129 (0.170)	0.542 (0.318)
Alternate	0.008 (0.002)	0.004 (<0.001)	2.046 (0.849)	0.122 (0.18)	0.544 (0.305)
Hypercarnivore notosuchians					
Nicholl <i>et al.</i> (2021)	0.007 (0.003)	0.006 (<0.001)	1.174 (0.604)	0.305 (0.209)	0.811 (0.210)
Alternate	0.009 (0.002)	0.005 (<0.001)	1.554 (0.300)	0.160 (0.072)	0.786 (0.231)

However, diet is significantly associated with skull length in both topologies (Table 2.5). The negative effect shows that omnivorous notosuchians have significantly shorter skulls than carnivores (Figure 2.4). The residuals are normally distributed and show no heteroscedasticity (Table 2.5).

Table 2.5: Results for the PGLS analyses testing the relationship between skull length and diet. Values for the estimates, StdErr, z, $\Pr(>|t|)$, and the p-values of the normality and homoscedasticity tests on the residuals, are the rounded means of the values obtained for every 200 trees in each analysis with the standard deviation in brackets. Significant p-values are indicated with an asterisk.

Topology	Estimate (sd)	StdErr (sd)	t.value (sd)	$\Pr(> t)$ (sd)	Residuals normality test p.value (sd)	Residuals homosc. test p.value (sd)
Nicholl <i>et al.</i> (2021)	-1.262 (0.062)	0.147 (0.041)	-9.109 (2.009)	<0.001* (<0.001)	0.411 (0.324)	0.973 (<0.001)
Alternate	-1.265 (0.075)	0.140 (0.040)	-9.548 (1.900)	<0.001* (<0.001)	0.314 (0.294)	0.973 (<0.001)

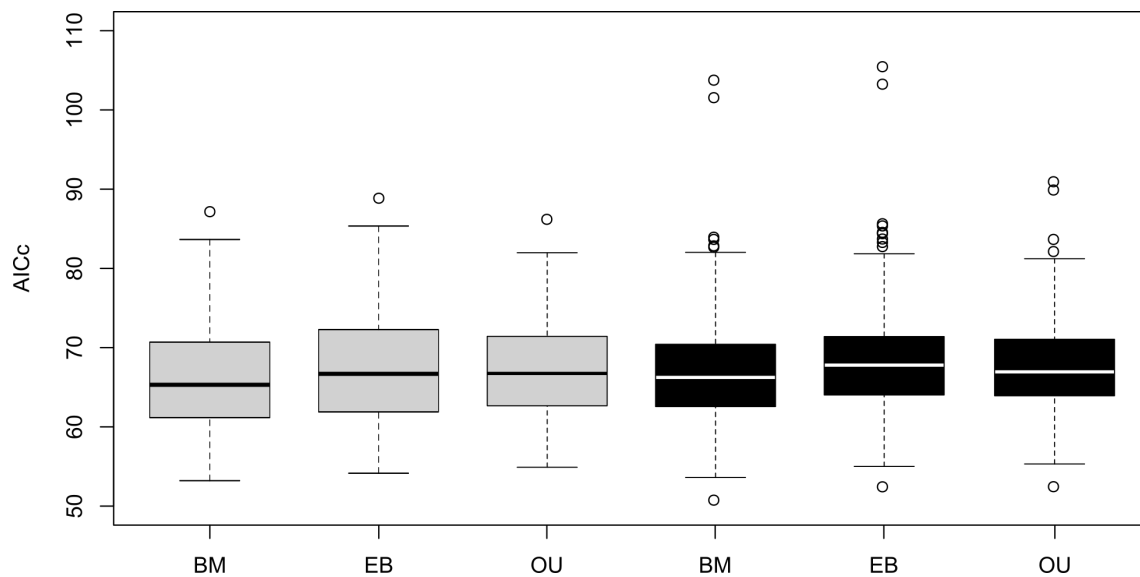


Figure 2.3: AICc scores for the three models tested: Brownian motion (BM), Early Burst (EB) and Ornstein-Uhlenbeck (OU). Grey boxes indicate supertrees constructed following the topology from Nicholl *et al.* (2021); black boxes indicate those constructed with the ‘alternate’ topology.

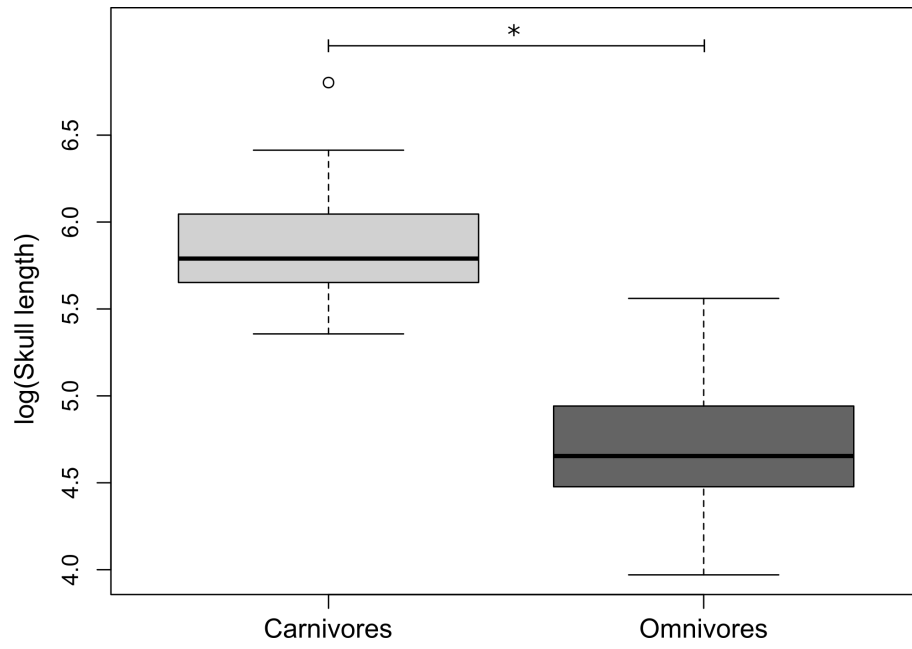


Figure 2.4: Boxplots of the log-transformed skull lengths depending on the diet. * indicates a significant difference (see Table 2.5).

2.6 Discussion

2.6.1 *K-Pg crisis: Phylogenetic structure of extinction and biotic factors explaining survivals*

The K-Pg crisis extinction was highly selective for Notosuchia, as shown by the D-statistic analyses. This means that there are specific factors, with a strong phylogenetic signal, that may explain the extinction/survival of notosuchians at this crisis. Palaeotemperature does not seem to be one of them. The geographic distribution of Notosuchia seems to be highly constrained, restricted to semi-arid to arid climates (Carvalho *et al.*, 2010). Their probable ectothermic metabolism (Cubo *et al.*, 2020, 2022) could have strongly restricted their possible dispersal to higher latitudes and habitats. Lower latitudes and habitats seem to be a limiting constraint too, maybe because the rainforest of tropical climates may have been problematic for terrestrial cursorial crocodyliforms. Our results are consistent with this strong climatic constraint on notosuchian geographic distribution. Our analyses failed to detect an effect of palaeotemperature on survival/extinction, which corroborates the hypothesis that notosuchians all lived under similar climatic conditions at the K-Pg crisis event. This does not mean that climate did not play a role during the K-Pg crisis, but rather that its effect, if present, was equally distributed among notosuchians due to their restricted latitudinal distribution. In other words, climate is not a variable but a constant parameter for Notosuchia in these analyses, so it was expected to find no effect on the response variable (the probability of survival). To investigate further the role of climate on the evolution of Notosuchia, future work may focus on inferring palaeotemperatures using latitudinal gradients not only relevant for the Maastrichtian but also for more recent times, since most of the sebecid diversity is distributed through the Palaeogene and Neogene. In the analyses that consider the Adamantina formation to be Campanian-Maastrichtian in age (*i.e.* when all species from this formation were included), the PLRs showed that small notosuchians have a high probability of extinction and that the longer the skull (and thus, the larger the body size), the higher the probability of survival. According to McKinney (1997), in closely related species, the positive relationship between survival and body size is explained by competitive advantage. This is dubious in the present case because sebecids were large, cursorial and hypercarnivorous whereas non-baurusuchid notosuchians were medium

to small, omnivorous or herbivorous. As a consequence, these taxa probably did not compete for the same resources.

2.6.2 Evolution of body size in Notosuchia and relationship with diet

According to the PGLS analyses, longer skulls seem to be associated with a carnivorous diet (Table 2.5, Fig. 2.4). This may explain, at least partially, this size increase for Notosuchia (Table 2.4). Traditionally, an increase in body size during the diversification of a clade has been seen as an anagenetic process ‘actively powered’ by natural selection because it was supposed to confer fundamental advantages (Newell, 1949; Simpson, 1953; Rensch, 1959; Brown & Maurer, 1986; Gould, 1988). A contrary view is that within clades, body size evolution was passively induced through adaptation to new ecological adaptive zones from small sizes, rather than actively directed toward big sizes (Stanley, 1973). Jablonski (1987) and Gould (1988) showed that for numerous groups, the observed increase in size was merely due to an increase in variance. Nevertheless, the ‘passive’ hypothesis has been supported by recent works that associate the increase in size with specialization and cladogenesis (Van Valkenburgh, 2004; Raia *et al.*, 2012; Bokma *et al.*, 2016). Yet, the ‘actively driven’ hypothesis may still not be discarded because Kingsolver & Pfennig (2004) found the individual-level selection to be the cause of size increase, with larger size associated with higher fitness. Here we show that skull length variance is not significantly different throughout different periods of notosuchian history. Thus, we discard the hypothesis of size increase as a statistical artefact. Godoy *et al.* (2018) found that for baurusuchids, cranial modifications were strongly linked with size variations. Furthermore, they hypothesized that changes in the shape and/or size of the skull might have occurred together with the shift to a hypercarnivorous diet. Van Valkenburgh (2004), discussing the evolution of Canidae, associated the increase in body size with the shift toward a hypercarnivorous diet. She concluded that ‘As mean body size increased, species evolved into specialized hypercarnivores’ (Van Valkenburgh, 2004, p. 102). The same relation may be at work here: a selective pressure favouring hypercarnivore adaptations led to larger body sizes because, within hypercarnivores, the ‘bigger species tend to dominate and kill small competitors’ (Van Valkenburgh, 2004, p. 103). Because crocodylomorphs were ancestrally homodont and carnivorous (Ősi, 2014), it can be assumed that peirosaurid carnivory (generalist carnivory) is a legacy from the ancestral condition, according to the phylogenetic framework used here. Furthermore, the PGLS analyses revealed a trend toward larger

body sizes for all Notosuchia, whether or not the Peirosauridae are included (Table 2.4). This suggests that body size increase (tested using PGLS) may be associated with the shift toward a hypercarnivorous diet (sebecosuchians). Furthermore, Godoy *et al.* (2019) found no support for Cope’s Rule in Notosuchia. Thus, the increase in body size is probably restricted to specific subgroups and did not occur uniformly in the various notosuchian lineages. Yet, if this mechanism was truly at work for Notosuchia, we should observe a trend toward larger body size when tested including only hypercarnivores, which is not the case in our analysis (Table 2.4). However, the diversity of the hypercarnivores is either very scarce with high stratigraphic uncertainty (Sebecidae) or composed of a high number of species that belong to the same formation (Baurusuchidae). Therefore, testing a temporal trend is hazardous for this group. The increase in notosuchian body size throughout the Cretaceous may not solely rely on this dietary shift. Indeed, Carvalho *et al.* (2010) interpreted the appearance of these larger forms partly as a response to hotter and drier climates. This may also be attributed to niche partitioning. Notosuchian dental complexity rivalled and even surpassed the complexity of extant mammals (Melstrom & Irmis 2019). Facing the high dental complexity of *Pakasuchus pakilimai*, it was proposed that notosuchians took advantage of the absence of competitive ecomorphs from other tetrapod groups to occupy ecological zones today occupied by mammals (O’Connor *et al.*, 2010). However, given the fact that numerous herbivorous notosuchian specimens have been found in assemblages containing synapsids, Melstrom & Irmis (2019) proposed instead that these notosuchians and herbivorous synapsids lived together and achieved an ecological partitioning that no longer exists. Following this, the increase in body size between Lower and Upper Cretaceous notosuchians could be attributed to the colonization of a new ecological adaptive zone, with forms that increasingly specialized from small, unspecialized root notosuchians.

2.6.3 *Effects of phylogenetic and stratigraphic uncertainty*

The PGLS, D-statistic and evolutionary model fitting analyses yielded very close results using both topologies. The PLR analyses are the only ones in which substantial differences could be observed (between analyses A and C, Table 2.3). Note that this difference is restricted to the degree of significance, and not the significance itself. However, we only compared two phylogenetic hypotheses in which Sebecidae is a clade included in Notosuchia. Other hypotheses have been proposed in which Sebecidae is not a notosuchian clade (Geroto & Bertini, 2019; Pinheiro *et al.*, 2018). Following these phylogenetic hy-

potheses, Notosuchia as a whole became extinct at the K-Pg crisis. Therefore, the uncertainty regarding the phylogenetic position of the Sebecidae does not only affect the question of how Notosuchia survived the K-Pg crisis but also if it survived it. In contrast, PLR analyses showed strongly different results depending on the dating of the Adamantina Formation (Table 2.3). When considered of Campanian-Maastrichtian age (*i.e.* all the species belonging to this formation are considered to have faced the K-Pg crisis), significant results for the log-transformed skull length are observed. But when a looser age of Santonian-Maastrichtian is considered, the significance is lost. Whether this loss of significance is explained by the reduction of the sample (and therefore is more a statistical artefact than a positive result) or not cannot be determined. However, this difference shows the importance of the Adamantina Formation in comparative phylogenetic analyses for Notosuchia. A more precise dating of this formation is necessary for clearer understanding of notosuchian evolutionary history.

2.7 Conclusions

Terrestrial notosuchians grew larger through the Cretaceous. This increase in body size during the Late Cretaceous may be restricted to specific lineages (Godoy *et al.*, 2019 found no support for Cope’s Rule for the clade Notosuchia) and may be attributed to the shift from omnivorous, medium-sized species to larger, carnivorous (and possibly hypercarnivorous) species. This shift led hypercarnivorous notosuchians to play a different ecological role than their omnivorous counterparts, as probable apex terrestrial predators (Montefeltro *et al.*, 2020). Kellner *et al.* (2014) proposed that this ecological specialization played a role in the survival/extinction of the hypercarnivores, and future work is needed to explore this hypothesis. Yet, the fact that all the survivors belong to a single clade (Sebecidae) prevents us from drawing any definitive reasons for their survival, because it may also simply be attributed to ‘chance’. Finally, our hypotheses about the role of diet and body length on the survival of the Notosuchia at the K-Pg crisis are only supported if the Adamantina Formation is of Campanian-Maastrichtian age, that is, if all species from this formation are considered to have faced this crisis. Given the richness of the notosuchian fossil record, the age of the formation highly influences the macroevolutionary conclusions of this work. This corroborates the arguments of Celis *et al.* (2020) who previously highlighted this Lagerstätten effect. The results of these analyses were largely the same with the two topologies we used. Thus, the phylogenetic placement of the Sebecidae does not seem to have a crucial effect, as long as they are considered monophyletic and part of the Notosuchia.

2.8 Acknowledgments

We would like to thank Mike Benton (University of Bristol, United Kingdom) and Kevin Padian (University of California, United States of America) for reading through the manuscript of this study. We also thank Philip Mannion, Pedro Godoy and an anonymous reviewer for their comments and remarks which strongly improved both the form and the substance of this study.

2.9 Author Contribution

Conceptualization: P Aubier, S Jouve, J Schnyder, J Cubo; **Data Curation:** P Aubier; **Formal Analysis:** P Aubier; **Investigation:** P Aubier; **Methodology:** P Aubier, S Jouve, J Schnyder, J Cubo;

Project Administration: P Aubier, S Jouve, J Schnyder, J Cubo; **Supervision:** J Cubo; **Validation:** P Aubier, S Jouve, J Schnyder, J Cubo; **Visualization:** P Aubier, S Jouve, J Schnyder, J Cubo; **Writing-Original Draft Preparation:** P Aubier; **Writing-Review & Editing:** P Aubier, S Jouve, J Schnyder and J Cubo.

2.10 References

Amiot R., Lécuyer C., Buffetaut E., Fluteau F., Legendre S., Martineau F. 2004. Latitudinal temperature gradient during the Cretaceous Upper Campanian–Middle Maastrichtian: $\delta^{18}\text{O}$ record of continental vertebrates. *Earth and Planetary Science Letters*. 226:255–272.

Bapst D.W. 2012. paleotree: an R package for paleontological and phylogenetic analyses of evolution: Analyses of Paleo-Trees in R. *Methods in Ecology and Evolution*. 3:803–807.

Bapst D.W., Hopkins M.J. 2017. Comparing cal3 and other a posteriori time-scaling approaches in a case study with the pterocephaliid trilobites. *Paleobiology*. 43:49–67.

Bapst D.W., Wright A.M., Matzke N.J., Lloyd G.T. 2016. Topology, divergence dates, and macroevolutionary inferences vary between different tip-dating approaches applied to fossil theropods (Dinosauria). *Biol. Lett.* 12:20160237.

Batezelli A. 2017. Continental systems tracts of the Brazilian Cretaceous Bauru Basin and their relationship with the tectonic and climatic evolution of South America. *Basin Res.* 29:1–25.

Benson R.B.J., Godoy P., Bronzati M., Butler R.J., Gearty W. 2022. Reconstructed evolutionary patterns for crocodile-line archosaurs demonstrate impact of failure to log-transform body size data. *Commun Biol.* 5:171.

Bokma F., Godinot M., Maridet O., Ladevèze S., Costeur L., Solé F., Gheerbrant E., Peigné S., Jacques F., Laurin M. 2016. Testing for Depéret’s Rule (Body Size Increase) in Mammals using Combined Extinct and Extant Data. *Syst Biol.* 65:98–108.

Bronzati M., Montefeltro F.C., Langer M.C. 2015. Diversification events and the effects of mass extinctions on Crocodyliformes evolutionary history. *R. Soc. open sci.* 2:140385.

Brown J.H., Maurer B.A. 1986. Body size, ecological dominance and Cope’s rule. *Nature*. 324:248–250.

Buckley G.A., Brochu C.A. 1999. An enigmatic new crocodile from the Upper Cretaceous of Madagascar. *Cretaceous Fossil Vertebrates*. 60:149–175.

Buckley G.A., Brochu C.A., Krause D.W., Pol D. 2000. A pug-nosed crocodyliform from the Late Cretaceous of Madagascar. *Nature*. 405:941–944.

Buffetaut E. 1990. Vertebrate extinctions and survival across the Cretaceous-Tertiary boundary. *Tectonophysics*. 171:337–345.

Busbey A. 1995. Structural consequences of skull flattening in crocodylians. *Functional morphology in vertebrate paleontology*. Cambridge: Cambridge University Press. p. 173–192.

Campos D.A., Oliveira G.R., Figueiredo R.G., Riff D., Azevedo S.A.K., Carvalho L.B., Kellner A.W.A. 2011. On a new peirosaurid crocodyliform from the Upper Cretaceous, Bauru Group, southeastern Brazil. *An. Acad. Bras. Ciênc.* 83:317–327.

Carvalho I. de S., de Gasparini Z.B., Salgado L., de Vasconcellos F.M., Marinho T. da S. 2010. Climate's role in the distribution of the Cretaceous terrestrial Crocodyliformes throughout Gondwana. *Palaeogeography, Palaeoclimatology, Palaeoecology*. 297:252–262.

Castro M.C., Goin F.J., Ortiz-Jaureguizar E., Vieytes E.C., Tsukui K., Ramezani J., Batezelli A., Marsola J.C.A., Langer M.C. 2018. A Late Cretaceous mammal from Brazil and the first radioisotopic age for the Bauru Group. *R. Soc. open sci.* 5:180482.

Celis A.D., Narváez I., Arcucci A., Ortega F. 2020. Lagerstätte effect drives notosuchian palaeodiversity (Crocodyliformes, Notosuchia). *Historical Biology*. 33:1–10.

Conover W.J., Johnson M.E., Johnson M.M. 1981. A Comparative Study of Tests for Homogeneity of Variances, with Applications to the Outer Continental Shelf Bidding Data. *Technometrics*. 23:351–361.

Cubo J., Aubier P., Faure-Brac M.G., Martet G., Pellarin R., Pelletan I., Sena M.V.A. 2022. Paleohistological inferences of thermometabolic regimes in Notosuchia (Pseudosuchia: Crocodylomorpha) revisited. *Paleobiology*.:1–11.

Cubo J., Sena M.V.A., Aubier P., Houee G., Claisse P., Faure-Brac M.G., Allain R., Andrade R.C.L.P., Sayão J.M., Oliveira G.R. 2020. Were Notosuchia (Pseudosuchia: Crocodylomorpha) warm-blooded? A palaeohistological analysis suggests ectothermy. *Biological Journal of the Linnean Society*. 131:154–162.

- Dias-Brito D., Musacchio E.A., Castro J.C., Maranhão M.S.A.S., Suárez J.M., Rodrigues R. 2001. The Bauru Group: A continental Cretaceous unit in Brazil - Concepts based on micropaleontological, oxygen isotope and stratigraphical data. *Revue de Paleobiologie*. 20:245–304.
- Drumheller S.K., Wilberg E.W. 2020. A synthetic approach for assessing the interplay of form and function in the crocodyliform snout. *Zoological Journal of the Linnean Society*. 188:507–521.
- Felsenstein J. 1985. Phylogenies and the Comparative Method. *The American Naturalist*. 125:1–15.
- Fritz S.A., Purvis A. 2010. Selectivity in Mammalian Extinction Risk and Threat Types: a New Measure of Phylogenetic Signal Strength in Binary Traits: Selectivity in Extinction Risk. *Conservation Biology*. 24:1042–1051.
- Geroto C.F.C., Bertini R.J. 2019. New material of *Pepesuchus* (Crocodyliformes; Mesoeucrocodylia) from the Bauru Group: implications about its phylogeny and the age of the Adamantina Formation. *Zoological Journal of the Linnean Society*. 185:312–334.
- Gobbo-Rodrigues S.R., Petri S., Bertini R.J. 1999. Ocorrências de ostrácodes na formação Araçatuba do Grupo Bauru, Cretáceo Superior da Bacia do Paraná, e possibilidades de correlação com depósitos isócronos argentinos-parte I: família Ilyocyprididae. *Acta Geologica Leopoliensia*. 23:3–13.
- Godoy P.L. 2020. Crocodylomorph cranial shape evolution and its relationship with body size and ecology. *J Evol Biol*. 33:4–21.
- Godoy P.L., Benson R.B.J., Bronzati M., Butler R.J. 2019. The multi-peak adaptive landscape of crocodylomorph body size evolution. *BMC Evol Biol*. 19:167.
- Godoy P.L., Bronzati M., Eltink E., Marsola J.C. de A., Cidade G.M., Langer M.C., Montefeltro F.C. 2016. Postcranial anatomy of *Pissarrachampsia sera* (Crocodyliformes, Baurusuchidae) from the Late Cretaceous of Brazil: insights on lifestyle and phylogenetic significance. *PeerJ*. 4:e2075.
- Godoy P.L., Ferreira G.S., Montefeltro F.C., Vila Nova B.C., Butler R.J., Langer M.C. 2018. Evidence for heterochrony in the cranial evolution of fossil crocodyliforms. *Palaeontology*. 61:543–558.

- Gomani E.M. 1997. A crocodyliform from the Early Cretaceous Dinosaur Beds, northern Malawi. *Journal of Vertebrate Paleontology*. 17:280–294.
- Gould S.J. 1988. Trends as changes in variance: a new slant on progress and directionality in evolution. *J. Paleontol.* 62:319–329.
- Grigg G., Kirshner D. 2015. *Biology and Evolution of Crocodylians*. Melbourne: CSIRO Publishing.
- Harvey P.H., Pagel M.D. 1991. *The comparative method in evolutionary biology*. Oxford: Oxford Univ. Press.
- Ho L. si T., Ané C. 2014. A Linear-Time Algorithm for Gaussian and Non-Gaussian Trait Evolution Models. *Systematic Biology*. 63:397–408.
- Iori F.V., Garcia K.L. 2012. *Barreirosuchus franciscoi*, um novo Crocodylomorpha Trematochampside da Bacia Bauru, Brasil. *Rev. bras. geociênc.* 42:397–410.
- Ives A.R., Garland T. 2010. Phylogenetic Logistic Regression for Binary Dependent Variables. *Systematic Biology*. 59:9–26.
- Jablonski D. 1987. Heritability at the Species Level: Analysis of Geographic Ranges of Cretaceous Mollusks. *Science*. 238:360–363.
- Jouve S. 2021. Differential diversification through the K-Pg boundary, and post-crisis opportunism in longirostrine crocodyliforms. *Gondwana Research*. 99:110–130.
- Jouve S., Menecart B., Douteau J., Jalil N.-E. 2017. Biases in the study of relationships between biodiversity dynamics and fluctuation of environmental conditions. *Palaeontologia Electronica*. 20:22.
- Kellner A.W.A., Pinheiro A.E.P., Campos D.A. 2014. A New Sebecid from the Paleogene of Brazil and the Crocodyliform Radiation after the K–Pg Boundary. *PLoS ONE*. 9:e81386.
- Kingsolver J.G., Pfennig D.W. 2004. Individual-level selection as a cause of Cope’s Rule of phyletic size increase. *Evolution*. 58:1608–1612.

Larsson H.C.E., Gado B. 2000. A new Early Cretaceous crocodyliform from Niger. *njgpa*. 217:131-141.

Larsson H.C.E., Sues H.-D. 2007. Cranial osteology and phylogenetic relationships of *Hamadasuchus rebouli* (Crocodyliformes: Mesoeucrocodylia) from the Cretaceous of Morocco. *Zoological Journal of the Linnean Society*. 149:533–567.

Lloyd G.T., Bapst D.W., Friedman M., Davis K.E. 2016. Probabilistic divergence time estimation without branch lengths: dating the origins of dinosaurs, avian flight and crown birds. *Biol. Lett.* 12:20160609.

Maganuco S., Dal Sasso C., Pasini G. 2006. A new large predatory archosaur from the Middle Jurassic (Bathonian) of Madagascar. *Atti della Società Italiana di Scienze Naturali e del Museo Civico di Storia Naturale di Milano*. 147:19–51.

Mannion P.D., Benson R.B.J., Carrano M.T., Tennant J.P., Judd J., Butler R.J. 2015. Climate constrains the evolutionary history and biodiversity of crocodylians. *Nat Commun*. 6:8438.

Martin J.E., Amiot R., Lécuyer C., Benton M.J. 2014. Sea surface temperature contributes to marine crocodylomorph evolution. *Nat Commun*. 5:4658.

McHenry C.R., Clausen P.D., Daniel W.J.T., Meers M.B., Pendharkar A. 2006. Biomechanics of the rostrum in crocodylians: A comparative analysis using finite-element modeling. *Anat. Rec.* 288A:827–849.

McKinney M.L. 1997. Extinction vulnerability and selectivity: Combining Ecological and Paleontological Views. *Annu. Rev. Ecol. Syst.* 28:495–516.

Melstrom K.M., Irmis R.B. 2019. Repeated Evolution of Herbivorous Crocodyliforms during the Age of Dinosaurs. *Current Biology*. 29:2389-2395.e3.

Montefeltro F.C., Lautenschlager S., Godoy P.L., Ferreira G.S., Butler R.J. 2020. A unique predator in a unique ecosystem: modelling the apex predator within a Late Cretaceous crocodyliform-dominated fauna from Brazil. *J. Anat.* 237:323–333.

Nascimento P.M., Zaher H. 2010. A new species of *Baurusuchus* (Crocodyliformes, Mesoeucrocodylia) from the Upper Cretaceous of Brazil, with the first complete postcranial skeleton described for the family Baurusuchidae. Pap. Avulsos Zool. (São Paulo). 50:323–361.

Newell N.D. 1949. Phyletic Size Increase, An Important Trend Illustrated by Fossil Invertebrates. Evolution. 3:103.

Nicholl C.S.C., Hunt E.S.E., Ouarhache D., Mannion P.D. 2021. A second peirosaurid crocodyliform from the Mid-Cretaceous Kem Kem Group of Morocco and the diversity of Gondwanan notosuchians outside South America. R. Soc. open sci. 8:211254.

Nieto M.N., Degrange F.J., Sellers K.C., Pol D., Holliday C.M. 2022. Biomechanical performance of the cranio-mandibular complex of the small notosuchian *Araripesuchus gomesii* (Notosuchia, Uruguay-suchidae). Anat Rec. 305.

O'Connor P.M., Sertich J.J.W., Stevens N.J., Roberts E.M., Gottfried M.D., Hieronymus T.L., Jinnah Z.A., Ridgely R., Ngasala S.E., Temba J. 2010. The evolution of mammal-like crocodyliforms in the Cretaceous Period of Gondwana. Nature. 466:748–751.

Orme D., Freckleton R., Thomas G., Petzoldt T., Fritz S., Isaac N., Pearse W. 2018. caper: Comparative Analyses of Phylogenetics and Evolution in R.

Ósi A. 2014. The evolution of jaw mechanism and dental function in heterodont crocodyliforms. Historical Biology. 26:279–414.

Paolillo A., Linares O.J. 2007. Nuevos cocodrilos Sebecosuchia del Cenozoico sudamericano (Mesosuchia: Crocodylia). Paleobiologia Neotropical. 3:1–25.

Pennell M.W., Eastman J.M., Slater G.J., Brown J.W., Uyeda J.C., FitzJohn R.G., Alfaro M.E., Harmon L.J. 2014. geiger v2.0: an expanded suite of methods for fitting macroevolutionary models to phylogenetic trees. Bioinformatics. 30:2216–2218.

Pierce S.E., Angielczyk K.D., Rayfield E.J. 2008. Patterns of morphospace occupation and mechanical performance in extant crocodylian skulls: A combined geometric morphometric and finite element modeling approach. J. Morphol. 269:840–864.

Pinheiro A.E., Pereira P.V.L.G. da C., de Souza R.G., Brum A.S., Lopes R.T., Machado A.S., Bergqvist L.P., Simbras F.M. 2018. Reassessment of the enigmatic crocodyliform “*Goniopholis*” *paulistanus* Roxo, 1936: Historical approach, systematic, and description by new materials. PLoS ONE. 13:e0199984.

Pol D. 2005. Postcranial remains of *Notosuchus terrestris* Woodward (Archosauria: Crocodyliformes) from the upper Cretaceous of Patagonia, Argentina. *Ameghiniana*. 42:21–38.

Pol D., Leardi J.M. 2015. Diversity patterns of Notosuchia (Crocodyliformes, Mesoeucrocodylia) during the Cretaceous of Gondwana. *PEAPA*. 15:172–186.

Pol D., Nascimento P.M., Carvalho A.B., Riccomini C., Pires-Domingues R.A., Zaher H. 2014. A New Notosuchian from the Late Cretaceous of Brazil and the Phylogeny of Advanced Notosuchians. PLoS ONE. 9:e93105.

Raia P., Carotenuto F., Passaro F., Fulgione D., Fortelius M. 2012. Ecological specialization in fossil mammals explains Cope’s rule. *The American Naturalist*. 179:328–337.

Rensch B. 1959. *Evolution Above the Species Level*. Columbia University Press.

Riff D., Kellner A.W.A. 2011. Baurusuchid crocodyliforms as theropod mimics: clues from the skull and appendicular morphology of *Stratiotosuchus maxhechti* (Upper Cretaceous of Brazil). *Zoological Journal of the Linnean Society*. 163:S37–S56.

Ruiz J.V., Bronzati M., Ferreira G.S., Martins K.C., Queiroz M.V., Langer M.C., Montefeltro F.C. 2021. A new species of *Caipirasuchus* (Notosuchia, Sphagesauridae) from the Late Cretaceous of Brazil and the evolutionary history of Sphagesauria. *Journal of Systematic Palaeontology*. 19:1–23.

Sellés A.G., Blanco A., Vila B., Marmi J., López-Soriano F.J., Llácer S., Frigola J., Canals M., Galobart À. 2020. A small Cretaceous crocodyliform in a dinosaur nesting ground and the origin of sebecids. *Scientific Reports*. 10:1–11.

Sena M.V.A., Andrade R.C.L.P., Sayão J.M., Oliveira G.R. 2018. Bone microanatomy of *Pepesuchus deiseae* (Mesoeucrocodylia, Peirosauridae) reveals a mature individual from the Upper Cretaceous of Brazil. *Cretaceous Research*. 90:335–348.

- Sereno P., Larsson H. 2009. Cretaceous Crocodyliforms from the Sahara. *ZK*. 28:1–143.
- Sereno P.C., Sidor C.A., Larsson H.C.E., Gado B. 2003. A new notosuchian from the Early Cretaceous of Niger. *Journal of Vertebrate Paleontology*. 23:477–482.
- Simpson G.G. 1953. *The Major Features of Evolution*. New York: Columbia University Press.
- Stanley S.M. 1973. An Explanation for Cope's Rule. *Evolution*. 27:1–26.
- Stockdale M.T., Benton M.J. 2021. Environmental drivers of body size evolution in crocodile-line archosaurs. *Commun Biol*. 4:38.
- Stubbs T.L., Pierce S.E., Elsler A., Anderson P.S.L., Rayfield E.J., Benton M.J. 2021. Ecological opportunity and the rise and fall of crocodylomorph evolutionary innovation. *Proc. R. Soc. B*. 288:10.
- Turner A.H. 2006. Osteology and phylogeny of a new species of *Araripesuchus* (Crocodyliformes: Mesoeucrocodylia) from the Late Cretaceous of Madagascar. *Historical Biology*. 18:255–369.
- Turner A.H., Buckley G.A. 2008. *Mahajangasuchus insignis* (Crocodyliformes: Mesoeucrocodylia) cranial anatomy and new data on the origin of the eusuchian-style palate. *Journal of Vertebrate Paleontology*. 28:382–408.
- Van Valkenburgh B. 2004. Cope's Rule, Hypercarnivory, and Extinction in North American Canids. *Science*. 306:101–104.
- Wilberg E.W. 2017. Investigating patterns of crocodyliform cranial disparity through the Mesozoic and Cenozoic. *Zoological Journal of the Linnean Society*. 181:189–208.
- Wilberg E.W., Turner A.H., Brochu C.A. 2019. Evolutionary structure and timing of major habitat shifts in Crocodylomorpha. *Sci Rep*. 9:10.
- Wu X., Sues H.-D., Sun A. 1995. A plant-eating crocodyliform reptile from the Cretaceous of China. *Nature*. 376:678–680.
- Wu X.-C., Sues H.-D. 1996. Anatomy and phylogenetic relationships of *Chimaerasuchus paradoxus*, an unusual crocodyliform reptile from the Lower Cretaceous of Hubei, China. *Journal of Vertebrate Paleontology*. 16:688–702.

Chapter 3

Phylogeny of Crocodylia

3.1 Foreword

After having developed a working methodology for the use of the PLR to analyse the evolution of palaeodiversity (see Chapter 2), the next objective was to reproduce it on neosuchian clades. We did so on the Tethysuchia (see Concluding remarks) but an issue prevented us from applying it to the Eusuchia. Indeed, most of the diversity of this group is made by the clade Crocodylia. As discussed above (see Chapter 1), the phylogenetic relationships of this group are still highly debated. The use of PCM relies on the assumptions (1) that the topology and (2) that the branch lengths of the tree are known. Neither of these assumptions were met for the Crocodylia. Indeed, two contradicting topologies have been consistently found for this group. The Brevirostres hypothesis (traditionally retrieved by morphological-based studies) in which Crocodyloidea and Alligatoroidea are closer to each other than to Gavialoidea, and the Longirostres hypothesis (traditionally retrieved by molecular-based studies) in which Crocodyloidea and Gavialoidea are closer to each other than to Alligatoroidea. The initial project was to produce a new phylogeny of the group in which we could have a high level of confidence. This phylogeny would then be used to perform PLR analysis on the Crocodylia. We planned visits to museum collections to critically review already published morphological characters, and to use the three-taxon analysis (3ta) to produce a robust phylogeny. However, a new phylogeny of the Crocodylia was published in 2021 (Rio & Mannion, 2021). This gave us the opportunity to work on an almost exhaustive dataset rather than on a new matrix produced by ourselves which, given the amount of time available, would have necessarily included less taxa and characters. Rio & Mannion (2021) carried out a complete review of the morphological characters and its taxonomic sampling was almost exhaustive. We thus developed a new methodology to assess phylogenetic support from the matrix. This task took the final year of my PhD. The initial objective (performing PLR analyses on the Crocodylia) unfortunately had to be dropped. The following work was submitted to the *Systematic Biology* journal in November 2023.

New perspectives in phylogenetic support assessment: the case of crocodylia

Paul Aubier¹, Valentin Rineau¹, Jorge Cubo¹ & Stéphane Jouve¹

¹ Sorbonne Université, Muséum national d'Histoire naturelle, CNRS, Centre de Recherche en Paléontologie de Paris (CR2P), 4 place Jussieu, 75005 Paris;

3.2 Abstract

The phylogenetic relationships of the Crocodylia have been highly debated in the past decades. The conflict revolves around the phylogenetic placement of gavialoids which are either the sister group of all other crocodylians (Brevirostres hypothesis) or, in a more nested position, the sister group of Tomistominae (Longirostres hypothesis). Identifying the differential contribution of the taxa and characters from the original matrix to the two competing hypotheses could help to determine the precise causes of incongruence. In parsimony, a phylogeny is the result of the interaction between all the characters during the analysis; we cannot therefore discuss the information carried by a single character, or a single taxon. Consequently, the link between the characters from the matrix and those as optimized on the tree can be lost. Thus, all methods aimed at measuring support only do so indirectly and the effect of individual character or taxa can only be assessed *a posteriori* of the analysis. These methods cannot explain why a given matrix produces a specific topology in the first place. In this study, we show how three-taxon analysis (3ta) can circumvent all these issues to precisely measure the support from the matrix from Rio & Mannion (2021). In 3ta, characters are coded as trees exactly as phylogenies and decomposed into three-taxon statements (3ts). The analysis is searching for the largest ensemble of non-contradicting minimal character hypotheses to compute the optimal phylogeny. Because the analysis is not an optimization procedure, but rather a compatibility one, character supports on the tree are independent from one another. This makes the assessment of support directly from the matrix both possible and relevant to explain the topology of the optimal trees. Moreover, the decomposition of characters into 3ts allows to quantify precisely the results. We show that the Longirostres hypothesis, despite being the best-supported one, is highly contradicted being only 1.6 times more supported than the Brevirostres hypothesis. Second, we show that the Tomistominae provide 61% of the supporting evidence of this hypothesis, such that, when removed, the matrix supports Brevirostres better. Furthermore, the contri-

bution of individual tomistomines only varies between 2% to 7% of the total support to the Longirostres hypothesis. We were, therefore, able to show that the result depends on the amount of Tomistominae species added to the taxonomic sampling, and that on average, the addition of only three Tomistominae is enough to shift towards the Longirostre hypothesis. Finally, we tested the effect of characters correlated to longirostry. We found that despite showing more support to the Longirostres relatively to the Brevirostres than the other characters, they play a minor role (22%) at the scale of the whole matrix.

Keywords: Crocodylia, Three-taxon analysis, phylogenetics, support.

3.3 Introduction

Crocodylia is the crown group of the extant crocodyliforms. It includes approximately 140 species, 26 of which are extant (Grigg & Kirshner, 2015) and is defined as the least inclusive clade including all Crocodyloidea, Gavialoidea and Alligatoroidea (Brochu *et al.*, 2009). The systematics of Crocodylia have been debated during the past three decades. Morphological cladistic analyses have traditionally pleaded for the grouping of Crocodyloidea and Alligatoroidea (Brevirostres) relative to Gavialoidea, considering Tomistominae as a basal crocodyloid (*e.g.* Norell, 1989; Brochu, 1997a,b; Salisbury *et al.*, 2006; Jouve *et al.*, 2015). On the other hand, according to phylogenetic studies using molecular data, Crocodyloidea and Gavialoidea (Longirostres) are more closely related to each other than either is to Alligatoroidea, considering *Tomistoma schlegelii* (the only extant representative of Tomistominae) as a basal gavialoid (*e.g.* Densmore, 1983; Densmore & Owen, 1989; Harshman *et al.*, 2003; Pan *et al.*, 2021). This conflict can be reduced to the phylogenetic position of the Gavialoidea: they are either the sister group of all the other crocodylians (Brevirostres) or they are included in a more nested node, forming the sister group of Crocodyloidea (Longirostres). In the first hypothesis, Gavialoidea includes a single subfamily, the Gavialinae, whereas in the second hypothesis, they also include the Tomistominae. Several studies have shown that Tomistominae might play a central role in this conflict. Indeed, when Gavialinae are considered to be the sister group of Tomistominae, within the Longirostres hypothesis, the interpretation of morphological data leads to a high number of reversals occurring in the Gavialinae (Gatesy, 2003). This has led some to hypothesize that this group shows a remarkable atavistic pattern. For instance, Iijima & Kobayashi (2019) described East Asian tomistomines that exhibit some of these ‘gavialine-specific’ atavistic character states, bridging the morphological gap between gavialines and tomistomines and therefore reinforcing the Longirostres hypothesis. As soon as 1985, it was proposed that if reinterpreted, morphological data could support the grouping of Gavialinae and Tomistominae (Buffetaut, 1985). It has long been recognized that there is an overall conservatism and a tendency toward parallel evolution and convergences within Crocodylia (Sill, 1968; Langston, 1965; Langston, 1973; Tarsitano *et al.*, 1989). Therefore, the conflict between morphological and molecular data might stem from undetected homoplasy in the formers. Thus, characters that initially supported groupings that contradict the Longirostres hypothesis may be reinterpreted in such a way that they are congruent with the groupings pleaded by the molecular data. This view has recently been supported by several

works. Ristevski *et al.* (2020, 2023) showed that all “morphological gavialoids” are closely related to tomistomines. Sookias (2020), focusing on extant species and character coding, demonstrated the influence of the outgroup choice on the results, and found that when reassessed, morphological matrices can yield topologies closer to the DNA tree. Rio & Mannion (2021) produced a new morphological dataset after having critically reviewed published ones (see Rio & Mannion, 2021, Table 1 and reference therein). This new matrix produced, using parsimony analyses, optimal trees supporting the Longirostres hypothesis. However, in these works, the molecular hypothesis for the dating of the clade Gavialoidea is incompatible with the fossil record, the oldest specimen known in the fossil register being much more older than the age given by molecular dating. This has led to hypothesize that ancient Late Cretaceous–Early Palaeogene gavialoids representatives were a distinct lineage (thoracosaurids), wrongly grouped with Gavialoidea because of a convergent adaptation of these two groups to piscivory (Gatesy *et al.*, 2003; Harshman *et al.*, 2003; Velez-Juarbe *et al.*, 2007; Lee and Yates, 2018; Ristevski *et al.*, 2020, 2023; Sookias, 2020). Lee & Yates (2018), using combined morphological and molecular data and Tip Dating method, is the sole study to retrieve the Longirostres hypothesis with thoracosaurids outside Crocodylia. All these results do not provide clear explanations of the reasons behind the origins and the persistence of this conflict. Indeed, although performing a return to the characters and analysing their optimization on the optimal tree provides knowledge regarding the role of each of them, it only does so *a posteriori* of the analysis: it does not shed light on the reasons why the analysis retrieved this particular optimal tree in the first place. Interpreting character optimizations on a specific tree is not the same thing as understanding why these characters produced such a tree. The former allows to know the optimization of a given character on the tree on which the whole matrix is best optimized (*i.e.* on which the number of transformation steps is minimized), and the latter should allow to know why it is so. The former is a result, the latter is the explanation of this result. Therefore, to understand the results from Rio & Mannion (2021), it is necessary to be able to investigate precisely which groupings are supported by each character or set of characters *a priori* of the analysis. In parsimony, the most simple estimate of grouping support is the branch length (*i.e.* the number of transformation steps; Bremer, 1994). However, because all steps do not necessarily provide similar support (*e.g.* homologous characters can be considered to provide greater support than homoplastic ones, Bremer, 1994), simply relying on branch lengths could be misleading (Bremer, 1994). Bremer (1988, 1994) proposed Branch Support (BS) as a

way to circumvent this problem. BS relies on the number of extra steps necessary to collapse a branch rather than on its mere length. Other support indices like the Bootstrap (Felsenstein, 1985) and the Jackknife (Farris *et al.*, 1996) are based on dataset perturbations. The former works by randomly overweighting or suppressing characters from the matrix whereas the latter randomly suppresses a given number of characters. However, BS, Bootstrap and Jackknife only provide a measure of global support. Indeed, despite providing support values at the node level (and not at the whole tree level), these indices always refer to the matrix as a whole because they rely on the results retrieved by the analysis with the whole matrix (or modified matrices in the case of Bootstrap and Jackknife). Hence, they cannot be used to assess the support of a targeted character or set of characters. Trueman (1988), proposed the Reversed Successive Weighting (RSW) as a way to distinguish and rank competing ‘hierarchical signals’ that represent different sets of characters which states are hierarchically congruent and therefore support the same groupings. Testing the RSW on Crocodylia using the dataset from Brochu (1997a), Trueman (1988) showed that, although the first signal (*i.e.* the largest set) supported the Breviostres, there was a secondary signal (*i.e.* the second largest set) supporting the Longirostres hypothesis. However, despite being more precise in that it can target the grouping(s) supported by specific sets of characters, RSW is similar to BS, Bootstrap and Jackknife in that it does not actually measure support from the matrix. Indeed, it follows essentially the same procedure as the two latter: secondarily changing the content of the matrix and observing the changes in the resulting trees. As shown by Goloboff *et al.* (2003), character interaction in parsimony produces post-hoc hypotheses: if the states of a character are not hierarchically congruent with the tree supported by the other characters, they can be reinterpreted as convergence/reversion. Convergences and reversions, as newly made hypotheses, provide additional steps that can (and will) participate in the support of groupings in the final tree(s). However, because these hypotheses (of convergence/reversion) were not made in the original matrix, such characters can support groupings in the final trees they did not support initially. Because character optimization during a parsimony analysis is dependent on the other characters included in the matrix, removing or adding characters might change the optimization of a given character and therefore change the groupings it supported prior to the removal/addition of characters. As such, a direct measure of support from the matrix prior to the analysis is irrelevant because groupings on the final tree are likely to be supported by data not originally present in the matrix. Thus, in parsimony, the support provided by a given

character or set of characters can only be assessed *a posteriori* of the phylogenetic analysis. This has led Goloboff *et al.* (2003) to state that “essentially all methods to measure support do so indirectly” (p.326). To summarize, because of character interactions, measuring grouping support in parsimony faces three difficulties: first, the removal of any taxa/character can change the optimization of any other therefore complicating the interpretations of the results; second, the relevancy of targeted taxa/character can only be assessed *a posteriori* of the procedure; third, results from this procedure are binary (the topology will change or not), thus providing no information on changes in the relative amounts of supporting evidence. We propose here a phylogenetic support assessment protocol that can circumvent all these issues by using three-taxon analysis (3ta), an alternative cladistic method to parsimony. Its methodological specificity (see the following section) makes it possible to assess grouping support from the character directly from the matrix, *a priori* of the analysis. Therefore, using this method, it is possible to investigate the reasons why a given set of characters produces a given optimal tree. Here, we exemplify our protocol using 3ta by producing a detailed analysis of the phylogenetic content from Rio & Mannion (2021) character matrix. We will focus on the Longirostres/Brevirostres node and the effect of Tomistominae by showing how the method stated here can answer why Longirostres or Brevirostres is raised given Rio & Mannion (2021) matrix. First, we present the methodological characteristics of the 3ta and explain how they make it suitable for phylogenetic support assesment. Second, we detail how we produced a 3ta phylogeny of the Crocodylia using the matrix from Rio & Mannion (2021). Finally, we present and discuss the phylogenetic support provided (1) by the whole matrix, (2) by the Tomistominae, (3) by the different anatomical parts of the crocodylian skeleton and (4) by characters considered to be correlated to longirostry.

3.4 Materials and Methods

3.4.1 *Three-taxon analysis(3ta)*

The 3ta was first introduced by Nelson & Platnick (1991). In 3ta, characters are coded hierarchically and decomposed into three-taxon statements (3ts). Optimal trees are recovered via the search of the larger set of compatible 3ts (*i.e.* the max-clique). Initially presented merely as a more precise way to use parsimony, it now constitutes an entirely different method from parsimony (Nelson *et al.*, 2003; Cao *et al.*, 2007; Zaragüeta-Bagils & Bourdon, 2007; Zaragüeta-Bagils *et al.*, 2012). Since the beginning of the 3ta, there has been extensive literature debating the pros and cons of this method relative to parsimony (Harvey, 1992; Farris *et al.*, 1995; Nelson & Ladiges, 1996; Platnick *et al.*, 1996; Farris & Kluge, 1998; Zaragüeta-Bagils & Bourdon, 2007; Farris, 2012) for phylogenetic inference. The aim of this study is not to take place within this debate. The 3ta method is used here as a tool to precisely and reliably quantify support directly from the matrix. 3ta is a method that maximizes the congruency through clique analysis of minimal phylogenetic statements. Any 3ts that support groupings incongruent with those supported by the max-clique are refuted and do not participate in the construction of the tree (Nelson & Platnick, 1991). Because of the exclusion of homoplastic hypotheses, the tree is constructed solely by hypotheses (3ts) that succeeded in the test of congruence. The decomposition of characters into minimal units, *e.g.* ‘atoms’ of cladistic information, allows to analyse and quantify precisely their content. It is thus possible to trace the support of a given group on the tree back to the data matrix and therefore to precisely assess the amount of information that supports a given grouping from each character and taxa. In the following section, we present the main characteristics of 3ta.

3.4.2 *Characters in 3ta*

Parsimony recovers unrooted trees, the polarization of the character only being performed *a posteriori* of the analysis. Because of that, the characters are coded as a set of mutually exclusive character states (Farris, 1970; Colless, 1985; Pimentel & Riggins, 1987; Pogue & Mickevich, 1990), a structure that is called in mathematics a partition. Particular cases like missing data (multiple states are possible), polymorphism (multiple states are present) or non-applicable data (no state is possible) are all treated the same way: the attribution of a single state following the optimization of the number of steps (Zaragüeta-

Bagils & Bourdon, 2007). In 3ta, characters represent clade(s) hypotheses and as such, like phylogenies, are coded as rooted hierarchies (Zaragüeta-Bagils & Bourdon, 2007). Each character state is either a differentiation (apomorphic state) of a more general one, or is included in the root (plesiomorphic state) (Nelson, 1978; Nelson & Platnick, 1981). The necessity of providing explicit hierarchical relationships between character states implies that the polarization of the character needs to be performed prior to the analysis. This can be done by relying on an outgroup (that can be different for each character) or on other sources (*e.g.* ontogeny, see Nelson, 1978). Even though 3ta characters are not partitions, they can still be coded in a two-dimensions table (*i.e.* a matrix) but with an additional row in which the hierarchical relationships between the states of each character can be stated in a Newick format (Cao *et al.*, 2007).

3.4.3 *Three-taxon statements (3ts)*

Hierarchical characters constitute both grouping and relationship hypotheses (Prin, 2015). As such, they can be decomposed into minimal assertions stating that of three taxa, two are more closely related to each other than either is to the third (hence, *three-taxon* statements). Indeed, for a binary character X , if taxa a and b are ‘0’ (plesiomorphic state) and taxa c and d are ‘1’ (apomorphic state), this character is congruent with the hypothesis that c and d are closer to each other than either is to a and b (in virtue of them sharing an apomorphic state absent from c and d) which is equivalent to the parenthesis notation $(ab(cd))$. This statement can be decomposed into two 3ts: (1) c and d are closer to each other than either is to a , and (2) c and d are closer to each other than either is to b . Decomposing characters into 3ts allows one to retain more information from the matrix during the analysis (Nelson & Platnick, 1991). Indeed, the character X is incongruent with the relationship $d(bc)$, but only partially. $d(bc)$ contradicts the second 3ts $b(cd)$, yielded by character X . However, it is compatible with the first 3ts $a(cd)$. In the congruency test phase, if $d(bc)$ is compatible with more 3ts than $b(cd)$, that is the clique that includes $d(bc)$ is larger than that which includes $b(cd)$, only the latter will be refuted. The other 3ts yielded by the character X , $a(cd)$, will not be refuted if it does not contradict any 3ts included in the same clique that includes $d(bc)$. Performing the analysis on 3ts, therefore, allows refuting only the fraction of the character that is incongruent with the max-clique, while keeping the fraction that is congruent, instead of refuting the character as a whole. The fact that a character can be only partially incongruent

with a grouping hypothesis can result, for instance, from a state having been wrongly attributed to a taxa, or by the fact that one or several taxa underwent reversals or convergences. In such cases, the grouping hypotheses (3ts) implied would contradict those yielded by the state attributed to the other taxa. Working at the level of the 3ts allows to decipher these contradicting signals and to put them aside without removing the whole content of the character. A most important feature of the 3ta is that any 3ts, whether it is retained in the final tree or not, can be traced back to the character it originates from. It is therefore possible to assess and quantify the contribution of each character to the tree, to any specific node of the tree or more generally to any relationship between three parts (whether these parts are species or more general groups).

3.4.4 *Fractional weighting*

In the example of character X above, the implied 3ts were independent (neither can be deduced from the other). However, dependency can happen, leading to redundancy among the set of phylogenetic statements. If we take a binary character Y $a(bcd)$ for which taxa a is '0' (plesiomorphic state) and b , c , and d are '1' (apomorphic state), it implies three 3ts: $a(bc)$, $a(bd)$ and $a(cd)$. Contrary to character X , there is a redundancy occurring within the same state (here character state 1) in the implied 3ts: any two of them are sufficient to logically deduce the third. As such, the amount of information given by the three 3ts is identical to that given by only two of them. To take charge of this redundancy, Nelson & Ladiges (1992) proposed to assign a fractional weight (fw) to each 3ts. Because in the case of character Y there are three implied 3ts that as a whole provide as much information as two 3ts, each should be assigned a fw of $2/3$. Rineau *et al.* (2021) showed that in addition to this redundancy among character states, a redundancy between character states can occur in characters with informative states nested in each other. They provided a fractional weighting procedure that took both kinds of redundancy in charge, which was followed in this study. The number of 3ts rescaled by the fractional weighting is considered here as the appropriate measure of supporting evidence.

3.4.5 *Measuring support in 3ta*

Because 3ts are structured as phylogenetic relationships, checking which ones are compatible with a given phylogenetic hypothesis and which ones are not is trivial. Regarding the relationships investigated here,

it is thus possible to check which 3ts implied by the characters from a given matrix are compatible with the Longirostres or with the Brevirostres hypotheses. This allows to decipher which character supports which topological (relationship) hypothesis and to quantify this support. Any hierarchical topology T can be decomposed into the set of implied 3ts $t(T)$. In hierarchical coding, each character can be assimilated to a tree-like hypothesis. Consequently, any hierarchical character can be decomposed into 3ts. Let's take $C = \{C_1, \dots, C_i\}$ a set of non-empty hierarchical characters; $t(C)$ is the set of 3ts deduced from C , and $|t(C)|_{fw}$ is the sum of the fractional weights of all the 3ts implied by C . Then, for a set T containing one topology, $|t(T) \cap t(C)|_{fw}$ corresponds to the quantification of the support from the matrix to the tree T in terms of independent phylogenetic hypotheses. Golobof & Farris (2001) proposed that relative support, *i.e.* the amount of favourable evidence for a topology relative to the favourable evidence for an alternative, contradicting one, is a better measure. Simply comparing the 3ts in agreement with a given phylogeny with those which contradict it would nonetheless be misleading. Indeed, the 3ts in agreement with a given phylogeny are all compatible with each other by definition. However, this is not the case of the set of 3ts in conflict with the phylogeny, because there are multiple ways to contradict it. For instance, the relationship $a(bc)$ conflicts with two 3ts: $b(ac)$ and $c(ab)$. For any of these three mutually exclusive incompatible statements, there are virtually twice as many contradicting 3ts than supporting ones. The ratio between the fractional weights (fw) of 3ts supporting and contradicting a relationship hypothesis could thus be inferior to 0.5 even if this grouping was the most supported in the matrix. Therefore, the ratio between two sets of 3ts supporting contradicting topologies would accurately measure the relative amount of support to a phylogeny compared to another. We present here the Contradiction Index (CI), a metric that computes such a relative support by measuring the amount of conflict using minimal cladistic statements (more precisely, of 3is fractional weights). Let's take T_a and T_b two conflicting topologies on the same terminal taxa. The support to T_a compared to that of T_b in a given matrix can be measured simply by computing the ratio of $|t(T_a)|_{fw}$ over $|t(T_b)|_{fw}$. However, some 3ts deduced from a character could be compatible with both hypotheses. These shared 3ts need to be removed because the aim of the CI is to quantify the contradiction between the two hypotheses. Therefore, the Contradictory Index of T_a compared to T_b would be equal to:

$$CI_{T_a/T_b} = \frac{|A - (A \cap B)|_{fw}}{|(A - (A \cap B)) + (B - (A \cap B))|_{fw}}$$

with $A = t(T_a) \cap t(C)$ and $B = t(T_b) \cap t(C)$. This index varies from 0 to 1. If greater than 0.5 then T_a is more supported than T_b (and reciprocally if lower than 0.5). If $CI = 1$, it means that there are 3ts supporting T_a in the matrix, but none supporting T_b . If $CI = 0$, it means that no 3ts are supporting T_a (but it doesn't say anything about the support of T_b). If no 3ts support either topology, the CI cannot be computed as the denominator would be equal to 0. The topology of the optimal tree retrieved in a phylogenetic analysis is by definition the most supported one in the matrix (in 3ta). Computing the CI between the optimal tree and the second most supported would adequately measure how the optimal phylogeny is supported relatively to its best 'contestant'. A CI value close to 0.5 for a specific topology means that the matrix holds a lot of contradiction (hence, *Contradiction Index*) whereas a value close to 1 would signal a large consensus in the matrix. The CI is a useful measure that can be used to provide a wide range of information. If T_a and T_b are respectively the optimal tree and the second optimal tree, the CI will quantify how closely their respective supports are. But T_a and T_b are not necessarily dichotomous phylogenies. For example, we can test the support of one clade in relation to another; we can also test the relationship between three known clades. Thus, T_a and T_b can be understood as two alternative backbone topologies (the only condition is that both must have the same taxonomic sampling).

3.4.6 *Phylogenetic dataset*

We used Rio & Mannion (2021) dataset. Following these authors, we defined *Bernissartia fagesii* as the outgroup. First, we reviewed this dataset and corrected 16 character states from 9 characters (see Supplementary File S3.1a). Second, to perform the 3ta analyses, the coding of the characters was changed to a hierarchical representation. This transformation of character representation was made without modifications (except for those mentioned above) of the original matrix from Rio & Mannion (2021). The use of 3ta requires *a priori* explicit polarization. Indications from Rio & Mannion (2021, Appendix 2) were followed when available. As an example, and considering '0' as the plesiomorphic state according to the outgroup, binary characters $0 \rightarrow 1$ were coded (0,(1)). For a character

<i>a</i>	0
<i>b</i>	0
<i>c</i>	1
<i>d</i>	1

the hierarchical coding (0,(1)) allows to explicitly deduce the relationship ($a, b, (c, d)$) (Cao *et al.* 2007). The character is thus a cladistic relationship hypothesis. The plesiomorphic state 0 is interpreted as the root, and the state 1 is interpreted as a differentiation from 0 stating that c is closer to d than to a and b . A multistate ordered character with four states $0 \rightarrow 1 \rightarrow 2 \rightarrow 3$ is coded (0,(1,(2,(3))))), and the same character unordered is coded (0,(1),(2),(3)). When no indications were available for the polarization of a given character, it was left unpolarized, with all states branching in the root. For example, an unordered character with four states and without polarisation information is coded as ((0),(1),(2),(3)). Finally, continuous characters were removed because hierarchical relationships are intrinsically discrete and qualitative. Matrices used for parsimony and 3ta analyses are available in Supplementary Files S3.1b and S3.1c, respectively.

3.4.7 *Phylogenetic analyses*

Because we amended the matrix from Rio & Mannion (2021), new analyses needed to be performed to assess the taxonomic content of crocodylian subgroups. A parsimony analysis was performed on the amended matrix (Supplementary File S3.1b) to ensure that the modifications we made (see above) did not substantially change the topology of the retrieved optimal trees regarding the Longirostres/Brevirostres conflict. The heuristic algorithm from PAUP v4.0a165 (Swofford & Sullivan, 2003) was used, with a set maxtrees of 500,000 trees and a simple addition sequence. A 3ta analysis was also performed on the hierarchical matrix (Supplementary File S3.1c). The decomposition of hierarchical characters into 3ts was performed using Agatta v0.7.15 (Rineau & Zaharias, 2022, <https://github.com/vrineau/Agatta>) and the tree search was performed using the heuristic algorithm from PAUPv4.0a165 (Swofford & Sullivan, 2003) with 50 replicates. A strict consensus was then computed. This was achieved using the following command into Agatta “>agatta analysis Matrixname.hmatrix -software=paup -chartest -consensus=strict -replicates=50 -analysis=heuristic”. The taxonomic contents of crocodylian clades were acknowledged on this consensus, following the same definitions of Rio & Mannion (2021, Table 1 and references therein). However, numerous species classically considered to be members of the Tomistominae were retrieved outside of this group. Indeed, nine gavialoid species placed outside of the Tomistominae in the 3ta consensus we produced (see Result section) were found to be members of this group in recent studies (Jouve *et al.*, 2015; Weems, 2018; Iijima & Kobayashi, 2019; Salas-Gismondi *et al.*, 2022): *Gavialosuchus eggen-*

burgensis, *Paratomistoma courti*, *Penghusuchus pani*, *Thecachampsa antiquus*, *Thecachampsa sericodon*, *Tomistoma dowsoni*, *Tomistoma cairensis*, *Tomistoma lusitanica* and *Toyotamaphimeia machikanensis*. This difference between our results and those of most of the published ones regarding the taxonomic content of the Tomistominae poses an issue. Indeed, both the Longirostres and Brevirostres hypotheses deal with the phylogenetic placement of this group (either included in the Gavialoidea or the Crocodyloidea, respectively). Therefore, the quantifications in support of both topologies will be affected by the taxonomic content of this group. Considering the nine aforementioned species as non-tomistomine would contradict the consistent results of most published studies. We thus chose to consider these nine species to be part of it. For clarity purposes, this ‘literature compatible’ Tomistominae group will be referred to as ‘Tomistominae’ in this study. Consequently, ‘Gavialoidea’ will refer to the group of the Gavialoidea as retrieved in our analysis but excluding all ‘Tomistominae’ members. Finally, secondary analyses were performed in 3ta and parsimony following the same protocol as the first ones after having removed the ‘Tomistominae’ from the taxa sample.

3.4.8 *Measuring the overall support from the matrix*

This study aims to investigate the phylogenetic conflict that stems from whether ‘Gavialoidea’ are grouped with the ‘Tomistominae’(see previous section) as the sister group of Crocodyloidea (Longirostres), or if they are branched more basally, as the sister group to all the other crocodylians (Brevirostres). In both the Longirostres and Brevirostres hypotheses, a relationship is not debated: all Crocodyloidea and Tomistominae are always closer to each other than either is to Alligatoidea. Because this relationship is undebated in this conflict, we did not discuss it and did not explore hypotheses that contradicted it. However, with the (A,(C,T)) relationship as the backbone tree (here and after, in the parenthesis format, A = Alligatoidea, C = Crocodyloidea, G = ‘Gavialoidea’ and T = ‘Tomistominae’), the Longirostres and Brevirostres hypotheses are only two out of five different hypotheses. Each of the five possible hypotheses, as well as the implied relationship for each, are represented in Figure3.1. The relationship (A,(C,T)) is the only one common to all five hypotheses. Other relationships are shared by multiple hypotheses (e.g. (G,(C,T)) is shared by *S2*, *S3* and Brevirostres, Fig. 3.1) but not all, and each hypothesis (except *S2*) implies at least one unique relationship not implied by any other hypothesis (see bold groupings in **Fig. 1**). Thus, each collection of four relationships is necessary and sufficient

to define a specific hypothesis. Support for each hypothesis (given definitions above of Alligatoroidea, Crocodyloidea, ‘Gavialoidea’ and ‘Tomistominae’) was measured using R v4.0.3 (R development Core Team, 2016) and Agatta. Because (A,(C,T)) is common to all five relationship hypotheses, 3ts supporting this relationship can be discarded as they will be common to all hypotheses. The R script is available in Supplementary File S3.2.

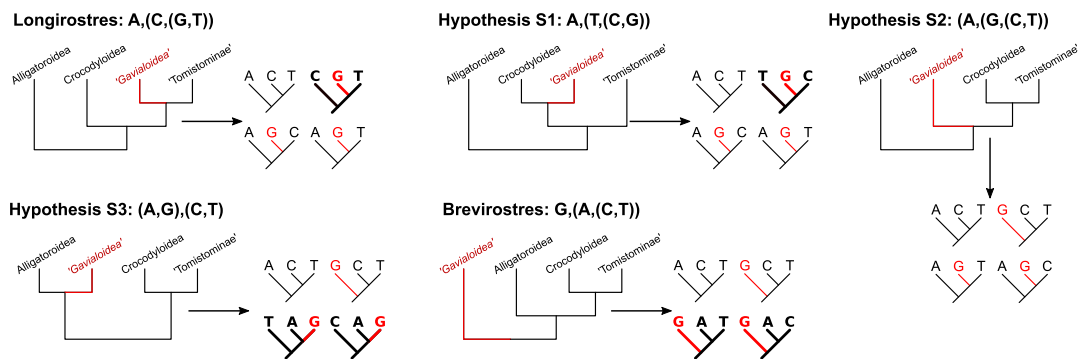


Figure 3.1: The five hypotheses corresponding to the possible phylogenetic placements of the ‘Gavialoidea’ if Crocodyloidea and ‘Tomistominae’ are considered to be closer to each other than either is to Alligatoroidea. For each hypothesis, the implied 3ts are given. In bold are those that are specific to a single hypothesis. A: Alligatoroidea; C: Crocodyloidea; ‘G’: ‘Gavialoidea’ and T: ‘Tomistominae’ (see main text)

3.4.9 Measuring the effect of ‘Tomistominae’

As stated above (see Introduction), Tomistominae has been at the centre of attention regarding the conflict under investigation here. Using 3ta, the support provided by this group can be precisely assessed by selecting from the statements deduced from the matrix only those that include at least one of their members. However, by doing so the impact of the ‘Tomistominae’ is only measured at the scale of the whole group. The individual contribution of each ‘Tomistominae’ member in the support of both the Longirostres and Brevirostres hypotheses was thus also assessed by selecting only the 3ts that both include a ‘Tomistominae’ and support one of the two hypotheses (see again Fig. 3.1).

3.4.10 Disparity in support among characters

Tracing back each 3ts to the character they come from, using the tripdec function from Agatta (command line: “>agatta tripdec Matrixname.hmatrix -detailed tripdec”), allowed us to compute the support pro-

vided by each character to the Longirostres and Brevirostres hypotheses (see Supplementary File S3.3a). Given the large number of characters, we considered anatomical groups of characters, *i.e.* sets of characters described at predetermined anatomical regions, to make the results more intelligible. We adopted the categories from Rio & Mannion (2021, Appendix 2). Consistently, characters and their associated 3ts, resulting from their decomposition, were grouped into five categories: Skull, Mandible, Postcranial, Soft tissue and Osteoderms. The support of a given category to each hypothesis was calculated by summing the fw of each 3ts originating from characters included in this category. We focused on the 3ts which played a role in discriminating Longirostres and Brevirostres hypotheses. We also investigated the effect of 'Tomistominae' for each anatomical category following the same method as in the previous section. The list of characters included in each category is available in Supplementary File S3.3b.

3.4.11 *Assessing the effect of 'Longirostrine' characters*

Rio & Mannion (2021) listed 22 characters that were identified as correlates of longirostry (*i.e.* 'longirostrine' characters) by Jouve (2009) and Groh *et al.* (2020). By analysing the set of 3ts deduced from the phylogenetic matrix, it is possible to measure the contribution of specific taxa but also of specific characters to the support of a given grouping. To test whether these characters highly contributed to their result, they performed a secondary analysis after having removed them. The fact that they retrieved final trees supporting the Longirostres hypothesis using a matrix lacking these 22 characters led them to consider that this result is "unrelated to longirostry" (p.58). However, as for taxa, this procedure only provides qualitative results: the topology might or might not change. They only showed that the evidence originating from these 'longirostrine characters' is not sufficient to change the results when removed. Using 3ta, it is however possible to precisely measure the support coming from 'longirostrine' characters and to quantify it. To do so, support to Longirostres and Brevirostres was measured for each character. We then compared the support values of 'longirostrine' characters (excluding continuous ones, see Phylogenetic Analyses section, n = 17) with those of 'non-longirostrine' characters (*i.e.* the other characters). $CI_{Longirostres}$ (see above) were also calculated for both sets of characters.

3.5 Results

3.5.1 *3ta and parsimony phylogenetic analyses*

The final matrix includes 304 characters (35 are ordered) and 144 taxa. The decomposition of the characters yielded 1,252,709 3ts (see Supplementary File S3.4a) and added up to 364,325 fw from which 221,915.51 have been retained (see Supplementary File S3.4b) for computing the optimal trees, resulting in a retention index of $\frac{221,915.51}{364,325} = 60.91$. The 3ta analysis retrieved three optimal trees, the consensus of which is illustrated in Figure 3.2a. It is well resolved, including only one apical polytomy between three species of *Borealosuchus*, and supports the Longirostres hypothesis. According to this result, the Alligatorioidea super-family includes 60 species, the Crocodyloidea includes 42 species and the Gavialoidea includes 33 species, five belonging to the Tomistominae. The ‘Tomistominae’ and ‘Gavialoidea’ (see Methods section) include 14 and 19 species, respectively. The parsimony analysis retrieved 500,000 optimal trees (*i.e.* the settled maxtree). The consensus, like that of the 3ta analysis and Rio & Mannion (2021)’s most discussed one (see Rio & Mannion, 2021, analysis 1.3, Figure 10), also supports the Longirostres hypothesis, with the Crocodyloidea and Gavialoidea (including the Tomistominae) being closer to each other than either is to the Alligatorioidea (Fig. 3.2b). Analyses performed in 3ta and parsimony after the removal of the ‘Tomistominae’ both support the Brevirostres hypothesis (Fig. 3.2c). The 3ta analysis found a single optimal tree whereas the parsimony analysis found again the maximum number of optimal trees (500,000). The complete consensuses of Figure 3.2b-c as well as the optimal trees of each analysis can be found in Newick and pdf formats in Supplementary Files S3.5a-S3.5h.

3.5.2 *Overall Support from the Matrix*

Overall support for each hypothesis is represented in Figure 3. The low retention index of 60.91 is already a first clue of the intensity of conflict. It indicates that on all phylogenetic statements from the matrix, 39.09% has been rejected during the analysis. When looking more precisely at the competing hypotheses, Longirostres is the most supported one (25,143.63 fw). This is expected because the results of both the parsimony and 3ta phylogenetic analyses retrieved optimal trees supporting it. Our quantification of cladistic relationships shows however unexpectedly that Brevirostres is not the second best-supported hypothesis, but the fourth. The phylogenetic placement of ‘Gavialoidea’ (1) as the sister group of the

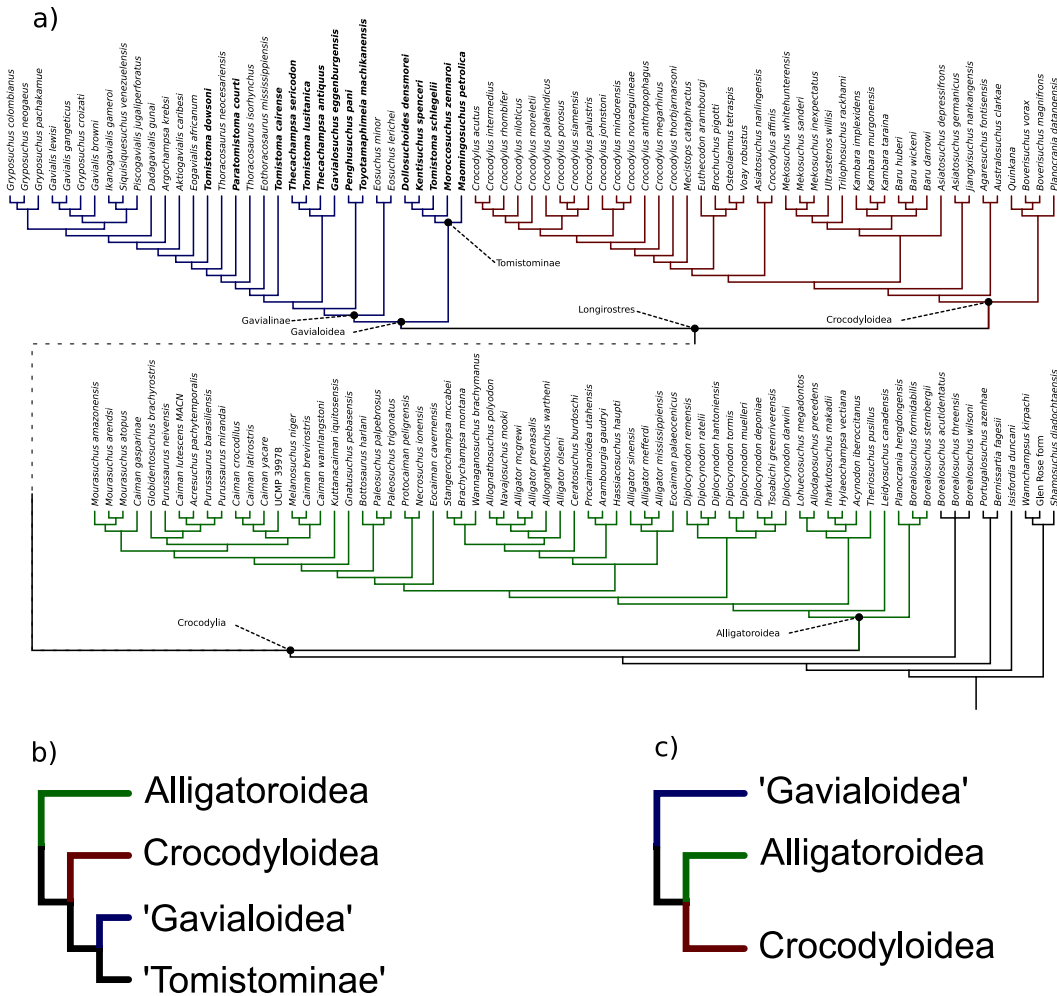


Figure 3.2: a) Strict consensus tree of the primary analysis in 3ta including the ‘Tomistominae’ (see main text) in bold. b) Simplified topology of the strict consensus of the parsimony analysis including the ‘Tomistominae’. c) Simplified topology of the strict consensuses of both the 3ta and parsimony analysis excluding the ‘Tomistominae’.

clade Crocodyloidea + ‘Tomistominae’ (S_2) or (2) as the sister group of Crocodyloidea (S_1) are more supported (21,132.821 and 19,827.732 fw, respectively). This is because hypotheses S_2 and S_1 share with Longirostres the two heavily supported relationships (A,(C,G)) and (A,(G,T)), with supports of 9,419.407 fw and 9,423.226 fw (Figure 3.3), respectively. These two relationships are by themselves more supported than the whole Brevirostres hypothesis. Consequently, S_2 and S_1 are respectively the second and the third most supported hypotheses. Brevirostres only comes fourth (15,736.321 fw), and S_3 fifth and last (11,153.283 fw, 44% of the support to Longirostres).

From these positive support values, relative support can easily be calculated. As stated above, the 3ts shared by two topologies are not considered when computing the Contradictory Index. Therefore,

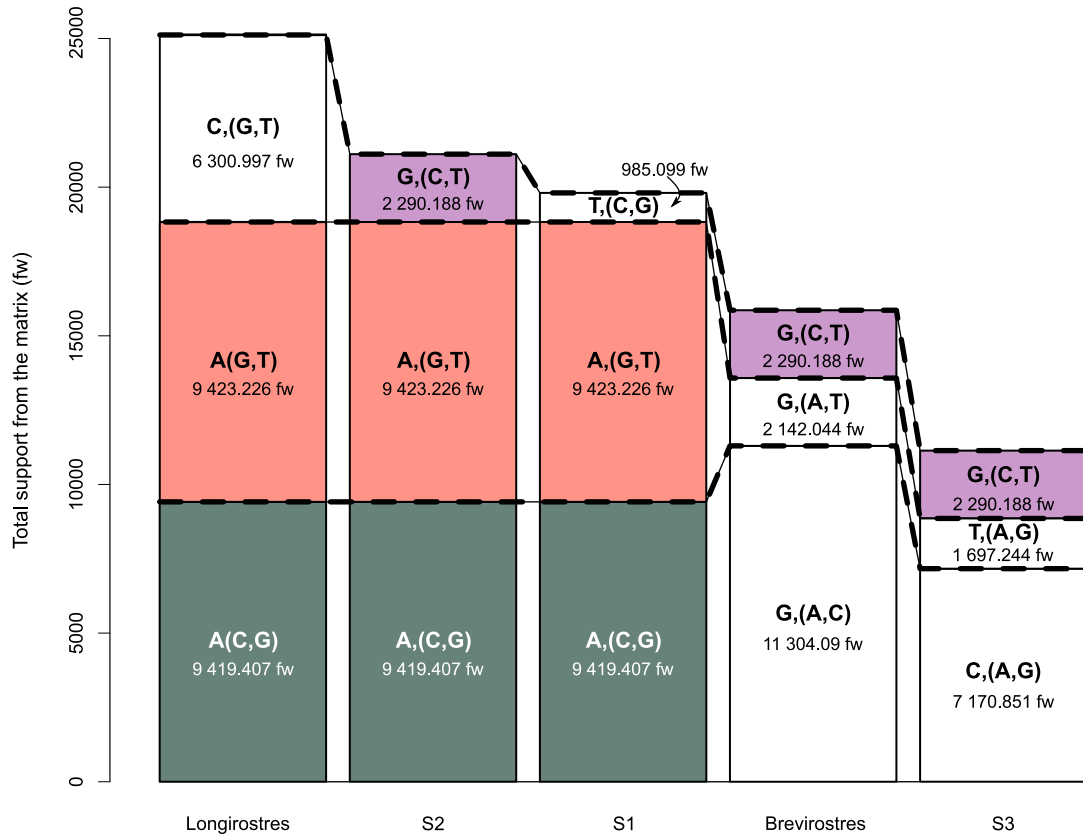


Figure 3.3: Overall support (in fw: fractional weights) from the complete matrix to the 5 hypotheses with the detailed contribution of each 3ts. Colours indicate the sharing of identical general 3ts by different hypotheses. A: Alligatoroidea, C: Crocodyloidea, G: ‘Gavialoidea’ (see main text) and T: ‘Tomistominae’ (see main text). Bold dotted lines separate the 3ts that deal with the same three taxa.

comparing Longirostres and $S2$ means comparing the $(C,(G,T))$ and $(G,(C,T))$ relationships that are supported by 6,300.997 and 2,290.180 fw, respectively. Thus:

$$CI_{Longirostres/S2} = \frac{|L - (L \cap S2)|_{fw}}{|(L - (L \cap S2)) + (S2 - (L \cap S2))|_{fw}} = \frac{6,300.997}{6,300.997 + 2,290.180} \approx 0.73$$

with L the 3ts from the matrix we used that support the Longirostres hypothesis and $S2$ the 3ts that support $S2$. When compared with $S1$, this index ≈ 0.86 . However, when compared with the Brevirostres hypothesis,

$$CI_{Longirostres/Brevirostres} = \frac{25,143.63}{25,143.63 + 15,736.321} \approx 0.62$$

3.5.3 Assessing the effect of ‘Tomistominae’

‘Tomistominae’ as a whole provides 15,724.223 fw in support of the Longirostres hypothesis and 4,432.232 fw in support of the Brevirostres one, which corresponds to a $CI_{Longirostres/Brevirostres} \approx 0.75$. Thus,

in the complete matrix, the ‘Tomistominae’ contributes to 63% (15,724.223 fw out of 25,143.63 fw) of the support to Longirostres and 28% (4,432.232 fw out of 15,736.321 fw) of the support to Brevirostres. This explains the results of the secondary analyses excluding the ‘Tomistominae’ (Fig. 3.2). Figure 3.4 shows the contribution to the whole matrix of each member of ‘Tomistominae’ in terms of support to both Longirostres and Brevirostres. Detailed results are available in Supplementary File S3.6. The mean individual contribution to the support to Longirostres (green bars, Fig. 3.4) is of 4.47% (sd = 1.4). It ranges from the lowest 1.6% of *Parastomistoma courti* to the highest 7.1% contribution of *Thecachampsa sericodon*. The mean individual contribution to Brevirostres (orange bars, Fig. 3.4) is, as expected, lower (2%, sd = 0.9). The lowest contribution is again that of *P. Courti* (0.8%) and, the highest, that of *Tomistoma schlegelii* (3.6%). *Maroccosuchus zennaroi* is the only ‘Tomistominae’ to provide more support to Brevirostres than to Longirostres, both contributions being nonetheless very similar. *Maomingosuchus petrolica*, *Kentisuchus spenceri* and *T. schlegelii*, to a lesser degree, also show a high level of conflict.

3.5.4 *Disparity in Support Between Anatomical Categories*

Figure 3.5 shows the proportions of supporting evidence for the Longirostres and Brevirostres hypotheses in each category. The Skull, Soft tissue and Osteoderms are the only categories with uneven supporting evidence. Indeed, 62.60% of the fractional weights from skull characters 3ts support the Longirostres hypothesis. This value is 58.20% for the Osteoderms category. On the contrary, 65.36% of the fractional weights from Soft tissue character 3ts support the Brevirostres hypothesis. The other two categories (Mandible and Post-cranial) show very balanced support, although the Longirostres hypothesis is slightly best supported in both (55.72% and 53.54%, respectively). Figure 3.6 illustrates the same information as Figure 3.5 but in absolute fractional weights. It shows that the 3ts from the skull characters provide the vast majority of the fractional weights supporting Longirostres (21,691.435 fw, or 86.27% of total support, Fig. 3.6) and Brevirostres (12,960.097 fw, or 82.36%, Fig. 3.6), which is expected given the substantial amount of character this category includes (see below). The Mandible is the second category to yield the most supporting evidence but it only accounts for 10.61% (2,677.168 fw) and 13.52% (2,127.646 fw) of total support to Longirostres and Brevirostres, respectively. The contribution of characters described at the post-cranial skeleton (1.86% for Longirostres against 0.09% for Brevirostres), soft tissues (>0.01%

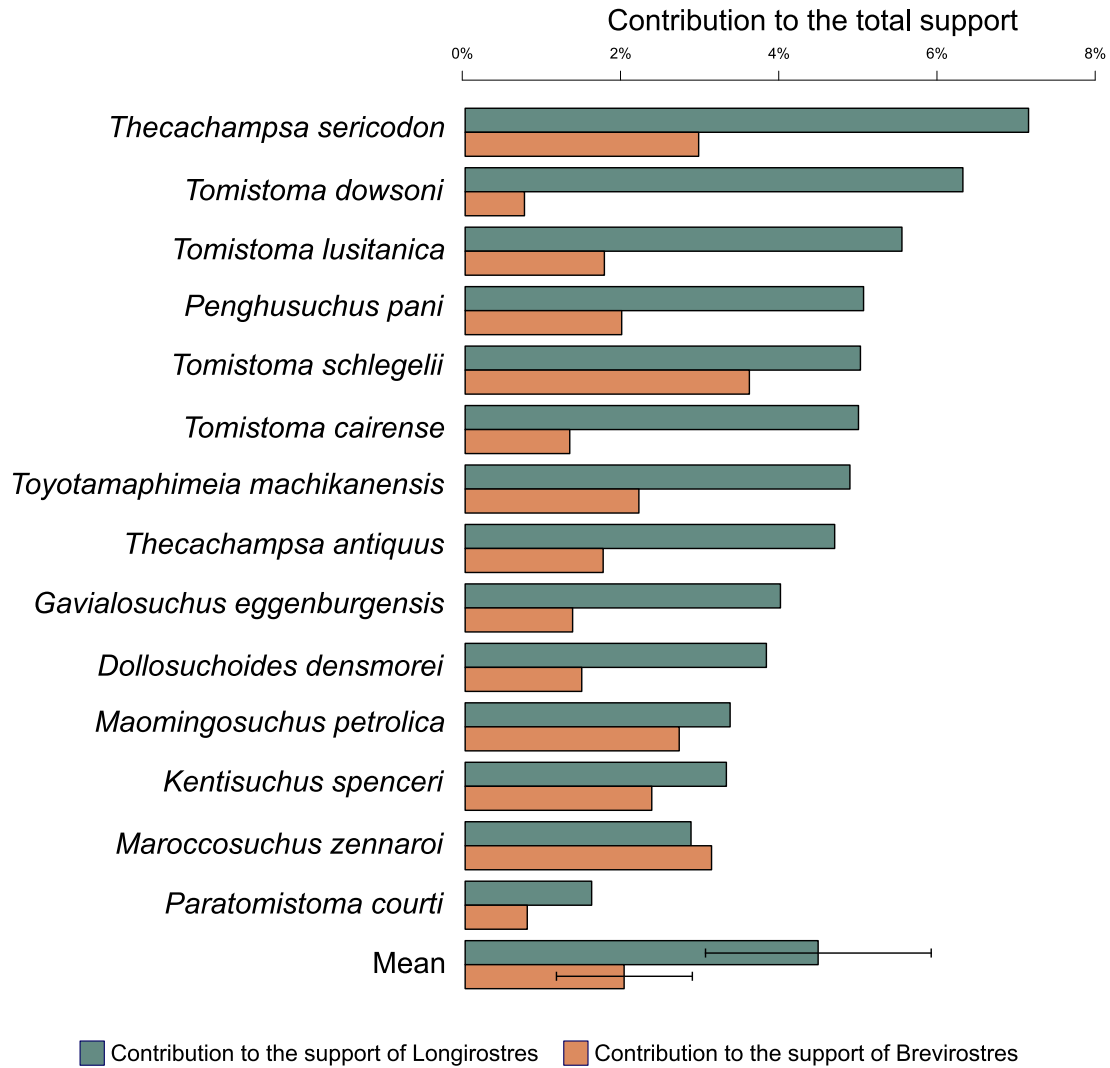


Figure 3.4: Contribution (in %) of each member of the ‘Tomistominae’ to the support of the Longirostres hypothesis (green bars) and Brevirostres hypothesis (orange bars).

against 2.97%) and osteoderms (1.16% against 1.86%) are marginal. Detailed results can be found in Supplementary File S3.7.

Our results showed that most of the support for the Longirostres hypothesis is provided by the ‘Tomistominae’ (61 %, see previous section). Here we assess the fraction of the support for both hypotheses that is accounted for by the ‘Tomistominae’ in each anatomical category. Figure 3.7 shows that, except for the Soft Tissue category, the contribution of the ‘Tomistominae’ in support of Longirostres (green bars, Fig. 3.7) is always higher than that in support of Brevirostres (orange bars, Fig. 3.7). Consequently, when no ‘Tomistominae’ is included in the taxa sample, all categories show more support to the Brevirostres than to the Longirostres hypothesis with very similar relative supports (Fig. 3.5b).

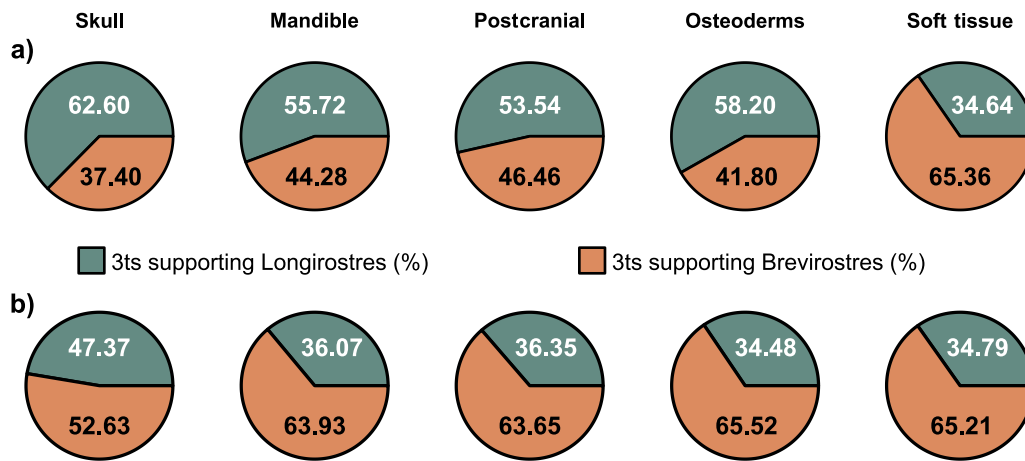


Figure 3.5: Relative support to Longirostres (green) and Brevirostres (orange) of the five anatomical categories when ‘Tomistominae’ are including (a) or excluded (b) from the taxa sample.

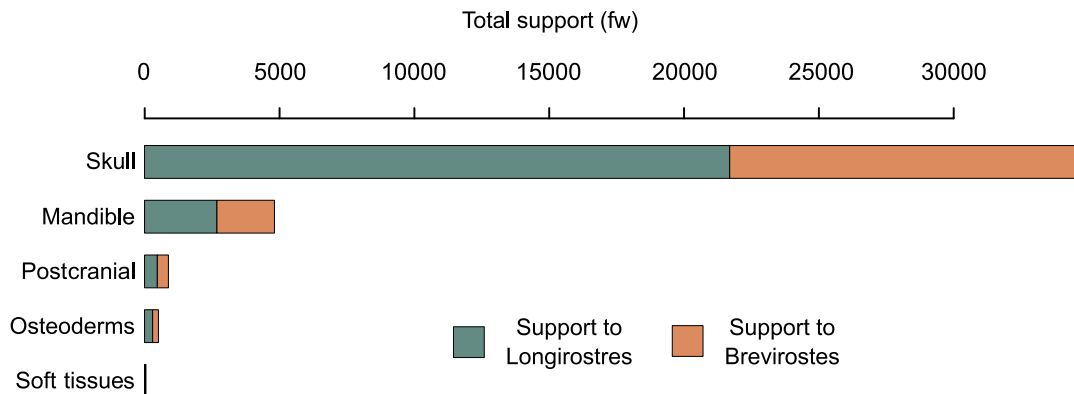


Figure 3.6: Absolute support (in fw) to Longirostres (green) and Brevirostres (orange) of the five anatomical categories.

The most unequal contributions concern the Mandible category, in which the contribution in support of Longirostres is 3.21 times that of support to Brevirostres, and the Osteoderms category in which this ratio is 2.59. It is slightly lower for the Postcranial and Skull categories (2.28 and 1.87, respectively). In every category except the Soft tissues one, ‘Tomistominae’ accounts for more than 60% (mean = 64%, $sd = 0.02$, see Supplementary File S3.7) of the support to Longirostres. On the other hand, they account for a minor part of the support to Brevirostres in these categories (mean = 0.27 %, $sd = 0.06$). Their contribution is least in the Soft tissues category in which they account for $\approx 14\%$ of the support to both hypotheses. It should be noted, however, that those relative contributions translate into very different absolute contributions in terms of the amount of fractional weights. Indeed, the fraction of the support to Longirostres from the Skull category that is accounted by the ‘Tomistominae’ (62%) corresponds to

13,091.87 fw whereas it only represents 1,688.07 fw in the Mandible category (in which this contribution is of 63%). Finally, the Soft tissues category is the only one in which both contributions are similar with a ratio of 0.96. This result is due to the fact that *Tomistoma schlegelii* is the only ‘Tomistominae’ for which these structures have been coded in the matrix we used (Rio & Mannion, 2021). As such, the fraction of support from this category accounted by the ‘Tomistominae ($\approx 14\%$ for both hypotheses) is actually accounted solely by this single species.

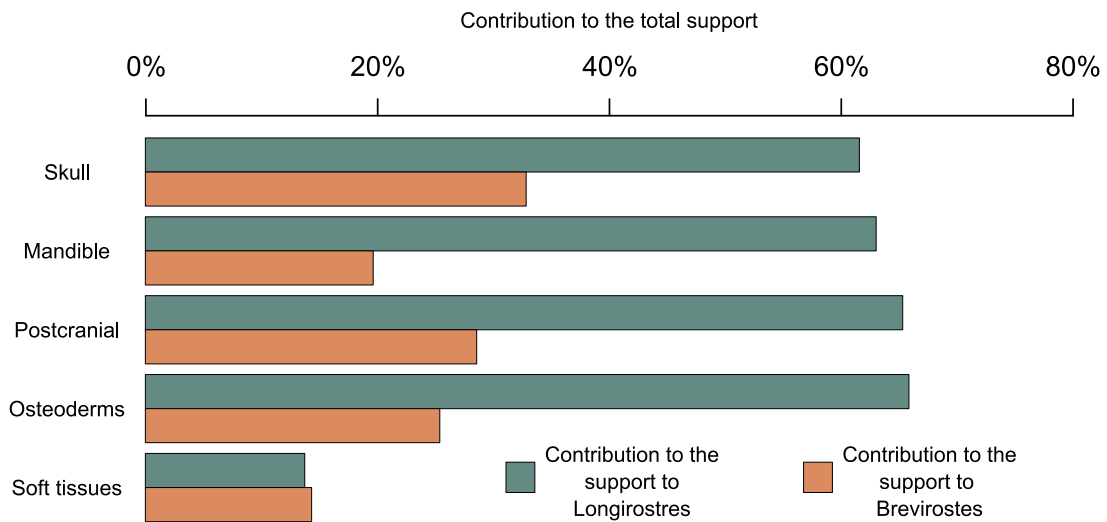


Figure 3.7: Contribution (in %) of the ‘Tomistominae’ to the support to Longirostres (green) and Brevirostres (orange) in the five anatomical categories.

3.5.5 Assessing the effect of ‘Longirostrine’ characters

Table 1 summarizes the quantification in terms of support provided by ‘longirostrine’ and ‘non-longirostrine’ characters. The formers provide 5,654.80 fw (22% of the supporting evidence to the Longirostres hypothesis from the whole matrix) in support of Longirostres and 2,946.42 fw (19%) in support of Brevirostres. For comparison, all other characters provide 19,487.79 and 12,783.09 fw in support of Longirostres and Brevirostres, respectively (larger amounts being due to a higher number of characters, $n = 200$). A ‘longirostrine’ character provides on average more evidence in support of Longirostres than others (245.86 fw vs 67.43 fw respectively). However, the same conclusion appears when looking at the Brevirostres support (128.11 fw vs 44.23 fw). Still, the $CI_{Longirostres/Brevirostre}$ of ‘longirostrine’ characters is higher (0.66) than that of ‘non-longirostrine’ ones (0.60).

Table 3.1: Support provided by ‘longirostrine’ and ‘non-longirostrine’ characters. All values are in fractional weights. In brackets are the standard deviation for the mean values.

	‘Longirostrine’ char. (n=17)	‘non-longirostrine’ char. (n=200)
Longirostres (total)	5,654.80	19,487.79
Longirostres (mean)	245.86 (sd = 332.94)	67.43 (sd = 178.64)
Bevirostres (total)	2,946.42	12,783.09
Bevirostres (mean)	128.11 (sd = 207.60)	44.23 (sd = 100.97)

3.6 Discussion

The fact that both methods (parsimony and 3ta) retrieved congruent optimal trees regarding the Longirostres/Brevirostres hypotheses both including and excluding the ‘Tomistominae’ shows that the difference in character coding (from partitions in parsimony to inclusive hierarchies in 3ta) do not impact this outcome. Therefore, investigating the support in 3ta can be used to draw conclusions relevant also to parsimony analyses. According to our results, the $S2$ and $S1$ hypotheses are better supported than the Brevirostres one. The computations of the CI explain why both of these phylogenetic hypotheses are not often retrieved in previously published phylogenetic analyses. With (A,(C,G)) and (A,(G,T)) as backbone relationships, Longirostres is much more supported than either $S1$ or $S2$ ($CI_{Longirostres/S1} = 0.86$ and $CI_{Longirostres/S2} = 0.73$). Furthermore, the $CI_{Longirostres/Brevirostres}$ value shows that although Longirostres is the most supported hypothesis, it is highly contradicted in the matrix when compared to the Brevirostres one, the support to the former being only 1.6 times that of the latter. The assessment of support via the decomposition of general relationships hypotheses into minimal relationships shows that the Longirostres hypothesis is better supported than the Brevirostres one because of the ‘Tomistominae’ (Fig. 3.3). Indeed, when discarding the relationships that include the ‘Tomistominae’, the relationship (A,(C,G)), implied by the Longirostres hypothesis, is actually less supported than (G,(A,C)), implied by the Brevirostres one (9,419.407 vs 11,304.09 fw, Fig. 3.3). If no ‘Tomistominae’ species are included in the taxa sample, both hypotheses would be solely defined by these two relationships and $CI_{Longirostres/Brevirostres} \approx 0.45$. Thus, the larger support for Longirostres is due to the phylogenetic placement of the ‘Tomistominae’ and more precisely, the relationship between ‘Tomistominae’, Alligatoroidea, and Gavialoidea (more than the relationship between ‘Tomistominae’, Crocodyloidea, and Gavialoidea) is decisive for the analysis. Longirostres is better supported than Brevirostres first because (A,(G,T)) is better supported (9,423.226 fw) than either of the two other possible relationships (2,142.044 and 1,697.244 fw, Fig. 3), and second because (C(G,T)) is also the best-supported relationship (6,300.997 fw) compared to the two other possibilities (2,290.188 and 985.099 fw, Fig. 3.3). Consequently, without ‘Tomistominae’, Brevirostres becomes the best-supported hypothesis. Our methodology allowed us to precisely quantify the magnitude of the effect of this group. Indeed, we showed that it provides 63% of the total support to the Longirostres hypothesis from the matrix. On the other hand, their contribution to the support of the Brevirostres hypothesis is only 28%. Thus, when the ‘Tomistominae’ are removed

from the analysis, the total phylogenetic information is logically decreasing (in terms of weighted triplets extracted from the matrix), concerning both statements supporting the Brevirostres and Longirostres hypotheses (losses of 28% and 63%, respectively). However, the information given by the characters supporting the Longirostres one falls drastically and becomes less than the total remaining amount of information supporting the Brevirostres hypothesis. Therefore, using 3ts matrix analysis, it becomes possible to add quantifications to the qualitative result that the supported relationships have changed. These results shed light on why the behaviour of analyses with and without Tomistominae is changing this way (Fig. 3.2), allowing precise quantification of the effect of differential taxonomic sampling. We were also able to assess the contribution of each member of 'Tomistominae'. Our results show that the contribution of the whole group is not reducible to that of one member. Indeed, this group accounts for 63% of the fractional weights supporting the Longirostres hypothesis while *T. sericodon*, which is the largest contributor only accounts for 7.1% of it. Therefore, rather than a specific species, this is globally the number of 'Tomistominae' included in the analysis that is essential. An analysis including too few 'Tomistominae' would be highly biased toward the Brevirostres hypothesis. On average (*i.e.* if each 'Tomistominae' species contribution is 1,123.920 fw in support of Longirostres, 4.47% of the total, and of 314.726 fw in support of Brevirostres, 2% of the total), the inclusion of three 'Tomistominae' in the taxonomic sampling is sufficient to shift the best-supported hypothesis from Brevirostres to Longirostres (12,791.167 fw in support to the latter and 12,248.268 fw in support to the former). In the context of sampling modifications that drastically change the outcome of a phylogenetic analysis, we are thus able to locate precisely the origin of the changes, explain the behaviour of the analyses, and quantify the impact of the taxonomic sampling on the results. It is, therefore, the characterisation of the origin of these conflicting relationships between these crocodylian major clades that promises to be a fruitful avenue of investigation for understanding the conflict within the Crocodylia. We also assessed the disparity in terms of provided support between characters dealing with different anatomical parts of the skeleton. Out of Figures 3.5 and 3.6, there seems to be a general congruency, four anatomical categories out of five of them supporting more Longirostres than Brevirostres (Fig. 3.5a). However, the fact that the Skull category (and the Osteoderms one, to a lesser extent) is the only one to show a marked preference toward Longirostres tends to temper this. Indeed, with relative supports of each hypothesis close to 50%, the Mandible and Postcranial categories reflect more the internal contradiction in support between

these two hypotheses than clearly showing that one prevails over the other. The broad support of the Soft tissue category to Brevirostres stands out compared to the other categories. It is the only one to provide more support to the Brevirostres hypothesis, by a strong margin (65.36%). The analysis of the relative supports provided by the anatomical categories can thus provide insights for targeting characters or groups of characters that stand out. In our case, nonetheless, the variations in provided supports between anatomical are marginal and play a minor role in the final result of the phylogenetic analysis. Indeed, the Skull category represents 64% of the characters from the matrix used here, reflecting the numerous characters hypothesized. As such the overall signal from the matrix is largely driven by the morphology of the skull, the Mandible, Postcranial, Osteoderms and Soft tissues categories accounting for respectively 16%, 14%, 4% and 2% of all characters. Additionally, Skull characters include less missing/inapplicable data (25%) than characters from the other categories (Mandible: 47%, Postcranial: 62%, Osteoderms: 73% and Soft tissue: 80%), inflating even more the weight of skull morphology. The result of this asymmetry that has direct consequences in terms of phylogenetic content can be measured in 3ta. The Skull category accounts for 86.27% of the total fractional weights of 3ts supporting Longirostres and 82.36% of that supporting Brevirostres (Fig. 3.6). This shows that the effect of postcranial characters regarding the Longirostres/Brevirostres conflict is marginal. Sookias (2020) pointed out that controversial phylogenetic placement can rely on very few characters, even in large matrices. The need for and the relevancy of postcranial characters have been recently assessed for crocodylians and other crocodyliforms (Pol *et al.*, 2012; Blanco *et al.*, 2014; Blanco *et al.*, 2015; Leardi *et al.*, 2015; Iijima & Kobayashi, 2019; Rio *et al.*, 2019 and Blanco, 2021). Our results suggest that such developments would not help in resolving the conflict under investigation here as an enormous amount of new postcranial characters would need to be hypothesized for them to play a part in it. Furthermore, the marginality of postcranial morphology is most probably not explained only by the lack of characters but also by the large amount of missing data in the fossil record. Our results showed that most of the support for the Longirostres hypothesis was provided by the ‘Tomistominae’ (63%). Here we assess the fraction of the support for both hypotheses that is accounted for by the ‘Tomistominae’ in each anatomical category. Figure 3.7 shows that, except for the Soft Tissue category, the contribution of the ‘Tomistominae’ in support of Longirostres (green bars, Fig. 3.7) is always higher than that in support of Brevirostres (orange bars, Fig. 3.7). Consequently, when no ‘Tomistominae’ is included in the taxa sample, all categories show

more support to the Brevirostres than to the Longirostres hypothesis with very similar relative supports (Fig. 3.5b). The most unequal contributions concern the Mandible category, in which the contribution in support of the Longirostres hypothesis is 3.21 times that of support of the Brevirostres one, and the Osteoderms category in which this ratio is 2.59. It is slightly lower for the Postcranial and Skull categories (2.28 and 1.87, respectively). In every category except the Soft tissues one, the ‘Tomistominae’ account for more than 60% (mean = 64%, sd = 0.02, see Supplementary File S3.7) of the support of the Longirostres hypothesis. On the other hand, they account for a minor part of the support of the Brevirostres hypothesis in these categories (mean = 0.27%, sd = 0.06). Their contribution is least in the Soft tissues category in which they account for $\approx 14\%$ of the support to both hypotheses. It should be noted, however, that those relative contributions translate into very different absolute contributions in terms of amount of fractional weights. Indeed, the fraction of the support to Longirostres from the Skull category that is accounted by the ‘Tomistominae’ (62%) corresponds to 13,091.87 fw whereas it only represents 1,688.07 fw in the Mandible category (in which this contribution is of 63%). Finally, the Soft tissues category is the only one in which both contributions are similar with a ratio of 0.96. This result is due to the fact that *Tomistoma schlegelii* is the only ‘Tomistominae’ for which these structures have been coded in the matrix we used (Rio & Mannion, 2021). As such, the fraction of support from this category accounted by the ‘Tomistominae’ ($\approx 14\%$ for both hypotheses) are actually accounted solely by this single species. These results show that overall, the effect of the ‘Tomistominae’ is similar in all categories (except in the Soft tissues one). Furthermore, when they are excluded from the quantifications, the supports provided by the Mandible, Postcranial and Osteoderms categories are almost identical to those provided by the Soft tissues one (Fig. 3.5b). Thus, the differences between the Soft tissue category (strong support to the Brevirostres hypothesis), the Mandible, Postcranial and Osteoderms one (almost similar support to both hypotheses) and the Skull one (strong support to the Longirostres hypothesis) can be explained by the quantity of ‘Tomistominae’ evidence present in each category. The Skull and the Soft tissue ones are at both end of the spectrum (very high number of character states coded on ‘Tomistominae’ species for the former, very low for the latter) while the three others lie in-between. We showed that ‘longirostrine’ characters provide greater support to the Longirostres hypothesis compared to the Brevirostres hypothesis than ‘non-longirostrine’ ones. Nonetheless, the $CI_{Longirostres/Brevirostres} \approx 0.62$ when all characters are included (see Results section) and ≈ 0.60 when ‘longirostrine’ characters are

removed. Therefore, ‘longirostrine’ characters only contribute to 3.2% of the CI Longirostres in the complete matrix. As such, we can confirm Rio & Mannion’s (2021) hypothesis: the results of the 3ta and parsimony analyses retrieving the Longirostres hypothesis can be said to be largely unrelated to the evidence yielded by these ‘longirostrine’ characters. To change the topology from Longirostres to Brevirostres when removed from the matrix (*i.e.* dropping the $CI_{Longirostres/Brevirostres}$ below 0.5), the contribution from ‘longirostrine’ characters to the $CI_{Longirostres/Brevirostres}$ would need to be at least six times larger (19%) than it is. These results have two explanations. First, we highlight that the ‘longirostrine’ characters list from Rio & Mannion (2021) does not include many of the characters that provide the highest evidence in support of the Longirostres hypothesis. Figure 3.8 displays the contribution of all the characters to both hypotheses, sorted by their contribution to the Longirostres one (excluding characters that do not contribute to the Longirostres nor the Brevirostres hypothesis). For example, our methodology used herein is able to highlight that despite not being included in the ‘longirostrine’ characters list, character 151 from Rio & Mannion (2021) which describes the occlusion pattern between dentary and maxillary teeth provides the most support to the Longirostres hypothesis out of all characters (1,757.38 fw, Fig. 3.8, see Supplementary File S3.3a for the detailed contribution of each character). Second, this list of ‘longirostrine’ characters also includes 5 characters (the characters number 30, 37, 90, 219 and 220 from Rio & Mannion, 2021, see Fig. 3.8) out of 17 that provide more support to Brevirostres than to Longirostres. This is explained by the fact that for almost all of these characters, Rio & Mannion (2021) identified the plesiomorphic state ‘0’ as correlated with longirostry. If these characters can be interpreted in 3ta on a tree as being affected by reversals, this conclusion can only be accepted *a posteriori* from the analysis, as the fundamental cladistic information for these characters originally coded in the matrix does not support it (Nelson, 1996; Nelson & Ladiges, 1996; Nelson *et al.*, 2003; Platnick *et al.*, 1996; Siebert & Williams 1998; Williams & Ebach, 2005; Zaragüeta & Bourdon, 2007). In a compatibility framework (on 3ts) such as ours, we can only depart statements that have been accepted from those that have been rejected. This framework is precisely the one that allows us to analyse the phylogenetic content hidden in the matrix, contrary to optimization procedures such as in parsimony.

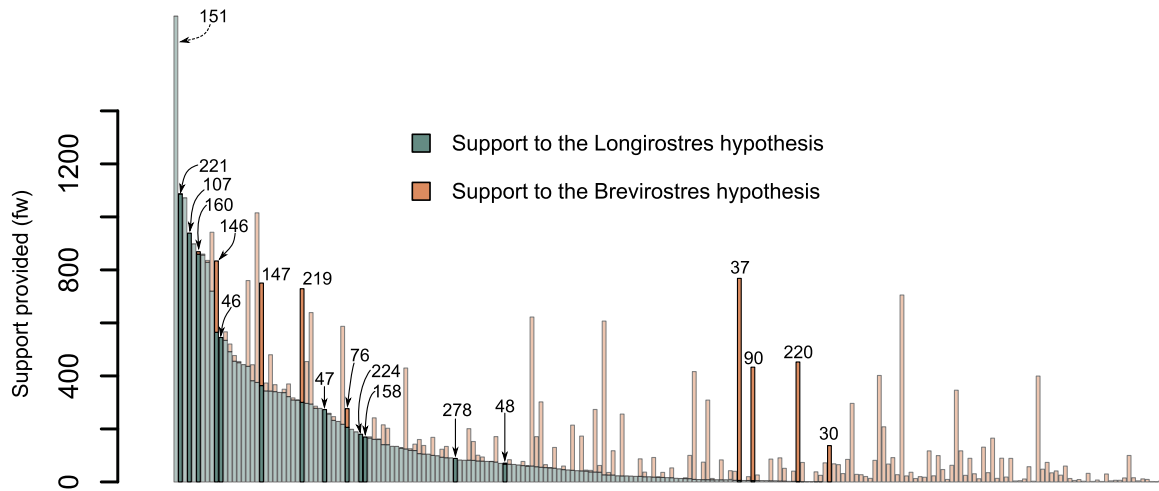


Figure 3.8: Support (in fw) provided by each character to the Longirostres (green bars) and the Brevirostres (orange bars) hypotheses. ‘Longirostrine’ characters (see main text) are highlighted. Characters are sorted by their support to the Longirostres hypothesis. Characters that provided no support to any hypothesis are excluded.

3.7 Conclusions

In parsimony, the assessment of the contribution of any given taxon(a) or character(s) to a given grouping can only be made by its removal. This has three limitations: first, the removal of any taxa/character(s) can change the optimization of any other character because of character interactions, therefore complicating the interpretations of results obtained using this procedure; second, the relevancy of the targeted taxa/character can only be assessed *a posteriori* of the procedure; third, the outcome of the procedure is qualitative (it either produces a change in retrieved groupings or not). We show that by using 3ta, it is possible to overcome these limitations. Using an amended matrix from Rio & Mannion (2021), we propose a protocol to quantify the support directly from the matrix and therefore to precisely target specific taxa and/or characters of interest. First, we quantified the support for each hypothesis regarding the Longirostres/Brevirostres conflict. We showed that the closer the ‘Gavialoidea’ are to the ‘Tomistominae’, the higher the topology is supported. As such, the Longirostres hypothesis is best supported while the Brevirostres is only the fourth out of five possible phylogenetic placement for the ‘Gavialoidea’. Furthermore, we showed that the relationship between the Alligatoroidea, the ‘Gavialoidea’ and the ‘Tomistominae’ is the most decisive one regarding this conflict. This better support to Longirostres hypothesis compared to the Brevirostres one was assessed in all anatomical categories except for the soft tissues. Quantifications pointed out the role of the ‘Tomistominae’, the precise contribution of which was measured, both as a whole and for each species. We showed that this group provides the majority of the evidence supporting Longirostres, both at the scale of the whole matrix and for most of the anatomical categories, and that this contribution is not reducible to that of a single terminal taxon. Furthermore, we investigated the contribution of ‘longirostrine’ characters (Rio & Mannion, 2021) and our results confirmed their hypothesis that they do not significantly contribute to the results of the phylogenetic analyses.

3.8 References

Blanco A. 2021. Importance of the postcranial skeleton in eusuchian phylogeny: Reassessing the systematics of allodaposuchid crocodylians. PLoS ONE. 16:e0251900.

Blanco A., Fortuny J., Vicente A., Luján À.H., García-Marçà J.A., Sellés A.G. 2015. A new species of *Allodaposuchus* (Eusuchia, Crocodylia) from the Maastrichtian (Late Cretaceous) of Spain: phylogenetic and paleobiological implications. PeerJ. 3:e1171.

Blanco A., Puértolas-Pascual E., Marmi J., Vila B., Sellés A.G. 2014. *Allodaposuchus palustris* sp. nov. from the Upper Cretaceous of Fumanya (South-Eastern Pyrenees, Iberian Peninsula): Systematics, Palaeoecology and Palaeobiogeography of the Enigmatic Allodaposuchian Crocodylians. PLoS ONE. 9:e115837.

Bremer K. 1988. The Limits of amino acid sequence data in Angiosperm phylogenetic reconstruction. Evolution. 42:795–803.

Bremer K. 1994. Branch support and tree stability. Cladistics. 10:295–304.

Brochu C.A. 1997a. Morphology, Fossils, Divergence Timing, and the Phylogenetic Relationships of *Gavialis*. Systematic Biology. 46:479–522.

Brochu C.A. 1997b. A review of “*Leidyosuchus*” (Crocodyliformes, Eusuchia) from the Cretaceous through Eocene of North America. Journal of Vertebrate Paleontology. 17:679–697.

Brochu C.A. 1999. Taxon Sampling and Reverse Successive Weighting. Systematic Biology. 48:808–813.

Brochu C.A. 2003. Phylogenetic Approaches Toward Crocodylian History. Annu. Rev. Earth Planet. Sci. 31:357–397.

Brochu C.A., Wagner J.R., Jouve S., Sumrall C.D., Densmore L.D. 2009. A Correction Corrected: Consensus Over the Meaning of Crocodylia and Why It Matters. Systematic Biology. 58:537–543.

Buffetaut E. 1985. The place of *Gavialis* and *Tomistoma* in eusuchian evolution: a reconciliation of palaeontological and biochemical data. njgpm. 1985:707–716.

- Cao N., Bagils R.Z., Vignes-Lebbe R. 2007. Hierarchical representation of hypotheses of homology. *Geodiversitas*.
- Colless D.H. 1985. On "Character" and Related Terms. *Systematic Zoology*. 34:229.
- Densmore L.D. 1983. Biochemical and Immunological Systematics of the Order Crocodylia. In: Hecht M.K., Wallace B., Prance G.T., editors. *Evolutionary Biology*. Boston, MA: Springer US. p. 397–465.
- Densmore L.D., Owen R.D. 1989. Molecular Systematics of the Order Crocodylia. *Am Zool*. 29:831–841.
- Farris J.S. 1970. Methods for Computing Wagner Trees. *Systematic Biology*. 19:83–92.
- Farris J.S. 2012. 3ta Sleeps with the fishes: Book review. *Cladistics*. 28:422–436.
- Farris J.S., Albert V.A., Källersjö M., Lipscomb D., Kluge A.G. 1996. Parsimony jackknifing outperforms neighbor-joining. *Cladistics*. 12:99–124.
- Farris J.S., Källersjö M., Albert V.A., Allard M., Anderberg A., Bowditch B., Bult C., Carpenter J.M., Crowe T.M., Laet J., Fitzhugh K., Frost D., Goloboff P., Humphries C.J., Jondelius U., Judd D., Karis P.O., Lipscomb D., Luckow M., Mindell D., Muona J., Nixon K., Presch W., Seberg O., Siddall M.E., Struwe L., Tehler A., Wenzel J., Wheeler Q., Wheeler W. 1995. Explanation. *Cladistics*. 11:211–218.
- Farris J.S., Kluge A.G. 1998. A/The Brief History of Three-Taxon Analysis. *Cladistics*. 14:349–362.
- Felsenstein J. 1985. Confidence limits on phylogenies: an approach using the Bootstrap. *Evolution*. 39:783–791.
- Gatesy J., Amato G., Norell M. 2003. Combined Support for Wholesale Taxic Atavism in Gavialine Crocodylians. *Systematic Biology*. 52.
- Goloboff P.A., Farris J.S. 2001. Methods for Quick Consensus Estimation. *Cladistics*. 17:S26–S34.
- Goloboff P.A., Farris J.S., Källersjö M., Oxelman B., Ramacuterez M.J., Szumik C.A. 2003. Improvements to resampling measures of group support. *Cladistics*. 19:324–332.

- Grigg G., Kirshner D. 2015. *Biology and Evolution of Crocodylians*. Melbourne: CSIRO Publishing.
- Groh S.S., Upchurch P., Barrett P.M., Day J.J. 2020. The phylogenetic relationships of neosuchian crocodiles and their implications for the convergent evolution of the longirostrine condition. *Zoological Journal of the Linnean Society*:zlj117.
- Harshman J., Huddleston C.J., Bollback J.P., Parsons T.J., Braun M.J. 2003. True and False Gharials: A Nuclear Gene Phylogeny of Crocodylia. *Systematic Biology*. 52:386–402.
- Harvey A.W. 1992. Three-taxon statements: more precisely, an abuse of parsimony? *Cladistics*. 8:345–354.
- Iijima M., Kobayashi Y. 2019. Mosaic nature in the skeleton of East Asian crocodylians fills the morphological gap between “Tomistominae” and Gavialinae. *Cladistics*. 35:623–632.
- Jouve S. 2009. The skull of *Teleosaurus cadomensis* (Crocodylomorpha; Thalattosuchia), and phylogenetic analysis of Thalattosuchia. *Journal of Vertebrate Paleontology*. 29:88–102.
- Jouve S., Bouya B., Amaghaz M., Mesloui S. 2015. *Maroccosuchus zennaroii* (Crocodylia: Tomistominae) from the Eocene of Morocco: phylogenetic and palaeobiogeographical implications of the basalmost tomistomine. *Journal of Systematic Palaeontology*. 13:421–445.
- Leardi J.M., Pol D., Novas F.E., Suárez Riglos M. 2015. The postcranial anatomy of *Yacarerani boliviensis* and the phylogenetic significance of the notosuchian postcranial skeleton. *Journal of Vertebrate Paleontology*. 35:e995187.
- Lee M.S.Y., Yates A.M. 2018. Tip-dating and homoplasy: reconciling the shallow molecular divergences of modern gharials with their long fossil record. *Proc. R. Soc. B*. 285:20181071.
- Nelson G. 1978. Ontogeny, Phylogeny, Paleontology, and the Biogenetic Law. *Systematic Zoology*. 27:324.
- Nelson G. 1996. *Nullius in Verba*. New York: Published by the author.
- Nelson G., Ladiges P.Y. 1992. Information Content and Fractional Weight of Three-Item Statements. *Systematic Biology*. 41:490.

- Nelson G., Ladiges P.Y. 1996. Paralogy in cladistic biogeography and analysis of paralogy-free subtrees. *American Museum novitates*.
- Nelson G., Platnick N. 1981. *Systematics and Biogeography*. Harcourt, Brace and World.
- Nelson G., Platnick N.I. 1991. Three-Taxon statements: a more precise use of parsimony? *Cladistics*. 7:351–366.
- Nelson G., Williams D.M., Ebach M.C. 2003. A question of conflict: Three-item and standard parsimony compared. *Systematics and Biodiversity*. 1:145–149.
- Norell M.A. 1989. The Higher Level Relationships of the Extant Crocodylia. *Journal of Herpetology*. 23:325.
- Norell M.A., Clark I.J.M., Hutchison J.H. 1994. The Late Cretaceous Alligatoroid *Brachychampsia Montana* (Crocodylia): New Material and Putative Relationships. *American Museum Novitates*.
- Pan T., Miao J.-S., Zhang H.-B., Yan P., Lee P.-S., Jiang X.-Y., Ouyang J.-H., Deng Y.-P., Zhang B.-W., Wu X.-B. 2021. Near-complete phylogeny of extant Crocodylia (Reptilia) using mitogenome-based data. *Zoological Journal of the Linnean Society*. 191:1075–1089.
- Pimentel R.A., Riggins R. 1987. The Nature of cladistic data. *Cladistics*. 3:201–209.
- Platnick N.I., Humphries C.J., Nelson G., Williams D.M. 1996. Is Farris optimization perfect?: Three-taxon statements and multiple branching. *Cladistics*. 12:243–252.
- Pogue M.G., Mickevich M.F. 1990. Character definitions and character state delineation: the bête noire of phylogenetic inference. *Cladistics*. 6:319–361.
- Pol D., Leardi J.M., Lecuona A., Krause M. 2012. Postcranial anatomy of *Sebecus icaeorhinus* (Crocodyliformes, Sebecidae) from the Eocene of Patagonia. *Journal of Vertebrate Paleontology*. 32:328–354.
- Prin S. 2015. Structure mathématique des hypothèses cladistiques et conséquences pour la phylogénie et l'évolution avec une perspective sur l'analyse cladistique.

Rineau V., Grand A., Zaragüeta-Bagils R., Laurin M. 2015. Experimental systematics: sensitivity of cladistic methods to polarization and character ordering schemes. *CTOZ*. 84:129–148.

Rineau V., Zaragüeta R., Bardin J. 2021. Information content of trees: three-taxon statements, inference rules and dependency. *Biological Journal of the Linnean Society*. 133:1152–1170.

Rineau V., Zaragüeta-Bagils R.Z., Laurin M. 2018. Impact of errors on cladistic inference: simulation-based comparison between parsimony and three-taxon analysis. *CTOZ*. 87:25–40.

Rio J.P., Mannion P.D. 2021. Phylogenetic analysis of a new morphological dataset elucidates the evolutionary history of Crocodylia and resolves the long-standing gharial problem. *PeerJ*. 9:e12094.

Rio J.P., Mannion P.D., Tschopp E., Martin J.E., Delfino M. 2019. Reappraisal of the morphology and phylogenetic relationships of the alligatoroid crocodylian *Diplocynodon hantoniensis* from the late Eocene of the United Kingdom. *Zoological Journal of the Linnean Society*.:zlj034.

Ristevski J., Weisbecker V., Scanlon J.D., Price G.J., Salisbury S.W. 2023. Cranial anatomy of the mekosuchine crocodylian *Trilophosuchus rackhami* Willis, 1993. *The Anatomical Record*. 306:239–297.

Ristevski J., Yates A.M., Price G.J., Molnar R.E., Weisbecker V., Salisbury S.W. 2020. Australia's prehistoric 'swamp king': revision of the Plio-Pleistocene crocodylian genus *Pallimnarchus* de Vis, 1886. *PeerJ*. 8:e10466.

Salas-Gismondi R., Ochoa D., Jouve S., Romero P.E., Cardich J., Perez A., DeVries T., Baby P., Urbina M., Carré M. 2022. Miocene fossils from the southeastern Pacific shed light on the last radiation of marine crocodylians. *Proc. R. Soc. B*. 289:20220380.

Salisbury S.W., Molnar R.E., Frey E., Willis P.M.A. 2006. The origin of modern crocodyliforms: new evidence from the Cretaceous of Australia. *Proc. R. Soc. B*. 273:2439–2448.

Siebert D.J., Williams D.M. 1998. Recycled. *Cladistics*. 14:339–347.

Sill W.D. 1968. The Zoogeography of the Crocodylia. *Copeia*. 1968:76.

Sookias R.B. 2020. Exploring the effects of character construction and choice, outgroups and analytical method on phylogenetic inference from discrete characters in extant crocodylians. *Zoological Journal of the Linnean Society*. 189:670–699.

Tarsitano S.F., Frey E., Riess J. 1989. The Evolution of the Crocodylia: A Conflict Between Morphological and Biochemical Data. *Am Zool*. 29:843–856.

Trueman J.W.H. 1998. Reverse Successive Weighting. *Systematic Biology*. 47:733–737.

Weems R.E. 2018. Crocodylians of the Calvert Cliffs. In: Godfrey S.J., editor. *The Geology and vertebrate paleontology of Calvert Cliffs, Maryland*. Smithsonian Institution Scholarly Press. p. 213–240.

Williams D.M., Ebach M.C. 2005. Drowning by Numbers: Rereading Nelson’s “Nullius in Verba.” *The Botanical Review*. 71:415–430.

Zaragüeta-Bagils R., Bourdon E. 2007. Three-item analysis: Hierarchical representation and treatment of missing and inapplicable data. *Comptes Rendus Palevol*. 6:527–534.

Zaragüeta-Bagils R.Z., Ung V., Grand A., Vignes-Lebbe R., Cao N., Ducasse J. 2012. LisBeth: New cladistics for phylogenetics and biogeography. *Comptes Rendus Palevol*. 11:563–566.

Chapter 4

General Conclusions

In the first chapter of this manuscript, we reviewed the diversity of Metasuchia. We have seen that the extant diversity of this group is a fraction of the fossil one. Metasuchian diversity was at its maximum during the Cretaceous, with multiple less inclusive clades radiating. During the Cenozoic, on the other hand, this diversity decreased, from an ecological and morphological point of view. It is during this time that Crocodylia imposes itself as the major representative clade, the diversity of the two others (Tethysuchia and Notosuchia) rapidly decreasing. Nonetheless, the diversity of Metasuchia as it is known today was not established until the late Neogene to Quaternary. During its evolutionary history, metasuchians lived under different climates. However, they remained largely associated with mostly freshwater environments all the way. Two major crises have strongly impacted them: the OAE2 and the K/Pg crisis. While the former seems to have had a uniform impact on the whole group, the effect of the latter varied importantly depending on the taxa.

The second chapter of this manuscript presents a study focused on the differential survival of Notosuchia clades at this crisis. To investigate this, we used the phylogenetic logistic regression (PLR) to test the effect of intrinsic and extrinsic factors on survival. This method had never been used before this way. The results showed that the survival of Sebecidae is significantly explained by large body size, a surprising result as larger organisms are usually more prone to become extinct during mass crises than smaller ones (that is the case, for instance, of the Dinosauria). We explained this relationship by the fact that body size is strongly correlated to the diet in notosuchians, with larger ones being carnivorous and smaller ones being omnivorous. This led us to hypothesize that the survival of sebecids is actually explained by their hypercarnivorous diet, and conversely, that non-sebecid notosuchians became extinct because of their omnivorous one (leaving open the reason for the extinction of baurusuchids). The foreword of this manuscript raises the question of the decrease in metasuchian diversity. This study provides some answers but also opens questions. Indeed, its results suggest that the drivers of metasuchian survival (large body size and carnivorous diet in the case of Notosuchia) are opposite to those of the dinosaurs. This can help to understand the dramatically different extant diversities of both birds and crocodylians. However, further studies are needed to understand the reasons explaining these opposite drivers. Nonetheless, the study presented in the second chapter of this manuscript confirms the value of smaller-scaled analyses, focused on specific groups at particular time intervals. Finally, it also shows how

important phylogenetic relationships are for macroevolutionary studies. The same approach was used on Tethysuchia, a group of neosuchians (see Fig. 1.1), as part of the internship of Tom Forêt (Sorbonne Université, CR2P) during the first year of his master's degree I co-supervised in 2022. This work was synthesized in a research article which is currently in review in the Paleobiology journal (Forêt et al., *accepted*, see Appendix of the manuscript). This study focused on the impact of the OAE2 and the K-Pg crisis on the diversity of Tethysuchia. We found that the OAE2 crisis is followed by an important turnover, with a pre-OAE2 fauna dominated by Pholidosauridae and a post-OAE2 one dominated by Dyrosauridae. On the other hand, the K-Pg crisis is associated with an increase in the diversity of Dyrosauridae, probably explained by the colonization of ecological niches left empty by the extinction of other organisms. Second, we showed that tethysuchians inhabited warmer environments after the OAE2 than before. Third, snout proportion significantly decreases in the post-Cretaceous fauna. This is most likely explained by niche partitioning. Thus, contrary to Notosuchia, post-Cretaceous tethysuchians are not larger than their Cretaceous counterparts. However, they included more short-snouted species. This result shows the morphologic plasticity of Tethysuchia as well as their ability to rapidly occupy new ecological niches left vacant due to extinction events. Both studies (on Notosuchia and Tethysuchia) show that because of their diversity, metasuchians were able to survive major crisis events and evolve rapidly, morphologically speaking, following such events. Furthermore, this study on Tethysuchia shows that the methodology we developed in Aubier *et al.* (2023) can be successfully applied to other groups. Finally, it showed that the impact of the OAE2 on the diversity can be quantitatively assessed. This is promising as we saw that this event may have negatively impacted several groups of Metasuchia (see Chapter 1). Therefore, a study could be performed to investigate the effect of the OAE2 on a larger scale. This may help in understanding the driving forces behind the metasuchian radiation that occurs following this event. However, working at small timescales prevents us from assessing long-term relationships between diversity and environmental drivers. This explains why we found that the palaeotemperature did not play a role in the notosuchian survival/extinction despite climatic variables having been shown to play an important role in the diversification as well as in the geographic distribution of the group. Moreover, we observed that both the apparition and the radiation of Notosuchia seem to have occurred during cold time intervals, at the Barremian-Aptian and Coniacian-Santonian, respectively. This led us to set up a project with F. Fluteau (IPGP) to simulate local palaeoclimatic conditions during these

specific geological stages. These simulations should allow us to precisely characterize the palaeoclimatic conditions under which notosuchians lived and under which they did not. This could lead us to identify precise climatic drivers for this group. Investigating the particularities of specific metasuchian clades could in turn help us to understand the global changes in climatic preferences this group displays, with a shift from arid to tropical climates following the K-Pg crisis.

Once the study presented in the second chapter of this manuscript had been accepted for publication and that I could finally consider it ‘from the outside’, I initially felt unsatisfied with it. My main concern was that even though the hypothesis that the differential survival of *Notosuchia* at the K-Pg crisis can be explained by differences in the diet is not frontally contradicted by the empirical evidence at hand, it was far from being overwhelmingly supported by them. This is all the more true given the scarcity, fragmentary and poorly dated nature of the fossil specimens. This criticism challenged me because on the one hand, I completely agreed with it (since I was myself raising it), but on the other hand I found it rather useless. Indeed, the empirical pieces of evidence used in this study do not unanimously support the hypothesis we developed. However, by themselves, they do not seem to unanimously support any hypothesis. If it is justified for the hypothesis developed in this study, this criticism is also justified for any other one. After wondering about this issue for a few weeks, I found a satisfactory answer that was actually neither new nor surprising, either to me or to anyone else, as it had been proposed by Popper (1935) and had been extensively discussed since: falsifiability. But because it took me weeks to link Popper’s falsifiability to this study on *Notosuchia*, and because it allowed me to consider the latter in a new way, I wish to briefly develop this here. In this study, we proposed a hypothesis (diet explains the differential survival of terrestrial notosuchians at the K-Pg crisis) based on the data we gathered. The limitations of these data prevent us from relying solely on them to support this hypothesis. We thus have to rely on an other source to make our hypothesis consistent: predictions. In Popper’s mind, the origin of a hypothesis’s production is irrelevant, only its easiness to be refuted is. In the present study, at least two predictions are associated with our hypothesis. The scarcity of the fossil record ‘forced’ us to consider the notosuchians from the Cenozoic as ‘survivors’ of the K-Pg crisis, even though most of them certainly never faced it. As said in the foreword of this chapter, this means that we considered that the post-Cretaceous fauna is representative of the notosuchian diversity that actually survived the crisis. One could consider this as a poorly supported assumption. However, this could also be seen as a prediction.

Indeed, if post-Cretaceous sebecids are representatives of the crisis survivors, we should expect (predict) the findings of similar organisms in Maastrichtian deposits. This first prediction, I would consider weak as the outcome can only corroborate our hypothesis. A second prediction is made: if hypercarnivory explains the survival of the sebecids, then we should expect (predict) that further fossil discoveries will confirm that omnivorous clades like Sphagesauria were severely impacted. The current knowledge of the fossil record corroborates that in the strongest way because no omnivorous species have yet been found in the Cenozoic. However, if such species were to be discovered in the future, this could dramatically impair our hypothesis. Indeed, this hypothesis can hold if only a very low number of species were to be discovered (still, it would need to be adjusted). But if numerous omnivorous species were to be excavated in post-Cretaceous formations, it would constitute a direct refutation. As such, this hypothesis, despite not being very strongly supported by empirical data, is theoretically rather simple to refute. Thus, in this study, it is not a 'somewhat sort of supported' hypothesis that is being developed, it is a proposed explanation, waiting to be falsified. I regret not having been able to adopt such a view before and during the redaction of this study. Had I to write it again, I would state explicitly these predictions so that in the future, if Cenozoic sphagesaurids were to be found, the impair it constitutes to our hypothesis would become clear to any reader. These reflections set aside, we show that the methodology developed in the second chapter can yield interesting results and can be applied to different groups. However, it relies on the use of phylogenetic comparative methods (PCM). The results obtained using such methods heavily rely on the topology and branch lengths of the phylogeny being used. Thus, having a strong phylogeny is necessary prior to the use of such methods. Regarding Crocodylia, the conflict between the Longirostres and Brevirostres hypotheses not only concerns the topology but also the dating of the nodes. This would strongly affect PCM analyses. Thus, analysing Crocodylia the same way we treated that of the Notosuchia would probably yield strongly contradicting results depending on the phylogenetic hypothesis, therefore impairing their discussion. Therefore, resolving the phylogenetic conflict should be the first objective.

The third chapter of this manuscript is a study, currently under review in the *Systematic Biology* Journal, that investigates the Brevirostres/Longirostres conflict. We argue that measuring directly in the matrix the phylogenetic support to each topology is a line of investigation that can help in the

understanding of the persistence of the conflict. Indeed, it would allow us to assess the evidence yielded by the taxa and character to each hypothesis and therefore to target taxa/characters of interest. Because such a measure is not possible in a parsimony framework, we use an alternative cladistic method, the three-taxon analysis (3ta) to analyse the most recently published phylogenetic matrix. We were able to quantify the impact of the Tomistominae in this Longirostres/Brevirostres conflict for the first time and we showed how dramatic it is. We showed that despite a comprehensive review of morphological characters, the contradiction is still very high in the matrix we analysed. Further questions arise. First, why is it that the Tomistominae provide so much support in favour of the Longirostres hypothesis? This question calls for a return to the characters and comparative anatomy. It is unlikely that this strong support for the Longirostres hypothesis originates from wrongly attributed character states because the 14 Tomistominae species are concerned. However, it could originate from characters dealing with homoplastic features. Finally, it could also be genuine. Second, what is the disparity in terms of provided support between non-tomistomine crocodylian clades? In this chapter, we were focused on quantifying the role of the Tomistominae. In doing so, we compared the support they provide to the support provided by all the other crocodylians. The same should be done in the future for the Alligatoroidea, Crocodyloidea and Gavialoidea to further locate the sources of contradiction. Third, what is the effect of the thoracosaur? We saw that this group was hypothesized to form an independent lineage, outside of the Crocodylia (Gatesy *et al.*, 2003; Harshman *et al.*, 2003; Vélez-Juarbe *et al.*, 2007; Lee and Yates, 2018; Ristevski *et al.*, 2020, 2023; Sookias, 2020). In the matrix we used, they were considered as gavialoids. A precise assessment of the support they provide may shed light on this controversy. We also showed that characters correlated to the longirostry did not play a major role in the Longirostres/Brevirostres conflict. However, the list we used is largely imperfect. Using our approach, we were able to quantify the support provided by each character. This allowed us to identify those providing the highest support for each hypothesis and show that they had not been included in this list. This ability to target important characters (regarding the conflict under investigation) provides new lines of investigation. However, our results are based on the analysis of Rio & Mannion (2021) matrix. They made a comprehensive review of previously published ones and substantially modified numerous characters. As a result, they retrieved a tree congruent with the Longirostres hypothesis, contrary to analyses performed using older matrices (Brochu, 1997a, 1997b; Salisbury *et al.*, 2006; Jouve *et al.*, 2015). This limits the generalization of

our results. Indeed, the role of the Tomistominae as the main provider of support to the Longirostres hypothesis is most probably diminished in matrices that yield topologies congruent with the Brevirostres one. Analysing these matrices using the same methodology would thus allow us to understand the results from Rio & Mannion (2021), that is to target which of their modifications had such a huge impact on the topology.

This approach is useful for dealing with contradictory phylogenetic hypotheses. This case is rather frequent. Indeed, we saw in the first chapter that numerous controversies exist regarding the phylogenetic relationships of Metasuchia. Most of the time, these controversies originate from distinct character matrices which yield different results. This is the case, for instance, of Thalattosuchia. The matrices from Jouve (2009) and Wilberg *et al.* (2019) respectively retrieved Thalattosuchia within and outside of Neosuchia. However, the latter was initially produced by modifying the former. Thus, an analysis of both of these matrices would allow us to precisely target which of these modifications produced such a change in the retrieved topology.

To summarise, two approaches were developed during this PhD. First, we demonstrated that the PLR could be used to investigate diversity changes for particular, short time intervals. Using this approach, we showed that metasuchian diversity was a key factor in its successful crossing of the K-Pg crisis. Sebecids survived the K-Pg crisis, seemingly unaffected by it, and retained their morphology until they became extinct. Dyrosaurids, on the other hand, colonized new ecological niches and displayed rapid and substantial morphological adaptations (brevirostry). Thus, because it was so diverse, Metasuchia survived the K-Pg crisis and still included marine and terrestrial groups during the Cenozoic. Non-crocodylian metasuchians became fully extinct when most of their diversity had already been wiped out by the K-Pg crisis, thus making them more fragile when facing new environmental changes, or new competition. Despite the approach using the PLR being fruitful, it cannot assess the long-term relationship between diversity and environmental factors. This relationship will be investigated in the future, using palaeoclimatic simulations for specific time intervals. Finally, we also developed a new method to measure phylogenetic support directly from the matrix. We showed that it could characterize the evidence provided by each taxa and characters included in a phylogenetic matrix and be used to target those of interest. This method can be used to investigate a wide range of phylogenetic controversies.

Analysing the content of a matrix using 3ta is thus a new tool that will help in the resolving of long-standing phylogenetic conflicts.

4.1 References

Brochu C.A. 1997a. A review of “*Leidyosuchus*” (Crocodyliformes, Eusuchia) from the Cretaceous through Eocene of North America. *Journal of Vertebrate Paleontology*. 17:679–697.

Brochu C.A. 1997b. Morphology, Fossils, Divergence Timing, and the Phylogenetic Relationships of *Gavialis*. *Systematic Biology*. 46:479–522.

Foret T., Aubier P., Jouve S., Cubo J. *Accepted* (Paleobiology). Biotic and abiotic factors and the phylogenetic structure of extinction in the evolution of Tethyuchia.

Gatesy J., Amato G., Norell M. 2003. Combined Support for Wholesale Taxic Atavism in Gavialine Crocodylians. *Systematic Biology*. 52.

Harshman J., Huddleston C.J., Bollback J.P., Parsons T.J., Braun M.J. 2003. True and False Gharials: A Nuclear Gene Phylogeny of Crocodylia. *Systematic Biology*. 52:386–402.

Jouve S. 2009. The skull of *Teleosaurus cadomensis* (Crocodylomorpha; Thalattosuchia), and phylogenetic analysis of Thalattosuchia. *Journal of Vertebrate Paleontology*. 29:88–102.

Jouve S., Bouya B., Amaghaz M., Meslough S. 2015. *Maroccosuchus zennaroi* (Crocodylia: Tomistominae) from the Eocene of Morocco: phylogenetic and palaeobiogeographical implications of the basalmost tomistomine. *Journal of Systematic Palaeontology*. 13:421–445.

Lee M.S.Y., Yates A.M. 2018. Tip-dating and homoplasy: reconciling the shallow molecular divergences of modern gharials with their long fossil record. *Proc. R. Soc. B*. 285:20181071.

Popper K. 1935. *The Logic of scientific discovery*. Verlag von Julius Springer.

Rio J.P., Mannion P.D. 2021. Phylogenetic analysis of a new morphological dataset elucidates the evolutionary history of Crocodylia and resolves the long-standing gharial problem. *PeerJ*. 9:e12094.

Ristevski J., Weisbecker V., Scanlon J.D., Price G.J., Salisbury S.W. 2023. Cranial anatomy of the mekosuchine crocodylian *Trilophosuchus rackhami* Willis, 1993. *The Anatomical Record*. 306:239–297.

Ristevski J., Yates A.M., Price G.J., Molnar R.E., Weisbecker V., Salisbury S.W. 2020. Australia's prehistoric 'swamp king': revision of the Plio-Pleistocene crocodylian genus *Pallimnarchus* de Vis, 1886. PeerJ. 8:e10466.

Salisbury S.W., Molnar R.E., Frey E., Willis P.M.A. 2006. The origin of modern crocodyliforms: new evidence from the Cretaceous of Australia. Proc. R. Soc. B. 273:2439–2448.

Sookias R.B. 2020. Exploring the effects of character construction and choice, outgroups and analytical method on phylogenetic inference from discrete characters in extant crocodylians. Zoological Journal of the Linnean Society. 189:670–699.

Vélez-Juarbe J., Brochu C.A., Santos H. 2007. A gharial from the Oligocene of Puerto Rico: transoceanic dispersal in the history of a non-marine reptile. Proc. R. Soc. B. 274:1245–1254.

Wilberg E.W., Turner A.H., Brochu C.A. 2019. Evolutionary structure and timing of major habitat shifts in Crocodylomorpha. Sci Rep. 9:10.

Appendix 1 - Were Notosuchia

(Pseudosuchia: Crocodylomorpha)

warm-blooded? A palaeohistological
analysis suggests ectothermy

Were Notosuchia (Pseudosuchia: Crocodylomorpha) warm-blooded? A palaeohistological analysis suggests ectothermy

JORGE CUBO^{1,*}, MARIANA V. A. SENA^{2,3}, PAUL AUBIER¹, GUILLAUME HOUÉE¹, PENELOPE CLAISSE¹, MATHIEU G. FAURE-BRAC¹, RONAN ALLAIN⁴, RAFAEL C. L. P. ANDRADE⁵, JULIANA M. SAYÃO⁵ and GUSTAVO R. OLIVEIRA⁶

¹Sorbonne Université, Muséum national d'Histoire naturelle, CNRS, Centre de Recherche en Paléontologie—Paris (CR2P, UMR 7207), Paris, France

²Universidade Federal de Pernambuco, Departamento de Geologia, Programa de Pós-Graduação em Geociências (PPGEOC), Recife, PE, Brazil

³Centro Universitário da Vitória de Santo Antão, Vitória de Santo Antão, PE, Brazil

⁴Muséum national d'Histoire naturelle, Sorbonne Université, CNRS, Centre de Recherche en Paléontologie—Paris (CR2P, UMR 7207), Paris, France

⁵Universidade Federal de Pernambuco, Laboratório de Paleobiologia e Microestruturas, Vitória de Santo Antão, PE, Brazil

⁶Universidade Federal Rural de Pernambuco, Departamento de Biologia, Laboratório de Paleontologia & Sistemática, Recife, PE, Brazil

Received 31 March 2020; revised 5 May 2020; accepted for publication 11 May 2020

Most Notosuchia were active terrestrial predators. A few were semi-aquatic, or were insectivorous, omnivorous or herbivorous. A question relative to their thermometabolism remains to be answered: were Notosuchia warm-blooded? Here we use quantitative bone palaeohistology to answer this question. Two variables were used as proxies to infer thermometabolism: resting metabolic rate and red blood cell dimensions. Resting metabolic rate was inferred using relative primary osteon area and osteocyte size, shape and density. Blood cell dimensions were inferred using harmonic mean canal diameter and minimum canal diameter. All inferences were performed using phylogenetic eigenvector maps. Both sets of analyses suggest that the seven species of Notosuchia sampled in this study were ectotherms. Given that extant Neosuchia (their sister group) are also ectotherms, and that archosaurs were primitively endotherms, parsimony suggests that endothermy may have been lost at the node Metasuchia (Notosuchia–Neosuchia) by the Early Jurassic. Semi-aquatic taxa such as *Pepesuchus* may have had thermoregulatory strategies similar to those of recent crocodylians, whereas the terrestrial taxa (*Araripesuchus*, *Armadillosuchus*, *Iberosuchus*, *Mariliasuchus*, *Stratiotosuchus*) may have been thermoregulators similar to active predatory varanids. Thermal inertia may have contributed to maintaining a stable temperature in large notosuchians such as *Baurusuchus*.

ADDITIONAL KEYWORDS: bone histology – ectothermy – endothermy – Metasuchia – Neosuchia – phylogenetic eigenvector maps – thermometabolism.

INTRODUCTION

Notosuchia is a group of extinct crocodyliforms that lived from the Middle Jurassic (*Razanandrongobe sakalavae*, Dal Sasso *et al.*, 2017) to the Middle

Miocene (*Sebecus*, Buffetaut & Hoffstetter, 1977; Busbey 1986). Some groups became extinct after the crisis at the end of the Cretaceous (Peirosauridae, Uruguaysuchidae), whereas others survived until the Miocene (Sebecosuchia). Notosuchians present a diverse array of body sizes, and inhabited different environments. Some small to medium-sized taxa

*Corresponding author. E-mail: jorge.cubo_garcia@upmc.fr

(e.g. *Araripesuchus*, Sereno & Larsson, 2009), and some large ones (e.g. *Baurusuchus*, Pol *et al.*, 2014) were terrestrial, whereas other forms were semi-aquatic (e.g. *Kaprosuchus*, *Mahajangasuchus*, *Stolokrosuchus* and *Pepesuchus*, Riff *et al.*, 2012; Pol *et al.*, 2014; Grigg & Kirshner, 2015; Wilberg *et al.*, 2019). Moreover, these crocodyliforms were diversified in terms of diet: carnivorous (e.g. *Notosuchus* and baurusuchids), insectivorous or omnivorous (e.g. *Araripesuchus*, *Candidodon* and *Mariliasuchus*), omnivorous (e.g. *Armadillosuchus*) and herbivorous (e.g. *Simosuchus*, *Pakasuchus* and *Chimaerasuchus*) (Marinho & Carvalho, 2009; Godoy *et al.*, 2014; Melstrom & Irmis, 2019). A question of their palaeobiology remains unanswered: were notosuchians warm-blooded? Endotherms (e.g. birds and mammals) have high metabolic rates (tachymetabolism) and generate enough internal heat to enable physiological regulation of body temperature, while ectotherms (e.g. most other vertebrates) have low metabolic rates (bradymetabolism) and must thermoregulate behaviourally. Archosaurs are considered as being primitively endotherms. This hypothesis is based on cardiovascular (Seymour *et al.*, 2004), respiratory (Farmer & Sanders, 2010) and osteohistological (Legendre *et al.*, 2016) evidence. As the outgroups *Calypotosuchus welllesi* (Aetosauria) and *Postosuchus kirkpatricki* (Rauisuchidae) are considered to have been endotherms (Cubo & Jalil, 2019), and many notosuchians were active terrestrial predators, the null hypothesis suggests that Notosuchia may have inherited endothermy whereas Neosuchia, their sister group, may have lost this condition when they became secondarily aquatic during the Early Jurassic. The last hypothesis is congruent with the fact that thermal conductivity in water is higher than in air [0.59 vs. 0.024 W/(m.K); Vogel, 2005]. The heat capacity (J/K) and density (kg/L) of water are also higher than those of air. Therefore, it is more costly to maintain a high body temperature in water than in air. As most extant Neosuchia are sit-and-wait predators and have lower energy budgets than active aquatic endothermic predators such as dolphins and penguins, natural selection may have favoured the loss of endothermy at the node Neosuchia. Qualitative histological analyses performed to date in Notosuchia are not conclusive. Cubo *et al.* (2017) found an isolated femoral bone tissue in *Iberosuchus macrodon* that can be interpreted as either radial fibrolamellar bone tissue formed at extremely high growth rates and suggesting endothermy, or as compacted spongiosa formed at lower growth rates typical of ectotherms. Sena *et al.* (2018) found in the appendicular bones of *Pepesuchus deiseae* bone tissues formed at moderate

growth rates. Here we use quantitative bone palaeohistology and the phylogenetic comparative method to uncover the thermometabolic condition of these amazing archosaurs.

MATERIAL AND METHODS

MATERIAL

We included seven species of Notosuchia:

1. *Araripesuchus wegneri* Buffetaut 1981. A partial femur (MNHN.F.GDF660) from the Aptian of Gadoufaoua (Niger), Museum national d'Histoire naturelle (MNHN) (Paris, France).
2. *Armadillosuchus arrudai* Marinho & Carvalho 2009. A partial femur (LPRP-USP 0774) from the Turonian–Maastrichtian of the Bauru Group (Brazil), Universidade de São Paulo (USP) (Ribeirão Preto, Brazil).
3. *Baurusuchus* sp. Price 1945. A partial femur (LPRP-USP 0634 C) from the Turonian–Maastrichtian of the Bauru Group (Brazil), USP.
4. *Iberosuchus macrodon* Antunes 1975. Two partial femora (IPS4930 and IPS4932) from the Palaeocene of La Boixedat (Spain), Institut Català de Paleontologia (ICP) (Sabadell, Spain). Histological descriptions of these bones can be found in Cubo *et al.* (2017).
5. *Mariliasuchus amarali* Carvalho & Bertini 1999. A right humerus (UFRPE 5311) from the Turonian–Maastrichtian of the Bauru Group (Brazil), Universidade Federal Rural de Pernambuco (UFRPE) (Recife, Brazil).
6. *Stratiotosuchus maxhechti* Campos *et al.*, 2001. A femur (MCT1714-R) and a tibia (DGM 1477-R) from the Campanian–Maastrichtian of the Bauru Group (Brazil), Museu de Ciências da Terra (MCT), under a temporary loan to Universidade Federal de Uberlândia (UFU).
7. *Pepesuchus deiseae* Campos *et al.*, 2011. A right tibia (MN 7466-V) from the Campanian–Maastrichtian of the Bauru Group (Brazil), Museu Nacional do Rio de Janeiro (Brazil).

The analyses aimed at inferring resting metabolic rates in fossils include 18 species of extant tetrapods. Resting metabolic rates were measured by Montes *et al.* (2007) using respirometry, with the exception of values for *Capreolus capreolus*, *Oryctolagus cuniculus* and *Lepus europaeus*, which were taken from Olivier *et al.* (2017). Analyses performed to infer red blood cell (RBC) size in fossils included 14 species of extant tetrapods. RBC sizes were taken from Huttenlocker & Farmer (2017), who measured them by imaging of stained blood smears.

OSTEOHISTOLOGICAL FEATURES

Bone histological features used to construct palaeobiological inference models were: relative primary osteon area (RPOA, described by Fleischle *et al.*, 2018, as primary osteon density), osteocyte size, shape and density (described by Cubo *et al.*, 2012), and vascular canal diameter (Huttenlocker & Farmer, 2017). Values for the sample of Notosuchia were quantified in this study (Supporting Information File S1) and values for the sample of extant taxa were taken from Faure-Brac & Cubo (2020) for the femoral RPOA, from Legendre *et al.* (2016) and Olivier *et al.* (2017) for humeral, femoral and tibiae osteocyte size, shape and density, and from Huttenlocker & Farmer (2017) for femoral canal harmonic mean and minimum diameter.

RPOA and osteocyte size, shape and density were used to infer resting metabolic rate (RMR in $\text{mL O}_2 \text{ h}^{-1} \text{ g}^{-0.67}$) in Notosuchia. As all sampled extant tetrapods were juveniles in the active growth phase (Legendre *et al.*, 2016), these variables were quantified in the deep cortex of the Notosuchia analysed. By deep cortex we mean primary bone near endosteal bone.

The reason for this is that the deep cortex of adults was formed when they were juveniles. For *Iberosuchus*, quantifications were performed on specimen IPS4930 as it is younger than IPS4932. Harmonic mean canal diameter and minimum canal diameter were used to infer RBC width (μm) and area (μm^2) in Notosuchia. The variable ‘canal diameter’ corresponds to the diameter of vascular spaces in bone tissue. Values for the sampled extant tetrapods were taken from Huttenlocker & Farmer (2017), who analysed adult specimens. Therefore, we quantified the vascular canal diameters in the outer cortex of the sampled Notosuchia, and we used *Iberosuchus* IPS4932 because it is older than IPS4930.

PHYLOGENY AND PHYLOGENETIC COMPARATIVE METHODS

For extant taxa, we used the phylogenies compiled by Legendre *et al.* (2016) and Faure-Brac & Cubo (2020) for Figures 1 and 3, and Supporting Information Figures S1 and S2, and by Huttenlocker & Farmer (2017) for Figure 2 and Figure S3. Several phylogenetic

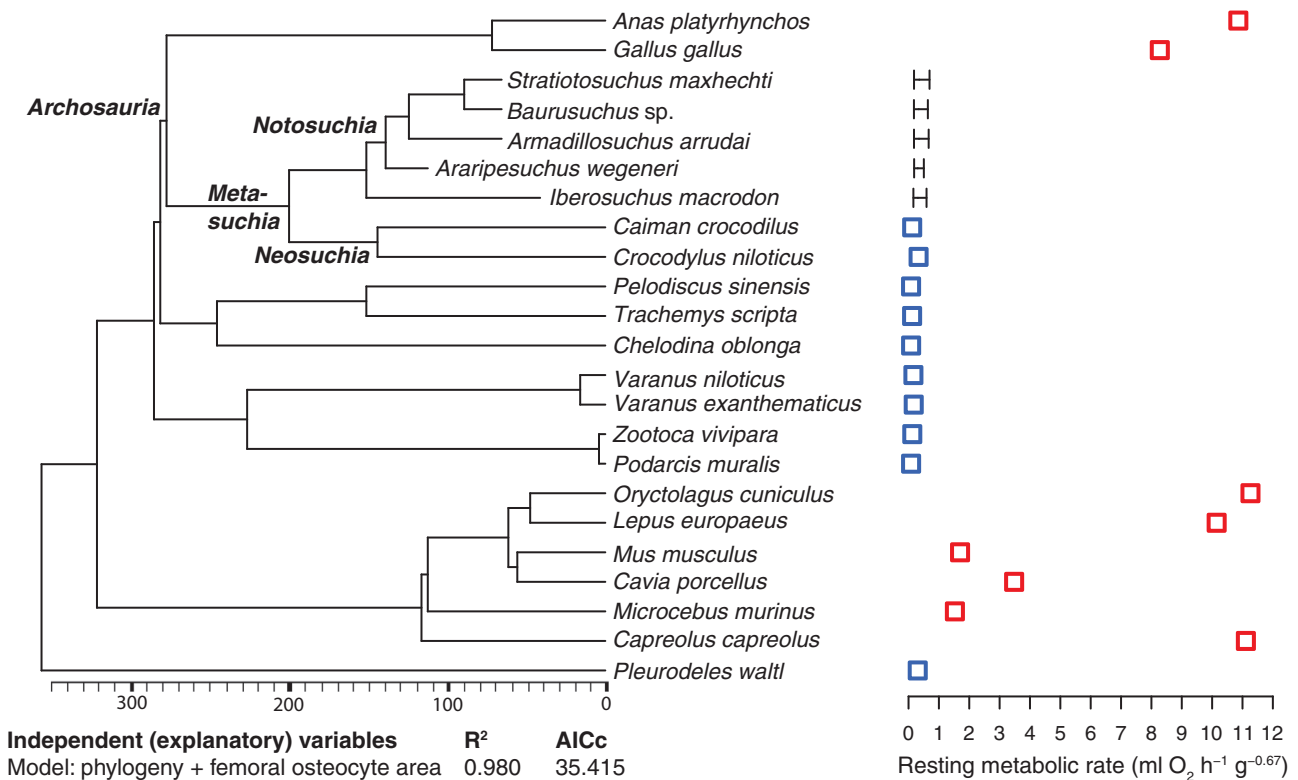


Figure 1. Resting metabolic rate inferred for a sample of Notosuchia using palaeohistology and phylogenetic eigenvector maps. We used a model that included phylogeny + osteocyte area for the femur as explanatory factors. Blue squares indicate ectothermy and red squares endothermy. For fossil taxa, segments represent the 95% confidence interval of the inferences. AIC, Akaike’s information criterion. Phylogeny for extant taxa has been compiled from Legendre *et al.* (2016) and Olivier *et al.* (2017), and for extinct taxa from Geroto & Bertini (2019).

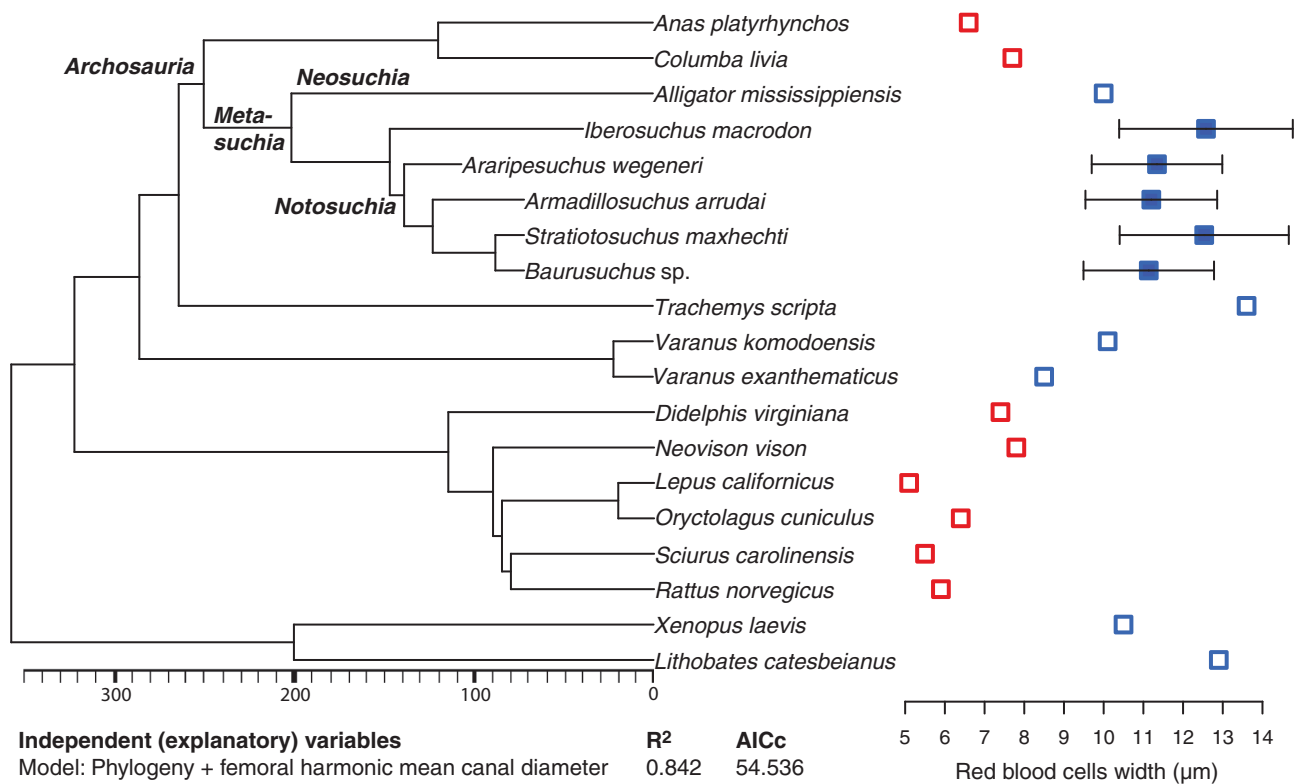


Figure 2. Red blood cell width inferred for a sample of Notosuchia using palaeohistology and phylogenetic eigenvector maps. We used a model that included phylogeny + harmonic mean canal diameter for the femur as explanatory factors. Blue squares indicate ectothermy and red squares endothermy. For fossil taxa, segments represent the 95% confidence interval of the inferences. AIC, Akaike's information criterion. Phylogeny for extant taxa has been taken from [Huttenlocker & Farmer \(2017\)](#), and for extinct taxa from [Geroto & Bertini \(2019\)](#).

analyses have been published for Notosuchia. [Pol et al. \(2014\)](#) found the following topology for the species of our sample: (*Araripesuchus* (*Mariliasuchus* (*Baurusuchus*–*Stratiosuchus*–*Iberosuchus*))). [Kellner et al. \(2014\)](#) proposed the same topology for these species. In contrast, [Geroto & Bertini \(2019\)](#) proposed a different topology for the species of our sample: ((*Iberosuchus*–*Pepesuchus*) (*Araripesuchus* ((*Mariliasuchus*–*Armadillosuchus*)(*Stratiosuchus*–*Baurusuchus*))). We followed the more recent topology (that published by [Geroto & Bertini, 2019](#)). Note that in the topologies published by [Pol et al. \(2014\)](#) and [Kellner et al. \(2014\)](#), all seven species of our sample are included in the node Notosuchia, whereas in the topology used in the present study (that published by [Geroto & Bertini, 2019](#)), *Iberosuchus* and *Pepesuchus* are not included in this node.

We used phylogenetic eigenvector maps (PEMs) and the 'MPSEM' package ([Guenard et al., 2013](#)) in R ([R Development Core Team, 2016](#)) to infer our dependent (response) variable using a set of explanatory variables. We checked the normality of residuals of the explanatory variables (the differences

between the values fitted by the PEM model and the actual values) using Shapiro–Wilk tests. If a distribution of residuals was significantly different from normality, the corresponding raw variable needs to be transformed. Finally, we performed leave-one-out cross-validation tests. For this, we estimated values of the dependent variable of extant taxa (for which these values are known) using the inference procedure of the 'MPSEM' package ([Guenard et al., 2013](#)), and compared these inferred values to the empirical ones using a phylogenetic generalized least squares (PGLS) regression and the 'caper' package ([Orme et al., 2013](#)) in R ([R Development Core Team, 2016](#)).

RESULTS

RESTING METABOLIC RATE INFERENCES PERFORMED USING RPOA AND OSTEOCYTE DENSITY, AREA AND SHAPE

The datasets used to perform analyses are available in [Supporting Information File S1](#). We used PEMs to infer the mass-independent RMRs of Notosuchia using

RMR values quantified in a sample of extant tetrapods, histological features quantified in both Notosuchia and extant tetrapods, and the phylogeny. The dependent (response) variable is RMR, and the explanatory variables are the phylogeny and osteohistological features: RPOA and osteocyte density, area and shape. The response variable (RMR) was transformed using natural logarithms because raw values are skewed. With a single exception, the distributions of residuals of the explanatory variables (the differences between the values fitted by the PEM models and the actual values) were not significantly different from normality (File S2). Transformation of explanatory variables was needed only for humerus osteocyte area, but this variable was not selected to infer the dependent variable. For each bone we chose the model that maximizes the R^2 value and, where these were equal, the model that minimizes the Akaike Information Criterion (AIC) value. The selected models were (File S2): phylogeny + osteocyte shape for the humerus (Figure S1), phylogeny + osteocyte area for the femur (Fig. 1) and phylogeny + osteocyte shape for the tibia (Figure S2). Inferences and 95% confidence intervals are given in Table 1. Additionally, we inferred values of the dependent variable of extant taxa (for which these values are known) using leave-one-out cross-validation tests. For the sample of extant taxa, regressions of inferred values to empirical values performed using PGLS were highly significant: $R^2 = 0.994$, $P = 2.2e-16$ for the humerus; $R^2 = 0.990$, $P = 2.2e-16$ for the femur; and $R^2 = 0.977$, $P = 1.521e-10$ for the tibia.

RBC SIZE INFERENCES MADE USING VASCULAR CANAL DIAMETER

The datasets used to perform analyses are available in Supporting Information File S1. We used PEMs to infer RBC dimensions of Notosuchia using RBC values quantified in a sample of extant tetrapods, vascular

canal diameters quantified in both Notosuchia and extant tetrapods, and the phylogeny. The dependent (response) variables were RBC_{width} and RBC_{area} , and the explanatory variables were femoral harmonic mean canal diameter and femoral minimum canal diameter. The distributions of residuals of the explanatory variables (the differences between the values fitted by the PEM model and the actual values) were not significantly different from normality (File S2). Therefore, no transformation of explanatory variables was needed. For each dependent variable we chose the model that maximizes the R^2 value and, where these were equal, the model that minimizes the AIC value. The selected models are (File S2): phylogeny + harmonic mean canal diameter to infer RBC width (Fig. 2); and phylogeny + minimum canal diameter to infer RBC area (Figure S3). Inferences and 95% confidence intervals are given in Table 2. Additionally, we inferred values of the dependent variable of extant taxa (for which these values are known) using leave-one-out cross-validation tests. For the sample of extant taxa, regressions of inferred values to empirical values performed using PGLS were significant: $R^2 = 0.891$, $P = 3.981e-07$ for RBC width and $R^2 = 0.425$, $P = 0.01154$ for RBC area.

DISCUSSION

METHODOLOGICAL CONSIDERATIONS

We used two variables as proxies to infer endothermy: resting metabolic rate (White *et al.*, 2006; Clarke & Pörtner, 2010) and RBC dimensions (Snyder & Sheafor, 1999; Huttenlocker & Farmer, 2017). For a range of body masses from 50 to 1000 g, the resting metabolic rate of birds and mammals exceed those of ectotherms by a factor of, respectively, 15 and 12 (Clarke & Pörtner, 2010). Furthermore, birds and mammals are characterized by smaller vascular canal minimum sizes

Table 1. Inferences of resting metabolic rate (RMR) of the sample of Notosuchia analysed in this study using phylogenetic eigenvector maps models

Bone	Taxa	Inferred RMR	Lower limit 95% CI	Upper limit 95% CI
Humerus	<i>Mariliasuchus amarali</i>	0.305	0.168	0.552
Femur	<i>Araripesuchus wegeneri</i>	0.304	0.183	0.504
	<i>Armadillosuchus arrudai</i>	0.345	0.179	0.663
	<i>Baurusuchus</i> sp.	0.336	0.177	0.636
	<i>Iberosuchus macrodon</i>	0.307	0.159	0.592
	<i>Stratiotosuchus maxhechti</i>	0.353	0.181	0.691
Tibia	<i>Pepesuchus deiseae</i>	0.255	0.110	0.590
	<i>Stratiotosuchus maxhechti</i>	0.267	0.119	0.601

The models included the following predictors: phylogeny + osteocyte shape for the humerus, phylogeny + osteocyte area for the femur, and phylogeny + osteocyte shape for the tibia. CI, confidence interval.

Table 2. Inferences of red blood cell dimensions of the sample of *Notosuchia* analysed in this study using a PEM model

Taxon	Inferred RBC variables	Inferred values	Lower limit 95% CI	Upper limit 95% CI
<i>Araripesuchus wegeneri</i>	RBC _{width} (µm)	11.343	9.699	12.988
	RBC _{area} (µm ²)	149.990	131.047	168.934
<i>Armadillosuchus arrudai</i>	RBC _{width} (µm)	11.200	9.541	12.859
	RBC _{area} (µm ²)	152.124	130.900	173.348
<i>Baurusuchus</i> sp.	RBC _{width} (µm)	11.136	9.492	12.780
	RBC _{area} (µm ²)	148.022	127.322	168.722
<i>Iberosuchus macrodon</i>	RBC _{width} (µm)	12.577	10.391	14.764
	RBC _{area} (µm ²)	155.884	132.297	179.470
<i>Stratiosuchus maxhechti</i>	RBC _{width} (µm)	12.533	10.403	14.663
	RBC _{area} (µm ²)	161.011	137.690	184.332

The model to infer red blood cells width (µm) included phylogeny + harmonic mean canal diameter as predictors. The model to infer red blood cell area (µm²) included phylogeny + minimum canal diameter. CI, confidence interval; RBC, red blood cell.

than ectotherms (Huttenlocker & Farmer, 2017). It has been shown that smaller capillaries produce higher diffusive gas exchange and higher resistance to blood flow (Snyder & Sheafor, 1999). In endotherms, RBCs undergo cell deformation during capillary flow (Snyder & Sheafor, 1999). Therefore, in these organisms, the presence of small capillaries increases resistance even if there are more capillaries in a given volume of tissue. The presence of smaller vascular canal minimum sizes in endotherms (birds and mammals) can thus be associated with their high oxygen uptake and their four-chambered heart, allowing high systemic blood pressures (Snyder & Sheafor, 1999; Huttenlocker & Farmer, 2017). Resting metabolic rate, RBC dimensions and thermometabolism (endothermy or ectothermy) are known in our sample of extant tetrapods. They are inferred in the sample of *Notosuchia* using a model that includes osteohistological features and the phylogeny. Interestingly, we performed two separate sets of analyses, using two independent samples of extant tetrapods, to infer two variables used as proxies of endothermy (resting metabolic rate, RBC dimensions), and we obtained the same inferences in *Notosuchia* (see below).

What is the effect of the number of extinct taxa (for which we performed inferences) relative to the number of extant ones used to construct the inference models? The results are the same irrespective of the relative number of extinct taxa included in the model: as an example, *Stratiosuchus maxhechti* was inferred as being ectothermic using a model based on the bone histology of the femur (five extinct taxa) and using a model based on the bone histology of the tibia (two extinct taxa).

Finally, we checked the reliability of our inferences by performing leave-one-out cross-validation tests: we estimated values of the dependent variable of extant taxa (for which these values are known) using the

inference procedure, and performed regressions of the inferred values to the measured (actual) values. All regressions were significant, suggesting that the inferences performed for *Notosuchia* are reliable.

PALEOBIOLOGICAL INFERENCES

The question here is: were *Notosuchia* warm-blooded? Considering that archosaurs were primitively endotherms (Seymour *et al.*, 2004; Farmer & Sanders, 2010; Legendre *et al.*, 2016), that the outgroups of *Notosuchia* analysed to date (*Calyptosuchus welllesi* and *Postosuchus kirkpatricki*) have been shown to be endotherms (Cubo & Jalil, 2019), and that *Notosuchia* includes a wide range of active terrestrial predator species (Carvalho *et al.*, 2004, 2005, 2007; Nascimento & Zaher, 2010; Godoy *et al.*, 2014), the null hypothesis suggests that *Notosuchia* were endotherms. This hypothesis has been refuted by our results. Both sets of analyses, those aimed at inferring resting metabolic rates and those performed to estimate RBC dimensions, show that the seven species of *Notosuchia* sampled in this study may have been ectotherms. Given that extant Neosuchia (their sister group) are also ectotherms, parsimony suggests that endothermy may have been lost at the node Metasuchia (*Notosuchia*–*Neosuchia*) by the Early Jurassic (Fig. 3). Among *Notosuchia*, semi-aquatic taxa such as *Pepesuchus* may have had thermoregulatory strategies akin to those of recent crocodylians (e.g. control of heat flow through the skin by basking, and opening the mouth to promote cooling by evaporation; Grigg & Kirshner, 2015), whereas the terrestrial species (*Araripesuchus*, *Armadillosuchus*, *Iberosuchus*, *Mariliasuchus*, *Stratiosuchus*) may have been thermoregulators similar to active predatory varanids. Varanid lizards have high aerobic capacities and can sustain higher activity levels than other lizards (Pough, 1980; Mendyk *et al.*, 2014). These terrestrial

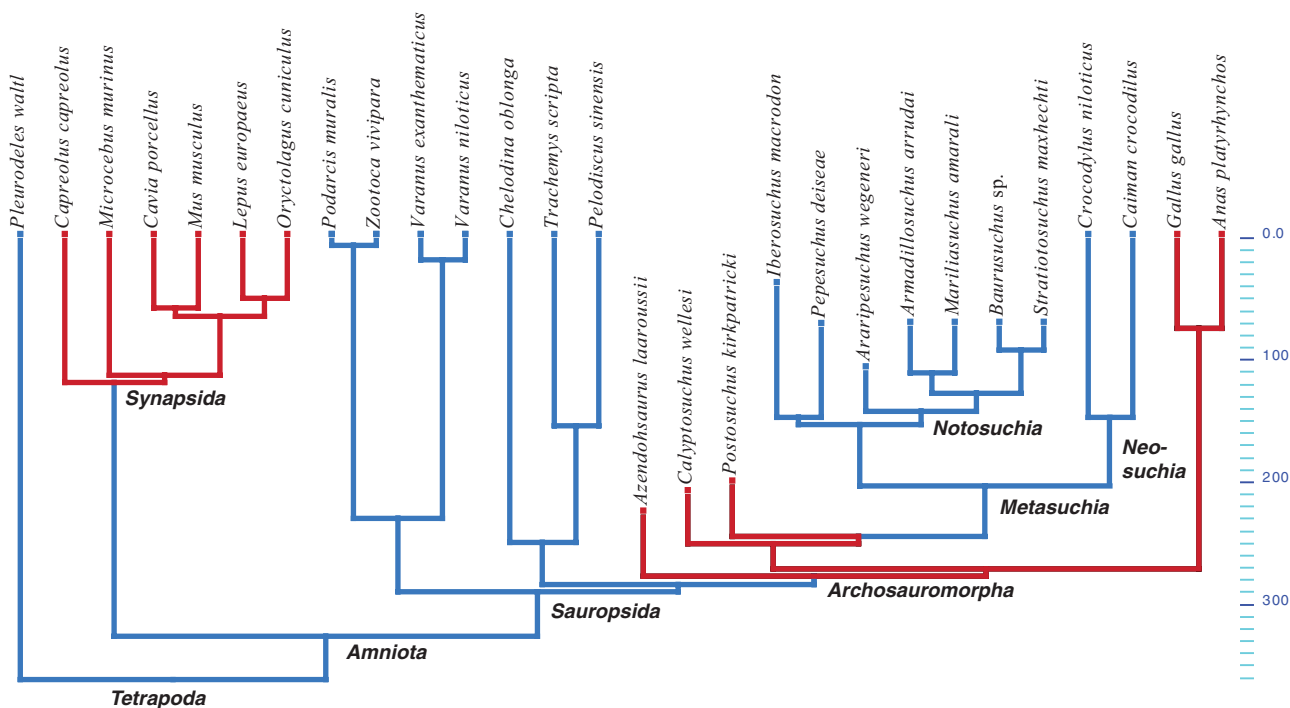


Figure 3. Optimization of the presence of endothermy onto a phylogeny of tetrapods. Inferences of extinct taxa have been made in this study, with the exception of *Azendohsaurus laaroussii*, *Calyptosuchus wellsi* and *Postosuchus kirkpatricki*, which were made by Cubo and Jalil (2019). Phylogeny for extant taxa has been compiled from Legendre *et al.* (2016) and Olivier *et al.* (2017), and for extinct taxa from Geroto & Bertini (2019). Red branches: endothermy. Blue branches: ectothermy.

notosuchians may have occupied sunlit areas for basking or while foraging, and they possibly entered burrows (Marinho & Carvalho, 2009; Carvalho *et al.*, 2010) to lower their body temperature when necessary. Clarac & Quilhac (2019) showed that, in crocodylians, “osteoderms collect the external heat during the basking periods as they become significantly warmer than the surrounding skin”. The presence of osteoderms in terrestrial Notosuchia (e.g. *Iberosuchus*), probably involved in heat intake during basking, suggests that these organisms relied on external heat to perform the high levels of activity inferred by functional morphology analyses. In the large sebecosuchians (e.g. *Baurusuchus*; Pol *et al.*, 2014) body temperature should have been more or less stable throughout the day because of thermic inertia. This feature made them more independent from external heating, which may have allowed extra time for hunting. The lifestyle of a few taxa remains debated. This is the case for *Mariliasuchus*. Nobre & Carvalho (2013) observed that *Mariliasuchus amarali* shares postcranial features with recent eusuchians, and concluded that this taxon probably had a sprawling-type posture and an amphibian lifestyle. However *Mariliasuchus amarali* also has cranial features which correspond to a terrestrial habit, such as a short and high skull, lateral orbits, frontal external nares, and long and robust

limbs, indicating a quadrupedal posture (Vasconcellos & Carvalho, 2005; Andrade & Bertini, 2008). In addition, some thin section histological and microanatomic features in *Mariliasuchus* (M. V. A. Sena, unpublished data) corroborate its terrestrial habits, such as the absence of bone specializations, tubular ribs and long bones showing a compact cortical bone and a free marrow cavity or a loose spongiosa filling the medullary region (Houssaye *et al.*, 2016). Moreover *Mariliasuchus amarali* is found in deposits of the Adamantina Formation from the Bauru group, which are interpreted as originating in semi-arid environments with sand sheets crossed by ephemeral river systems surrounding an interior desert within the Paraná basin of Gondwana during the Late Cretaceous (Fernandes and Ribeiro, 2015). For all these reasons we consider that *Mariliasuchus* had a terrestrial lifestyle. Future research on the palaeophysiology, lifestyle, diet and general palaeobiology of Notosuchia is needed to fully understand their ecological role and the causes of their extinction

ACKNOWLEDGEMENTS

We thank Roger Seymour (The University of Adelaide), Holly Woodward (Oklahoma State University) and an

anonymous reviewer for helpful comments that improved the quality of the manuscript. We gratefully thank Dr Max Langer (Universidade de São Paulo), Dr Douglas Riff (Universidade Federal de Uberlândia) and Dr Felipe Chinaglia Montefeltro (Universidade Estadual Paulista) and Alexander W. A. Kellner (Museu Nacional—UFRJ) for making available the thin-section images of *Baurusuchus* sp., *Armadillosuchus arrudai* and *Stratiotosuchus maxhecthi*. We thank the curator of the archosaur collection of the Muséum national d'Histoire naturelle (Paris, France) for allowing us to make thin sections of a partial femur (GDF660) of *Araripesuchus wegneri*, and to Hayat Lamrous (Sorbonne Université) for making these sections. We thank the curators of the Paleovertebrate Sector of the Museu Nacional (MN/UFRJ) which provided fossils of *Pepesuchus deiseae*, *Mariliasuchus amarali* and *Stratiotosuchus maxhecthi*. Some of the specimens used here were prepared in the Paleohistology lab at Des Moines University (Medical and Health Sciences Institution). The authors thank Des Moines University and, especially, Dr Sarah Werning for having R.C.L.P.A. as an exchange student, and the opportunity to use their facilities.

REFERENCES

- Andrade MB, Bertini RJ. 2008.** Morphological and anatomical observations about *Mariliasuchus amarali* and *Notosuchus terrestris* (Mesoeucrocodylia) and their relationships with other South American notosuchians. *Arquivos do Museu Nacional (Rio de Janeiro)* **66**: 5–62.
- Buffetaut E, Hoffstetter R. 1977.** Discovery of crocodylian *Sebecus* in Miocene of eastern Peru. *Comptes Rendus Hebdomadaires des Séances de l'Académie des Sciences Serie D* **284**: 1663–1666.
- Busbey AB. 1986.** New material of *Sebecus* cf. *huilensis* (Crocodylia: Sebecosuchidae) from the Miocene La Venta Formation of Colombia. *Journal of Vertebrate Paleontology* **6**: 20–27.
- Campos DA, Oliveira GR, Figueiredo RG, Riff D, Azevedo SAK, Carvalho LB, Kellner AWA. 2011.** On a new peirosaurid crocodyliform from the Upper Cretaceous, Bauru Group, southeastern Brazil. *Anais da Academia Brasileira de Ciências* **83**: 317–327.
- Carvalho IS, Brandoni de Gasparini Z, Salgado L, de Vasconcellos FM, Marinho TS. 2010.** Climate's role in the distribution of the Cretaceous terrestrial Crocodyliformes throughout Gondwana. *Palaeogeography Palaeoclimatology Palaeoecology* **297**: 252–262.
- Carvalho IS, Campos ACA, Nobre PH. 2005.** *Baurusuchus salgadoensis*, a new Crocodylomorpha from the Bauru Basin (Cretaceous), Brazil. *Gondwana Research* **8**: 11–30.
- Carvalho IS, Ribeiro LCB, Avilla LS. 2004.** *Uberabasuchus terrificus* sp. nov., a new Crocodylomorpha from the Bauru Basin (Upper Cretaceous), Brazil. *Gondwana Research* **7**: 975–1002.
- Carvalho IS, Vasconcellos FM, Tavares SAS. 2007.** *Montealtosuchus arrudacamposi*, a new peirosaurid crocodile (Mesoeucrocodylia) from the Late Cretaceous Adamantina Formation of Brazil. *Zootaxa* **1607**: 36–46.
- Clarac F, Quilhac A. 2019.** The crocodylian skull and osteoderms: a functional exaptation to ectothermy? *Zoology (Jena, Germany)* **132**: 31–40.
- Clarke A, Pörtner HO. 2010.** Temperature, metabolic power and the evolution of endothermy. *Biological Reviews of the Cambridge Philosophical Society* **85**: 703–727.
- Cubo J, Jalil NE. 2019.** Bone histology of *Azendohsaurus laaroussii*: implications for the evolution of thermometabolism in Archosauromorpha. *Paleobiology* **45**: 317–330.
- Cubo J, Kohler M, De Buffrenil V. 2017.** Bone histology of *Iberosuchus macrodon* (Sebecosuchia, Crocodylomorpha). *Lethaia* **50**: 495–503.
- Cubo J, Le Roy N, Martinez-Maza C, Montes L. 2012.** Paleohistological estimation of bone growth rate in extinct archosaurs. *Paleobiology* **38**: 335–349.
- Dal Sasso C, Pasini G, Fleury G, Maganuco S. 2017.** *Razanandrongobe sakalavae*, a gigantic mesoeucrocodylian from the Middle Jurassic of Madagascar, is the oldest known notosuchian. *PeerJ* **5**: e3481.
- Farmer CG, Sanders K. 2010.** Unidirectional airflow in the lungs of alligators. *Science (New York, N.Y.)* **327**: 338–340.
- Faure-Brac MG, Cubo J. 2020.** Were the synapsids primitively endotherms? A palaeohistological approach using phylogenetic eigenvector maps. *Philosophical Transactions of the Royal Society of London B: Biological Sciences* **375**: 20190138.
- Fernandes LA, Ribeiro CM. 2015.** Evolution and palaeoenvironment of the Bauru Basin (Upper Cretaceous, Brazil). *Journal of South American Earth Science* **61**: 71–90.
- Fleischle C, Wintrich T, Sander PM. 2018.** Quantitative histological models suggest endothermy in plesiosaurs. *PeerJ* **6**: e4955.
- Geroto CF, Bertini RJ. 2019.** New material of *Pepesuchus* (Crocodyliformes; Mesoeucrocodylia) from the Bauru Group: implications about its phylogeny and the age of the Adamantina Formation. *Zoological Journal of the Linnean Society* **185**: 312–334.
- Godoy PL, Montefeltro FC, Norell MA, Langer MC. 2014.** An additional *Baurusuchid* from the Cretaceous of Brazil with evidence of interspecific predation among crocodyliformes. *PLoS One* **9**: e97138.
- Guenard G, Legendre P, Peres-Neto P. 2013.** Phylogenetic eigenvector maps: a framework to model and predict species traits. *Methods in Ecology and Evolution* **4**: 1120–1131.
- Grigg G, Kirshner D. 2015.** *Biology and evolution of crocodylians*. New York: Cornell University Press.
- Houssaye A, Martin Sander P, Klein N. 2016.** Adaptive patterns in aquatic amniote bone microanatomy – more complex than previously thought. *Integrative and Comparative Biology* **56**: 1349–1369.
- Huttenlocker AK, Farmer CG. 2017.** Bone microvasculature tracks red blood cell size diminution in Triassic mammal and dinosaur forerunners. *Current Biology: CB* **27**: 48–54.

- Kellner AWA, Pinheiro AEP, Campos DA. 2014.** A new sebecid from the Paleogene of Brazil and the crocodyliform radiation after the K-Pg boundary. *PLoS One* **9**: e81386.
- Legendre LJ, Guénard G, Botha-Brink J, Cubo J. 2016.** Palaeohistological evidence for ancestral high metabolic rate in archosaurs. *Systematic Biology* **65**: 989–996.
- Marinho TS, Carvalho IS. 2009.** An armadillo-like sphagesaurid crocodyliform from the Late Cretaceous of Brazil. *Journal of South American Earth Sciences* **27**: 36–41.
- Melstrom KM, Irmis RB. 2019.** Repeated evolution of herbivorous crocodyliforms during the age of dinosaurs. *Current Biology: CB* **29**: 2389–2395.e3.
- Mendyk RW, Augustine L, Baumer M. 2014.** On the thermal husbandry of monitor lizards. *Herpetological Review* **45**: 619–632.
- Montes L, Le Roy N, Perret M, De Buffrenil V, Castanet J, Cubo J. 2007.** Relationships between bone growth rate, body mass and resting metabolic rate in growing amniotes: a phylogenetic approach. *Biological Journal of the Linnean Society* **92**: 63–76.
- Nascimento PM, Zaher H. 2010.** A new Baurusuchidae from the Upper Cretaceous of Brazil. *Papéis Avulsos de Zoologia* **50**: 323–361.
- Nobre PH, Carvalho I de S. 2013.** Postcranial skeleton of *Mariliasuchus amarali* Carvalho and Bertini, 1999 (Mesoeucrocodylia) from the Bauru Basin, Upper Cretaceous of Brazil. *Ameghiniana* **50**: 98–113.
- Olivier C, Houssaye A, Jalil NE, Cubo J. 2017.** First palaeohistological inference of resting metabolic rate in an extinct synapsid, *Moghreberia nmachouensis* (Therapsida: Anomodontia). *Biological Journal of the Linnean Society* **121**: 409–419.
- Orme D, Freckleton R, Thomas G, Petzoldt T, Fritz S, Isaac N, Pearse W. 2013.** *Caper: comparative analyses of phylogenetics and evolution in R*. Available at: <https://cran.rproject.org/web/packages/caper/vignettes/caper.pdf>.
- Pol D, Nascimento PM, Carvalho AB, Riccomini C, Pires-Domingues RA, Zaher H. 2014.** A new notosuchian from the Late Cretaceous of Brazil and the phylogeny of advanced notosuchians. *PLoS One* **9**: e93105.
- Pough FH. 1980.** The advantages of ectothermy for tetrapods. *The American Naturalist* **115**: 92–112.
- R Development Core Team. 2008.** R: a language and environment for statistical computing. Vienna, Austria: R Foundation for Statistical Computing. Available at: <http://www.R-project.org>.
- Riff D, Souza RG, Cidade GM, Martinelli AG, Souza-Filho JP. 2012.** Crocodilomorfos: a maior diversidade de répteis fósseis do Brasil. *Terræ* **9**: 12–40.
- Sena MVA, Andrade RCLP, Sayao JM, Oliveira GR. 2018.** Bone microanatomy of *Pepesuchus deiseae* (Mesoeucrocodylia, Peirosauridae) reveals a mature individual from the Upper Cretaceous of Brazil. *Cretaceous Research* **90**: 335–348.
- Sereno PC, Larsson HCE. 2009.** Cretaceous crocodyliforms from the Sahara. *Zookeys* **28**: 1–143.
- Seymour RS, Bennett-Stamper CL, Johnston SD, Carrier DR, Grigg GC. 2004.** Evidence for endothermic ancestors of crocodiles at the stem of archosaur evolution. *Physiological and Biochemical Zoology: PBZ* **77**: 1051–1067.
- Snyder GK, Sheafor BA. 1999.** Red blood cells: centerpiece in the evolution of the vertebrate circulatory system. *American Zoologist* **39**: 189–198.
- Vasconcellos FM, Carvalho IS. 2005.** Estágios de desenvolvimento de *Mariliasuchus amarali*, Crocodyliformes Mesoeucrocodylia da Formação Adamantina, Cretáceo Superior da Bacia Bauru, Brasil. *Anuário do Instituto de Geociências* **28**: 49–69.
- Vogel S. 2005.** Living in a physical world. V. Maintaining temperature. *Journal of Biosciences* **30**: 581–590.
- White CR, Phillips NF, Seymour RS. 2006.** The scaling and temperature dependence of vertebrate metabolism. *Biology Letters* **2**: 125–127.
- Wilberg EW, Turner AH, Brochu CA. 2019.** Evolutionary structure and timing of major habitat shifts in Crocodylomorpha. *Scientific Reports* **9**: 514.

SUPPORTING INFORMATION

Additional Supporting Information may be found in the online version of this article at the publisher's web-site.

File S1. Datasets.

File S2. Results.


Figure S1. Resting metabolic rate inferred for *Mariliasuchus amarali* using palaeohistology and phylogenetic eigenvector maps.

Figure S2. Resting metabolic rate inferred for *Stratiosuchus maxhechti* and *Pepesuchus deiseae* using palaeohistology and phylogenetic eigenvector maps.

Figure S3. Red blood cell area inferred for a sample of *Notosuchia* using palaeohistology and phylogenetic eigenvector maps.

Appendix 2 - Paleohistological
inferences of thermometabolic regimes
in Notosuchia (Pseudosuchia:
Crocodylomorpha) revisited

Osteohistological characterization of notosuchian osteoderms: Evidence for an overlying thick leathery layer of skin

Mariana Valéria de Araújo Sena^{1,2}  | Thiago da Silva Marinho^{3,4} | Felipe Chinaglia Montefeltro⁵ | Max Cardoso Langer⁶ | Thiago Schneider Fachini⁶ | William Roberto Nava⁷ | André Eduardo Piacentini Pinheiro⁸ | Esaú Victor de Araújo⁹ | Paul Aubier¹ | Rafael César Lima Pedroso de Andrade² | Juliana Manso Sayão⁹ | Gustavo Ribeiro de Oliveira¹⁰ | Jorge Cubo¹

¹Centre de Recherche en Paléontologie Paris (CR2P, UMR 7207), Muséum national d'Histoire naturelle, CNRS, Sorbonne Université, Paris, France

²Centro de Ciências Biológicas e da Saúde, Laboratório de Paleontologia da URCA, Universidade Regional do Cariri, Rua Carolino Sucupira–Pimenta, Crato, Ceará, Brazil

³Centro de Pesquisas Paleontológicas “Llewellyn Ivor Price”, Complexo Cultural e Científico Peirópolis, Pró-Reitoria de Extensão Universitária, Universidade Federal do Triângulo Mineiro, Uberaba, Minas Gerais, Brazil

⁴Instituto de Ciências Exatas, Naturais e Educação, Universidade Federal do Triângulo Mineiro, Uberaba, Minas Gerais, Brazil

⁵Departamento de Biologia e Zootecnia, Faculdade de Engenharia de Ilha Solteira, Universidade Estadual Paulista, Ilha Solteira, São Paulo, Brazil

⁶Faculdade de Filosofia, Ciências e Letras de Ribeirão Preto, Laboratório de Paleontologia de Ribeirão Preto, Universidade de São Paulo, Ribeirão Preto, São Paulo, Brazil

⁷Museu de Paleontologia de Marília, Prefeitura Municipal de Marília, Marília, São Paulo, Brazil

⁸Faculdade de Formação de Professores, Universidade do Estado do Rio de Janeiro, Rio de Janeiro, Brazil

⁹Museu Nacional do Rio de Janeiro, Universidade Federal do Rio de Janeiro, Rio de Janeiro, Brazil

¹⁰Laboratório de Paleontologia e Sistemática (LAPASI), Departamento de Biologia, Universidade Federal Rural de Pernambuco, Recife, Pernambuco, Brazil

Correspondence

Mariana Valéria de Araújo Sena, Muséum national d'Histoire naturelle, CNRS, Centre de recherche en paléontologie Paris (CR2P, UMR 7207), Sorbonne Université, 4 Place Jussieu, Paris, BC 104, 75005, France.
Email: mari.araujo.sena@gmail.com

Funding information

Centre National de la Recherche Scientifique; Conselho Nacional de Desenvolvimento Científico e Tecnológico; Université Sorbonne Paris Cité; Fundação Cearense de Apoio ao Desenvolvimento Científico e Tecnológico

Abstract

Osteoderms are mineralized structures embedded in the dermis, known for nonavian archosaurs, squamates, xenarthrans, and amphibians. Herein, we compared the osteoderm histology of Brazilian Notosuchia of Cretaceous age using three neosuchians for comparative purposes. Microanatomical analyses showed that most of them present a diploe structure similar to those of other pseudosuchians, lizards, and turtles. This structure contains two cortices (the external cortex composed of an outer and an inner layers, and the basal cortex) and a core in-between them. Notosuchian osteoderms show high bone compactness (>0.85) with varying degrees

Abbreviations: CAV, Centro Acadêmico da Vitória, Universidade Federal de Pernambuco, Vitória de Santo Antão, Brazil; CPPLIP, Centro de Pesquisas Paleontológicas “Llewellyn Ivor Price”, Complexo Cultural e Científico de Peirópolis, Universidade Federal do Triângulo Mineiro, Peirópolis, Uberaba, Brazil; CR2P, Centre de Recherche en Paléontologie, Sorbonne Université, Paris, France; LAPASI, Laboratório de Paleontologia e Sistemática, Universidade Federal Rural de Pernambuco, Recife, Brazil; LAPEISA, Laboratório de Paleontologia e Evolução de Ilha Solteira, Universidade Estadual Paulista, Ilha Solteira, Brazil; LPRP/USP, Laboratório de Paleontologia, Universidade de São Paulo, Ribeirão Preto, Brazil; MCT, Museu de Ciências da Terra, Serviço Geológico do Brasil, Rio de Janeiro, Brazil; MPM, Museu de Paleontologia de Marília, Marília, Brazil.

This is an open access article under the terms of the Creative Commons Attribution-NonCommercial-NoDerivs License, which permits use and distribution in any medium, provided the original work is properly cited, the use is non-commercial and no modifications or adaptations are made.

© 2022 The Authors. *Journal of Morphology* published by Wiley Periodicals LLC.

of cancellous bone in the core. The neosuchian *Guarinisuchus* shows the lowest bone compactness with a well-developed cancellous layer. From an ontogenetic perspective, most tissues are formed through periosteal ossification, although the mineralized tissues observed in baurusuchid LPRP/USP 0634 suggest a late metaplastic development. Histology suggests that the ossification center of notosuchian osteoderm is located at the keel. Interestingly, we identified Sharpey's fibers running perpendicularly to the outer layer of the external cortex in *Armadillosuchus arrudai*, *Itasuchus jesuinoi*, and Baurusuchidae (LPRP/USP 0642). This feature indicates a tight attachment within the dermis, and it is evidence for the presence of an overlying thick leathery layer of skin over these osteoderms. These data allow a better understanding of the osteohistological structure of crocodylomorph dermal bones, and highlight their structural diversity. We suggest that the vascular canals present in some sampled osteoderms connecting the inner layer of the external cortex and the core with the external surface may increase osteoderm surface and the capacity of heat transfer in terrestrial notosuchians.

KEYWORDS

ossification, osteoderm, osteohistology, Pseudosuchia

1 | INTRODUCTION

The reptile skin acts as an interface of the organism with the environment. It is composed of two layers, the epidermis and the dermis, separated by a fibrous membrane (Nyström & Bruckner-Tuderman, 2019). The outermost layer, the epidermis, is formed by three main strata: *stratum basale* or *germinativum* (inner), *stratum granulosum*, and *stratum corneum* (outer) (e.g., Rutland et al., 2019). The underlying layer, the dermis, is bilaminar and organized into the *stratum superficiale* and the *stratum compactum* (Williams et al., 2022). The dermis, where the osteoderms are located, includes blood vessels, cutaneous nerves, pigmentary cells, epidermic glandular tissues invaginating into the fibrous connective tissue (Rutland et al., 2019; Williams et al., 2022) and sometimes skeletal elements known as osteoderms.

Osteoderms are widespread integumentary features that occur in diverse extinct and extant amniotes, including turtles, nonavian archosaurs, lepidosaurs, and cingulatan mammals (Burns et al., 2013; Hill, 2005; Moss, 1972; Romer, 1956; Vickaryous & Sire, 2009; Witzmann, 2009). Osteoderms can bear superficial ornamentation in the dorsal surface, which may show different morphological patterns, such as tubercles in lizards, turtles, temnospondyls, and armadillos (de Buffrénil et al., 2011; Scheyer et al., 2007; Sena et al., 2021; Vickaryous & Hall, 2006; Witzmann & Soler-Gijón, 2010), and pits and grooves in crocodylomorphs (Marinho et al., 2006; Montefeltro, 2019). The osteohistology of osteoderms is heterogeneous (Vickaryous & Sire, 2009) comprising blood vessels, nerves, yellow marrow, a collagenous meshwork, and cancellous and cortical bone (Kirby et al., 2020; Moss, 1972; Vickaryous & Sire, 2009). Their microstructural organization reflects the mode of development, and it

is useful to infer evolutionary patterns and test hypotheses of homology (de Buffrénil et al., 2011). Osteoderms have a flexible resistant nature and Sharpey's fibers have a key role in anchoring them to the underlying musculature and connective tissue, thus contributing to the integrity of the skin (Chen et al., 2014; Kirby et al., 2020; Scheyer et al., 2007). Some studies already proposed different functions for osteoderms besides protection, including mineral storage (Dacke et al., 2015) and thermoregulation (Farlow et al., 2010; Inacio Veenstra & Broeckhoven, 2022; Seidel, 1979).

Crocodylomorpha, an archosaur group with an evolutionary history from Late Triassic (Bronzati et al., 2015; Mannion et al., 2015) are characterized by the presence of osteoderms (Hill, 2005; Marinho et al., 2006; Montefeltro, 2019). Only few exceptions have been described, the most important being the absence of these structures in metriorhynchoids as an adaptation to a fully aquatic lifestyle (Ósi et al., 2018). The spatial distribution of osteoderms in crocodylomorph bodies varies among groups. In Crocodylidae there are no osteoderm rows in the ventral surface, except by *Crocodylus johnstoni* and *C. cataphactus* (Brochu, 1999; Burns et al., 2013; Fuchs, 2006), whereas the extinct terrestrial *Simosuchus clarki* had a heavily armored body covered by osteoderms including dorsal and ventral surface of the body, as well as the limbs (Hill, 2010). In extant semi-aquatic Crocodylia osteoderms may help to stiffen the back to facilitate terrestrial locomotion (Molnar et al., 2014; Salisbury & Frey, 2001).

One of the most diverse groups of extinct crocodyliforms are the Notosuchia (sensu Ruiz et al., 2021), a clade of mostly terrestrial organisms limited to the Gondwanan landmasses during the Cretaceous. This group is characterized by a great diversity in osteoderms morphology, anatomy, and arrangements in the body ranging from

the complete absence of osteoderm cover in *Pissarrachampsia sera* (Godoy et al., 2016; Montefeltro, 2019) to the extreme dorsal shield present in *Armadillosuchus arrudai* (Marinho & Carvalho, 2009). In this paper, we investigate the microstructure of notosuchian osteoderms based on the comparison of a sample coming from the Cretaceous and the Cenozoic of Brazil, and a few Neosuchia for comparative purposes. Moreover, we infer developmental aspects based on published data obtained for extant taxa.

2 | MATERIALS AND METHODS

2.1 | Material

We performed thin-sections of 10 disarticulated osteoderms (seven notosuchians and three neosuchians; Figure S1) as listed below:

- *Marialiasuchus amarali* Carvalho and Bertini (1999). Partial osteoderm (MPM 087) from Late Cretaceous Bauru Group, Marilia-SP, Brazil.
- *Armadillosuchus arrudai* Marinho and Carvalho (2009). Partial osteoderm (LPRP/USP 0774) from Late Cretaceous Bauru Group, Jales-SP, Brazil.
- *Itasuchus jesuinoi* Price 1955. Complete osteoderm (CPPLIP 332) from Late Cretaceous Bauru Group, Uberaba-MG, Brazil.
- *Uberabasuchus terrificus* Carvalho, Ribeiro, and Avilla (2004). Complete osteoderm (CPPLIP 501) from Late Cretaceous Bauru Group, Uberaba-MG, Brazil.
- *Aplestosuchus sordidus* Godoy, Montefeltro, Norell, and Langer (2014). Complete osteoderm (LPRP/USP 0229-9) from the Uberaba-MG Bauru Group, General Salgado-SP, Brazil.
- Baurusuchidae indet. Two complete osteoderms (LPRP/USP 0634 and 0642) from Late Cretaceous Bauru Group, Brazil.
- Bernissartiidae indet. Fragmented osteoderm (LAPEISA 026) from Early Cretaceous, United Kingdom.
- *Caiman* sp. Complete osteoderm (LPRP/USP 0708, Castro et al., 2014) from the Pleistocene deposits at Ioiô cave Iraquara-BA, Brazil.
- *Guarinisuchus* cf. *G. munizi*, Barbosa, Kellner & Viana, 2008. Fragmented osteoderm (CAV 0013-V) from the Danian of Paraíba Basin, Brazil.

2.2 | Sampling and methods for histological analysis

Samples were removed from each osteoderm to prepare the histological slides. Except for that of Bernissartiidae indet., the osteoderms were sectioned transversely (Clarac et al., 2017). Thin sections were prepared using standard fossil histology techniques (Chinsamy & Raath, 1992) at LAPAMI, CAV/UFPE and housed at the LAPASI, UFRPE. The specimens were embedded in clear epoxy resin Resapol T-208, catalyzed with Butanox M50 and cut with a diamond-

tipped blade mounted on a saw. The mounting side of the sections was wet-ground using a metallographic polishing machine (Aropol-E, Arotec Ltda) with Arotec abrasive sandpapers of increasing grit size (80/P80, 320/P400, 1200/P1500) and grounded to a thickness 100–80 µm. Samples were observed using a petrographic polarizing microscope under normal and cross-polarized light with lambda compensator. Images were obtained using a Nikon Eclipse E600 POL microscope mounted to a Nikon Digital Sight DS-L 1, at CR2P. Our terminology follows Francillon-Vieillot et al. (1900) and Scheyer and Sander (2004).

2.3 | Bone compactness analysis

We transformed photographs of the thin sections into binary images using Adobe Photoshop® CS6. This method marks the bone tissue in black and vascular spaces (medullary cavity, vascular canals, and resorption cavities) in white. The binary images (Figure S2) were quantitatively analyzed in R using the Bone Profile R package, (Girondot & Laurin, 2003; Gônet et al., 2022) to calculate the compactness parameters. We quantified the bone compactness (ratio between the surface occupied by bone tissues and the total bone surface (Laurin et al., 2004), as well as the relative width of the transition zone between the medulla and the cortex (S), the distance of this transition zone from the center of the sections (P), and the minimum (Min) and maximum (Max) values of bone compactness (Girondot & Laurin, 2003) (Table S1).

3 | RESULTS

3.1 | Osteohistological descriptions

Most osteoderms possess superficial ornamentations on their external surface, which consists of shallow rounded pits or deep elongated grooves or sulci, whereas their basal surfaces are smooth. The general microstructural corresponds to the diploe structure, i.e., a central cancellous core framed by compact cortices, with different degrees of remodeling and the presence of cancellous bone. All osteoderms show high bone compactness (Buffrénil et al., 2010).

3.2 | *Armadillosuchus arrudai* (LPRP/USP 0774)

Although fragmentary, this osteoderm is well preserved, with its dorsal surface strongly ornamented (Figure 1a) by pits and four vascular canals connecting the inner and outer layers of the external cortex to the surface. The thin section shows a high level of bone compactness (0.873). The external cortex exhibits a ridged pattern with depressions. This cortex is formed by an outer thin layer of an almost avascular parallel-fibered bone tissue with flattened rows of osteocyte lacunae. One resorption line separates the outer and the inner layers of the external cortex (Figure 1b). This cortex

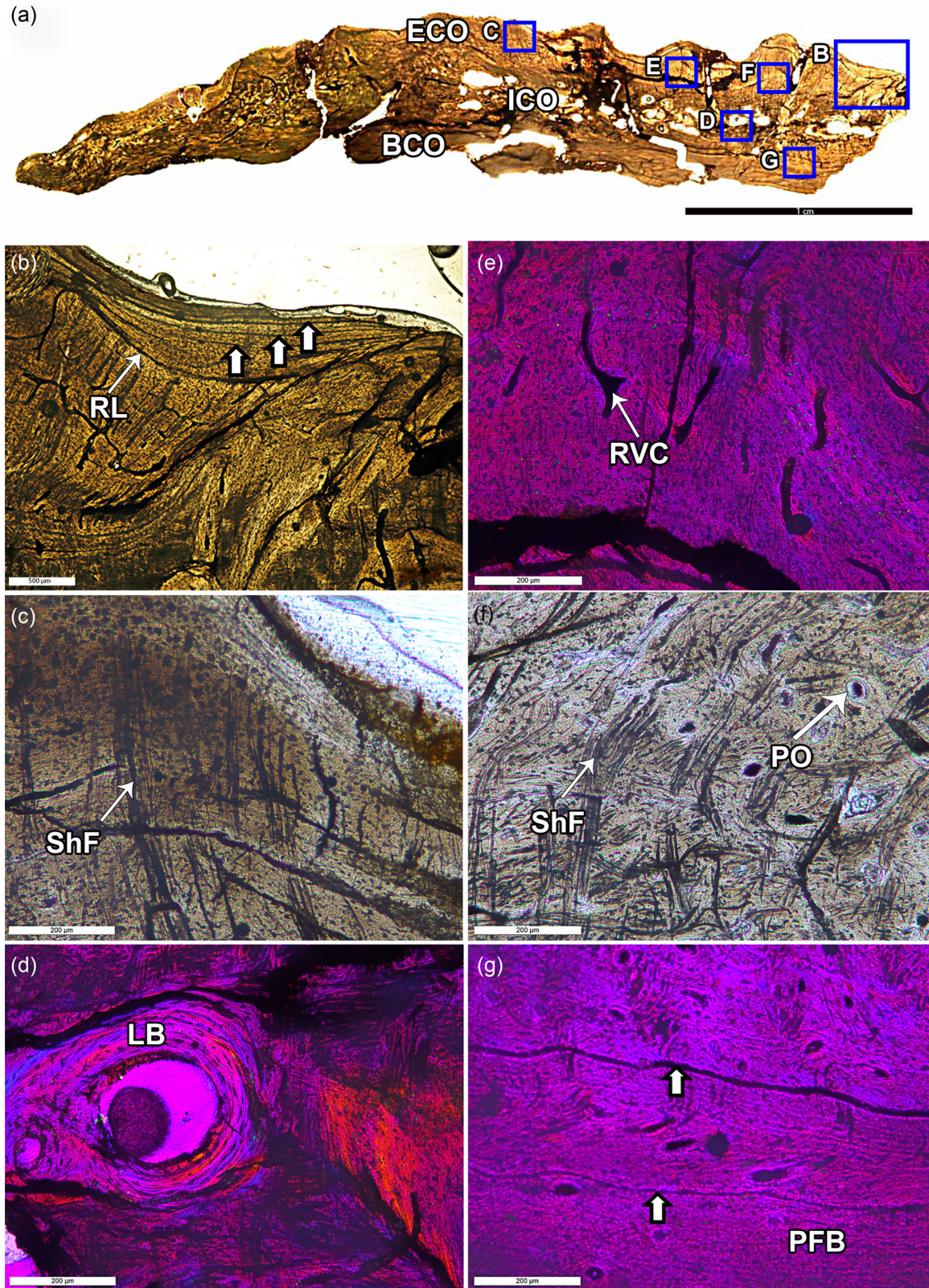


FIGURE 1 Histological section of an osteoderm of the notosuchian *Armadillosuchus arrudai* (LPRP/USP 0774) from Bauru Group, Brazil. (a) Microanatomical overview of the thin section of the osteoderm. (b) Note the presence of growth marks in the outermost cortex and a resorption line separating the two types of bone matrix. (c) Long Sharpey's fibers oriented nearly perpendicularly to the outer surface. (d) Close-up of the basal cortex exhibiting LAGs. (e) Detail of remodeling process in the inner core of the osteoderm. (f) Detail of the inner core showing short Sharpey's fibers. (g) Close-up of the basal cortex interrupted by growth marks. White arrow indicates line of arrested growth. Images: Normal transmitted light (a–c, f) and polarized light with lambda compensator (e, d, g). BCO, basal cortex; ECO, external cortex; ICO, inner core; LB, lamellar bone; PFB, parallel-fibered bone; PO, primary osteon; RL, resorption line; RVC, reticular vascular canal; ShF, Sharpey's fibers.

incorporates long Sharpey's fibers, i.e., mineralized in growing fibrillary processes from adjacent soft bone tissues (Francillon-Vieillot et al., 1990, p. 504), which are perpendicularly projected to the external surface (Figure 1c). The core is composed of woven bone with abundant osteocyte lacunae which are densely arranged and vascularized by reticular vascular canals (Figure 1f). It contains portions of remodeled bone with irregular erosion cavities and secondary osteons surrounded by lamellar bone (Figure 1d). The basal cortex reveals periodic growth, with parallel-fibered bone tissue interrupted by growth marks (Figure 1g). The osteocyte lacunae have a round shape in both woven and parallel-fibered matrix. However, a flattened aspect is observed in the lamellar matrix (Figure 1f,g). Vascularization mainly consists of simple or anastomosed vascular canals and scarce primary osteons.

3.3 | *Itasuchus jesuinoi* (CPPLIP 332)

This osteoderm presents ornamentation composed of pits and grooves (Figure 2a) and a bone compactness of 0.967. The external surface shows a smooth pattern of valleys and ridges. The outer layer of the external cortex consists of lamellar-zonal bone tissue interrupted by closely spaced growth marks. A resorption line is observed as the boundary between the outer and the inner layers of the external cortex. The vascular network is composed of a few simple or anastomosed primary vascular canals. Long Sharpey's fiber bundles are observed perpendicular to the external surface (Figure 2b). Osteocyte lacunae are elongated and orientated parallel to the fiber's orientation. The core presents a woven matrix with some portions of fibrolamellar tissue (Figure 2d), which is well-vascularized by primary osteons. The osteocyte lacunae are abundant and rounded in shape. Remodeling is identified by scattered secondary osteons (Figure 2e). The basal cortex is composed of parallel-fibered bone tissue interrupted by growth marks and vascularized by some primary osteons and reticular vascular canals (Figure 2c). Osteocyte lacunae show a flattened or irregular aspect oriented in parallel rows.

3.4 | *Mariliasuchus amarali* (MPM 087)

The superficial ornamentation of the osteoderm is formed by deep grooves, rare pits and vascular canals opening up from the inner core to the external surface (Figure 3a). The thin section shows a bone compactness of 0.857. The osteoderm exhibits a diploe structure and the cortices have similar thicknesses. The core is composed of heavily remodeled bone with numerous resorption cavities and secondary osteons surrounded by lamellar bone tissue (Figure 3d,e). The basal and external cortices are thin and formed by parallel-fibered and woven bone tissues vascularized by anastomosed and longitudinal vascular canals

(Figure 3b,c). The osteocyte lacunae have either irregular or round shapes, randomly distributed.

3.5 | *Uberabasuchus terrificus* (CPPLIP 501)

The external cortex bears some depressions, which form the superficial ornamentation composed of pits and grooves above the parallel-fibered bone tissue layer (Figure 4a). The osteoderm presents a high bone compactness degree of 0.989. The inner core is composed of woven bone (Figure 4b) tissue, vascularized by anastomosed and longitudinal vascular canals and primary osteons; other portions show osteoclastic activity in the form of erosion cavities. In these parts, osteocyte lacunae are more abundant and they are randomly distributed. Scarce secondary osteons are present in the core toward the basal cortex (Figure 4e), which is thicker than the external cortex and it is composed of parallel-fibered bone tissue and interrupted by growth marks and poorly vascularized (lamellar-zonal bone tissue) (Figure 4d). Osteocyte lacunae are less numerous than in the inner core, they also have a flat appearance oriented in parallel rows; short Sharpey's fibers cross perpendicularly the growth marks (Figure 4c).

3.6 | *Aplestosuchus sordidus* (LPRP/USP 0229-9)

This is a keeled osteoderm, with no superficial ornamentation and bone compactness of 0.920 (Figure 5a). The basal and external cortices are formed by parallel-fibered bone tissue with a reticular and longitudinal vascular pattern (Figure 5b and 5e). The basal cortex is thicker than the external one. The core presents some resorption cavities surrounded by remodeled lamellar bone tissue (Figure 5c). The growth marks are deposited in the cortices and core with some of them obliterated by remodeling. The osteocyte lacunae present either irregular or round shape and they follow the fibers orientation forming subparallel rows. The cortical bone incorporated Sharpey's fibers with oblique orientation, probably to keep the adhesion among osteoderms.

3.7 | *Baurusuchidae* indet. (LPRP/USP 0634 and 0642)

LPRP/USP 0634 is an osteoderm with a smooth ridge in the dorsal region and no superficial ornamentation and a bone compactness of 0.948 (Figure 6a). The basal and external cortices are well-vascularized showing a reticular and radial vascular pattern (Figure 6b). Some anastomosed vascular canals open towards the outer bone surface. The primary bone is mainly composed of woven and parallel-fibered bone. The inner region presents Haversian bone formed by different generations of

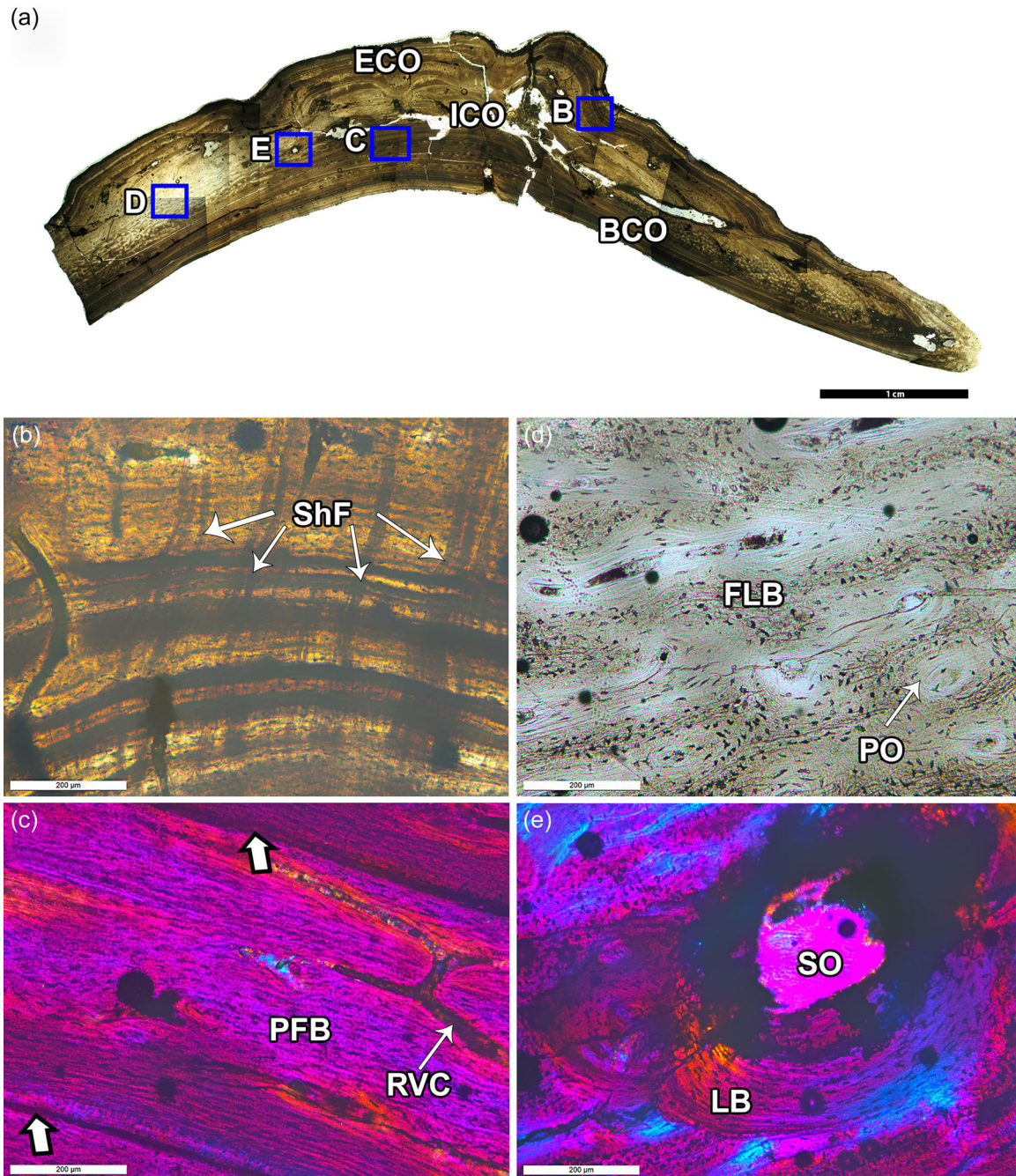


FIGURE 2 Histological section of an osteoderm of the notosuchian *Itasuchus jesuinoi* (CPPLIP 332) from Bauru Group, Brazil. (a) Microanatomical overview of the perpendicular section of the osteoderm's ridge. (b) Detail of Long Sharpey's fibers bundles oriented nearly perpendicularly to the outer surface. (c) Parallel-fibered cortical bone interrupted by cyclical growth marks. (d) Detail of the inner core formed by fibrolamellar bone. (e) Isolated secondary osteon representing the remodeling process in the inner core. White arrow indicates line of arrested growth. Images: Normal transmitted light (a–c) and polarized light with lambda compensator (c, e). BCO, basal cortex; ECO, external cortex; FLB, fibrolamellar bone; ICO, inner core; LB, lamellar bone; PFB, parallel-fibered bone; PO, primary osteon; RVC, reticular vascular canal; ShF, Sharpey fibers; SO, secondary osteon.

secondary osteons (Figure 6c,d) surrounded by lamellar bone tissue. Abundant Sharpey's fibers are embedded in the primary cortex but show no preferential orientation. Inner cortical portions are composed of parallel-fibered bone tissue which preserves few LAGs (Figure 6e). These growth marks look

obliterated by the remodeling process in the inner core (Figure 6d). The Osteocyte lacunae present round or irregular shapes that are abundant in the woven bone tissue. These cell lacunae exhibit a highly disorganized arrangement even in the parallel-fibered bone tissue.

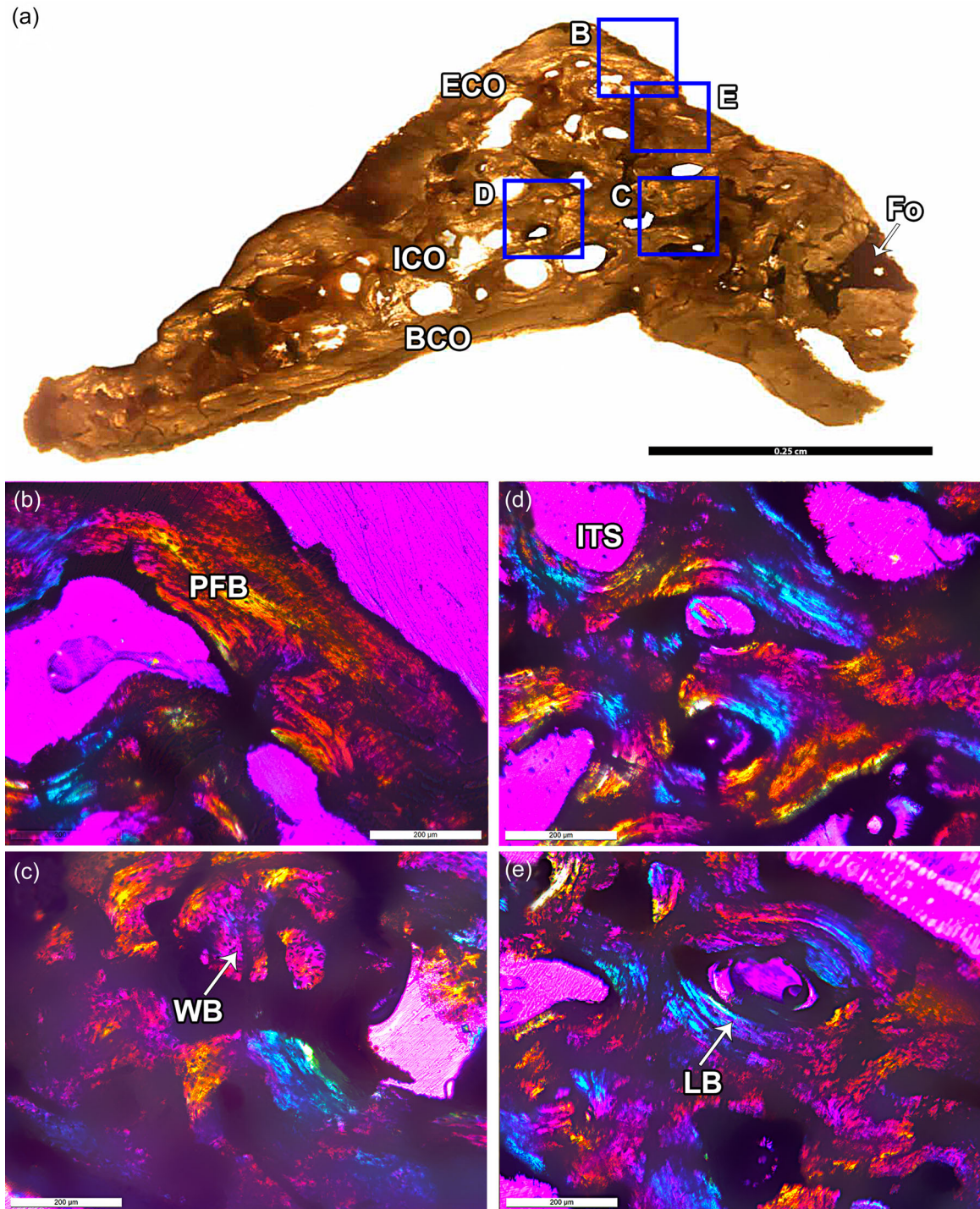


FIGURE 3 Histological section of an osteoderm of the notosuchian *Mariliasuchus amarali* (MPM 087) from Bauru Group, Brazil. (a) Microanatomical overview of the perpendicular section of the osteoderm's keel. (b) Detail of the external cortex constituted by disorganized parallel-fibered bone. (c) Portions of woven bone in the inner core. (d) Secondary cancellous bone featured by short trabeculae. (e) Lamellar bone surrounding the vascular spaces in the inner core. Images: Normal transmitted light (a) and polarized light with lambda compensator (b–e). BCO, basal cortex; ECO, external cortex; Fo, foramen; ICO, inner core; ITS, inter-trabecular space; LB, lamellar bone; PFB, parallel-fibered bone; WB, woven bone.

LPRP/USP 0642 exhibits a superficial ornamentation composed of shallow pits. A foramen canal connects the osteoderm core to the external surface (Figure 7a). The thin section reveals a high bone compactness of 0.912. The external cortex is formed by parallel-fibered

bone tissue. A circular cavity is seen in the central core of the keel (Figure 7b) surrounded by secondary lamellar bone tissue. A few growth marks are visible in some surfaces of the external parts, but these are more abundant in the basal cortex. Primary, parallel-fibered bone tissue

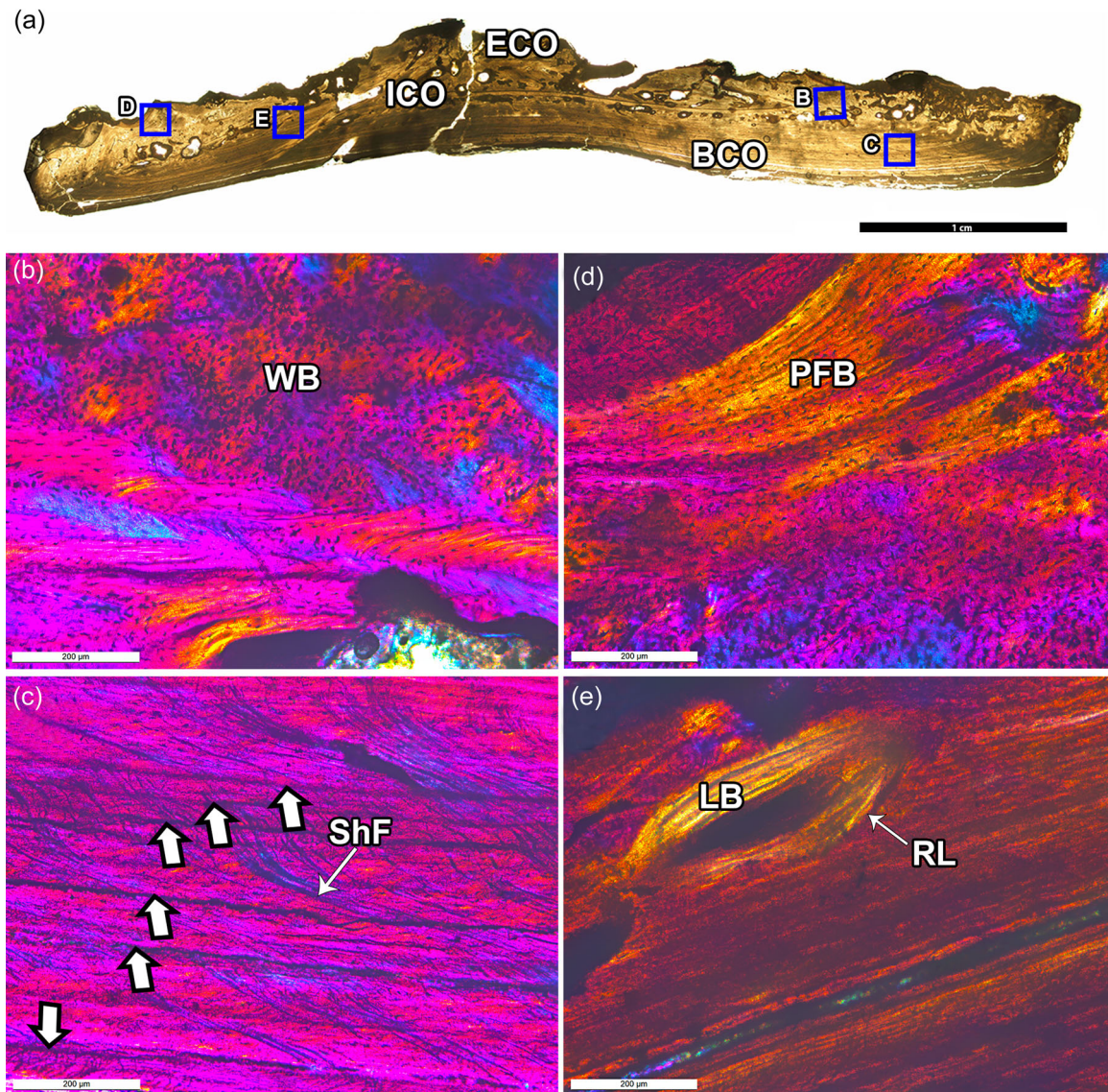


FIGURE 4 Histological section of an osteoderm of the notosuchian *Uberabasuchus terrificus* (CPPLIP 501) from Bauru Group, Brazil. (a) Microanatomical overview of the thin section of the osteoderm. (b) Close-up of the inner core composed of woven bone tissue with abundant osteocyte lacunae. (c) Detail of the short Sharpey's fibers attached to growth lines. (d) Close-up of the most external layer of the external cortex formed by parallel-fibered bone tissue. (e) Close-up of the remodeling process expanding into the basal cortex. White arrow indicates line of arrested growth. Images: Normal transmitted light (a) and polarized light with lambda compensator (b–e). AVC, anastomosed vascular canal; BCO, basal cortex; ECO, external cortex; ICO, inner core; LB, lamellar bone; PFB, parallel-fibered bone; PO, primary osteon; RL, resorption line; ShF, Sharpey's fibers; WB, woven bone.

vascularized by reticular vascular canals composes some portions of osteoderm core (Figure 7d). This region also presents scattered secondary osteons and erosion cavities surrounded by lamellar bone tissue. Some erosion cavities are anastomosed and others are concentrated towards the superficial keel. The basal cortex is formed by parallel-fibered bone tissue interrupted by growth marks (Figure 7e). Abundant bundles of Sharpey's fibers have diverse orientations, i.e., parallel, oblique or perpendicular towards the surface, in the compact cortex surface (Figure 7c). In the cortices, osteocyte lacunae possess an elongated or irregular aspect, and their arrangement follows the orientation of intrinsic fibers in which they are embedded.

3.8 | Bernissartiidae indet. (LPRP/USP 026)

Adiploe structure with a bone compactness of 0.956 is observed (Figure 8a). It is formed by a compact cortex, which is less vascularized than the inner region. The central core is mainly formed by small primary osteons and longitudinal vascular canals (Figure 8b). The cortices consist of woven bone tissue with abundant rounded or irregular osteocyte lacunae, randomly distributed (Figure 8c). The cortices are poorly vascularized by primary osteons, longitudinal or anastomosed vascular canals. The dark color of the thin section is probably due to impregnation of iron oxides during the fossil diagenetic processes.

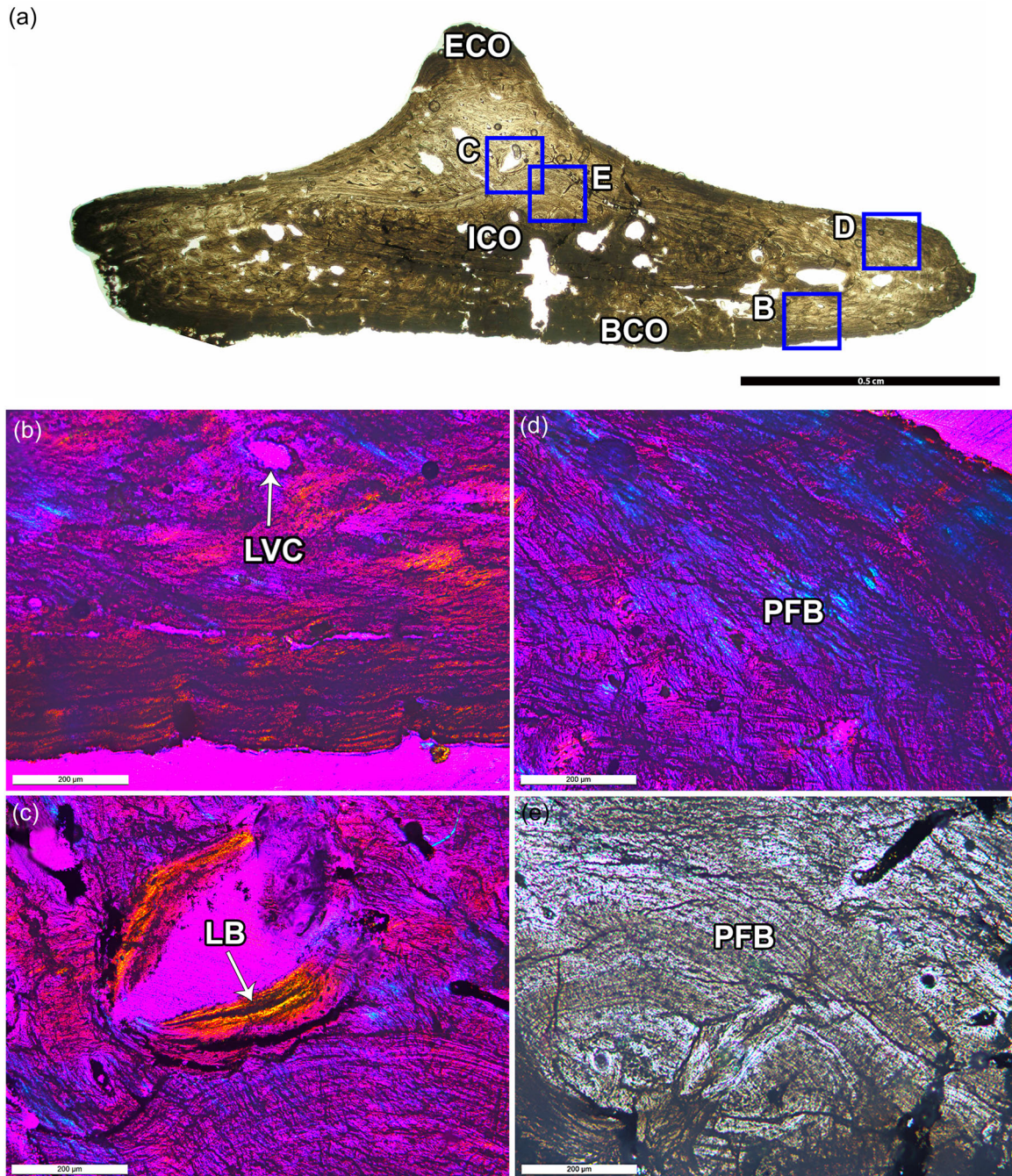


FIGURE 5 Histological section of an osteoderm of the notosuchian *Aplestosuchus sordidus* (LPRP/USP 0229-9) from Bauru Group, Brazil. (a) Microanatomical overview of the perpendicular section of the osteoderm's keel. (b) Slightly vascularized basal cortex showing mainly simple vascular canals. (c) Note the remodeling process in the inner core. (d, e) Close-up of the parallel-fibered bone tissue in external cortex and inner core. Images: Normal transmitted light (a, e) and polarized light with lambda compensator (b–d). BCO, basal cortex; ECO, external cortex; ICO, inner core; LB, lamellar bone; LVC, longitudinal vascular canal; and PFB, parallel-fibered bone.

3.9 | *Caiman* sp. (LPRP/USP 0708)

This is an ornamented and keeled osteoderm and its compactness reaches 0.963 (Figure 9a). A foramen is observed near the basis of the keel, crossing the entire external cortex (Figure 9b). The basal cortex and most of the core present iron oxides impregnations

from the fossil diagenesis and its microstructural pattern cannot be completely assessed. In the visible portions, the compact external cortex is formed by lamellar-zonal bone tissue with a parallel-fibered bone matrix interrupted by several growth marks (Figure 9c and 9e). The cortical bone is poorly vascularized with the presence of scattered primary osteons (Figure 9c). The core

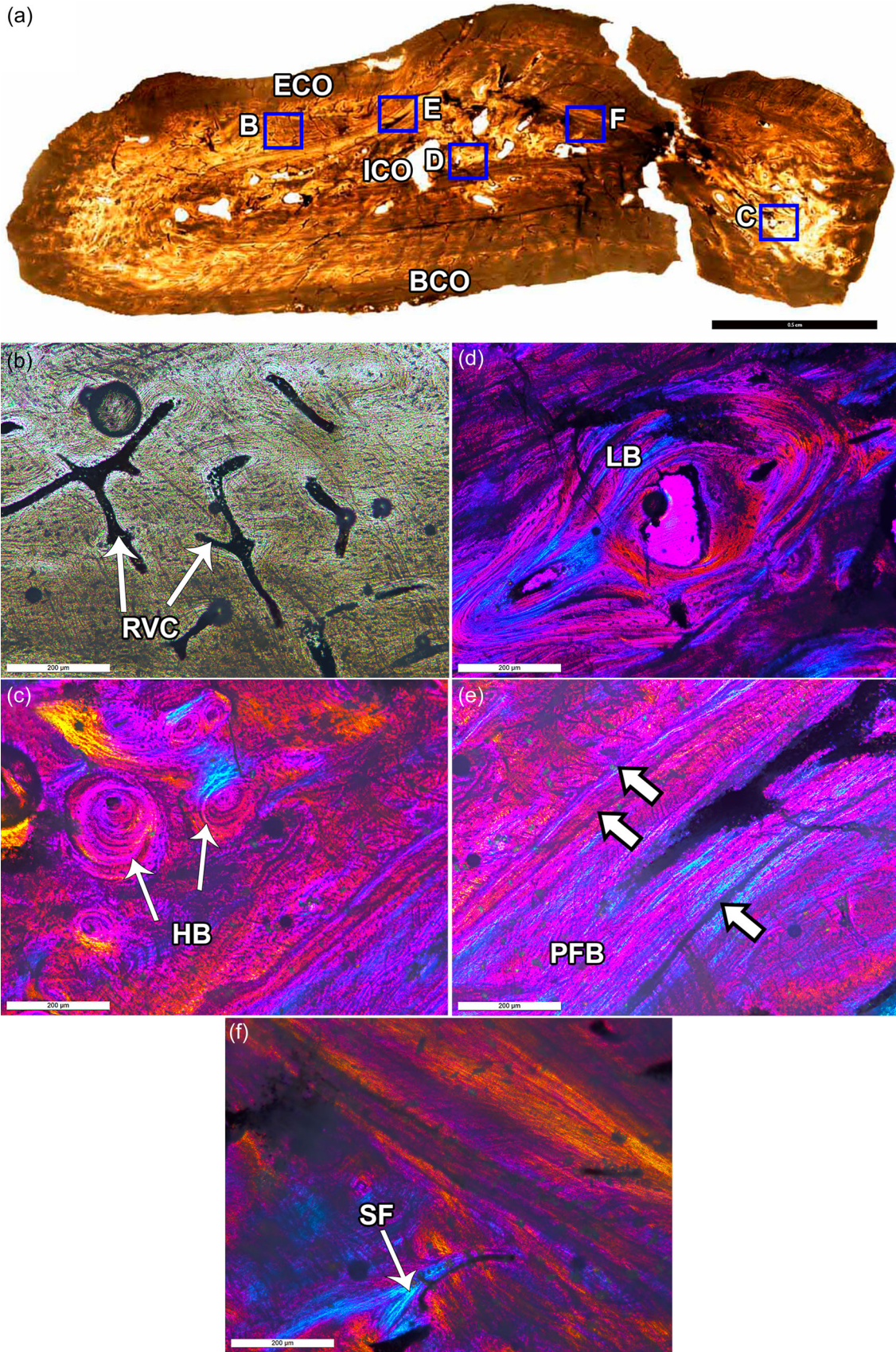


FIGURE 6 (See caption on next page)

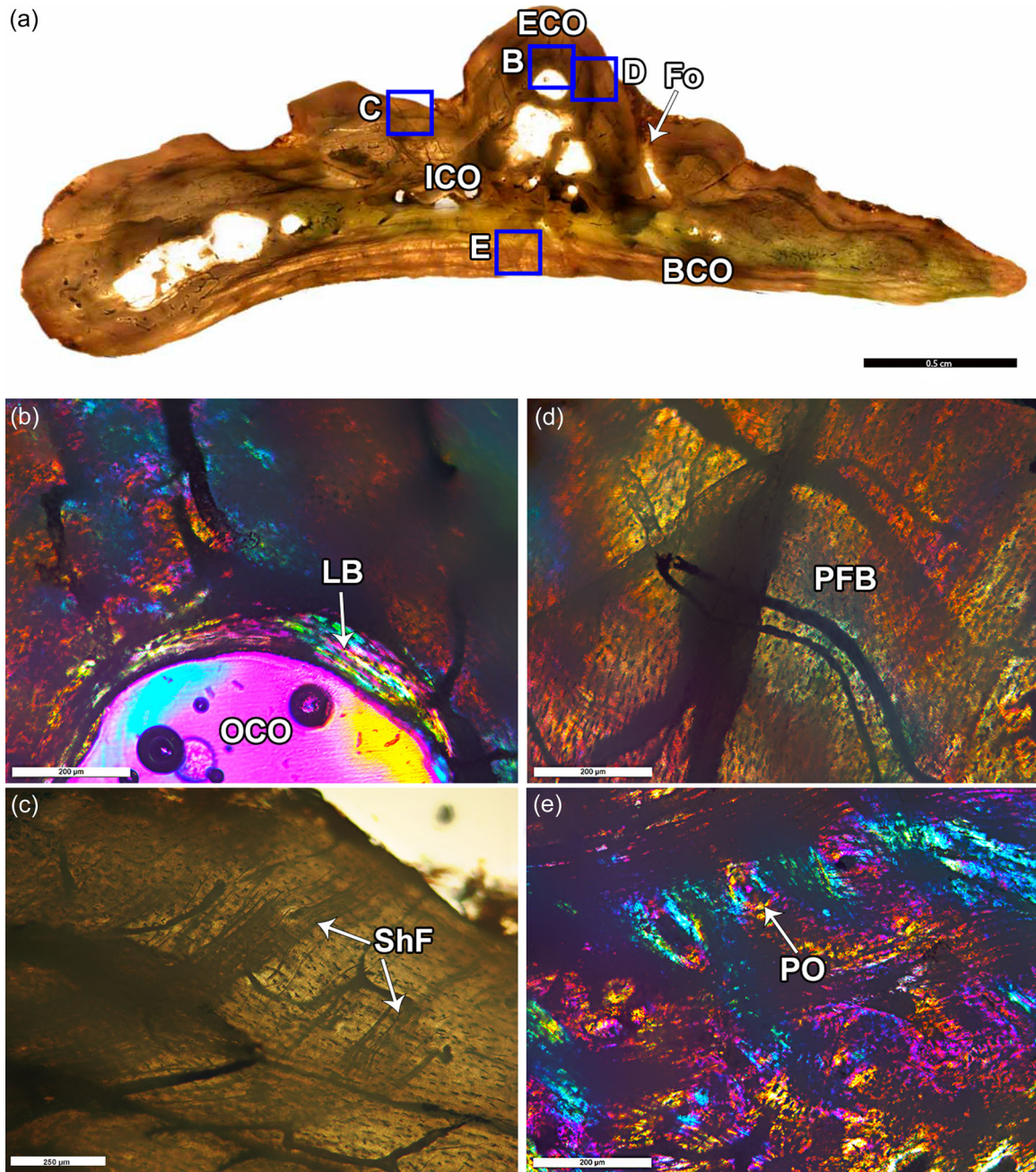


FIGURE 7 Histological section of an osteoderm of Baurusuchidae indet. (LPRP/USP 0642) from Bauru Group, Brazil. (a) Microanatomical overview of the perpendicular section of the osteoderm's keel. (b) Ossification center of the osteoderms surrounded by secondary lamellar bone tissue. (c) Note the presence of numerous Sharpey's fibers perpendicularly oriented in the outermost part of the cortex. (d, e) Detail of the disorganized parallel-fibered bone tissue. Images: Normal transmitted light (a, c) and polarized light with lambda compensator (b, d, e). BCO, basal cortex; ECO, external cortex; Fo, foramen; ICO, inner core; LB, lamellar bone; OCO, ossification center of osteoderms; PFB, parallel-fibered bone; PO, primary osteon; ShF, Sharpey's fibers.

FIGURE 6 Histological section of an osteoderm of Baurusuchidae indet. (LPRP/USP 0634) from Bauru Group, Brazil. (a) Microanatomical overview of the perpendicular section of the osteoderm's ridge. (b) Reticular vascular pattern in the primary bone tissue. (c) Detail of the inner core formed by Haversian bone. (d) Secondary osteons anastomosed. (e) Close up of primary bone with three cyclical growth marks preserved. (f) Detail of inner core showing structural fibers. White arrow indicates line of arrested growth. Images: Normal transmitted light (a, b) and polarized light with lambda compensator (c–e). BCO, basal cortex; ECO, external cortex; HB, Haversian bone; ICO, inner core; LB, lamellar bone; PFB, parallel-fibered bone; RVC, reticular vascular canal; SF, structural fibers.

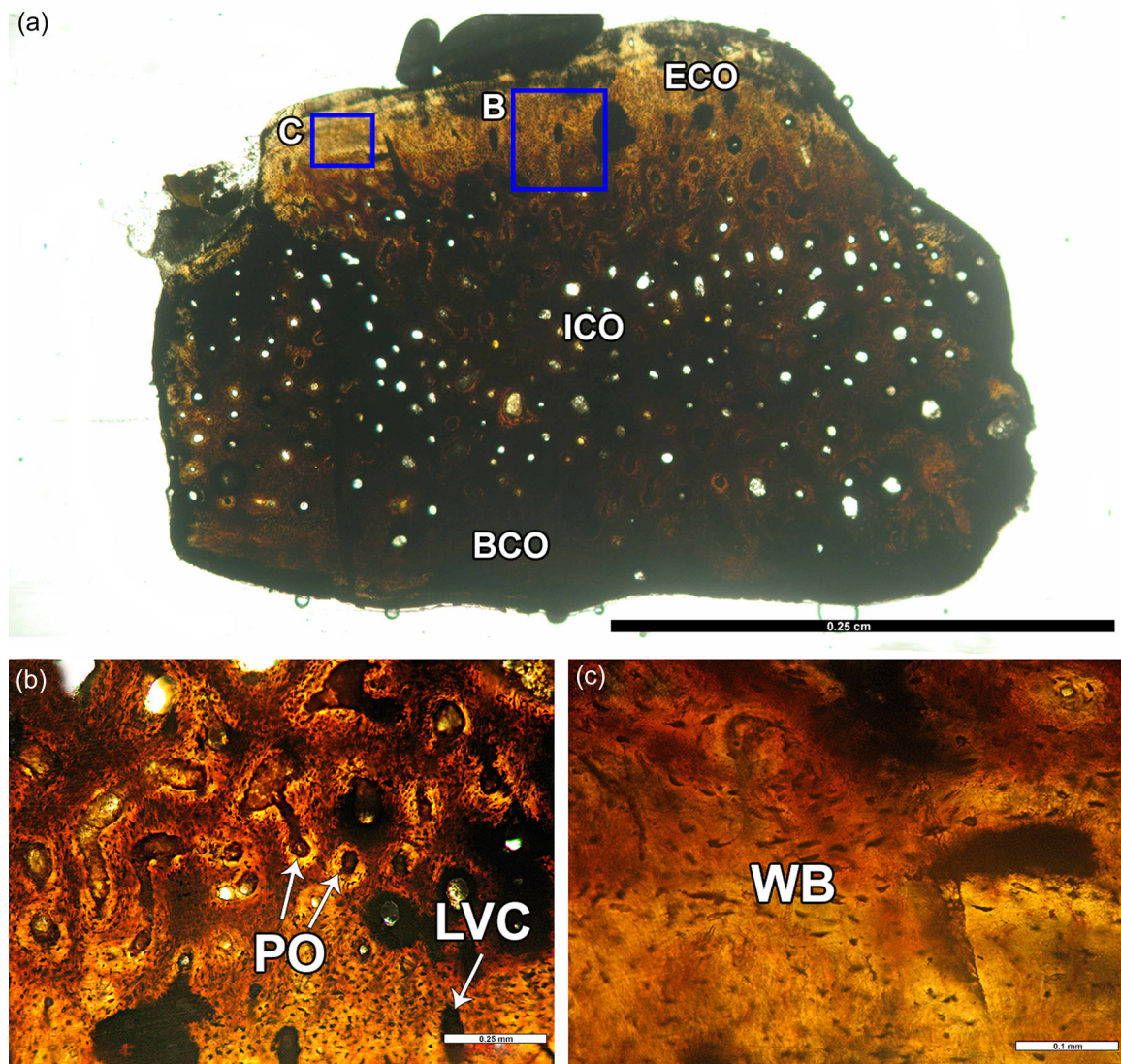


FIGURE 8 Histological section of an osteoderm of the neosuchian Bernissartiidae indet. (LAPEISA 026) from Alpercatas Basin, Brazil. (a) Microanatomical overview of the fragmented osteoderms. (b) Inner core is mainly vascularized by primary osteons and longitudinal vascular canals. (c) Cortical bone seems to be formed by woven bone tissue. Images: Normal transmitted light. BCO, basal cortex; ECO, external cortex; ICO, inner core; LVC, longitudinal vascular canal; PO, primary osteon; WB, woven bone.

shows resorption cavities and secondary bone tissues sectioned in different orientations (Figure 9d). Osteocyte lacunae show elongated or irregular aspect, following orientation of the fibers in the primary bone tissue.

3.10 | *Guarinisuchus* cf. *G. munizi* (CAV 0013-V)

Both cortices are narrow and formed by avascular parallel-fibered bone tissue (Figure 10b). The cancellous bone is the largest layer; it is constituted by thin and long trabeculae (Figure 10a), intertrabecular spaces and erosion cavities (Figure 10d). The walls of the trabeculae bone constitute secondary lamellar bone lining vascular spaces and the primary interstitial bone areas within the trabeculae (Figure 10e). Osteocyte lacunae show different shapes, they are flattened in the

secondary lamellar bone tissue of the inner core, irregular in the primary parallel-fibered bone tissue and rounded in the primary interstitial bone tissue (Figure 10c-e).

4 | DISCUSSION

4.1 | General microstructural pattern

We sampled osteoderms with distinct external morphologies from different body positions. *Itasuchus* (dorsal), *Uberabasuchus* (dorsal) and *Armadillosuchus* (dorsal accessory) show a reduced cancellous layer. *Guarinisuchus* presents thin cortices and a well-developed secondary cancellous bone with long and slender trabeculae. The structure of baurusuchid LPRP/USP 0634 is

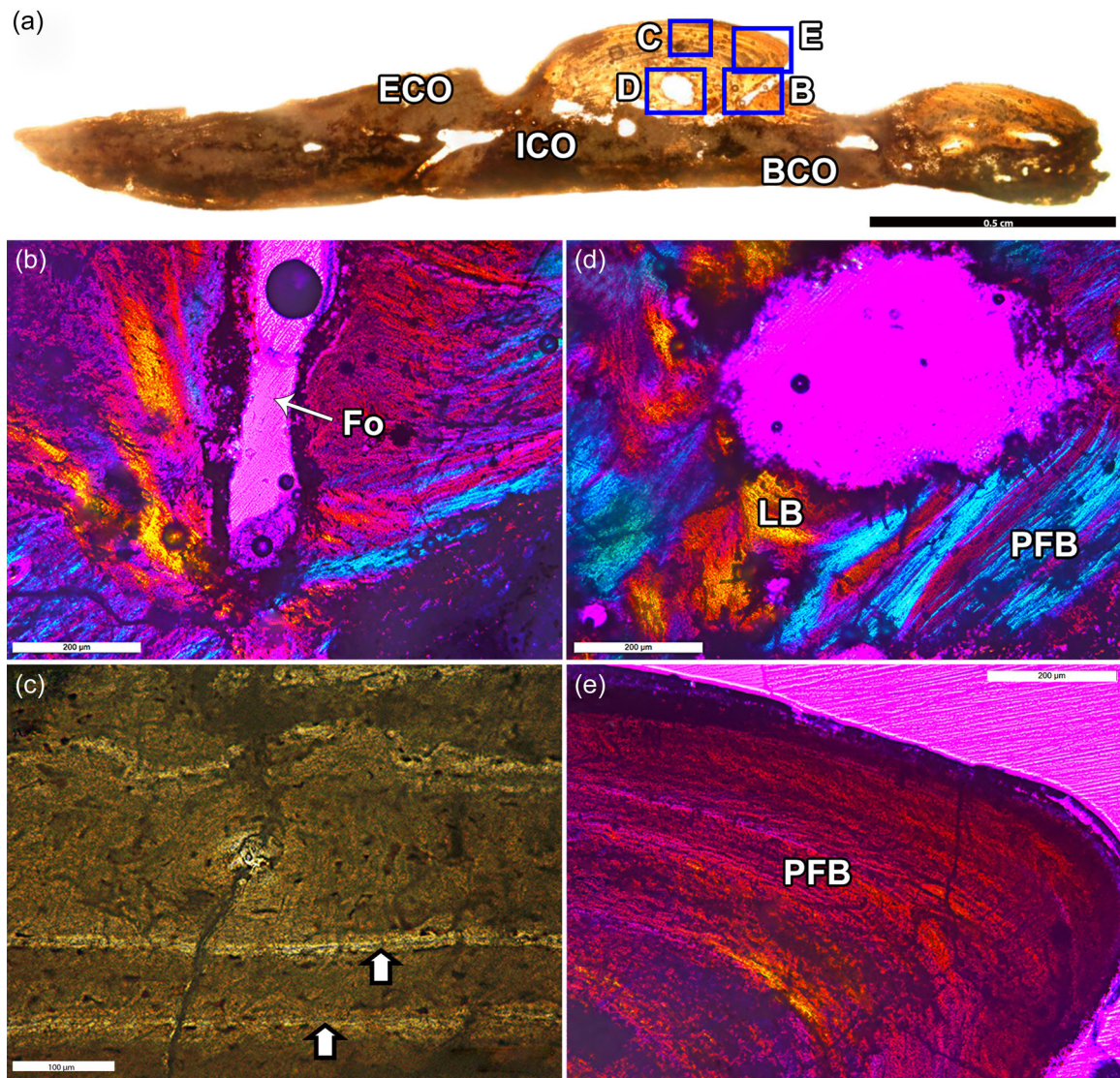


FIGURE 9 Histological section of an osteoderm of the neosuchian *Caiman* sp. (LPRP/USP 0708) from Gruta do Ioiô, Brazil. (a) Microanatomical overview of the osteoderm's keel. (b) Detail of a foramen situated in the bottom of the keel. (c) Note two lines of arrested growth in the external cortex. (d) Close-up of different orientations of the fibers bundles. (e) Poorly vascularized parallel-fibered bone tissue. White arrow indicates line of arrested growth. Images: Normal transmitted light (a, c) and polarized light with lambda compensator (b, d, e). BCO, basal cortex; ECO, external cortex; Fo, foramen; ICO, inner core; LB, lamellar bone; PFB, parallel-fibered bone.

similar to Baurusuchidae (MPMA 62.0002.02; Marchetti et al., 2022) characterized by the presence of cancellous bone containing small erosion cavities and highly vascularized cortices. The cancellous bone in Bernissartiidae osteoderm (indeterminate position) has a primary origin similar to the Aetosaurinae paramedian plate, MLP 61-VIII-2-34 (Cerde & Desojo, 2011). The inner core is the most histologically diverse layer besides the remodeled bone; it could present portions of parallel-fibered or fibrolamellar bone tissues (Figure 2d). Scheyer et al. (2014) indicated that the remodeling degree is directly related to the external ornamentation of the osteoderms. We did not observe this pattern in our sample since the highest degrees of remodeling was found in the scarcely ornamented *Guarinisuchus* osteoderm, while well-ornamented osteoderms (*Caiman* sp., *Armadillosuchus*

arrudai and *Uberabasuchus terrificus*) show lower degree of resorption and secondary bone deposition.

Most of the osteoderms investigated in this study possess a diploe structure containing two cortices, the external and the basal cortices, and a core between them. This structure is similar to that observed in xenarthran osteoderms (Vickaryous & Hall, 2006), early tetrapods (Witzmann & Soler-Gijón, 2010), the aetosaurus *Calyptosuchus wellsi* and *Stagonolepis olenkae* (Scheyer et al., 2014); raiusuchians (Scheyer & Desojo, 2011) and turtle shell bones (e.g., Sena et al., 2021; Skutschas et al., 2017). This pattern differs from that observed in the Aetosaurinae specimens described by (Cerde & Desojo, 2011) and in the doswelliid *Tarjadia ruthae* dermal plates (Ponce et al., 2017), which lack the cancellous bone layer, and from the pareiasaurians (Scheyer & Sander, 2009), which exhibit a spongy

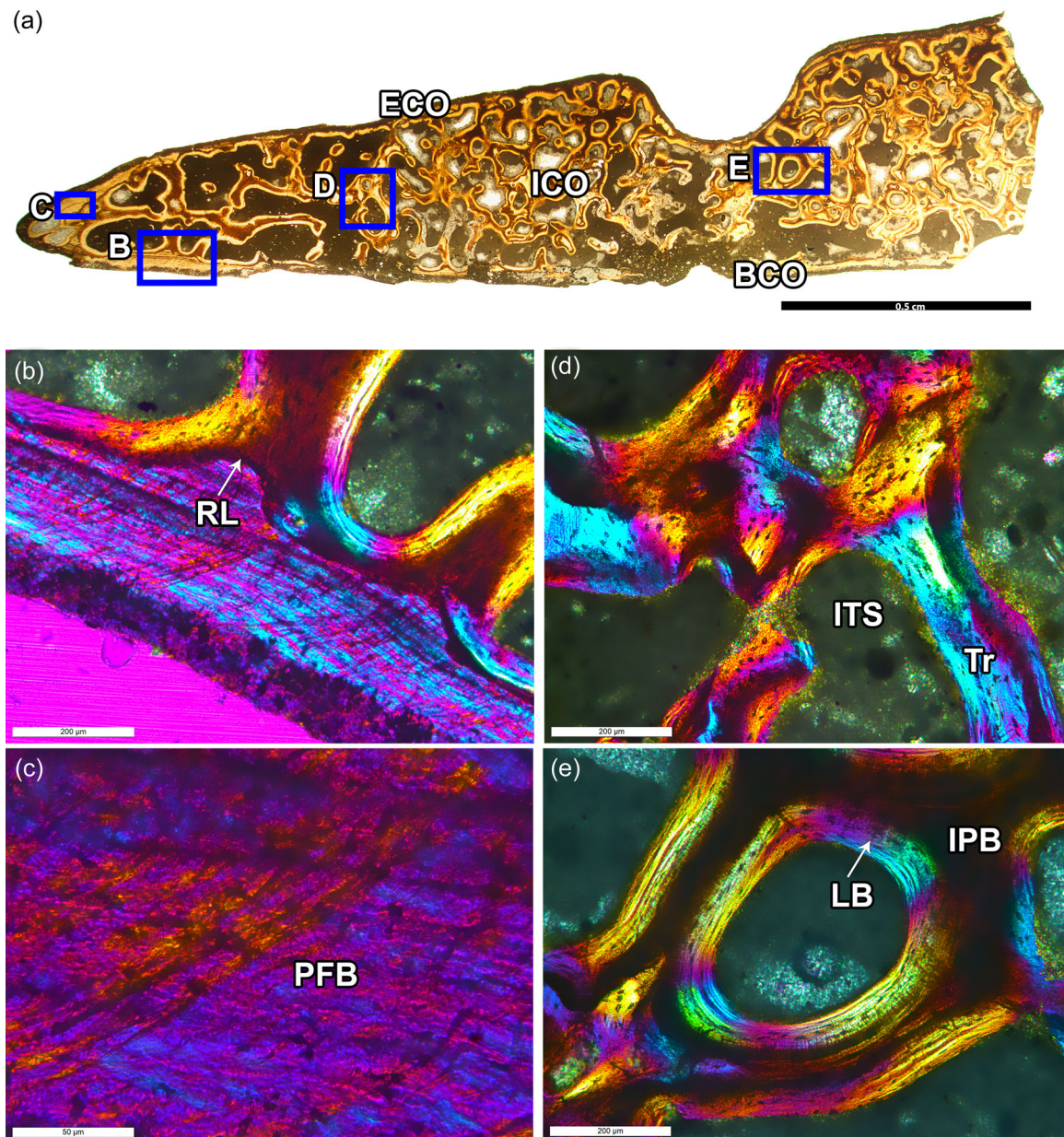


FIGURE 10 Histological section of an osteoderm of the neosuchian *Guarinisuchus* cf. *Guarinisuchus munizi* (CAV 0013-V) from Paraíba Basin. (a) Microanatomical overview of the thin section of the osteoderm. (b) Resorption line delimits the transition between basal cortex and inner core. (c) Close-up of the thin cortex formed by parallel-fibered bone tissue. (d) Trabecular bone tissue forms the intermediate layer. (e) Interstitial primary bone is preserved inside the trabeculae. Images: Normal transmitted light (a) and polarized light with lambda compensator (b–e). BCO, basal cortex; ECO, external cortex; ICO, inner core; IPB, interstitial primary bone; ITS, inter-trabecular space; LB, lamellar bone; PFB, parallel-fibered bone; RL, resorption line; Tr, trabecula.

osteoderm. In the osteoderms studied here, the cortices display a homogenous aspect formed by parallel-fibered with some cyclical growth marks. The bone compactness of these Notosuchia specimens is higher than 85% included in the range of bone compactness of pseudosuchian osteoderms from 0.987 to 0.660 (e.g., Cerda et al., 2018; Ponce et al., 2017). *Armadillosuchus arrudai* presents the lowest bone compactness among notosuchians analyzed. Scheyer & Sander (2009) reported that the association of bone compactness and lifestyle is controversial for amniote osteoderms. In

crocodyliforms, the bone compactness seems to have no influence on their lifestyle. It is probably related to the extension of osteoderm covering of the body. For instance, the dermal plates in *Simosuchus clarki* (Hill, 2010) and *Guarinisuchus* are extremely porous and lightly constructed. This high degree of porosity might be biomechanically relevant because it decreases the weight of the armor, ensuring its mobility as proposed by Chen et al. (2014) for *Alligator*.

The osteoderms of *Uberabasuchus terrificus*, *Itasuchus jesuinoi*, *Armadillosuchus arrudai*, *Marillasuchus amarali*, and *Baurusuchidae*

indet. (LPRP/USP 0642) have basal cortices similar to those of aetosaurs, other pseudosuchian, and turtle shell plates (Scheyer et al., 2007; Sena et al., 2020, 2021). They are composed of parallel-fibered bone tissue poorly vascularized interrupted by growth marks.

However, *Aplestosuchus sordidus* and Baurusuchidae indet. (LPRP/USP 0634) show highly vascularized basal cortices, similar to those of phytosaur osteoderms (Scheyer et al., 2014; Figure 5d). The vascular pattern in the osteoderms of bernissartiid resembles that of the Aetosaurinae, which was interpreted as a true fibrolamellar complex (Cerdeña & Desojo, 2011; Figure 3e). However, we could not assess whether this dermal plate of bernissartiid presents fibrolamellar bone tissue due to the impregnation of the bone matrix by iron oxides from the fossil diagenesis.

The structure of Sharpey's fibers varies between the external and basal cortices. In the external cortex these fibers are long and thick while in the basal cortex they are shorter, thinner and more abundant intercepting growth marks. This pattern is also recognized in other extinct and extant archosaurs and turtles (e.g., de Buffrénil et al., 2015; Hill, 2010; Sena et al., 2018; Woodward, Horner & Farlow, 2014). This pattern reflects the connection between the basal cortex and *stratum compactum* of the dermis (Burn et al., 2013) and suggests a tight anchorage of the osteoderm within the dermis (Scheyer et al., 2007). Sharpey's fibers are inserted perpendicularly to the external surface of the bone in the external cortices of *Armadillosuchus arrudai*, *Itasuchus jesuinoi* and Baurusuchidae indet. (LPRP/USP 0642). It suggests that during postembryonic growth, pre-existing collagen bundles of the dermis are incorporated perpendicularly into the element. The presence of Sharpey's fibers perpendicular to the outer layer of the external cortex is recorded also in recent trionychid turtle shell bones, in the marine turtle *Dermochelys coriacea* (Scheyer et al., 2007) and in the extinct aetosaur *Stagonolepis olenkae* (ZPAL Ab III/2379) (Scheyer et al., 2014). We suggest that this feature is associated with the presence of a leathery dermis layer covering the osteoderms, similar to that covering the shell plates of recent soft-shelled turtles and the marine leatherback turtle. Because of that we suggest that *Armadillosuchus arrudai*, *Itasuchus jesuinoi* and baurusuchid indet. (LPRP/USP 0642) also had their dermal bones firmly anchored within the dermis covered by a leathery layer. This feature should increase the flexibility of their dermal armor as proposed by Chen et al. (2015) for *Dermochelys coriacea*.

4.2 | Osteoderm skeletogenesis

At least three different ossification mechanisms were already proposed for the formation of reptile osteoderms and scute plates: metaplastic ossification (Scheyer & Sander, 2004), intramembranous ossification (von Baczko et al., 2020) and fibrocartilaginous ossification (Scheyer, 2007). Here, we propose that most notosuchian osteoderms sampled show the intramembranous ossification similar to what has been described in *Riojasuchus tenuisiceps* (von Baczko et al., 2020), where a periosteal layer replaces a primary

noncartilaginous connective tissue. Portions of structural fibers found in the osteoderms of the Baurusuchid indet. (LPRP/USP 0634) can be interpreted as metaplastic tissue as proposed by Scheyer and Sander (2004) for ankylosaur osteoderms and Scheyer and Sánchez-Villagra (2007) for the turtle shells. The metaplastic development, which is the direct transition from the dermis into mineralized tissue (*sensu* Beresford, 1981), is rare for squamate (Vickaryous et al., 2015; Williams et al., 2022) and archosaur (Scheyer & Sander, 2004; Vickaryous & Hall, 2008) osteoderms. Also, it is worth noting that, unlike lizards, crocodyliform osteoderms do not regenerate (Vickaryous et al., 2015; Williams et al., 2022). In contrast, metaplasia is the main ossification type of shell plates of some turtle taxa (Scheyer & Sánchez-Villagra, 2007; Sena et al., 2020). Finally, metaplasia in Baurusuchidae indet. (LPRP/USP 0634; Figure 6f) seems to have occurred after the initial step of intramembranous ossification, as postulated by Vickaryous and Hall (2006) for *Dasypus*. Our findings corroborate Dubansky & Dubansky (2018) results suggesting that intramembranous ossification is the main process involved in the development of crocodyliform osteoderms.

According to von Baczko et al. (2020) the intramembranous ossification appears to be involved with the origin of osteoderms in Pseudosuchia being observed in early stages of osteoderms development, and also in basal group (Cerdeña et al., 2018), whereas the metaplastic ossification is more unusual. The osteoderms studied here also present a plesiomorphic set of growth pattern typical of turtles and crocodiles, represented by the lamellar zonal bone composing the basal cortex (Klein, 2010), i.e., parallel-fibered and/or lamellar bone matrix showing several cyclical growth marks (see Francillon-Vieillot et al., 1990).

In addition, similar to turtle shells, the Baurusuchidae indet. (LPRP/USP 0642) and the *Caiman* sp. osteoderms present an isolated and enlarged circular space situated in the keel (Figures 7b and 9a). Such vascular canals are interpreted as the ossification centers of the osteoderms and are seen in shell plates of the extinct *Araripemys barretoii* (Sena et al., 2021), *Heckerochelys romani* (Scheyer et al., 2014), the testudinatan *Condorchelys antiqua* (Cerdeña et al., 2016) and the extant *Podocnemis expansa* (Vieira et al., 2016) turtles. Osteoderms have a late ontogeny; they develop after the postcranial skeleton has formed within the well-differentiated dermis (Vickaryous & Hall, 2006). Similar to the formation of alligator osteoderm begins with calcium mineralization at the center (keel region) and proceeds radially, 1 year after hatching; calcium is gradually deposited on the collagen fibers from the surrounding dermis layer (Vickaryous & Hall, 2008).

5 | CONCLUSION

The osteohistological data presented here suggest that notosuchian osteoderms are conservative regarding their microstructure. They show features like lamellar-zonal growth and mainly intramembranous ossification. Nonetheless, mineralized structural fibers were identified in osteoderms of baurusuchid (LPRP/USP 0634) indicating

the contribution of metaplastic mineralization of collagenous fibers during skeletogenesis. Also, the presence of long and dense Sharpey's fibers perpendicular to the external cortex of *Armadillosuchus arrudai*, *Itasuchus jesuinoi*, and *Baurusuchid* indet. (LPRP/USP 0642) osteoderms suggest their tight anchorage to an overlying leathery dermis layer increasing the dermal armor flexibility.

AUTHOR CONTRIBUTIONS

Mariana Sena: Formal analysis (lead); funding acquisition; investigation (lead); methodology (lead); writing—original draft (lead); writing—review and editing (lead). **Thiago S Marinho:** Investigation; resources; writing—original draft; writing—review and editing. **Felipe C Montefeltro:** Investigation; resources; writing—original draft; writing—review and editing. **Max C Langer:** Investigation; resources; writing—original draft; writing—review and editing. **Thiago Schneider Fachini:** Investigation; resources; writing—original draft; writing—review and editing. **William R Nava:** Investigation; resources; writing—original draft; writing—review and editing. **Andre E. Piacentini Pinheiro:** Investigation; resources; writing—original draft; writing—review and editing. **Esau Victor de Araujo: Paul Aubier:** Investigation; resources; writing—original draft; writing—review and editing. **Rafael Cesar Pedrosa Andrade:** Investigation; resources; writing—original draft; writing—review and editing. **Juliana Manso Sayao:** Investigation; resources; writing—original draft; writing—review and editing. **Gustavo Ribeiro de Oliveira:** Investigation; resources; writing—original draft; writing—review and editing. **Jorge Cubo:** Conceptualization (lead); funding acquisition (lead); methodology (equal); project administration (lead); supervision (equal); writing—review and editing (lead).

ACKNOWLEDGMENTS

We thank D. Germain, curator of the Vertebrate Hard Tissue Collection of the Centre de Recherche en Paleontologie – Paris (MNHN, CNRS, and Sorbonne Université), Dr. A. Houssaye, CNRS professor, and Dr. A. Herrel, head of the Function and Evolution team of the Unite Mixte de Recherche UMR 7179 (MNHN) for permitted acquisition of the pictures in their laboratories. We also thank the reviewers Dr. T. Scheyer and an anonymous reviewer for their comments and suggestions that helped improve the quality of the manuscript. We also thank Fundação Cearense de Apoio ao Desenvolvimento Científico e Tecnológico (FUNCAP) and Conselho Nacional de Desenvolvimento Científico e Tecnológico (CNPq) for financial support grants. This research was supported by Sorbonne Université (Projet Emergences 2019 No. 243374 to J. Cubo).

DATA AVAILABILITY STATEMENT

The data that support the findings of this study are openly available in Hal Sorbonne Université at <https://hal-sorbonne-universite-fr.ezproxy.u-pec.fr/>.

ORCID

Mariana Valéria de Araujo Sena  <http://orcid.org/0000-0003-4708-999X>

REFERENCES

- von Baczko, M. B., Desojo, J. B., & Ponce, D. (2020). Postcranial anatomy and osteoderm histology of *Riojasuchus tenuisiceps* and a phylogenetic update on Ornithosuchidae (Archosauria, Pseudosuchia). *Journal of Vertebrate Paleontology*, 39, e1693396.
- Beresford, W. A. (1981). Chondroid bone, secondary cartilage, and metaplasia, *Baltimore, Md.* Urban & Schwarzenberg.
- Brochu, C. A. (1999). Phylogenetics, taxonomy, and historical biogeography of alligatoroidea. *Journal of Vertebrate Paleontology*, 19, 9–100.
- Bronzati, M., Montefeltro, F. C., & Langer, M. C. (2015). Diversification events and the effects of mass extinctions on Crocodyliformes evolutionary history. *Royal Society Open Science*, 2, 140385.
- de Buffrénil, V., Clarac, F., Fau, M., Martin, S., Martin, B., Pellé, E., & Laurin, M. (2015). Differentiation and growth of bone ornamentation in vertebrates: A comparative histological study among the Crocodylomorpha. *Journal of Morphology*, 276, 425–445.
- de Buffrénil, V., Dauphin, Y., Rage, J. C., & Sire, J. Y. (2011). An enamel-like tissue, osteodermine, on the osteoderms of a fossil anguid (Glyptosaurinae) lizard. *Comptes Rendus Palevol*, 10, 427–437.
- de Buffrénil, V., Sire, J.-Y., & Rage, J.-C. (2010). The histological structure of glyptosaurine osteoderms (Squamata: Anguidae), and the problem of osteoderm development in squamates. *Journal of Morphology*, 271, NA.
- Burns, M. E., Vickaryous, M. K., & Currie, P. J. (2013). Histological variability in fossil and recent alligatoroid osteoderms: Systematic and functional implications. *Journal of Morphology*, 274, 676–686.
- Castro, M. C., Montefeltro, F. C., & Langer, M. C. (2014). The quaternary vertebrate fauna of the limestone cave Gruta do Ioiô, northeastern Brazil. *Quaternary International*, 352, 164–175.
- Cerda, I. A., & Desojo, J. B. (2011). Dermal armour histology of aetosaurs (Archosauria: Pseudosuchia), from the upper triassic of Argentina and Brazil: Aetosaurinae osteoderm bone histology. *Lethaia*, 44, 417–428.
- Cerda, I. A., Desojo, J. B., & Scheyer, T. M. (2018). Novel data on aetosaur (Archosauria, Pseudosuchia) osteoderm microanatomy and histology: Palaeobiological implications. *Palaeontology*, 61, 721–745.
- Cerda, I. A., Sterli, J., & Scheyer, T. M. (2016). Bone shell microstructure of *Condorchelys antiqua* Sterli, 2008, a stem turtle from the Jurassic of Patagonia. *Comptes Rendus Palevol*, 15, 128–141.
- Chen, I. H., Yang, W., & Meyers, M. A. (2014). Alligator osteoderms: Mechanical behavior and hierarchical structure. *Materials Science and Engineering: C*, 35, 441–448.
- Chen, I. H., Yang, W., & Meyers, M. A. (2015). Leatherback sea turtle shell: A tough and flexible biological design. *Acta Biomaterialia*, 28, 2–12.
- Chinsamy, A., & Raath, M. (1992). Preparation of fossil bone for histological examination. *Palaeontologia Africana*, 29, 39–44.
- Clarac, F., Goussard, F., Teresi, L., de Buffrénil, V., & Sansalone, V. (2017). Do the ornamented osteoderms influence the heat conduction through the skin? A finite element analysis in Crocodylomorpha. *Journal of Thermal Biology*, 69, 39–53.
- Dacke, C. G., Elsey, R. M., Trosclair, P. L., Sugiyama, T., Nevarez, J. G., & Schweitzer, M. H. (2015). Alligator osteoderms as a source of labile calcium for eggshell formation. *Journal of Zoology*, 297, 255–264.
- Dubansky, B. H., & Dubansky, B. D. (2018). Natural development of dermal ectopic bone in the american alligator (*Alligator mississippiensis*) resembles heterotopic ossification disorders in humans. *Anatomical Record*, 301, 56–76.
- Farlow, J. O., Hayashi, S., & Tattersall, G. J. (2010). Internal vascularity of the dermal plates of *Stegosaurus* (Ornithischia, Thyreophora). *Swiss Journal of Geosciences*, 103, 173–185.
- Francillon-Vieillot, H., de Buffrénil, V., Castanet, J., Géraudie, J., Meunier, F. J., Sire, J. Y., Zylberberg, L., & Ricqlès, A. (1990). Microstructure and mineralization of vertebrate skeletal tissues. In J. G. Carter, (Ed.) *Skeletal biomineralization: Patterns, processes and evolutionary trends* (pp. 175–234). American Geophysical Union.

- Fuchs, K. (2006). The Crocodile skin: The important characteristics in identifying. Edition, Chimaira, Frankfurt, HE, Germany.
- Girondot, M., & Laurin, M. (2003). Bone profiler: A tool to quantify, model, and statistically compare bone-section compactness profiles. *Journal of Vertebrate Paleontology*, 23, 458–461.
- Godoy, P. L., Bronzati, M., Eltink, E., Marsola, J. C. A., Cidade, G. M., Langer, M. C., & Montefeltro, F. C. (2016). Postcranial anatomy of *Pissarrachampsia sera* (Crocodyliformes, Baurusuchidae) from the Late Cretaceous of Brazil: Insights on lifestyle and phylogenetic significance. *PeerJ*, 4, e2075.
- Gónet, J., Laurin, M., & Girondot, M. (2022). Bone Profiler: The next step to quantify, model and statistically compare bone section compactness profiles. *Paleontologica Electronica*. In press.
- Hill, R. V. (2010). Osteoderms of *Simosuchus clarki* (Crocodyliformes: Notosuchia) from the Late Cretaceous of Madagascar. *Journal of Vertebrate Paleontology*, 30, 154–176.
- Hill, R. V. (2005). Integration of morphological data sets for phylogenetic analysis of Amniota: The Importance of integumentary characters and increased taxonomic sampling. *Systematic Biology*, 54, 530–547.
- Inacio Veenstra, L. L., & Broeckhoven, C. (2022). Revisiting the thermoregulation hypothesis of osteoderms: A study of the crocodylian *Paleosuchus palpebrosus* (Crocodylia: Alligatoridae). *Biological Journal of the Linnean Society*, 135, 679–691.
- Kirby, A., Vickaryous, M., Boyde, A., Olivo, A., Moazen, M., Bertazzo, S., & Evans, S. (2020). A comparative histological study of the osteoderms in the lizards *Heloderma suspectum* (Squamata: Helodermatidae) and *Varanus komodoensis* (Squamata: Varanidae). *Journal of Anatomy*, 236, 1035–1043.
- Klein, N. (2010). Long bone histology of Sauropterygia from the lower muschelkalk of the germanic basin provides unexpected implications for phylogeny. *PLoS One*, 5, e11613.
- Laurin, M., Girondot, M., & Loth, M. M. (2004). The evolution of long bone microstructure and lifestyle in lissamphibians. *Paleobiology*, 30, 589–613.
- Mannion, P., Benson, R., Carrano, M., Tennant, J., Judd, J. & Butler, R. (2015). Climate constrains the evolutionary history and biodiversity of crocodylians. *Nature Communications*, 6, 8438. <https://doi.org/10.1038/ncomms9438>
- Marchetti, I., Delcourt, R., Tavares, S. A. S., Canalli, J., Nascimento, P. M., & Ricardi-Branco, F. (2022). Morphological and paleohistological description of a new Baurusuchidae specimen from the adamantina formation, upper cretaceous of Brazil. *Journal of South American Earth Sciences*, 114, 103693.
- Marinho, T. D. S., Ribeiro, L. C. B., & Carvalho, I. D. S. (2006). Morfologia de osteodermos de crocodylomorfos do Sítio Paleontológico de Peirópolis (Bacia Bauru, Cretáceo Superior). *Anuário do Instituto de Geociências*, 29, 44–53.
- Molnar, J. L., Pierce, S. E., & Hutchinson, J. R. (2014). An experimental and morphometric test of the relationship between vertebral morphology and joint stiffness in Nile crocodiles (*Crocodylus niloticus*). *Journal of Experimental Biology*, 217, 758–768.
- Montefeltro, F. C. (2019). The osteoderms of baurusuchid crocodyliforms (Mesoeucrocodylia, Notosuchia). *Journal of Vertebrate Paleontology*, 39, e1594242.
- Moss, M. L. (1972). The vertebrate dermis and the integumental skeleton. *American Zoologist*, 12, 27–54.
- Nyström, A., & Bruckner-Tuderman, L. (2019). Matrix molecules and skin biology. *Seminars in Cell & Developmental Biology*, 89, 136–146.
- Ósi, A., Young, M. T., Galász, A., & Rabi, M. (2018). A new large-bodied thalattosuchian crocodyliform from the Lower Jurassic (Toarcian) of Hungary, with further evidence of the mosaic acquisition of marine adaptations in Metriorhynchoidea. *PeerJ*, 6, e4668.
- Ponce, D., Cerda, I., Desojo, J., & Nesbitt, S. (2017). The osteoderm microstructure in doswelliids and proterochampsids and its implications for palaeobiology of stem archosaurs. *Acta Palaeontologica Polonica*, 62, 819–831.
- Romer, A. S. (1956). *Osteology of the Reptiles* (p. 772). University of Chicago Press.
- Ruiz, J. V., Bronzati, M., Ferreira, G. S., Martins, K. C., Queiroz, M. V., Langer, M. C., & Montefeltro, F. C. (2021). A new species of *Caipirasuchus* (Notosuchia, Sphagesauridae) from the Late Cretaceous of Brazil and the evolutionary history of *Sphagesauria*. *Journal of Systematic Palaeontology*, 19, 1–23.
- Rutland, C. S., Cigler, P., & Kubale Dvojmoč, V. (2019). Reptilian skin and its special histological structures. In eds. C. S. Rutland & V. Kubale Dvojmoč, *Veterinary anatomy and physiology* (pp. 1–21). Rijeka, Shanghai: InTech.
- Salisbury, S. W., & Frey, E. (2001). A biomechanical transformation model for the evolution of semi-spheroidal articulations between adjoining vertebral bodies in crocodylians. In G. C. Grigg, F. Seebacher & C. E. Franklin, (Eds.) *Crocodylian Biology and Evolution* (pp. 121–148). Surrey Beatty & Sons.
- Scheyer, T., Martinsander, P., Joyce, W., Bohme, W., & Witzel, U. (2007). A plywood structure in the shell of fossil and living soft-shelled turtles (Trionychidae) and its evolutionary implications. *Organisms Diversity & Evolution*, 7, 136–144.
- Scheyer, T. M. (2007). Skeletal histology of the dermal armor of Placodontia: The occurrence of 'postcranial fibro-cartilaginous bone' and its developmental implications. *Journal of Anatomy*, 211, 737–753.
- Scheyer, T. M., Danilov, I. G., Sukhanov, V. B., & Syromyatnikova, E. V. (2014). The shell bone histology of fossil and extant marine turtles revisited. *Biological Journal of the Linnean Society*, 112, 701–718.
- Scheyer, T. M., & Desojo, J. B. (2011). Palaeohistology and external microanatomy of rauisuchian osteoderms (*Archosauria: Pseudosuchia*). *Palaeontology*, 54, 1289–1302.
- Scheyer, T. M., Desojo, J. B., & Cerda, I. A. (2014). Bone histology of Phytosaur, Aetosaur, and Other Archosauriform Osteoderms (Eureptilia, Archosauromorpha): Archosauriform osteoderm microstructures. *The Anatomical Record*, 297, 240–260.
- Scheyer, T. M., & Sánchez-Villagra, M. R. (2007). Carapace bone histology in the giant pleurodiran turtle *Stupendemys geographicus*: Phylogeny and function. *Acta Palaeontologica Polonica*, 52, 137–154.
- Scheyer, T. M., & Sander, P. M. (2004). Histology of ankylosaur osteoderms: Implications for systematics and function. *Journal of Vertebrate Paleontology*, 24, 874–893.
- Scheyer, T. M., & Sander, P. M. (2009). Bone microstructures and mode of skeletogenesis in osteoderms of three pareiasaur taxa from the Permian of South Africa. *Journal of Evolutionary Biology*, 22, 1153–1162.
- Seidel, M. R. (1979). The osteoderms of the American *Alligator* and their functional significance. *Herpetologica*, 35, 375–380.
- Sena, M. V. A., Andrade, R. C. L. P., Sayão, J. M., & Oliveira, G. R. (2018). Bone microanatomy of *Pepesuchus deiseae* (Mesoeucrocodylia, Peirosauridae) reveals a mature individual from the upper cretaceous of Brazil. *Cretaceous Research*, 90, 335–348.
- Sena, M. V. A., Bantim, R. A. M., Saraiva, A. Á. F., Sayão, J. M., & Oliveira, G. R. (2020). Osteohistology and microanatomy of a new specimen of *Cearachelys placidoi* (Testudines: Pleurodira) a side-necked turtle from the lower cretaceous of Brazil. *The Anatomical Record*, 304, 1294–1304.
- Sena, M. V. A., Bantim, R. A. M., Saraiva, A. A. F., Sayão, J. M., & Oliveira, G. R. (2021). Shell and long-bone histology, skeletochronology, and lifestyle of *Araripemys barretoii* (Testudines: Pleurodira), a side-necked turtle of the lower cretaceous from Brazil. *Anais da Academia Brasileira de Ciências*, 93, e20201606.
- Skutschas, P. P., Boitsova, E. A., Cherepanov, G. O., & Danilov, I. G. (2017). Shell bone histology of the pan-caretochelyid turtle *Kizylkumemys schultzi* from the upper cretaceous of Uzbekistan and shell bone morphology transformations in the evolution of pan-trionychian turtles. *Cretaceous Research*, 79, 171–181.

- Vickaryous, M. K., & Hall, B. K. (2006). Osteoderm morphology and development in the nine-banded armadillo, *Dasypus novemcinctus* (Mammalia, Xenarthra, Cingulata). *Journal of Morphology*, 267, 1273–1283.
- Vickaryous, M. K., & Hall, B. K. (2008). Development of the dermal skeleton in *Alligator mississippiensis* (Archosauria, Crocodylia) with comments on the homology of osteoderms. *Journal of Morphology*, 269, 398–422.
- Vickaryous, M. K., Meldrum, G., & Russell, A. P. (2015). Armored geckos: A histological investigation of osteoderm development in *Tarentola* (Phyllodactylidae) and *Gekko* (Gekkonidae) with comments on their regeneration and inferred function: Gecko Osteoderm Development. *Journal of Morphology*, 276, 1345–1357.
- Vickaryous, M. K., & Sire, J. Y. (2009). The integumentary skeleton of tetrapods: Origin, evolution, and development. *Journal of Anatomy*, 214, 441–464.
- Vieira, L. G., Santos, A. L. Q., Moura, L. R., Orpinelli, S. R. T., Pereira, K. F., & Lima, F. C. (2016). Morphology, development and heterochrony of the carapace of giant Amazon River turtle, *Podocnemis expansa* (Testudines, Podocnemidae). *Pesquisa Veterinária Brasileira*, 36, 436–446.
- Williams, C., Kirby, A., Marghoub, A., Kéver, L., Ostashevskaya-Gohstand, S., Bertazzo, S., Moazen, M., Abzhanov, A., Herrel, A., Evans, S. E., & Vickaryous, M. (2022). A review of the osteoderms of lizards (Reptilia: Squamata). *Biological Reviews*, 97, 1–19.
- Witzmann, F. (2009). Comparative histology of sculptured dermal bones in basal tetrapods, and the implications for the soft tissue dermis. *Palaeodiversity*, 2, 233–270.
- Witzmann, F., & Soler-Gijón, R. (2010). The bone histology of osteoderms in temnospondyl amphibians and in the chroniosuchian *Bystrowiella*. *Acta Zoologica*, 91, 96–114.
- Woodward, H. N., Horner, J. R., & Farlow, J. O. (2014). Quantification of intraskeletal histovariability in *Alligator mississippiensis* and implications for vertebrate osteohistology. *PeerJ*, 2, e422.

SUPPORTING INFORMATION

Additional supporting information can be found online in the Supporting Information section at the end of this article.

How to cite this article: Sena, M. V. d. A., Marinho, T. d. S., Montefeltro, F. C., Langer, M. C., Fachini, T. S., Nava, W. R., Pinheiro, A. E. P., Araújo, E. V. d., Aubier, P., Andrade, R. C. L. P. d., Sayão, J. M., Oliveira, G. R. d., & Cubo, J. (2022). Osteohistological characterization of notosuchian osteoderms: Evidence for an overlying thick leathery layer of skin. *Journal of Morphology*, 284, e21536. <https://doi.org/10.1002/jmor.21536>

Appendix 3 - Were Notosuchia

(Pseudosuchia: Crocodylomorpha)

warm-blooded? A palaeohistological
analysis suggests ectothermy

Article

Paleohistological inferences of thermometabolic regimes in Notosuchia (Pseudosuchia: Crocodylomorpha) revisited

Jorge Cubo* , Paul Aubier , Mathieu G. Faure-Brac , Gaspard Martet, Romain Pellarin, Idriss Pelletan, and Mariana V. A. Sena 

Abstract.—Notosuchia is a group of mostly terrestrial crocodyliforms. The presence of a prominent crest overhanging the acetabulum, slender straight-shafted long bones with muscular insertions close to the joints, and a stable knee joint suggests that they had an erect posture. This stance has been proposed to be linked to endothermy, because it is present in mammals and birds and contributes to the efficiency of their respiratory systems. However, a bone paleohistological study unexpectedly suggested that Notosuchia were ectothermic organisms. The thermophysiological status of Notosuchia deserves further analysis, because the methodology of the previous study can be improved. First, it was based on a relationship between red blood cell size and bone vascular canal diameter tested using 14 extant tetrapod species. Here we present evidence for this relationship using a more comprehensive sample of extant tetrapods (31 species). Moreover, contrary to previous results, bone cross-sectional area appears to be a significant explanatory variable (in addition to vascular canal diameter). Second, red blood cell size estimations were performed using phylogenetic eigenvector maps, and this method excludes a fraction of the phylogenetic information. This is because it generates a high number of eigenvectors requiring a selection procedure to compile a subset of them to avoid model overfitting. Here we inferred the thermophysiology of Notosuchia using phylogenetic logistic regressions, a method that overcomes this problem by including all of the phylogenetic information and a sample of 46 tetrapods. These analyses suggest that *Araripesuchus wegeneri*, *Armadillosuchus arrudai*, *Baurusuchus* sp., *Iberosuchus macrodon*, and *Stratiotosuchus maxhechti* were ectothermic organisms.

Jorge Cubo, Paul Aubier, Mathieu G. Faure-Brac, Gaspard Martet, Romain Pellarin, and Idriss Pelletan. Sorbonne Université, Muséum national d'Histoire naturelle, CNRS, Centre de Recherche en Paléontologie—Paris (CR2P, UMR 7207), Paris, France. E-mail: jorge.cubo_garcia@sorbonne-universite.fr, paul.aubier@gmail.com, faurebrac.mathieu@gmail.com, gaspard.martet@gmail.com, romain.pellarin74@gmail.com, idriss.pelletan@laposte.net

Mariana V. A. Sena. Sorbonne Université, Muséum national d'Histoire naturelle, CNRS, Centre de Recherche en Paléontologie—Paris (CR2P, UMR 7207), Paris, France; and Laboratório de Paleontologia da URCA-LPU, Centro de Ciências Biológicas e da Saúde, Universidade Regional do Cariri, Rua Carolino Sucupira–Pimenta, Crato, Ceará 63105-010, Brazil. E-mail: mari.araujo.sena@gmail.com

Accepted: 14 July 2022

*Corresponding author.

Introduction

Notosuchia is a group of extinct, mostly terrestrial crocodyliforms. The presence of several morphological features suggests that they had an erect posture: the prominent crest overhanging the acetabulum observed in *Chimaerasuchus paradoxus* (Wu and Sues 1996), *Notosuchus terrestris* (Pol 2005), *Araripesuchus tsangatsangana* (Turner 2006), *Baurusuchus albertoi* (Nascimento and Zaher 2010), and *Stratiotosuchus maxhechti* (Riff and Kellner 2011); the straight-shafted long bones described in

Anatosuchus minor and *Araripesuchus* spp. (Serenó and Larsson 2009); the slender limb bones with muscular insertions close to the joints reported in *Malawisuchus mwakasyungutiensis* (Gomani 1997); and the tight/stable knee joint shown in *Pissarrachampsa sera* (Godoy et al. 2016). Among extant tetrapods, only endotherms (mammals and birds) show an upright stance. This last feature has been proposed to be linked to endothermy, because it contributes to the efficiency of the respiratory system (Carrier 1987). Thus, according to this morphological evidence,

we can reasonably hypothesize that Notosuchia were endothermic. However, Cubo et al. (2020) concluded that they were primitively ectothermic using two proxies: resting metabolic rate (RMR) and red blood cell size (RBC_{size}).

RMR is the minimal consumption of oxygen over time per unit of body mass measured under postabsorptive conditions during the period of normal activity of the daily cycle in resting, nonreproductive specimens (Andrews and Pough 1985; Montes et al. 2007). RMRs of extant endotherms are at least one order of magnitude higher than those of extant ectotherms of similar body mass, because the mechanisms of thermogenesis operating in the former are costly in terms of energy (Clarke and Pörtner 2010; Legendre and Davesne 2020). RMRs inferred by Cubo et al. (2020) for Notosuchia were significantly lower than the threshold separating ectotherms from endotherms.

Within extant tetrapods, RBC_{size} is lower in endotherms (mammals and birds) than in ectotherms (Amphibia, Squamata, Testudines, and Crocodylia) (Hartman and Lessler 1964; Snyder and Sheafor 1999; Soslau 2020). It has been suggested that the acquisition of lungs together with the subsequent evolution of the cardiovascular system was the driving force explaining the evolution of vertebrate RBC_{size} (Snyder and Sheafor 1999). In endotherms, thermogenetic mechanisms use a huge amount of oxygen, producing high RMRs. Considering that “Smaller capillaries [and smaller RBCs] are associated with increased potential for diffusive gas exchange” (Snyder and Sheafor 1999: 189), these features may have been positively selected in endotherms. Huttenlocker and Farmer (2017) found that RBC_{size} values are related to, and can be inferred from, bone vascular canal diameter. Cubo et al. (2020) inferred notosuchian RBC_{size} values using this last relationship and concluded that they were significantly higher than the threshold separating ectotherms from endotherms.

To sum up, both proxies (RMR and RBC_{size}) suggest that Notosuchia were ectothermic organisms. Considering that paleohistological evidence (suggesting low RMR, large RBC_{size} , and ectothermy) is not congruent with morphological evidence (suggesting an erect posture, cursoriality, and endothermy), the

thermophysiological status (i.e., either ectothermic or endothermic) of Notosuchia deserves further analysis.

The approach used by Cubo et al. (2020) to perform these inferences can be improved in two ways. First, notosuchian thermophysiological status inferred using RBC_{size} is based on the quoted relationship between RBC_{size} and bone vascular canal diameter (Cubo et al. 2020). This relationship was tested by Huttenlocker and Farmer (2017) using a rather small sample size (14 extant tetrapod species). Here we tested this relationship using a more comprehensive sample of extant tetrapods (31 species) and phylogenetic generalized least-squares regression (PGLS). Second, RBC_{size} estimations were performed using phylogenetic eigenvector maps (PEMs), and this method excludes a fraction of phylogenetic information. This is because PEM generates a high number of eigenvectors ($n - 1$, with n being the number of terminal taxa analyzed), thus requiring a selection procedure to compile a subset of eigenvectors to avoid model overfitting (Guénard et al. 2013; Legendre et al. 2016). Here we inferred the thermophysiology of Notosuchia using phylogenetic logistic regression (PLR) (Ives and Garland 2010; Tung Ho and Ané 2014), a method that overcomes this problem, because it includes all (instead of a fraction) of the phylogenetic information.

Material and Methods

Phylogenies in Figure 1 and Supplementary File 1 contain the tetrapod samples used in this study. Topologies were taken from Pyron and Wiens (2011) for amphibians; Meredith et al. (2011), Zurano et al. (2019), Kumar et al. (2013), and Upham et al. (2019) for mammals; Ast (2001) and Villa et al. (2018) for *Varanus*; Man et al. (2011) for crocodiles; Prum et al. (2015) for birds; and Pol et al. (2014) for Notosuchia. Both phylogenies were dated using Time Tree of Life (<http://www.timetree.org>). When the ages of two successive nodes collapsed, we arbitrarily added 1 Myr in between the more-inclusive and less-inclusive nodes to facilitate the graphic visualization of the topology. For Notosuchia, nodes were dated according to the last appearance datum (LAD) of the oldest

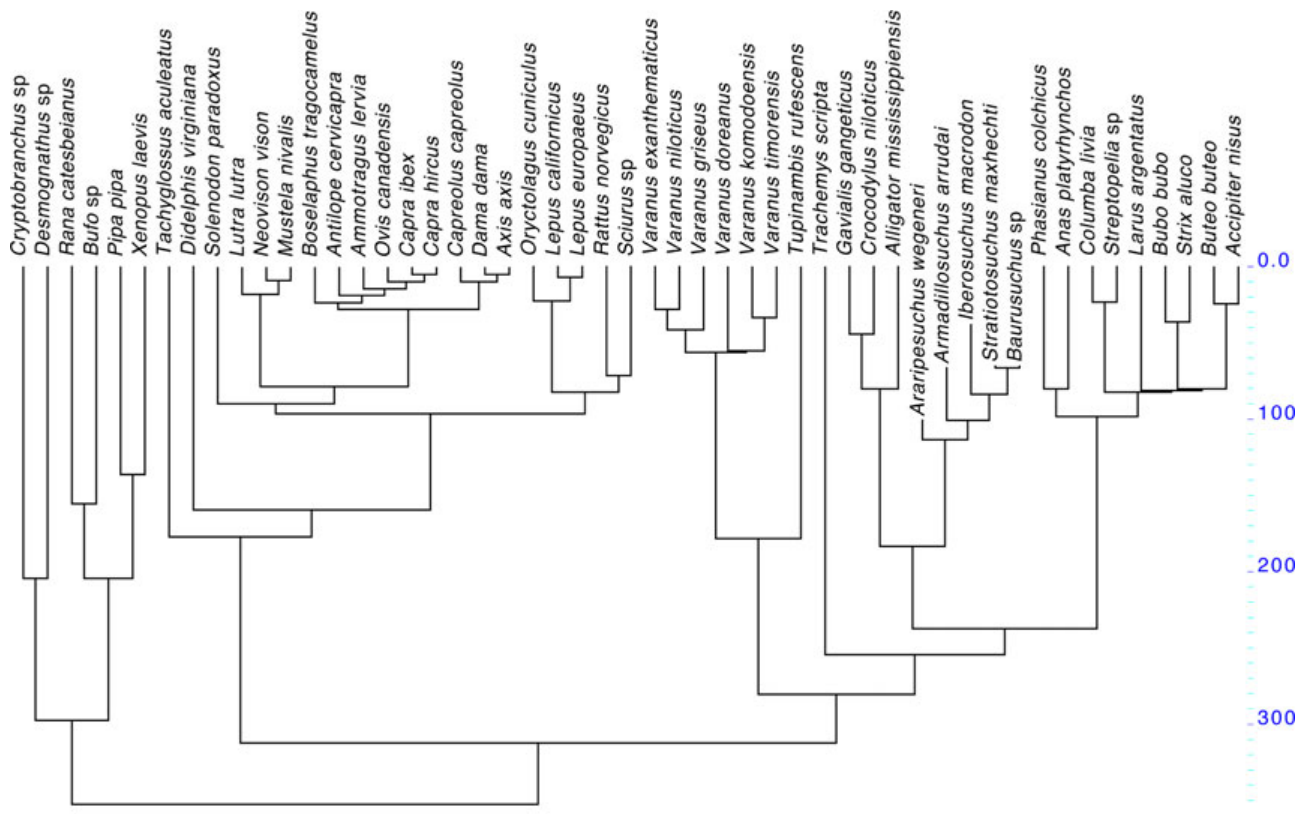


FIGURE 1. Phylogenetic relationships among extant taxa used to construct the thermophysiology inference model and the extinct Notosuchia for which we performed paleobiological inferences. Sources of topology and divergence times are cited in the main text. Scale on the right: geologic time in millions of years (Myr).

fossil included in each node taken from the Paleobiology Database (<https://paleobiodb.org>). The age of the node Notosuchia (113 Myr) corresponds to the LAD of *Malawisuchus mwakasyungutiensis*. The age of the node *Armadillosuchus–Baurusuchus* (100.5 Myr) corresponds to the LAD of *Chimaerasuchus paradoxus*. The age of the node *Iberosuchus–Baurusuchus* (83.6 Myr) corresponds to the LAD of *Comahuesuchus brachybuccalis*, *Pehuenchesuchus enderi*, *Cynodontosuchus rothi*, and *Wargosuchus australis*. Finally, the age of the node *Stratiotosuchus–Baurusuchus* (66 Myr) corresponds to the LAD of these taxa. The latter (*Stratiotosuchus–Baurusuchus*), as well as *Armadillosuchus arrudai*, come from the Adamantina Formation, the age of which is still debated. We follow the hypothesis of a Campanian–Maastrichtian age proposed by some authors (e.g., Gobbo-Rodrigues et al. 1999; Batezelli 2017).

Testing the Relationship between RBC_{size} and Bone Vascular Canal Diameter Using PGLS.—Supplementary File 1 contains the sample (31 species of extant tetrapods) and the

phylogeny (topology and divergence times) used to test the relationships between the response variables (RBC_{width} and RBC_{area}) and the explanatory variables (femoral vascular canal diameter and femoral cross-sectional area including the medullary cavity). Thin sections of extant taxa are curated at the Vertebrate Hard Tissue Collection of the Museum national d’Histoire naturelle, Paris, and are available on request to the curator (D. Germain). RBC_{width} (defined as RBC minimum diameter) and RBC_{area} (either published values or values computed using maximum and minimum published diameters and assuming an ellipse) were taken from the literature (Supplementary File 2). Femoral vascular canal diameters (white arrowheads in Fig. 2) were computed as Can_{harmean} and Can_{minv} as defined by Huttenlocker and Farmer (2017). Can_{harmean}, Can_{minv}, and femoral cross-sectional area were either quantified in this study or taken from Huttenlocker and Farmer (2017) (data available in Supplementary File 2).

The method of ordinary least-squares regression makes the assumption of no covariance

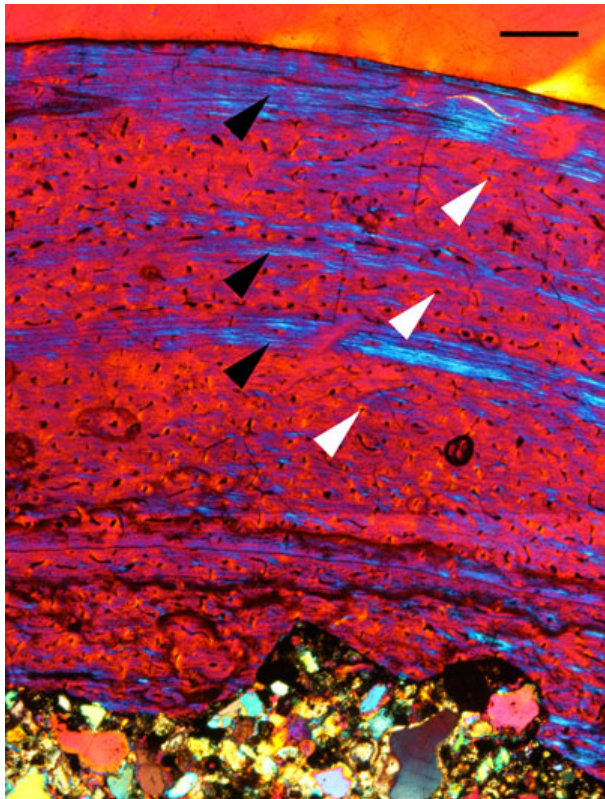


FIGURE 2. Transverse thin section, lateral side, of the femur of *Araripesuchus wegeneri* Buffetaut, 1981, observed in cross-polarized light with lambda wave plate. The thin section was made from a partial femur (MNHN.F.GDF660) from the Aptian of Gadoufaoua (Niger), and is curated at the Museum national d'Histoire naturelle (MNHN) (Paris, France). The cortex is made of lamellar-zonal bone. It is composed of three zones formed at moderate growth rate and containing vascular canals (white arrowheads) included in primary osteons, and three annuli formed at low growth rates and made of parallel fibered bone (black arrowheads). Periosteum is on the top and medullary cavity on the bottom. The continuous black line occurring near the medullary cavity is an artifact. Scale bar, 0.5 mm.

between residuals obtained from the regression equation (i.e., the off-diagonals of the variance–covariance matrix are expected to contain zeros) (Symonds and Blomberg 2014). In analyses using interspecific data, this assumption is not verified because of the hierarchical, shared phylogenetic history among terminal taxa (i.e., closely related species are more similar than expected by chance). PGLS (Grafen 1989; Martins and Hansen 1996; Rohlf 2001; Symonds and Blomberg 2014) overcomes this problem by using a variance–covariance matrix in which off-diagonals correspond to the phylogenetic history shared by the two species under comparison. Symonds and Blomberg (2014) described PGLS as a “weighted regression” in which data points corresponding to

closely related species are “downweighted.” We ran PGLS using the function *pgls* of the package *caper* (Orme et al. 2013) in R (R Development Core Team 2008).

Inferring the Thermophysiology of Notosuchia Using PLR.—Figure 1 shows the phylogenetic relationships among extant taxa (46 species of tetrapods) used to construct the thermophysiology inference model (to infer the probability of being endothermic) and the extinct *Notosuchia* for which we performed paleobiological inferences. This model was constructed using femoral vascular canal diameter (Can_{harmean} and Can_{min}) and femoral cross-sectional area as explanatory variables. As noted earlier, femoral Can_{harmean} , Can_{min} , and femoral cross-sectional area were either quantified in this study or taken from Huttenlocker and Farmer (2017) (data available in Supplementary File 3). As before, thin sections of extant taxa are curated at the Vertebrate Hard Tissue Collection of the Museum national d'Histoire naturelle, Paris. Data for *Notosuchia* are taken from Cubo et al. (2020): *Araripesuchus wegeneri*, *Armadillosuchus arrudai*, *Baurusuchus* sp., *Iberosuchus macrodon*, and *Stratiosuchus maxhechti*. Considering that the model was constructed using femora of extant species, we performed inferences only for those *Notosuchia* for which data for femora were available. Sample size was smaller for PGLS analyses, because data for RBC_{size} were not available for many species analyzed in PLR analyses. PLR is a generalized linear model explaining the probability of occurrence of the state “presence” of a binary response (dependent) variable (here the “presence of endothermy”) using continuous explanatory (independent) variables when residual variation of the former variable is phylogenetically structured (Ives and Garland 2010). The regression coefficients computed do account for phylogenetic correlation; when data are not phylogenetically structured, these coefficients are those of standard logistic regression (Ives and Garland 2010). PLR models contain two components. The first is controlled by parameters α (the transition rate) and μ (the asymptotic probability of being in state 1 [here the asymptotic probability of being endotherm]). Parameter α equals $\alpha_1 + \alpha_0$; α_1 being the probability that the response

variable switches from 0 to 1 in each small time increment when it evolves up a phylogenetic tree, whereas the α_0 parameter is the probability that it evolves from 1 to 0 (Ives and Garland 2010). The transition rate α is a measure of phylogenetic signal, because the larger the α , the quicker the evolutionary transitions and the lower the phylogenetic structure of data (Ives and Garland 2010). In the second component, the probability of occurrence of the state “presence of endothermy” is modeled using values of the independent (explanatory) variable (here bone vascular canal diameter). Parameters α and μ are estimated using an iterative process in which μ is estimated given α , using the quasi-likelihood function, and α is estimated given μ , using least squares until convergence (Ives and Garland 2010). Analyses were performed using the package *phyloglm* (Tung Ho and Ané 2014) in R (R Development Core Team 2008).

Results

Testing the Relationship between RBC_{size} and Bone Vascular Canal Diameter Using PGLS.—We used PGLS to test the relationships between RBC_{width} and RBC_{area} and the explanatory variables femoral vascular canal diameter (computed as Can_{harmean} and Can_{min}) and femoral cross-sectional area (data available in Supplementary File 2). Shapiro-Wilk normality tests showed that residuals of PGLS regression of RBC_{area} to Can_{harmean} + bone cross-sectional area and the regression RBC_{area} to Can_{min} + bone cross-sectional area do not follow a normal distribution (*p*-values of 0.0007557 and 0.001896, respectively). Thus, we performed a log transformation of all variables. After log transformation, residuals of all four PGLS regressions (RBC_{area} and RBC_{area} to the explanatory variables bone cross-sectional area and either Can_{min} or Can_{harmean}) do follow a normal distribution. All four of these PGLS regressions were significant and, in each regression, both explanatory variables (bone cross-sectional area and either Can_{min} or Can_{harmean}) were significant (Table 1).

Inferring the Thermophysiology of Notosuchia Using PLR.—We used PLR to construct models aimed at computing the probability of being

endothermic using paleohistological features (data available in Supplementary File 3). When Can_{harmean} was used as the explanatory variable, we obtained a model with a transition rate α of 0.00144, an intercept estimate of 6.04 (*p*-value = 0.004) and an estimate for the coefficient of Can_{harmean} of -0.45 (*p*-value = 0.001). The negative sign of the Can_{harmean} coefficient indicates that the probability of being endothermic decreases as vascular canal diameter increases. Figure 3 shows the distribution of probabilities of being endothermic as a function of Can_{harmean} variation. The corresponding equation is:

$$\ln[p(\text{endothermy})/p(\text{ectothermy})] = -0.45 * \text{Can}_{\text{harmean}} + 6.04 \quad (1)$$

or

$$p(\text{endothermy}) = \exp(-0.45 * \text{Can}_{\text{harmean}} + 6.04) / [1 + \exp(-0.45 * \text{Can}_{\text{harmean}} + 6.04)] \quad (2)$$

Ives and Garland (2010: p. 17) stated that “we assume that if $\mu_i < \bar{\mu}$, then trait Y will evolve toward 0; [...] Conversely, if $\mu_i > \bar{\mu}$, then trait Y will evolve toward 1,” where $\bar{\mu}$ is the mean probability of being endotherm in our sample. Thus, we considered that $\bar{\mu}$ is the cutoff probability, so that an inferred probability higher than $\bar{\mu}$ would be evidence for endothermy. Conversely, a probability lower than $\bar{\mu}$ would be evidence for ectothermy. When Can_{harmean} was used as the explanatory variable, $\bar{\mu} = 0.59$. To evaluate the predictive power of the model, we constructed a contingency table in which we inferred the thermometabolic regime of each extant species of the sample using its Can_{harmean}. Lines contain predictions (0, inferred ectothermy; 1, inferred endothermy) and columns contain true states (0, observed ectothermy; 1, observed endothermy):

	state 0	state 1
prediction 0	14	2
prediction 1	3	27

The specificity (the ratio of quantity of true 1 inferred as 1 on the quantity of true 1; $Sp = 27 / (27 + 2)$) equals 0.931. The sensitivity (the ratio of quantity of true 0 inferred as 0 on the quantity of true 0; $Se = 14 / (14 + 3)$) equals 0.824. The

TABLE 1. Testing the relationship between the dependent variables used to quantify red blood cell size (RBC_{size} ; RBC_{width} and RBC_{area}) and the explanatory variables femoral vascular canal diameter (computed either as Can_{min} or $Can_{harmean}$) and femoral cross-sectional area using phylogenetic generalized least-squares regression. * p -value < 0.05; ** p -value < 0.01; *** p -value < 0.001.

Dependent (response) variable	Adjusted R^2		Estimate	p -value
RBC_{width}	0.624	Intercept	0.895	0.001603**
		Can_{min}	0.714	2.08×10^{-6} ***
		Bone cross-sectional area	-0.095	0.001249**
RBC_{width}	0.341	Intercept	1.250	0.000888***
		$Can_{harmean}$	0.459	0.001557**
		Bone cross-sectional area	-0.101	0.006239**
RBC_{area}	0.399	Intercept	1.910	0.016427*
		Can_{min}	1.398	0.000315***
		Bone cross-sectional area	-0.158	0.027307*
RBC_{area}	0.189	Intercept	2.757	0.002499**
		$Can_{harmean}$	0.852	0.013002*
		Bone cross-sectional area	-0.176	0.043913*

classification error (the ratio (quantity of true 0 inferred as 1 + quantity of true 1 inferred as 0)/ total; error = $(3 + 2)/(14 + 2 + 3 + 27)$) equals 0.109. This classification error is quite low, so we used the cutoff probability of 0.59 to perform paleobiological inferences using $Can_{harmean}$ as the explanatory (predictor) variable.

When Can_{min} was used as the explanatory variable, we obtained a model with a transition rate α of 0.00052, an intercept estimate of 2.58 (p -value = 0.032), and an estimate for the

coefficient of Can_{min} of -0.49 (p -value = 0.018). Figure 4 shows the distribution of probabilities of being endothermic as a function of Can_{min} variation. The corresponding equation is:

$$\ln[p(\text{endothermy})/p(\text{ectothermy})] = -0.49 * Can_{min} + 2.58 \tag{3}$$

or

$$p(\text{endothermy}) = \frac{\exp(-0.49 * Can_{min} + 2.58)}{[1 + \exp(-0.49 * Can_{min} + 2.58)]} \tag{4}$$

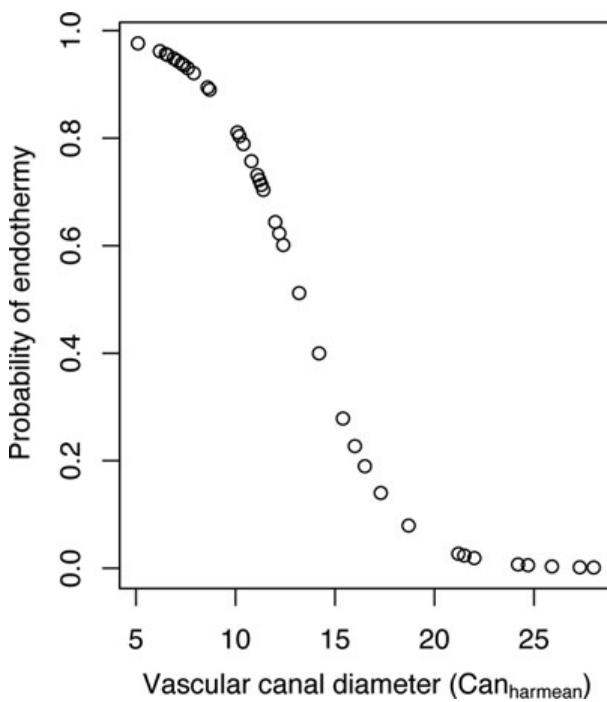


FIGURE 3. Distribution of probabilities of being endothermic inferred for our sample of extant tetrapods using a phylogenetic logistic regression model that includes femoral vascular canal diameter (computed as $Can_{harmean}$) as the explanatory variable.

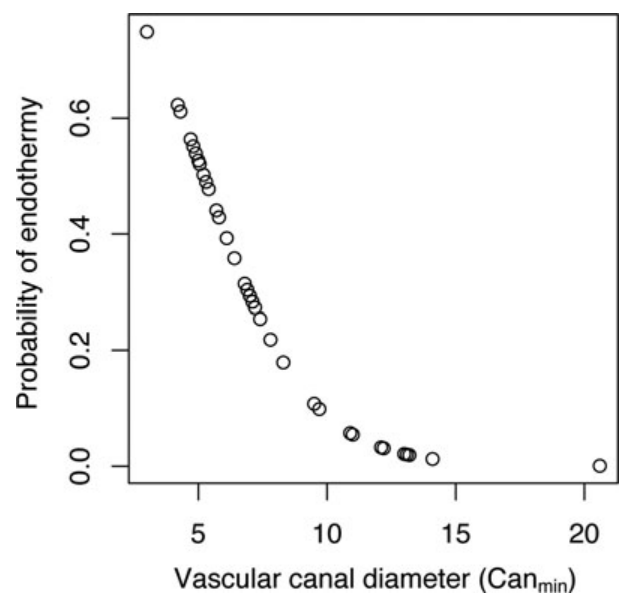


FIGURE 4. Distribution of probabilities of being endothermic inferred for our sample of extant tetrapods using a phylogenetic logistic regression model that includes femoral vascular canal diameter (computed as Can_{min}) as the explanatory variable.

Again we evaluated the quality of the model by constructing a contingency table in which we inferred the thermophysiological regime of each extant species of the sample using its Can_{min} . We used a cutoff probability of $\bar{\mu} = 0.32$ (the mean probability of being endothermic in our sample), so that an inferred probability lower than 0.32 is evidence for ectothermy and a probability higher than 0.32 is evidence for endothermy:

	state 0	state 1
prediction 0	15	9
prediction 1	2	20

The specificity (the ratio of quantity of true 1 inferred as 1 on the quantity of true 1; $Sp = 20/(20 + 9)$) equals 0.690. The sensitivity (the ratio of quantity of true 0 inferred as 0 on the quantity of true 0; $Se = 15/(15 + 2)$) equals 0.882. The classification error (the ratio (quantity of true 0 inferred as 1 + quantity of true 1 inferred as 0)/total; $error = (2 + 9)/(15 + 9 + 2 + 20)$) equals 0.239. This classification error is quite high, so we recomputed a new cutoff probability of 0.22 using the receiver operating characteristic curve. Then we constructed a new contingency table in which we inferred the thermophysiological regime of each extant species of the sample using its Can_{min} and considering that an inferred probability higher than 0.22 is evidence for endothermy:

	state 0	state 1
prediction 0	15	1
prediction 1	2	28

With this contingency table, the classification error [the ratio (quantity of true 0 inferred as 1 + quantity of true 1 inferred as 0)/total; $error = (2 + 1)/(15 + 1 + 2 + 28)$] equals 0.0652. This classification error is quite low, so we used the cutoff probability of 0.22 to perform paleobiological inferences using Can_{min} as the explanatory (predictor) variable.

We used these equations and cutoff probabilities and femoral $Can_{harmean}$ and Can_{min} values published by Cubo et al. (2020) for Notosuchia to compute the probability of these taxa being endotherms (Table 2).

Discussion

Notosuchia is an extremely diversified group of crocodyliforms. This diversity is particularly striking regarding their diet, suggesting that they occupied various ecological niches (Carvalho and Bertini 1999; Iori and Carvalho 2018). Uruguaysuchidae (Pol et al. 2014), the most basal notosuchians, of which *Araripesuchus wegeneri* (in our sample) is a representative, range from the Aptian (*Araripesuchus gomesii*) to the Maastrichtian (*Araripesuchus tsangatsangana*) (Price 1959; Turner 2006). Several species of this group have been inferred as being omnivorous, or even insectivorous, based on their dental complexity (Sereno and Larsson 2009; Soto et al. 2011; Nieto et al. 2021) and postcranial remains suggest that they had an erect posture (see “Introduction”). Uruguaysuchids were smaller than Sphagesauridae (Carvalho et al. 2010; Godoy et al. 2019). *Armadillosuchus* (also sampled by us) belongs to the large-bodied sphagesaurids group (Melstrom and Irmis 2019). The diagnosis of this clade is based on its peculiar dentition morphology (Price 1950). They show extremely complex manducatory systems, with evidence of “chewing” mechanisms, dental wear, and propalinal movements (e.g., see Ősi 2014; Iori and Carvalho 2018). The foraging abilities of some notosuchians, such as *Armadillosuchus*, *Mariliasuchus*, or *Malawisuchus*, to locate food or water have led some authors to propose the presence of burrowing habits (Gomani 1997; Nobre et al. 2008; Marinho and Carvalho 2009), a behavior that might play a role in thermoregulation (e.g., to search for a cooler shelter during dry periods, as in extant crocodylian species; Campos and Magnusson 2013). This behavior has also been proposed for the sebecosuchian *Baurusuchus salgadoensis* (Vasconcellos and Carvalho 2010). Sebecosuchia (to which *Iberosuchus* and *Stratiotosuchus*, also sampled by us, belong) were large predators with an erect posture (see “Introduction”) and cursorial abilities (Nascimento and Zaher 2010; Riff and Kellner 2011), feeding on large prey, including small sphagesaurids (Godoy et al. 2014). Indeed, their ziphodont teeth (unicuspidated, laterally compressed with serrated carinae) associated with the biomechanical performances of their skull allowed sebecosuchians

TABLE 2. Inferring the probability of endothermy for the sample of *Notosuchia* analyzed in this study using femoral vascular canal diameters (computed either as Can_{min} or $Can_{harmean}$) as explanatory variables and phylogenetic logistic regressions. Vascular canal diameters for *Notosuchia* were taken from Cubo et al. (2020).

	$Can_{harmean}$	Probability of being endothermic	Inferred status at cutoff probability of 0.59	Can_{min}	Probability of being endothermic	Inferred status at cutoff probability of 0.22
<i>Araripesuchus wegeneri</i>	25.99	0.0035	Ectothermy	13	0.0221	Ectothermy
<i>Armadillosuchus arrudai</i>	25.32	0.0047	Ectothermy	13.36	0.0186	Ectothermy
<i>Baurusuchus</i> sp.	25.02	0.0054	Ectothermy	12.67	0.0259	Ectothermy
<i>Iberosuchus macrodon</i>	31.76	0.0003	Ectothermy	14	0.0137	Ectothermy
<i>Stratiotosuchus maxhechti</i>	31.55	0.0003	Ectothermy	14.87	0.0090	Ectothermy

to effectively handle prey after wounding it (Montefeltro et al. 2020). It is noteworthy that the inferred ectothermic sebecosuchians occupy a niche usually occupied by endothermic theropod dinosaurs (Benson et al. 2013; Zanno and Makovicky 2013).

The ectothermic condition of *Notosuchia* suggested by Cubo et al. (2020) is supported by the results of the present study using larger sample sizes of extant species and a more robust phylogenetic comparative method (PLR). First, the finding that RBC_{size} is related to bone vascular canal diameter (Huttenlocker and Farmer 2017) is supported by our results obtained using a sample size more than twice of that used by these authors. Thus bone vascular canal diameter can be used as a proxy to infer RBC_{size} , and then endothermy (because within tetrapods, RBC_{size} is lower in endotherms than in ectotherms; Snyder and Sheafor 1999). Huttenlocker and Farmer (2017) included bone cross-sectional area (in addition to bone vascular canal diameter) as an explanatory variable in models aimed at explaining the variation of RBC_{size} . However, in their study, bone cross-sectional area did not improve the explanatory power of models and was not retained (Huttenlocker and Farmer 2017; Supplemental Information, “Analysis I, Training Data Set for Extant Taxa”). Unexpectedly, our analyses (using a larger sample size) showed that bone cross-sectional area significantly improves the explanatory power of models and is retained, together with bone vascular canal diameter, in models explaining the variation of RBC_{size} . The fact

that the estimate for bone cross-sectional area is always negative (Table 1) indicates that RBC_{size} decreases as bone cross-sectional area increases. Second, notosuchian thermometabolism is inferred here using a larger sample of extant tetrapods (more than three times the sample used by Cubo et al. [2020]) and logistic phylogenetic regressions (a method more reliable than those used in previous studies; see below). We are aware of the fact that Huttenlocker and Farmer (2017) showed that histological changes reflect changes in VO_{2max} better than changes in thermometabolism. However, we have found here that microstructural variation is linked to thermometabolism too. The models constructed to infer the probability of endothermy using vascular canal size as an explanatory (predictive) variable were highly significant, and the classification errors obtained are quite low (6.5% using Can_{min}). Thus we conclude that we can use these models confidently in paleobiological inference of thermometabolism.

Thermal paleophysiology is an emergent discipline (Cubo and Huttenlocker 2020). It has great potential resulting from the synergy between physiological studies aimed at deciphering the mechanisms of thermogenesis in extant amniotes (e.g., Bal and Periasamy 2020; Jastroch and Seebacher 2020; Grigg et al. 2021) and paleobiological inferences in extinct amniotes using phylogenetic comparative methods (e.g., Cubo et al. 2012, 2020, 2022; Legendre et al. 2016; Huttenlocker and Farmer 2017; Olivier et al. 2017; Fleischle et al. 2018; Cubo and Jalil 2019; Faure-Brac et al. 2021;

Knaus et al. 2021). Logistic phylogenetic regressions are the third step in efforts performed during the last decade to carry out reliable inferences of thermometabolic status in extinct amniotes. A decade ago, Cubo et al. (2012) inferred bone growth rates using bone histological features and multiple linear regressions tested for significance using permutations in order to circumvent the nonindependence of the observations due to the phylogeny. Considering that bone growth rates are significantly related to RMR in amniotes (Montes et al. 2007), the former was used by Cubo et al. (2012) as a proxy to infer the thermometabolic status of extinct archosaurs. This method was used by Legendre et al. (2013) to infer the bone growth rate and the thermometabolic status of *Euparkeria*. In a second step, Legendre et al. (2016) adapted Guénard et al.'s (2013) PEMs to perform paleobiological inferences of RMR. This contribution represented significant methodological progress, because paleobiological inference models included the phylogeny (rather than circumventing its effects, as did the preceding method), assuming an evolutionary model (Molina-Venegas et al. 2018). PEMs have been widely used to infer the thermometabolic status of extinct amniotes (Legendre et al. 2016; Olivier et al. 2017; Fleischle et al. 2018; Cubo and Jalil 2019; Cubo et al. 2020, 2022; Faure-Brac and Cubo 2020; Faure-Brac et al. 2021; Knaus et al. 2021). Using logistic phylogenetic regressions is a new step in this sequence. This method improves upon the previous approach by using all of the phylogenetic information (rather than a fraction of it, as did PEMs in order to avoid model overfitting). An encouraging sign is that results are congruent in spite of the diversity of methods used to obtain them. Inferring the maximum metabolic rate of *Notosuchia* using the size of femoral nutrient foramina (Seymour et al. 2012) would be the next promising step to fully understand the thermophysiology of these amazing crocodylomorphs.

Acknowledgments

We thank H. Lamrous (Sorbonne Université) for helping us with picture acquisition using bone thin sections at the Vertebrate Hard

Tissue Collection of the Museum national d'Histoire naturelle (Paris). This study was partly funded by the project Emergences Sorbonne Université 2019 no. 243374 to J.C. The authors declare no competing interests.

Data Availability Statement

Data available from the Dryad and Zenodo Digital Repositories: <https://doi.org/10.5061/dryad.80gb5mktb>, <https://doi.org/10.5281/zenodo.6795231>.

Literature Cited

- Andrews, R. M., and F. H. Pough. 1985. Metabolism of squamate reptiles: allometric and ecological relationships. *Physiological Zoology* 58:214–231.
- Ast, J. C. 2001. Mitochondrial DNA evidence and evolution in Varanoidea (Squamata). *Cladistics* 17:211–226.
- Bal, N. C., and M. Periasamy. 2020. Uncoupling of sarcoendoplasmic reticulum calcium ATPase pump activity by sarcolipin as the basis for muscle non-shivering thermogenesis. *Philosophical Transactions of the Royal Society of London B* 375:20190135.
- Batezelli, A. 2017. Continental systems tracts of the Brazilian Cretaceous Bauru Basin and their relationship with the tectonic and climatic evolution of South America. *Basin Research* 29:1–25.
- Benson, R. B. J., P. D. Mannion, R. J. Butler, P. Upchurch, A. Goswami, and S. E. Evans. 2013. Cretaceous tetrapod fossil record sampling and faunal turnover: implications for biogeography and the rise of modern clades. *Palaeogeography, Palaeoclimatology, Palaeoecology* 372:88–107.
- Buffetaut, E. 1981. Die biogeographische Geschichte der Krokodilier, mit Beschreibung einer neuen Art, *Araripesuchus wegeneri*. *Geologische Rundschau* 70:611–624.
- Campos, Z., and W. E. Magnusson. 2013. Thermal relations of dwarf caiman, *Paleosuchus palpebrosus*, in a hillside stream: evidence for an unusual thermal niche among crocodylians. *Journal of Thermal Biology* 38:20–23.
- Carrier, D. R. 1987. The evolution of locomotor stamina in tetrapods: circumventing a mechanical constraint. *Paleobiology* 13:326–341.
- Carvalho, I. S., and R. J. Bertini. 1999. *Mariliasuchus*: um novo Crocodylomorpha (Notosuchia) do Cretáceo da Bacia Bauru. *Geología Colombiana* 24:83–105.
- Carvalho, I. de S., Z. B. de Gasparini, L. Salgado, F. M. de Vasconcelos, and T. da S. Marinho. 2010. Climate's role in the distribution of the Cretaceous terrestrial Crocodyliformes throughout Gondwana. *Palaeogeography, Palaeoclimatology, Palaeoecology* 297:252–262.
- Clarke, A., and H.-O. Pörtner. 2010. Temperature, metabolic power and the evolution of endothermy. *Biological Reviews* 85:703–727.
- Cubo, J., and A. K. Huttenlocker. 2020. Vertebrate palaeophysiology. *Philosophical Transactions of the Royal Society of London B* 375:20190130.
- Cubo, J., and N.-E. Jalil. 2019. Bone histology of *Azendohsaurus laaroussii*: implications for the evolution of thermometabolism in Archosauromorpha. *Paleobiology* 45:317–330.
- Cubo, J., N. Le Roy, C. Martinez-Maza, and L. Montes. 2012. Paleohistological estimation of bone growth rate in extinct archosaurs. *Paleobiology* 38:335–349.
- Cubo, J., M. V. A. Sena, P. Aubier, G. Houee, P. Claisse, M. G. Faure-Brac, R. Allain, R. C. L. P. Andrade, J. M. Sayão, and G. R. Oliveira. 2020. Were *Notosuchia* (*Pseudosuchia*:

- Crocodylomorpha) warm-blooded? A palaeohistological analysis suggests ectothermy. *Biological Journal of the Linnean Society* 131:154–162.
- Cubo, J., A.D. Buscalioni, L. J. Legendre, E. Bourdon, J. L. Sanz and A. de Ricqlès. 2022. Palaeohistological inferences of resting metabolic rates in *Concornis* and *Iberomesornis* (Enantiornithes, Ornithothoraces) from the Lower Cretaceous of Las Hoyas (Spain). *Palaeontology* 65:e12583.
- Faure-Brac, M. G., and J. Cubo. 2020. Were the synapsids primitively endotherms? A palaeohistological approach using phylogenetic eigenvector maps. *Philosophical Transactions of the Royal Society of London B* 375:20190138.
- Faure-Brac, M. G., R. Amiot, C. de Muizon, J. Cubo, and C. Lécuyer. 2021. Combined paleohistological and isotopic inferences of thermometabolism in extinct Neosuchia, using *Goniopholis* and *Dyrosaurus* (Pseudosuchia: Crocodylomorpha) as case studies. *Paleobiology* 48:302–323.
- Fleischle, C. V., T. Wintrich, and P. M. Sander. 2018. Quantitative histological models suggest endothermy in plesiosaurs. *PeerJ* 6:e4955.
- Gobbo-Rodrigues S. R., S. Petri and R. J. Bertini. 1999. Ocorrências de ostrácodes na Formação Araçatuba do Grupo Bauru, Cretáceo Superior da Bacia do Paraná e possibilidades de correlação com depósitos isócronos argentinos—parte i: Família Hylocyprididae. *Acta Geologica Leopoldensia* 23:3–13.
- Godoy, P. L., F. C. Montefeltro, M. A. Norell, and M. C. Langer. 2014. An additional Baurusuchid from the Cretaceous of Brazil with evidence of interspecific predation among Crocodyliformes. *PLoS ONE* 9:e97138.
- Godoy, P. L., M. Bronzati, E. Eltink, J. C. A. Marsola, G. M. Cidade, M. Langer, and F. Montefeltro. 2016. Postcranial anatomy of *Pisarrachampsa sera* (Crocodyliformes, Baurusuchidae) from the Late Cretaceous of Brazil: insights on lifestyle and phylogenetic significance. *PeerJ* 4:e2075.
- Godoy, P. L., R. B. J. Benson, M. Bronzati, and R. J. Butler. 2019. The multi-peak adaptive landscape of crocodylomorph body size evolution. *BMC Evolutionary Biology* 19:167.
- Gomani, E. M. 1997. A crocodyliform from the Early Cretaceous Dinosaur Beds, northern Malawi. *Journal of Vertebrate Paleontology* 17:280–294.
- Grafen, A. 1989. The phylogenetic regression. *Philosophical Transactions of the Royal Society of London B* 326:119–157.
- Grigg, G., J. Nowack, J. E. Bicudo, W. Pereira, N. C. Bal, H. N. Woodward, and R. S. Seymour. 2021. Whole-body endothermy: ancient, homologous and widespread among the ancestors of mammals, birds and crocodylians. *Biological Reviews* 97:766–801.
- Guénard, G., P. Legendre, and P. Peres-Neto. 2013. Phylogenetic eigenvector maps: a framework to model and predict species traits. *Methods in Ecology and Evolution* 4:1120–1131.
- Hartman, F. A., and M. A. Lessler. 1964. Erythrocyte measurements in fishes, amphibia and reptiles. *Biological Bulletin* 126:83–88.
- Huttenlocker, A. K., and C. G. Farmer. 2017. Bone microvasculature tracks red blood cell size diminution in Triassic mammal and dinosaur forerunners. *Current Biology* 27:48–54.
- Iori, F.V., and I. S. Carvalho. 2018. The Cretaceous crocodyliform *Caipirasuchus*: behavioral feeding mechanisms. *Cretaceous Research* 84:181–187.
- Ives, A. R., and T. Garland. 2010. Phylogenetic logistic regression for binary dependent variables. *Systematic Biology* 59:9–26.
- Jastroch, M., and F. Seebacher. 2020. Importance of adipocyte browning in the evolution of endothermy. *Philosophical Transactions of the Royal Society of London B* 375:20190134.
- Knaus, P. L., A. H. Van Heteren, J. K. Lungmus, and P. M. Sander. 2021. High blood flow into the femur indicates elevated aerobic capacity in synapsids since the reptile-mammal split. *Frontiers in Ecology and Evolution* 9:751238.
- Kumar, V., B. M. Hallström, and A. Janke. 2013. Coalescent-based genome analyses resolve the early branches of the Euarchontoglires. *PLoS ONE* 8:e60019.
- Legendre, L. J., and D. Davesne. 2020. The evolution of mechanisms involved in vertebrate endothermy. *Philosophical Transactions of the Royal Society of London B* 375:20190136.
- Legendre, L. J., L. Segalen, and J. Cubo. 2013. Evidence for high bone growth rate in *Euparkeria* obtained using a new paleohistological inference model for the humerus. *Journal of Vertebrate Paleontology* 33:1343–1350.
- Legendre, L. J., G. Guénard, J. Botha-Brink, and J. Cubo. 2016. Palaeohistological evidence for ancestral high metabolic rate in archosaurs. *Systematic Biology* 65:989–996.
- Man, Z., W. Yishu, Y. Peng, and W. Xiaobing. 2011. Crocodylian phylogeny inferred from twelve mitochondrial protein-coding genes, with new complete mitochondrial genomic sequences for *Crocodylus acutus* and *Crocodylus novaeguineae*. *Molecular Phylogenetics and Evolution* 60:62–67.
- Marinho, T. S., and I. S. Carvalho. 2009. An armadillo-like sphaesaurid crocodyliform from the Late Cretaceous of Brazil. *Journal of South American Earth Sciences* 27:36–41.
- Martins, E. P., and T. F. Hansen. 1996. The statistical analysis of interspecific data: a review and evaluation of phylogenetic comparative methods. Pp. 22–75 in E. P. Martins, ed. *Phylogenies and the comparative method in animal behavior*. Oxford University Press, New York.
- Melstrom, K. M., and R. B. Irmis. 2019. Repeated evolution of herbivorous crocodyliforms during the age of dinosaurs. *Current Biology* 29:2389–2395.e3.
- Meredith, R. W., J. E. Janečka, J. Gatesy, O. A. Ryder, C. A. Fisher, E. C. Teeling, A. Goodbla, E. Eizirik, T. L. L. Simão, T. Stadler, D. L. Rabosky, R. L. Honeycutt, J. J. Flynn, C. M. Ingram, C. Steiner, T. L. Williams, T. J. Robinson, A. Burk-Herrick, M. Westerman, N. A. Ayoub, M. S. Springer, and W. J. Murphy. 2011. Impacts of the cretaceous terrestrial revolution and KPg extinction on mammal diversification. *Science* 334:521–524.
- Molina-Venegas, R., J. C. Moreno-Saiz, I. Castro Parga, T. J. Davies, P. R. Peres-Neto, and M. Á. Rodríguez. 2018. Assessing among-lineage variability in phylogenetic imputation of functional trait datasets. *Ecography* 41:1740–1749.
- Montefeltro, F. C., S. Lautenschlager, P. L. Godoy, G. S. Ferreira, and R. J. Butler. 2020. A unique predator in a unique ecosystem: modelling the apex predator within a Late Cretaceous crocodyliform-dominated fauna from Brazil. *Journal of Anatomy* 237:323–333.
- Montes, L., N. Le Roy, M. Perret, V. de Buffrénil, J. Castanet, and J. Cubo. 2007. Relationships between bone growth rate, body mass and resting metabolic rate in growing amniotes: a phylogenetic approach. *Biological Journal of the Linnean Society* 92:63–76.
- Nascimento, P. M., and H. Zaher. 2010. A new species of *Baurusuchus* (Crocodyliformes, Mesoeucrocodylia) from the Upper Cretaceous of Brazil, with the first complete postcranial skeleton described for the family Baurusuchidae. *Papéis Avulsos de Zoologia* 50:323–361.
- Nieto, M. N., F. J. Degrange, K. C. Sellers, D. Pol, and C. M. Holliday. 2021. Biomechanical performance of the cranio-mandibular complex of the small notosuchian *Araripesuchus gomesii* (Notosuchia, Uruguaysuchidae). *Anatomical Record*, <https://doi.org/10.1002/ar.24697>.
- Nobre, P. H., I. de Souza Carvalho, F. M. de Vasconcellos, and P. R. Souto. 2008. Feeding behavior of the Gondwanic Crocodylomorpha *Mariliasuchus amarali* from the Upper Cretaceous Bauru Basin, Brazil. *Gondwana Research* 13:139–145.
- Olivier, C., A. Houssaye, N.-E. Jalil, and J. Cubo. 2017. First palaeohistological inference of resting metabolic rate in an extinct synapsid, *Moghreberia nmachouensis* (Therapsida: Anomodontia). *Biological Journal of the Linnean Society* 121:409–419.
- Orme, D., R. Freckleton, G. H. Thomas, T. Petzoldt, S. Fritz, N. Isaac, and W. Pearse. 2013. Caper: comparative analyses of

- phylogenetics and evolution in R. <https://CRAN.R-project.org/package=caper>, accessed 23 May 2022.
- Ósi, A. 2014. The evolution of jaw mechanism and dental function in heterodont crocodyliforms. *Historical Biology* 26:279–414.
- Pol, D. 2005. Postcranial remains of *Notosuchus terrestris* Woodward (Archosauria: Crocodyliformes) from the upper Cretaceous of Patagonia, Argentina. *Ameghiniana* 42:21–38.
- Pol, D., P. M. Nascimento, A. B. Carvalho, C. Riccomini, R. A. Pires-Domingues, and H. Zaher. 2014. A new notosuchian from the Late Cretaceous of Brazil and the phylogeny of advanced notosuchians. *PLoS ONE* 9:e93105.
- Price, L. I. 1950. On a new Crocodylia, *Sphagesaurus* from the Cretaceous of State of São Paulo, Brazil. *Anais da Academia Brasileira de Ciências* 22:77–83.
- Price, L. I. 1959. Sobre um crocodilídeo notossuquío do Cretácico Brasileiro. Serviço Gráfico do Instituto Brasileiro de Geografia e Estatística, Rio de Janeiro.
- Prum, R. O., J. S. Berv, A. Dornburg, D. J. Field, J. P. Townsend, E. M. Lemmon, and A. R. Lemmon. 2015. A comprehensive phylogeny of birds (Aves) using targeted next-generation DNA sequencing. *Nature* 526:569–573.
- Pyron, R. A., and J. J. Wiens. 2011. A large-scale phylogeny of Amphibia including over 2800 species, and a revised classification of extant frogs, salamanders, and caecilians. *Molecular Phylogenetics and Evolution* 61:543–583.
- R Development Core Team. 2008. R: a language and environment for statistical computing. R Foundation for Statistical Computing, Vienna, Austria.
- Riff, D., and A. W. A. Kellner. 2011. Baurusuchid crocodyliforms as theropod mimics: clues from the skull and appendicular morphology of *Stratiotosuchus maxhechti* (Upper Cretaceous of Brazil). *Zoological Journal of the Linnean Society* 163:S37–S56.
- Rohlf, F. J. 2001. Comparative methods for the analysis of continuous variables: geometric interpretations. *Evolution* 55:2143–2160.
- Sereno, P., and H. Larsson. 2009. Cretaceous crocodyliforms from the Sahara. *ZooKeys* 28:1–143.
- Seymour, R. S., S. L. Smith, C. R. White, D. M. Henderson, and D. Schwarz-Wings. 2012. Blood flow to long bones indicates activity metabolism in mammals, reptiles and dinosaurs. *Proceedings of the Royal Society of London B* 279:451–456.
- Snyder, G. K., and B. A. Sheaffer. 1999. Red blood cells: centerpiece in the evolution of the vertebrate circulatory system. *Integrative and Comparative Biology* 39:189–198.
- Soslau, G. 2020. The role of the red blood cell and platelet in the evolution of mammalian and avian endothermy. *Journal of Experimental Zoology B* 334:113–127.
- Soto, M., D. Pol, and D. Perea. 2011. A new specimen of *Uruguaysuchus aznarezi* (Crocodyliformes: Notosuchia) from the middle Cretaceous of Uruguay and its phylogenetic relationships. *Zoological Journal of the Linnean Society* 163:S173–S198.
- Symonds, M. R. E., and S. P. Blomberg. 2014. A primer on phylogenetic generalised least squares. Pp. 105–130 in L. Z. Garamszegi, ed. *Modern phylogenetic comparative methods and their application in evolutionary biology: concepts and practice*. Springer, Berlin.
- Tung Ho, L.-s., and C. Ané. 2014. A linear-time algorithm for Gaussian and non-Gaussian trait evolution models. *Systematic Biology* 63:397–408.
- Turner, A. H. 2006. Osteology and phylogeny of a new species of *Araripesuchus* (Crocodyliformes: Mesoeucrocodylia) from the Late Cretaceous of Madagascar. *Historical Biology* 18:255–369.
- Upham, N. S., J. A. Esselstyn, and W. Jetz. 2019. Inferring the mammal tree: species-level sets of phylogenies for questions in ecology, evolution, and conservation. *PLoS Biology* 17:e3000494.
- Vasconcellos, F. M., and I. D. S. Carvalho. 2010. Paleoichnological assemblage associated with *Baurusuchus salgadoensis* remains, a Baurusuchidae Mesoeucrocodylia from the Bauru Basin, Brazil (Late Cretaceous). *Bulletin of the New Mexico Museum of Natural History and Science* 51:227–237.
- Villa, A., J. Abella, D. M. Alba, S. Almécija, A. Bolet, G. D. Koufos, F. Knoll, À. H. Luján, J. Morales, J. M. Robles, I. M. Sánchez, and M. Delfino. 2018. Revision of *Varanus marathonensis* (Squamata, Varanidae) based on historical and new material: morphology, systematics, and paleobiogeography of the European monitor lizards. *PLoS ONE* 13:e0207719.
- Wu, X.-C., and H.-D. Sues. 1996. Anatomy and phylogenetic relationships of *Chimaerasuchus paradoxus*, an unusual crocodyliform reptile from the Lower Cretaceous of Hubei, China. *Journal of Vertebrate Paleontology* 16:688–702.
- Zanno, L. E., and P. J. Makovicky. 2013. Neovenatorid theropods are apex predators in the Late Cretaceous of North America. *Nature Communications* 4:2827.
- Zurano, J. P., F. M. Magalhães, A. E. Asato, G. Silva, C. J. Bidau, D. O. Mesquita, and G. C. Costa. 2019. Cetartiodactyla: updating a time-calibrated molecular phylogeny. *Molecular Phylogenetics and Evolution* 133:256–262.

Appendix 4 - Biotic and abiotic factors
and the phylogenetic structure of
extinction in the evolution of
Tethysuchia

<RRH>*Factors explaining the evolution of Tethysuchia*

<LRH>Forêt *et al.*

Biotic and abiotic factors and the phylogenetic structure of extinction in the evolution of Tethysuchia

Tom Forêt, Paul Aubier, Stéphane Jouve, and Jorge Cubo

Sorbonne Université, Muséum National d'Histoire Naturelle, CNRS, Centre de Recherche en Paléontologie-Paris (CR2P), 75005 Paris, France

1 **Corresponding author:**

Tom Foret; Email: tomforet@gmail.com

2 **Non-technical Summary**

3 Crocodylomorpha is a large group of reptiles now restricted to modern crocodylians. Among
4 them, Tethysuchia is a small group of semi-amphibious crocodiles that crossed two biological
5 crises: the second Oceanic Anoxic Event (OAE 2) and the Cretaceous/Paleogene (K/Pg) crisis.
6 Numerous studies have sought to find the driving factors explaining crocodylomorph evolution,
7 producing contradictory conclusions. Studies of smaller groups may help find new exclusive
8 patterns. Here, we studied factors driving tethysuchian evolution using phylogenetically
9 informed statistical analyses. First, we tested whether or not tethysuchian extinction was random
10 across the tips of phylogeny for both crises. Then we tested the influence of biological (body
11 size, snout proportion) and climatic (temperature, paleolatitude) factors on the evolution of
12 tethysuchian diversity at the OAE 2 and the K/Pg crises. Finally, we tested whether temperature
13 influenced the evolution of body size. We conclude that (1) extinction was not random in regard
14 to phylogeny for Tethysuchia at the OAE 2 and K/Pg crises; (2) while an important tethysuchian
15 turnover follows OAE 2, the K/Pg crisis was followed by an explosion in diversity of

16 tethysuchians, which may be explained by the disappearance of marine competitors such as
17 mosasaurs; (3) tethysuchians lived in warmer environments after OAE 2, possibly because of
18 both global warming and changes in latitudinal distribution; (4) there is an ecological
19 diversification after both crises, observable by snout reduction, probably caused by niche
20 partitioning; and (5) there is a positive correlation between body size and temperature, possibly
21 because of a longer growth season.

22 **Abstract**

23 Crocodylomorpha is a large and diverse clade with a long evolutionary history now restricted to
24 modern crocodylians. Tethysuchia is a less-inclusive clade of semi-amphibious taxa that crossed
25 two biological crises: the second Oceanic Anoxic Event (OAE 2) and the Cretaceous/Paleogene
26 (K/Pg) crisis. Numerous studies have sought to find the driving factors explaining
27 crocodylomorph evolution, producing contradictory conclusions. Studies of included groups may
28 be useful. Here, we study factors driving tethysuchian evolution using phylogenetically informed
29 statistical analyses. First, we tested the phylogenetic structure of tethysuchian extinction at the
30 OAE 2 and K/Pg crises. We then used phylogenetic comparative methods to test the influence of
31 intrinsic (body size, snout proportion) and extrinsic (temperature, paleolatitude) factors on the
32 evolution of tethysuchian diversity at the OAE 2 and the K/Pg crises. Finally, we tested whether
33 temperature influenced the evolution of body size. We conclude that (1) extinction was not
34 random in regard to phylogeny for Tethysuchia at the OAE 2 and K/Pg crises; (2) while an
35 important tethysuchian turnover follows OAE 2, the K/Pg crisis was followed by an explosion in
36 diversity of tethysuchians, probably linked to the colonization of emptied ecological niches; (3)
37 tethysuchians lived in warmer environments after the OAE 2 crisis, possibly because of both
38 global warming and latitudinal distribution shifts; (4) there is a significant change of snout

39 proportion after the OAE 2 and the K/Pg crises, likely caused by niche partitioning; and (5) there
40 is a positive correlation between body size and temperature, possibly because of a longer growth
41 season.

42 Received: 7 April 2023

43 Accepted: 7 February 2024

44 **Introduction**

45 Crocodylomorpha is a diverse clade that emerged during the Late Triassic (Irmis et al. 2013) and
46 occupied many ecological niches (Wilberg et al. 2019). It crossed major extinction events such
47 as the Triassic/Jurassic (T/J) crisis, after which it radiated (Toljagić and Butler 2013; Bronzati et
48 al. 2015), and the Cretaceous/Paleogene (K/Pg) crisis. Its diversity declined during the Cenozoic,
49 probably due to climate cooling (Markwick 1998) or to competition with mammals in the case of
50 terrestrial crocodylomorphs (Notosuchia) until modern days, when they are limited to 26 species
51 sharing a similar semi-aquatic ecology (Grigg and Kirshner 2015).

52 Among crocodylomorphs, Tethysuchia Buffetaut, 1982 is a group of semi-aquatic
53 freshwater and marine neosuchians (Andrade and Sayão 2014) that extended from the
54 Kimmeridgian to the Bartonian (Jouve et al. 2021). They were probably ectothermic animals
55 (Faure-Brac et al. 2021). While tethysuchians are ancestrally freshwater organisms (Martin et al.
56 2014b), independent events of colonization of the marine environment have been reported (Jouve
57 et al. 2005a,b; Hua et al. 2007; Wilberg et al. 2019; Jouve 2021). This group is composed of two
58 clades (Jouve 2021): Pholidosauridae Eastman *in* Zittel and Eastman 1902, which extended from
59 the Kimmeridgian (Mones 1980) to the Danian (Jouve and Jalil 2020) and Dyrosauroidea Jouve
60 et al., 2021, which extended from the Barremian (Buffetaut and Hutt 1980) to the Bartonian
61 (Buffetaut 1978). Tethysuchians faced two major extinction events. The second Oceanic Anoxic

62 Event (OAE 2) occurred during the Cenomanian/Turonian transition, coinciding with intense
63 volcanic activity, especially in the Caribbeans, which produced metallic nutrients (Turgeon and
64 Creaser 2008). These nutrients increased primary production, leading to greater oxygen
65 consumption, which causes anoxia (Bralower 2008; Turgeon and Creaser 2008). Coupled with
66 this, an important greenhouse effect may have been generated by the volcanic CO₂, leading to a
67 stratified ocean that hampered oxygen delivery to deep waters (Bralower 2008; Turgeon and
68 Creaser 2008). This event was linked to the extinction of ichthyosaurs (Fischer et al. 2016). The
69 second event that tethysuchians crossed was the K/Pg crisis. That event coincides with a
70 meteoric impact in the Gulf of Mexico (Hildebrand et al. 1991) and important volcanism in the
71 Deccan Traps (Courtilot 1980). The timing and importance of each event remain heavily
72 discussed (Schoene et al. 2019; Sprain et al. 2019). The K/Pg crisis was linked to the extinction
73 of non-avian dinosaurs (Novacek 1999); pterosaurs (Barrett et al. 2008 *in* Hone and Buffetaut
74 2008); and many marine reptiles, including mosasaurs and plesiosaurs (Bardet 1995).

75 Numerous studies have tried to identify factors driving crocodylomorph evolution.
76 Martin et al. (2014a) suggested that sea-surface temperature (SST) was positively correlated with
77 crocodylomorph diversity, as well as with the marine colonization by tethysuchians, but they did
78 not find a correlation between SST and tethysuchian diversity drops. Jouve et al. (2017)
79 questioned the reliability of these results, stating that minor taxonomic updates heavily affected
80 the results. Mannion et al. (2015) found that diversification patterns for crocodylomorphs tracked
81 environmental variations, but contrary to Martin et al. (2014a), no significant correlation
82 between diversity and temperature was found for marine taxa. Jouve and Jalil (2020) found a
83 significant positive correlation between paleotemperature and diversity during the Oxfordian–
84 Cenomanian time interval followed by a significant negative correlation during the Turonian–

85 Thanetian period. Bronzati et al. (2015) found that crocodylomorph diversification shifts were
86 patchy and restricted to small intervals, whereas none was found for tethysuchians. On the other
87 hand, Jouve (2021) found an important diversification event for longirostrine (i.e., long-snouted)
88 crocodylomorphs after the K/Pg crisis, especially dyrosaurid tethysuchians. Godoy et al. (2019)
89 did not find significant correlations between mean body size and temperature for
90 crocodylomorphs, except for the period that extends from the Late Cretaceous to recent times. As
91 for tethysuchians, the authors found different results depending on the body-size proxy and the
92 paleotemperature data used. More recently, Stockdale and Benton (2021) found a significant
93 correlation between mean body size and paleotemperature for crocodylomorphs. However,
94 Benson et al. (2022) contested these results, pointing out the absence of log transformation
95 before the statistical analyses. To sum up, no clear diversification driver has been found at the
96 phylogenetic level of Crocodylomorpha. A wide ecological diversity, marked by many different
97 lifestyles among crocodylomorphs (terrestrial, semi-aquatic, fully marine; see Wilberg et al.
98 2019) may explain these problems. Studies on less-inclusive groups, such as Tethysuchia, may
99 help in finding new patterns and resolving this issue. Such studies, however, remain scarce. A
100 new approach coding extinction/survival as a binary variable was applied recently to Notosuchia,
101 a group of largely terrestrial crocodylomorphs (Aubier et al. 2023). These authors tested the
102 phylogenetic structure of the extinction during the K/Pg crisis and used phylogenetic logistic
103 regression (PLR) to test the factors influencing survival during the K/Pg crisis. These analyses
104 revealed a phylogenetic structure in notosuchian extinction at the K/Pg crisis and an evolutionary
105 trend toward larger body sizes after this crisis. This last trend was tentatively explained as being
106 the outcome of a dietary shift (Aubier et al. 2023).

107 The present paper is aimed at elucidating the phylogenetic structure of extinction and
108 identifying the biotic and abiotic factors driving the evolution of tethysuchian paleobiodiversity.
109 More precisely, we tested the phylogenetic structure of tethysuchian extinction at the OAE 2 and
110 K/Pg crises. Then, we tested the effect of intrinsic (body size, snout proportion) and extrinsic
111 (paleolatitude, paleotemperature) factors on the evolution of tethysuchians at both crises. As
112 paleotemperature seems to play a varying role in tethysuchian diversity depending on the time
113 period considered (Jouve and Jalil 2020; Jouve 2021), we expect temperature to be significantly
114 associated with the probability of belonging to the fauna that existed after the OAE 2 and the
115 K/Pg crises. As there seems to be an overall increase in mean body size in crocodylomorphs
116 through time (Godoy et al. 2019), we expect this overall trend to remain unaffected by the crises
117 and body size to be correlated with the probability of belonging to the fauna that existed after the
118 OAE 2 and the K/Pg crises. Finally, we tested whether paleotemperature is linked to body-size
119 evolution. Previous studies did not find significant correlations between these variables in
120 crocodylomorphs (Godoy et al. 2019; Benson et al. 2022). However, mixed results were obtained
121 when focusing on Tethysuchia (Godoy et al. 2019). As most of these results were not significant,
122 we do not expect to find a correlation between size and temperature in tethysuchians.

123 **Materials and Methods**

124 *Data Acquisition*

125 A primary set of taxa was gathered using the Paleobiology Database (PBDB;
126 <https://paleobiodb.org>). To account for potential errors, we returned to the primary literature to
127 ensure the reliability of the data on various aspects (location, age, taxonomy, etc.). As most of
128 the fossil record consists of skulls (Buffetaut and Hutt 1980; Hastings et al. 2011; Jouve et al.
129 2021), we initially chose three cranial variables: skull length (SL; from the anterior tip of the

130 premaxilla to the posterior end of skull table), skull width (SW) at mid-orbital length, and snout
131 proportion (SP; from the tip of the premaxilla to the anterior margin of the orbits, relative to SL).
132 If the measurements were not available from the literature or not explicitly stated to be the same
133 as defined, we measured them using Photofiltre software (see Supplementary File 1 for details),
134 using published figures. As complete tethysuchian remains are scarce (Sereno et al. 2001; Jouve
135 et al. 2006), we cannot compare body sizes. Therefore, one of our cranial measurements had to
136 be selected as a proxy of body size. O'Brien et al. (2019) mention that SW at the quadrates is a
137 good proxy for body size for extant crocodylians. In their study, this proxy seemed to provide
138 accurate results for *Sarcosuchus imperator* De Broin De Lapparent and Taquet, 1966. However,
139 varying degrees of lateral compression of the specimens, as well as the state of conservation of
140 the specimens, only allow measurements at mid-orbital length, which remains a missing variable
141 in most of our sample (see Supplementary File 1 for more information). As a result, SW was
142 excluded from further analyses. SL is the most available skull variable and has previously been
143 used as a proxy of body size (e.g., Godoy et al. 2019; Aubier et al. 2023). However, many
144 studies have criticized this variable as subject to biases linked to group differences and have tried
145 to address this problem using various methods (Young et al. 2011; Stockdale and Benton 2021).
146 Most recently, Stockdale and Benton (2021) have applied principal component analysis (PCA)
147 using various body size indicators to distinguish independent components linked to body size.
148 However, Benson et al. (2022) pointed out that the first principal component was still heavily
149 linked to SL. Therefore, their analyses were still heavily biased by SL. Furthermore, specimens
150 included in this study are not well preserved enough to provide a satisfying amount of available
151 measurements. Another approach is to use equations to estimate the total body size using long
152 bones (Farlow et al. 2005; Vandermark et al. 2007). However, most of these equations are based

153 on extant crocodylians, particularly *Alligator mississippiensis* (Daudin, 1802), and assume that
154 there is not much difference in allometry between extant and extinct crocodylomorphs. Young et
155 al. (2011) considered this assumption unlikely and devised an entirely new equation for
156 metriorhynchids to counter the problem. As we lack complete tethysuchian remains, we cannot
157 test whether this assumption is true for Tethysuchia or whether an entirely new equation is
158 needed. Therefore, we chose to keep SL as a body-size proxy. *Meridiosaurus vallisparadisi*
159 Mones, 1980 and *Sabinosuchus coahuilensis* Shiller et al., 2016 obtained SL estimates based on
160 the length from the tip of the premaxilla to the last maxillary tooth (Fortier et al. 2011) and on
161 the mandible length (Shiller et al. 2016), respectively. We coded their SLs accordingly and then
162 conducted another set of analyses that excluded these estimations (see details in Supplementary
163 File 1). Before any analysis, we log-transformed the measurements, as advised by Benson et al.
164 (2022).

165 We gathered the inferred paleoenvironments of analyzed taxa using Jouve (2021). It can
166 be hypothesized that some Tethysuchia could possibly move between fresh and salt water, like
167 some modern crocodylians (Grigg and Kirshner 2015). However, modern crocodylians capable
168 of this behavior can only stay in salt water for a limited period and need at least partly functional
169 salt glands to deal with various osmolarity problems (Grigg and Kirshner 2015). Although some
170 species have been described as living in a “marine-influenced” environment that has intermediate
171 levels of salinity, the capacity to move “at will” between marine and freshwater environments
172 seems unlikely. Most of the species included in this study are buried either in freshwater-only or
173 marine-only localities (Jouve 2021). Therefore, we considered that the various specimens were
174 buried in their preferred environments and were coded consistently. *Dakotasuchus kingi* Mehl,
175 1941 is the only exception, as it was found in one marine and two freshwater localities (Jouve

176 2021). It seems more likely that it had been transported from freshwater to a marine environment
177 than the opposite, so we considered *D. kingi* a freshwater species. On another note, *MHNM-kh01*
178 is a heavily damaged specimen in the abundant and well-preserved Ouled Abdoun Basin which
179 is marine (Jouve and Jalil 2020). Its state of preservation is striking compared with the other
180 Tethysuchia from this formation (Jouve et al. 2005a,b, 2006, 2008b). Such a difference in
181 preservation suggests transport from a freshwater to a marine locality (Jouve 2021). Therefore,
182 we considered *MHNM-kh01* to be a freshwater organism.

183 Moreover, the local maximum absolute paleolatitude recorded for each species was
184 gathered using the PBDB, and local paleotemperatures were inferred using latitudinal
185 temperature gradients from the literature considering the aforementioned paleolatitudes.
186 However, we lack latitudinal temperature gradients for freshwater environments. Freshwater
187 temperatures have been proposed to be close to the terrestrial ones (Newton and Mudge 2003;
188 Pouech et al. 2014). Furthermore, tethysuchians spent time out of the water, as they had a semi-
189 aquatic lifestyle (Andrade and Sayão 2014). Therefore, we used terrestrial temperature gradients
190 for the species inferred as coming from freshwater environments. For marine species, we used
191 SST gradients gathered from the literature (Frakes et al. 1994; Amiot et al. 2004; Pouech et al.
192 2014; Alberti et al. 2017; Zhang et al. 2019; Laugié et al. 2020; see details in Supplementary File
193 1). Note that no extensive latitudinal temperature gradient study has been made for the Danian.
194 As $\delta^{18}\text{O}$ levels between the Maastrichtian and Selandian are rather similar (Prokoph et al. 2008),
195 we considered the mean value between Campanian–Maastrichtian and Selandian–Thanetian to
196 be a proxy for the value of the Danian.

197 ***Supertree***

198 Because phylogenetic comparative methods require a phylogeny, we decided to use the topology
199 from Jouve (2021) as a reference, because it includes the largest tethysuchian sample ($n = 35$)
200 and provides an extensive review of phylogenetic relationships among both pholidosaurids and
201 dyrosaurids. We added *Brachiosuchus kababishensis* Salih et al., 2022, which has been
202 recovered as the second-earliest diverging dyrosaurid (Salih et al. 2022). *Dakotasuchus kingi* has
203 a debated phylogenetic position (Jouve and Jalil 2020). It is considered to be part of the clade
204 including *Terminonaris robusta* (Mook 1934), *Terminonaris browni* (Osborn, 1904), and
205 *MHNM-kh01*, a poorly preserved Danian specimen (Jouve and Jalil 2020) or the sister species of
206 *Pholidosaurus* Meyer, 1841. We constructed a supertree for each of these two hypotheses,
207 subsequently named Jouve 1 and Jouve 2, respectively. We also tested the topologies obtained by
208 Sachs et al. (2021), the only ones with a satisfying Tethysuchia sample (i.e., more than 20
209 species), although this phylogeny was initially designed for testing phylogenetic relationships
210 among crocodyliforms and not specifically Tethysuchia. Its most striking difference with Jouve 1
211 and 2 was that *Vectisuchus leptognathus* Buffetaut and Hutt, 1980 and *Elosuchus* De Broin De
212 Lapparent, 2002 are considered pholidosaurids. Their analyses yielded two topologies: the first
213 one retrieves *Pholidosaurus schauburgensis* Meyer, 1841 in a clade with *Oceanosuchus*
214 *boecensis* Hua, 2007 and *T. robusta*. The second, on the other hand, retrieves *P.*
215 *schauburgensis* as a sister species of the clade including *O. boecensis*, *T. robusta*, *Chalawan*
216 *thailandicus* (Buffetaut and Ingavat, 1980) and *Sarcosuchus* De Broin and Taquet, 1966. These
217 topologies are subsequently named Sachs 1 and Sachs 2, respectively. Other species listed in the
218 PBDB could have been added but were excluded for various reasons. *Anglosuchus geoffroyi*
219 (Owen, 1884) and *Anglosuchus laticeps* (Owen, 1884) are considered Bathonian. However, their
220 ages remain doubtful, and they closely resemble *Pholidosaurus purbeckensis* (Mansel-Pleydell,

221 1888), so they may be synonyms of the latter (Jouve and Jalil 2020). The pholidosaurids
222 *Pholidosaurus milwardi* Roxo, 1929 and *Pholidosaurus meyeri* Dunker, 1843 and the
223 dyrosaurids *Tilemsisuchus lavocati* Buffetaut, 1980, *Congosaurus compressus* (Buffetaut, 1980),
224 and *Rhabdognathus acutirostris* Bergounioux, 1955 combine poor information on their anatomy,
225 locality, age, and/or phylogenetic position.

226 As mentioned earlier (see previous section), stratigraphic data were gathered using both
227 the PBDB and primary literature. For taxa restricted to a single formation, we considered their
228 FAD (first appearance datum) and LAD (last appearance datum) to match the stratigraphic extent
229 of the formation. For species having occurrences in multiple formations, we considered their
230 FADs and LADs to be as restrictive as possible: we selected the shortest time interval in which
231 the species could be present in all of its recorded localities. However, some adjustments have to
232 be made. Phu Kradung Formation (Thailand), where *C. thailandicus* was recovered, has been
233 traditionally considered as Kimmeridgian–Tithonian according to vertebrate data (Buffetaut and
234 Suteethorn 2007). However, recent palynology studies suggested a Berriasian age (Racey and
235 Goodall 2009). Therefore, we considered *C. thailandicus* to be of Berriasian age. *Hyposaurus*
236 *natator* Troxell, 1925 is noted as being Maastrichtian in the PBDB (Cope, 1866; Marsh, 1870).
237 However, reviews argued that there was probably a reworking caused by bioturbation that caused
238 Danian fossils to be trapped in an apparent Maastrichtian site (Landman et al. 2007; Wiest et al.
239 2016). Therefore, in our analyses, we considered it to be Danian.

240 The topologies were dated using the *timePaleoPhy* function on the paleotree package
241 (Bapst 2012) in R v. 4.2.2 (R Core Team 2013). We used the *firstLast* dating method, which
242 considers the FAD–LAD interval as a positive presence of the taxa. The nodes were dated using
243 the *mbl* (minimum branch length) method, which considers the age of a node to be the same age

244 as the FAD of the oldest fossil of the node. Therefore, FADs and LADs remain the only range
245 data used. Our analyses did not involve incorporating ghost lineages. We must consider that this
246 method may generate zero-length branches (ZLBs), which are intractable for many PCMs (Soul
247 and Wright 2021). A minimal branch length can be selected to prevent ZLBs (Laurin 2004;
248 Wang and Lloyd 2016). Here, we set it to 1 Myr using the “vartime” argument. The complete
249 dated supertrees include 36 Tethysuchia for the phylogenies adapted from Jouve 1 and 2 and 25
250 Tethysuchia for Sachs 1 and 2 (see Fig. 1 and Supplementary File 2). The complete dataset, R
251 script, and generated nexus trees are in Supplementary Files 3–5.

252

253 *Faunal Attribution*

254 Each species was assigned to a fauna depending on whether its stratigraphic interval extended
255 before or after the OAE 2 and the K/Pg crises. For the OAE 2 crisis, 15 taxa from Jouve 1 and 2
256 in the Kimmeridgian–Turonian time bin are referred to as “pre-OAE 2 fauna” (12 taxa for Sachs
257 1 and 2). The other 21 taxa (13 in Sachs 1 and 2) extend from the Campanian to the Ypresian and
258 are referred to as “post-OAE 2 fauna.” Regarding the K/Pg crisis, 18 taxa extend from the
259 Kimmeridgian to the Maastrichtian and are defined as “pre-K/Pg fauna” (13 in Sachs 1 and 2).
260 The other 18 taxa (12 in Sachs 1 and 2) extend from the Danian to the Ypresian and are defined
261 as “post-K/Pg fauna.” Thus, each crisis separates two large time bins. These time bins will be
262 used to test differences between pre- and postcrisis faunae (see following sections) rather than to
263 analyze the evolution of a trait through time as previous studies have done (this last procedure
264 requires a larger sample to infer evolutionary rates; see Stockdale and Benton 2021). Here, these
265 faunae are assumed to be homogeneous, which is a strong assumption considering the long time
266 bins involved.

267 **D-statistic**

268 To check whether the extinction across the OAE 2 and K/Pg has a phylogenetic structure or not,
269 we used the *D*-statistic (Fritz and Purvis 2010). This method measures the randomness of the
270 extinction distribution across the tips of a given tree. More precisely, it compares the observed
271 distribution of a binary variable (in this case, extinction vs. survival, coding each species in the
272 “precrisis” fauna as 0 and each species in the “postcrisis” fauna as 1) with two other
273 distributions: one that simulates the evolution of the binary trait under a Brownian model of
274 evolution and one that simulates the evolution of the same trait under a random model of
275 evolution. The analysis generates a *D*-value. If this value is equal to 1, extinction is not
276 considered to be phylogenetically structured (i.e., the observed distribution is the same as the one
277 produced under the simulated random evolutionary model). If extinction is clustered in the
278 phylogeny as if it followed a Brownian evolutionary model, the *D*-value would equal zero. *D*-
279 values can fall outside this range. This method has been used before to check extinction risk for
280 extant organisms (Fritz and Purvis 2010; Yessoufou et al. 2012; Fontana et al. 2021) or
281 extinction selectivity in the fossil record (Allen et al. 2019; Wilke et al. 2020; Aubier et al.
282 2023). We used the *d.phylo* function of the caper package (Orme et al. 2013) in R v. 4.2.2 (R
283 Core Team 2013), selecting 1000 permutations (i.e., repetition of the simulations to scale *D*-
284 values), as suggested by Fritz and Purvis (2010). This function provides the *D*-value, as well as
285 the probability of obtaining this *D*-value if extinction was phylogenetically random and if it was
286 phylogenetically structured. We performed four analyses depending on the phylogenies (Jouve 1
287 and 2, Sachs 1 and 2; see previous section). We also excluded *V. leptognathus*, as it caused
288 heteroscedasticity in the phylogenetic generalized least squares (PGLS) analysis (see “PGLS and

289 Variation Partitioning”). The complete dataset and script can be found in the Supplementary
290 Files 3 and 6.

291

292 ***PLR***

293 We used PLR (see Ives and Garland 2010) to test whether body size, SP, paleolatitude, and
294 paleotemperature affected the probability of belonging to the post-OAE 2 or post-K/Pg faunae.
295 We used the *phylglm* function from the *phylolm* R package (Tung Ho and Ané 2014) in R v.
296 4.2.2 (R Core Team 2013). The PLR allows the production of predictive models for a binary
297 dependent variable using a set of explanatory variables and the phylogeny. As observations
298 between organisms are not independent (Felsenstein 1985), we included the dated trees (see
299 “Supertree”). PLR has been used to infer the probability of endothermy in tetrapods (Cubo et al.
300 2022) and the probability of survival after the K/Pg crisis in *Notosuchia* (Aubier et al. 2023),
301 similar to our study. We used the same coding as in the *D*-statistic (see previous section). We
302 performed four sets of analyses depending on the phylogenies (Jouve 1 and 2, Sachs 1 and 2; see
303 “Supertree”). In each set, we tested four models: log-transformed SL (model A), SP (model B),
304 paleotemperature (model C), and paleolatitude (model D). For the latter two, we considered that
305 closely related species can have a tendency to live in close areas and/or share similar habitats,
306 following phylogenetic niche conservatism (PNC; Ackerly 2003; Cooper et al. 2010). However,
307 the alternative may be possible. Therefore, we also tested the influence of paleolatitude and
308 paleotemperature using non-phylogenetic logistic regressions with generalized linear models
309 (GLMs). Furthermore, for each set, we considered an alternative hypothesis that excluded SL
310 estimations for *M. valissparadisi* and *S. coahuilensis* (see “Data Acquisition”). In total, each set
311 comprised 24 analyses with 12 per biological crisis (8 comprising PNC, and 4 discarding it).

312 Early analyses suggested that *V. leptognathus* caused heteroscedasticity in the PGLS analysis
313 (see next section). Therefore, it was subsequently removed from both PLR and PGLS analyses.
314 The complete dataset and script can be found in Supplementary Files 3 and 7.

315 ***PGLS and Variation Partitioning***

316 Many studies have previously tried to find a correlation between body size and paleotemperature,
317 producing mixed results (see “Introduction”). Here, we used the PGLS method (see Grafen and
318 Hamilton 1989) to test whether temperature affected log-transformed SL. We used the *pgls*
319 function from the caper R package (Orme 2013) in R v. 4.2.2 (R Core Team 2013). We
320 performed four sets of analyses depending on the phylogenies (Jouve 1 and 2, Sachs 1 and 2; see
321 “Supertree”). In each set, we tested the relationship for tethysuchians as a whole, as well as for
322 pholidosaurids and dyrosauroids separately. As mentioned earlier, temperature may be
323 independent from phylogeny (see previous section); therefore, we also used generalized least
324 squares (GLS) and classic linear models (LMs) that do not take phylogenies into account.
325 Furthermore, for each set, we considered an alternative hypothesis that excluded SL estimation
326 for *M. valissparadisi* and *S. coahuilensis* (see “Data Acquisition”). Each set had a total of 18
327 analyses (6 per group). Shapiro-Wilk tests (Shapiro and Wilk 1965) were used to test the
328 normality of the residual distribution. To check for homoscedasticity, we used the Breusch-
329 Pagan test, which measures the regression error variance (Breusch and Pagan 1979).
330 Homoscedasticity was not respected if *V. leptognathus*, which had a very short skull (Salisbury
331 and Naish 2011 *in* Batten 2011) and lived in very cold temperatures (Frakes et al. 1994), was
332 included. Thus, it was removed from the sample. Then, to test the quality of the
333 paleotemperature-influenced model, we calculated the corrected Akaike information criterion
334 (AICc) using the *AICc* function from the AICcmodavg package (Mazerolle 2013) in R v. 4.2.2

335 (R Core Team 2013) and compared it with a null model (i.e., no influence). We used the same
336 sets of analysis as in the test of correlation between body size and temperature (see above).
337 Finally, to estimate the impact of PNC on log-transformed SL variation, we used the variation
338 partitioning method, which allows quantification of the relative impact of various components on
339 an explanatory variable (Borcard et al. 1992). This method has been further developed to
340 consider phylogeny as a component using a matrix of principal coordinates representing
341 phylogeny (Desdevises et al. 2003; Peres-Neto et al. 2006; Montes et al. 2007; Piras et al. 2009;
342 Sakamoto et al. 2010). We used the *varpart* function from the *vegan* R package (Dixon 2003) in
343 R v. 4.2.2 (R Core Team 2013). We analyzed the variation of log-transformed SL using two
344 components: ecology, which can be represented either by paleotemperature or paleolatitude; and
345 phylogeny. For the latter, we retained the axes that contributed the most (i.e., more than 80%) of
346 the total variation of the phylogenetic distance matrix. As a result, we obtained four different
347 partitions (Fig. 2): a fraction corresponding to a strictly ecological impact on log-transformed SL
348 variation (partition A), a fraction corresponding to a strictly phylogenetic impact on log-
349 transformed SL variation (partition B), a fraction corresponding to a combined effect of ecology
350 phylogeny on log-transformed SL variation (partition C), and a partition corresponding to the
351 unexplained variation (partition D). We may test the significance of partitions using redundancy
352 analysis, except for partitions C and D. The complete dataset and script can be found in
353 Supplementary Files 3, 8, and 9.

354

355 **Results**

356 *Testing the Phylogenetic Structure of Extinction at the OAE 2 and the K/Pg Crises*

357 Similar results were provided by all four analyses. Indeed, in the topology Jouve 1, which
358 considers that *Dakotasuchus kingi* belongs to the clade including *Terminonaris* and *MHNM-*
359 *kh01*, we observe *D*-values of -1.004 for the OAE 2 crisis and -0.751 for the K/Pg one (Table 1,
360 Jouve 1). These values mean that the distribution of the extinction is more phylogenetically
361 structured than that obtained from the simulations performed under a Brownian evolutionary
362 model. Likewise, negative *D*-values were yielded for the topology Jouve 2, which considers that
363 *D. kingi* belongs to the clade including *Pholidosaurus* ($D_{\text{OAE2}} = -1.037$ and $D_{\text{K/Pg}} = -0.723$; Table
364 1, Jouve 2). This was also the case for Sachs 1 and 2, which respectively consider that
365 *Pholidosaurus schauburgensis* is in a clade comprising *Oceanosuchus boecensis* and
366 *Terminonaris robusta* ($D_{\text{OAE2}} = -1.388$ and $D_{\text{K/Pg}} = -0.704$, Sachs 1), and that *P. schauburgensis*
367 is the sister species of a clade including *O. boecensis*, *T. robusta*, *Chalawan thailandicus*, and
368 both *Sarcosuchus* species ($D_{\text{OAE2}} = -1.331$ and $D_{\text{K/Pg}} = -0.74$; Table 1, Sachs 2). These results
369 show that extinction was not phylogenetically random at both of the studied crises. Rather, they
370 show a phylogenetic structure of extinction (i.e., closely related species went extinct during both
371 of the studied crises) that is robust enough to be independent from the phylogenetic placement of
372 one or two species depending on topologies.

373 ***Testing the Effect of Biotic and Abiotic Factors on the Evolution of Tethysuchia after the*** 374 ***OAE 2 and K/Pg Crises***

375 For the first Jouve topology (Table 2, Jouve 1), the probability of belonging to the post-OAE 2
376 fauna is significantly explained by SP (model B) and paleotemperature (model C) but not by the
377 log-transformed SL (model A) or paleolatitude (model D). The probability of belonging to the
378 post-K/Pg crisis fauna is significantly explained by SP (model B) but not by paleotemperature
379 (model C), log-transformed SL (model A), and paleolatitude (model D). The second topology

380 produced similar results (Table 2, Jouve 2). The alternative analysis excluding *Meridiosaurus*
381 *vallisparadisi* and *Sabinosuchus coahuilensis* (see “Materials and Methods”) produced similar
382 results for both topologies (Supplementary File 10, PLR, Jouve 1 and 2). The paleotemperature
383 estimate is positive and significant for each analysis testing its effect on the probability of
384 belonging to the post-OAE 2 fauna, which means the variable is positively correlated with the
385 probability of belonging to the post-OAE 2 fauna. Tethysuchians in the post-OAE 2 fauna are
386 more likely to live in warmer climates. According to analyses using Jouve’s (2021) topologies.
387 The coefficient for SP is significant and negative for each analysis testing its effect on the
388 probability of belonging to the post-OAE 2 and post K/Pg faunae, which means the variable is
389 negatively correlated with the probability of belonging to the post-OAE 2 and the post-K/Pg
390 faunae. Tethysuchians belonging to the postcrisis faunae are more likely to be short-snouted
391 according to analyses using Jouve’s (2021) topologies. However, analyses using Sachs 1 and 2
392 topologies yielded different results: the probability of belonging to the post-OAE 2 or to the
393 post-K/Pg fauna is not affected by any of our models regardless of topology (Table 2, Sachs 1
394 and 2). The alternative hypothesis that excludes *M. vallisparadisi* and *S. coahuilensis* yields
395 similar results (Supplementary File 10, PLR, Sachs 1 and 2). Finally, GLMs that discard PNC for
396 paleotemperature and paleolatitude (see “Materials and Methods”) show a positive effect of
397 paleotemperature on the probability of belonging to the post-OAE 2 and K/Pg faunae regardless
398 of topology (Table 2, Supplementary File 10, PLR). Paleolatitude also has a negative effect on
399 the probability of belonging to the post-OAE 2 fauna. Discarding PNC shows that Tethysuchia
400 are more likely to live in lower latitudes and warmer environments after OAE 2 and in warmer
401 environments after the K/Pg crisis. The alternative hypothesis that excludes *M. vallisparadisi* and
402 *S. coahuilensis* yielded similar results. To sum up, analyses using Jouve’s (2021) hypotheses

403 indicate a trend to warmer climates after OAE 2 and shorter snouts after K/Pg, whereas analyses
404 using Sachs et al.'s (2021) hypotheses indicates none, if PNC is taken into consideration.

405 ***Testing the Correlation between Body Size and Temperature***

406 Both Jouve topologies yielded similar results (Table 3, Jouve 1 and 2, and Fig. 3). We found a
407 significant positive correlation between paleotemperature and log-transformed SL for
408 tethysuchians and pholidosaurids. On the other hand, we found no significant correlation for
409 dyrosauroids. In both Sachs topologies, we found a significant positive correlation between
410 paleotemperature and log-transformed SL for tethysuchians (Table 3, Sachs 1 and 2). However,
411 it should be noted that in the latter two, residuals did not follow a normal distribution. Therefore,
412 these results are not statistically definitive. The alternative analysis considering *M. vallisparadisi*
413 and *S. coahuilensis* SL as missing provides different results: we find no significant correlation
414 between paleotemperature and log-transformed SL for any groups and topologies (see
415 Supplementary File 10, PGLS). The paleotemperature model has a lower AICc than the null
416 model for Tethysuchia in both Jouve topologies (Table 4, Jouve 1 and 2). However, the null
417 model has a lower AICc than the paleotemperature model for dyrosauroids and pholidosaurids.
418 For both Sachs topologies, we see close AICc values between the null model and the
419 paleotemperature model for Tethysuchia ($<0,5$; see Table 4, Supplementary File 10, AICc),
420 which indicates that they are not different. However, for dyrosaurids and pholidosaurids, AICc is
421 lower in the null model. The alternative hypothesis excluding *M. vallisparadisi* and *S.*

422 *coahuilensis* yields similar results for the first two topologies (Supplementary File 10, AICc).

423 However, for the third and fourth topologies, AICc is lower in the null model for Tethysuchia.

424 If we discard PNC (i.e., if we rely on GLS and LM), no correlation is found between log-
425 transformed SL and paleotemperature regardless of topologies and coding for *M. vallisparadisi*

426 and *S. coahuilensis* (Table 3, Supplementary Table 27). Using this assumption, AICc is always
427 lower in the null model (Table 4, Supplementary File 10, AICc). To sum up, paleotemperature
428 has a positive correlation with log-transformed SL in Tethysuchia only if PNC is considered and
429 if *M. vallisparadisi* and *S. coahuilensis* are not excluded. The paleotemperature model generally
430 has lower AICc values than the null model (and therefore is the better model) in Jouve's (2021)
431 topologies for Tethysuchia if PNC is considered and if *M. vallisparadisi* and *S. coahuilensis* are
432 not excluded.

433 Finally, when testing for variation partitioning, both Jouve topologies yield similar results
434 (Table 5, Jouve 1 and 2). Regardless of the explanatory variable composing the ecological
435 component (i.e., paleolatitude or paleotemperature), we observe that partition B accounts for
436 around 5% of the variation. However, we note that most of the variation remains unexplained.
437 Neither partition A nor partition B is significant when tested with redundancy analysis. The
438 alternative hypothesis that excludes *M. vallisparadisi* and *S. coahuilensis* provides slightly
439 different results. Partitions A and B remain nonsignificant in redundancy analyses, but partition
440 B provides a negative R^2 , while partition D accounts for around 100% of the variation for each of
441 the analyses (Supplementary File 10, Variation Partitioning, Jouve 1 and 2). These results
442 suggest an important effect of the two removed species on the results. In both Sachs topologies,
443 partition D accounts for around 100% of the variation and the R^2 values for the other partitions
444 are either negative or up to 2% of the variation (Table 5, Sachs 1 and 2). Similar results can be
445 observed when *M. vallisparadisi* and *S. coahuilensis* are excluded from the analysis: partition C
446 contributes to around 2% of log-transformed SL when paleotemperature is the ecological
447 component and less than 1% if paleolatitude is the ecological component. The rest of the
448 variation is unexplained (Supplementary File 10, Variation Partitioning, Sachs 1 and 2).

449 **Discussion**

450 *A Differential and Phylogenetically Structured Response to Biotic Crises*

451 The first major peak of tethysuchian diversity occurs during Cenomanian (Jouve and Jalil 2020;
452 Jouve 2021; Fig. 1, Supplementary File 2). This period corresponds to the highest temperature
453 and sea level of the Mesozoic (Vérard et al. 2015; Scotese et al. 2021), which may explain the
454 important tethysuchian fossil record, because sea level has long been considered a factor of
455 enhanced diversity (Martin et al. 2014a; Mannion et al. 2015; Tennant et al. 2016). During the
456 Cenomanian/Turonian transition, Tethysuchia experienced a major diversity drop corresponding
457 to OAE 2 (Jouve and Jalil 2020; Fig. 1, Supplementary File 2). Because half of the tethysuchians
458 at the time were marine (Jouve 2021), they were probably heavily affected by this event, which
459 was also linked to the extinction of ichthyosaurs (Fischer et al. 2016) and the diversification of
460 mosasaurs (Bardet 1995). These patterns suggest an important marine faunal turnover previously
461 mentioned in the literature (Kauffman 1995 in National Research Council 1995; Wan et al. 2003;
462 Caron et al. 2006; Monnet 2009). This turnover is supported by the *D*-statistic analysis, which
463 shows a phylogenetic structure of extinction at OAE 2 (Table 1). Indeed, most pholidosaurids do
464 not survive the crisis (Fig. 1, Supplementary File 2) and all known Dyrosauridae De Stefano,
465 1903 appear after the crisis. OAE 2 marks a transition from a pholidosaur- to dyrosaurid-
466 dominated faunae.

467 Following the OAE 2, a gap in the tethysuchian fossil record occurs from the Coniacian
468 to the Santonian (Jouve and Jalil 2020; Fig. 1, Supplementary File 2). The only known putative
469 tethysuchian remains during this period is from a partial maxilla fragment from the In Beceten
470 Formation of Niger that is described as being similar to Tethysuchia, although no phylogenetic
471 analysis is possible because of its fragmentary nature (Buffetaut 1974; Meunier and Larsson

472 2018). The Coniacian–Santonian interval coincides with a marine regression (Jouve and Jalil
473 2020), which can explain this drop in diversity. However, if we look at crocodylomorphs as a
474 whole, most of the fossil record during the Coniacian–Santonian consists of fragmentary remains
475 (Puértolas-Pascual et al. 2016; Meunier and Larsson 2018). Therefore, some of these
476 crocodylomorph elements may have belonged to tethysuchians but have not been identified as
477 such because the material is too fragmentary to provide a more precise taxonomic attribution.
478 Tethysuchian biodiversity may also have been further underestimated due to sampling biases:
479 Coniacian–Santonian formations may suffer from a lack of interest compared with other Late
480 Cretaceous periods that are closer to major events such as OAE 2 and the K/Pg crisis. The next
481 tethysuchian occurrences are recorded during the Campanian and the Maastrichtian (Halstead
482 1975; Shiller et al. 2016; Jouve and Jalil 2020; Salih et al. 2022). Most Late Cretaceous
483 tethysuchians lived in freshwater environments (Jouve 2021). These environments were
484 relatively spared during the K/Pg crisis, as increased potential for dormancy (i.e., a metabolically
485 slowed or inactive state in response to harsh conditions that limits starvation), faster production
486 recovery, more abundant detrital food sources, and the presence of eventual thermal refuges in
487 those environments may have helped stabilize the trophic networks (Robertson et al. 2013).

488 Following the K/Pg crisis, an explosion in diversity occurs (Jouve 2021; Fig. 1,
489 Supplementary File 2). Most Cenozoic tethysuchians lived in marine environments (Jouve 2021).
490 This colonization from freshwater to marine environments may have been made possible because
491 tethysuchians took over the niches vacated by mosasaurs and plesiosaurs that became extinct
492 during K/Pg (Jouve et al. 2008a,b; Barbosa et al. 2008; Bardet et al. 2017; Jouve 2021). As
493 shown by the *D*-statistic analysis, this diversification was phylogenetically structured (Table 1),
494 because most of early-diverging Dyrosauridae do not cross the K/Pg boundary. Because

495 extinction is phylogenetically structured, so is the subsequent diversification. Indeed, the
496 postcrisis diversification affects mostly dyrosaurids, especially Hyposaurinae Nopcsa, 1928 (Fig.
497 1, Supplementary File 2) that heavily colonized the marine realm during the Paleogene (Jouve
498 2021).

499 Both crises had an impact on tethysuchian biodiversity: OAE 2 caused a turnover in
500 tethysuchian diversity, likely by destabilizing the marine food chain, causing top predators such
501 as marine pholidosaurids to become extinct (Jouve and Jalil 2020), whereas the K/Pg crisis made
502 tethysuchian diversity explode, likely as a result of the colonization of niches vacated by
503 mosasaurs and plesiosaurs. After a thriving period during Paleocene, Tethysuchia's evolutionary
504 history ends with their extinction during the Bartonian (Jouve 2021). The factors explaining their
505 extinction are uncertain (Amoudji et al. 2021). The Bartonian coincides with the beginning of the
506 late Eocene–Oligocene cooling (Scotese et al. 2021), which may have impacted tethysuchians
507 (Jouve 2021). Another hypothesis involving competition with new predators, including
508 cetaceans, was mentioned by Hastings (2012). It was considered unlikely by Martin et al.
509 (2014a), but was still mentioned by Stubbs et al. (2021). These hypotheses remain to be tested.
510 Most recently, Scott and Anderson (2022) have tested, under the postulate that competition
511 increases as morphological similarity increases, the competitive interactions between
512 gnathostomes and agnathans during the late Silurian–Devonian using distance-based
513 morphometrics. However, we lack fossil sites bearing both Tethysuchia and cetaceans to support
514 the competition. Therefore, such an assumption cannot be tested.

515

516 *An Adaptation to Warmer Temperatures and Morphological Changes after the Biotic Crises*

517 PLR analyses showed that post-OAE 2 tethysuchians lived under higher temperatures than those
518 pre-OAE 2 if we follow Jouve's (2021) hypotheses. We observe similar results if we discard
519 PNC for Sachs et al.'s (2021) hypotheses (Table 2). Climatic data suggest that, except for the
520 Cenomanian, post-OAE 2 mean temperatures values were generally higher than those of the pre-
521 OAE 2 periods (Scotese et al. 2021). Therefore, these results could be explained by an overall
522 global warming after OAE 2. A change in latitudinal distribution between the two faunae could
523 also explain these results. However, we find no significant difference between them if we
524 consider PNC (Table 2). On the contrary, if we discard PNC, we observe that Tethysuchia were
525 more likely to live at lower latitudes after the OAE 2. Both pre- and post-OAE 2 faunae have a
526 wide latitudinal range (11.6° – 53.9° and 3.5° – 40.6° , respectively; see Fig. 4A-3B). However, two
527 post-OAE 2 tethysuchians (*Sabinosuchus coahuilensis* and *Hyposaurus natator*, located in
528 Mexico and the eastern United States, respectively) have positions relatively isolated from the
529 others. These are not clear outliers; however, if they are excluded, the latitudinal range of the
530 post-OAE 2 fauna is highly reduced (3.5° – 27° ; see Fig. 4B). Thus, the width of the latitudinal
531 range of this fauna is largely due to only two species. Therefore, temperature differences
532 between both faunae may be caused by the combined effect of an overall temperature increase
533 and a generally more restrictive latitudinal distribution (although not necessarily statistically
534 different). GLM analyses that discard PNC show that post K/Pg Tethysuchia also lived in
535 warmer environments. Although paleolatitude is similar between both faunae, the literature
536 shows an overall warming heating after K/Pg, most notably during the end of the Danian and the
537 Paleocene–Eocene thermal maximum (see Scotese et al. 2021).

538 We do not find any correlation between paleotemperature and the probability of
539 belonging to the post K/Pg fauna if we consider PNC. However, the recorded fauna between the

540 Campanian and Maastrichtian, which is the period right before the K/Pg crisis, is still quite
541 limited ($n = 3$). Therefore, a larger Campanian–Maastrichtian sample could heavily impact the
542 statistical analyses. Further exploration may be needed in methods that would consider that
543 tethysuchian distribution and local temperatures may be influenced by the formation of
544 paleocurrents; especially for Paleogene, where marine forms are numerous (Jouve 2021). Indeed,
545 a proto–Gulf Stream has been suggested in literature (Watkins and Self-Trail 2005). It could
546 explain the presence of *H. natator* and *S. coahuilensis* in high latitudes during the Late
547 Cretaceous–Paleogene, as there were warm currents on North America’s eastern coast (Jouve
548 2021). On the other hand, colder currents have been predicted near the European islands (Puc at
549 et al. 2005; Herman and Spicer 2010; Herman 2013). These cold currents may have excluded
550 tethysuchians from Europe, as there are no consensual occurrences of this clade in this region
551 during the end of the Cretaceous–Paleogene.

552 PLR analyses using Jouve’s (2021) topologies showed that the post-OAE 2 fauna was
553 more prone to brevirostry than the pre-OAE 2 one (Table 2). These cases of snout reduction have
554 been described in dyrosauroids, especially during the Paleogene (Jouve et al. 2005a, 2021;
555 Hastings et al. 2011). SP and shape classification in crocodyliforms have been widely discussed
556 in the literature, with proposals of differing categories for various clades. However, a consensus
557 emerges, suggesting that longer and thinner snouts are generally associated with a mainly
558 piscivorous diet and shorter snouts are generally associated with a more durophageous diet
559 (Brochu 2001; Pierce et al. 2009; Drumheller and Wilberg 2020). Early dyrosauroids such as the
560 opportunistic predator *Elosuchus* have a much longer snout than Cenozoic forms such as
561 *Chenanisuchus lateroculi* Jouve et al., 2005a, *Anthracosuchus balrogus* Hastings et al., 2011 and
562 *Rodeosuchus machukiru* Jouve et al., 2021. This pattern is absent when using Sachs et al.’s

563 (2021) topologies. This might, at least partly, be explained by the fact that 11 species included in
564 Jouve (2021) are not present in Sachs et al. (2021). Indeed, among these missing species are
565 *Terminonaris browni*, a longirostrine pre-OAE 2 pholidosaurid; *Dorbignysuchus niatu* Jouve et
566 al., 2020, a brevirostrine (i.e., short-snouted) post-K/Pg dyrosaurid; and many post-K/Pg
567 dyrosaurids that have a mesorostrine (i.e., a medium-sized) snout. The inclusion of these 11
568 species in Sachs et al.'s (2021) sample would be of interest for testing whether phylogeny,
569 sample, or both are affecting the results. We note that Sachs et al.'s (2021) matrix is designed to
570 test crocodyliform relationships and not intraclade relationships. In contrast, Jouve (2021)
571 provides a matrix designed for Tethysuchia. Different statistical results between topologies may
572 also be caused by these differing approaches. We consider that a significant variation in snout
573 length after a crisis may indicate a selective extinction of a particular diet and/or diversification
574 caused by character displacement, both being characteristic of niche partitioning (Brown and
575 Wilson 1956). Longirostrine Tethysuchia are still very abundant after K/Pg, with species such as
576 *Atlantosuchus coupatezi* Buffetaut and Wouters, 1979 and *Luciasuchus luringa* Jouve et al.,
577 2021, among others. Furthermore, brevirostrine Tethysuchia are only known after the K/Pg
578 crisis, which marks the extinction of mosasaurs and plesiosaurs (Bardet 1995; Jouve et al. 2008b,
579 2021; Hastings et al. 2015). As mentioned earlier (see "A Differential and Phylogenetically
580 Structured Response to Biotic Crises"), dyrosaurids may have taken the mosasaur's ecological
581 position after the extinction of the latter. Colonization of now-empty environments may have
582 allowed cases of niche partitioning. Niche partitioning has been described in thalattosuchians
583 (De Andrade et al. 2010), eusuchians (Hastings and Hellmund 2017), and marine Mesozoic
584 squamates (Bardet 2012; Bardet et al. 2015). Such a pattern is also present in dyrosaurids.
585 Indeed, Paleogene dyrosaurid-bearing formations often include longirostrine, brevirostrine, and

586 mesorostrine forms, each associated with a specific diet (piscivorous, durophagous, and
587 generalist, respectively). We observe such a pattern for the formations of the Ouled Abdoun
588 Basin (Paleocene–Ypresian) in Morocco (Bardet et al. 2010), the Cerrejon Formation
589 (Paleocene) in Colombia (Hastings et al. 2015), and the Santa Lucia Formation (Paleocene) in
590 Bolivia (Jouve et al. 2021).

591

592 *A Trend toward Larger Body Sizes and Warm Climates?*

593 A relationship between body size and temperature has already been tested for tethysuchians,
594 yielding contrasting results depending on how body size is measured (Godoy et al. 2019).
595 However, these analyses excluded PNC and used ordinary least squares and GLS instead of
596 phylogenetic comparative methods. A significant relationship has been found for the crocodylian
597 crown-group using the same methodology (Godoy et al. 2019; Godoy and Turner 2020),
598 suggesting that larger body sizes are associated with cooler climates. Similar results were found
599 when only extant crocodylomorphs were analyzed (Lakin et al. 2020). However, these
600 relationships were tested using GLMs and not PGLS (Lakin et al. 2020). By contrast, the PGLS
601 performed here shows that tethysuchians were larger in warmer climates (Table 3). The
602 subsequently created paleotemperature-influenced model has a better linear fit than the null
603 model that postulates no correlation (Table 4).

604 Tethysuchia were probably ectotherms (Faure-Brac et al. 2021). Ectothermic organisms
605 are known to have a cyclic growth linked to seasonality that can be recorded in bone histology.
606 Indeed, we can observe periods of rapid growth (zones) and periods of slow (annuli) or arrested
607 (lines) growth (De Buffrénil and Quilhac 2021 *in* De Buffrénil et al. 2021). Such a pattern has
608 been identified in extant crocodylians (Hutton, 1987) and the crocodylomorph fossil record

609 (Castanet et al. 1977; De Buffrénil et al. *in* De Buffrénil et al. 2021). Various histological
610 sections of tethysuchians show the presence of lines of arrested growth (Andrade and Sayão
611 2014; Faure-Brac et al. 2021; De Buffrénil et al. *in* De Buffrénil et al. 2021). Furthermore, some
612 extant vertebrate ectotherms have been known to have a preferential season of growth during
613 warm periods and hence have larger sizes in warmer climates (Hjernquist et al. 2012). Therefore
614 it is possible that Tethysuchia living in warmer temperatures had a longer preferred growth
615 season. With a longer growth season, they may have grown larger, thus explaining the results
616 shown by the PGLS. However, extant crocodylians, which are also ectothermic, have been noted
617 to follow the opposite pattern (Godoy and Turner 2020; Lakin et al. 2020). Both groups share an
618 overall similar thermophysiology; hence, this difference in body-size distribution cannot be
619 explained by the thermometabolism. However, temperature tolerance differences have been
620 noted to exist among extant crocodylians and have been suggested for extinct crocodylians
621 (Jouve 2019) or between dyrosaurids and gavialoids (Jouve 2021), the latter being present in
622 warmer climatic zones than dyrosarids. Therefore, there may be a different response in growth to
623 paleotemperature for tethysuchians compared with modern crocodiles. Further exploration is
624 required to assert the origins of these differences. We also tested the correlation for dyrosauroids
625 and pholidosaurids separately. We observe a similar correlation for pholidosaurids if we follow
626 Jouve's (2021) topologies. However, because the pholidosaurid sample is very small ($n < 8$) and
627 the null model generally has a better linear fit than the paleotemperature-influenced one, we
628 consider that there is not enough statistical evidence to prove any correlation for pholidosaurids
629 separately. Finally, the null model remains the better linear fit, and no correlation is found for
630 dyosauroids after *Vectisuchus leptognathus* is excluded from the analysis. *Vectisuchus*
631 *leptognathus* is a clear outlier in our sample, as it caused heteroscedasticity in PGLS analyses if

632 it was not excluded. Furthermore, it is both the smallest known tethysuchian and the one that
633 lives in the coldest environment (Frakes et al. 1994; Salisbury and Naish 2011 *in* Batten 2011).
634 Its unique specimen has been found in the Upper Wessex Formation (Barremian) of England,
635 and it lived among many other crocodylomorphs, mostly goniopholidids (Salisbury and Naish
636 2011 *in* Batten 2011). Its small size may result from niche partitioning with these other
637 crocodylomorphs: smaller-sized species do not feed from the same resources as larger species.
638 Such a pattern has been observed in Metriorhynchidae: species with similar ecologies have a
639 wide size range and different prey (Young et al. 2011). However, *V. leptognathus* lived at a high
640 paleolatitude, which may explain its low inferred paleotemperature (see Supplementary File 1).
641 Such a temperature cannot be explained by paleolatitude alone, as it is not the highest
642 paleolatitude of our sample (see Supplementary File 1 for details). Furthermore, during the
643 Barremian, many crocodylomorphs were living at similarly high paleolatitudes (Salisbury and
644 Naish 2011 *in* Batten 2011). The notably low paleotemperature we inferred for *V. leptognathus*
645 may result from cold environmental conditions during the Barremian. Indeed, its stratigraphic
646 extent stands during the Tithonian–early Barremian cool interval, which is the coldest period in
647 the Mesozoic (Scotese 2021). Therefore, a combination of a high latitude during a notably cold
648 period explains its low paleotemperature, and niche partitioning may explain its small size.
649 Finally, no significant correlation is found if the SL estimations of *Meridiosaurus vallisparadisi*
650 and *S. coahuilensis* are excluded. Hence, all of these elements suggest that our results must be
651 treated with caution, because changing the interpretation for one or two species heavily affects
652 the results. This caution is strengthened by the results of variation partitioning that suggest
653 different results, indicating that paleotemperature and phylogeny had a nonsignificant influence
654 on log-transformed SL variation. According to the analyses, most of the variation remains

655 unexplained. These differing results may be explained by the relative scarcity of SL data. Indeed,
656 some species were excluded from both variation partitioning and PGLS analyses because they
657 had no available SL. These missing values may have impacted the results differently depending
658 on the methodology used. We note that variation partitioning may show that, apart from
659 temperature, various other factors may explain log-transformed SL variation. One of these
660 factors may be dietary differences. Indeed, dietary shifts have been shown to explain body-size
661 variation in Canidae and Notosuchia (Van Valkenburgh et al. 2004; Aubier et al. 2023). Another
662 possible component may be species competitiveness: species with a relatively similar ecology
663 may limit competition for the same resources because of their larger range of body sizes.
664 Therefore, they feed on different prey while having a similar ecology. This pattern has been
665 suggested in metriorhynchid crocodylomorphs (Young et al. 2011). However, we lack
666 tethysuchian fossil data to further test both of these assumptions. Finally, other poorly
667 understood or yet undiscovered biological factors may explain more log-transformed SL
668 variation.

669

670 **Conclusion**

671 Tethysuchians crossed two biological crises, the OAE 2 and K/Pg, during their evolutionary
672 history. Extinction was phylogenetically structured in both of them. These crises had differential
673 effects on paleobiodiversity: first, the OAE 2 crisis was followed by a turnover of tethysuchian
674 diversity with a pholidosaurid-dominated fauna replaced by a dyrosaurid-dominated one.
675 Second, the K/Pg crisis was followed by increased biodiversity, especially regarding dyrosaurids,
676 which remained high until the Eocene. Post-OAE 2 tethysuchians lived in warmer environments
677 than the pre-OAE 2 fauna thanks to an overall global warming, possibly combined with a more

678 restricted lower-latitude extension. The possible colonization of new ecological niches, likely left
679 vacant by the extinction of mosasaurs and plesiosaurs, may also have allowed morphological
680 diversification regarding the SP and shape in the same formations. This niche partitioning is
681 shown by the co-occurrences of multiple tethysuchians associated with diverse diets. Finally,
682 unlike other studies (Godoy et al. 2019; Godoy and Turner 2020; Lakin et al. 2020), we found a
683 positive correlation between body length (using the log-transformed SL as proxy) and
684 temperature. These results may be explained by the difference in a preferential season of growth
685 duration. Nevertheless, these results must be treated with caution, as the fossil record of
686 tethysuchians is scarce, most notably during the Late Cretaceous with many ghost lineages.
687 These results also depend heavily on the size estimations from two taxa in our sample,
688 suggesting that the SL sample may be an issue. Finally, variation partitioning suggested that
689 other factors may explain body-size variation in Tethysuchia. Therefore, further exploration is
690 required to uncover body-size evolution in Tethysuchia.

691 **Acknowledgments.** We thank N. Campione (University of New England), C. Brochu
692 (University of Iowa), and two anonymous reviewers for their suggestions. We thank J. Schnyder
693 (Sorbonne Université) for helping us with climatic data treatment. We thank J. Bardin (Sorbonne
694 Université) for his statistical advice. We thank M. G. Faure-Brac (University of Oslo) and M. V.
695 A. Sena (Sorbonne Université) for their help.

696 **Competing Interests.** The authors declare no competing interests.

697 **Data Availability Statement.** Data available from the Dryad and Zenodo Digital Repositories:

698 <https://doi.org/10.5061/dryad.bnzs7h4j3>, <https://doi.org/10.5281/zenodo.10548562n>.

699 **Literature Cited**

700 **Ackerly, D. D.** 2003. Community assembly, niche conservatism, and adaptive evolution in
701 changing environments. *In* C. Caruso, ed. *Evolution of functional traits in plants*.
702 *International Journal of Plant Sciences* **164** (Suppl. to No. 3): S165–S184.

703 **Alberti, M., F. T. Fürsich, A. A. Abdelhady, and N. Andersen.** 2017. Middle to Late Jurassic
704 equatorial seawater temperatures and latitudinal temperature gradients based on stable
705 isotopes of brachiopods and oysters from Gebel Maghara, Egypt. *Palaeogeography,*
706 *Palaeoclimatology, Palaeoecology* **468**:301–313.

707 **Allen, B. J., T. L. Stubbs, M. J. Benton, and M. N. Puttick.** 2019. Archosauromorph
708 extinction selectivity during the Triassic–Jurassic mass extinction. *Palaeontology*
709 **62**:211–224.

710 **Amiot, R., C. Lécuyer, E. Buffetaut, F. Fluteau, S. Legendre, and F. Martineau.** 2004.
711 Latitudinal temperature gradient during the Cretaceous Upper Campanian–Middle
712 Maastrichtian: $\delta^{18}\text{O}$ record of continental vertebrates. *Earth and Planetary Science*
713 *Letters* **226**:255–272.

714 **Amoudji, Y. Z., G. Guinot, L. Hautier, K. E. Kassegne, N. Chabrol, A-L. Charruault, A. K.**
715 **C. Johnson, R. Sarr, P. Y. D Da Costa, and J. E. Martin.** 2021. New data on the
716 Dyrosauridae (Crocodylomorpha) from the Paleocene of Togo. *Annales de Paléontologie*
717 **107**:102472.

718 **Andrade, R. C. L. P., and J. M Sayão.** 2014. Paleohistology and lifestyle inferences of a
719 dyrosaurid (Archosauria: Crocodylomorpha) from Paraíba Basin (northeastern Brazil).
720 *PLOS ONE* **9**:e102189.

- 721 **Aubier, P., S. Jouve, J. Schnyder, and J. Cubo.** 2023. Phylogenetic structure of the extinction
722 and biotic factors explaining differential survival of terrestrial notosuchians at the
723 Cretaceous–Palaeogene crisis. *Palaeontology* **66**:e12638.
- 724 **Bapst, D. W.** 2012. paleotree: an R package for paleontological and phylogenetic analyses of
725 evolution. *Methods in Ecology and Evolution* **3**:803–807.
- 726 **Barbosa, J. A., A. W. A. Kellner, and M. S. S. Viana.** 2008. New dyrosaurid crocodylomorph
727 and evidences for faunal turnover at the KP transition in Brazil. *Proceedings of the Royal*
728 *Society of London B* **275**:1385–1391.
- 729 **Bardet, N.** 1995. Evolution et extinction des reptiles marins au cours du Mésozoïque.
730 *Paleovertebrata* **24**:177–283.
- 731 **Bardet, N.** 2012. Maastrichtian marine reptiles of the Mediterranean Tethys: a
732 palaeobiogeographical approach. *Bulletin de la Société Géologique de France* **183**:573–
733 596.
- 734 **Bardet, N., X. P. Suberbiola, S. Jouve, E. Bourdon, P. Vincent, A. Houssaye, J-C. Rage, N-**
735 **E. Jalil, B. Bouya, and M. Amaghaz.** 2010. Reptilian assemblages from the latest
736 Cretaceous–Palaeogene phosphates of Morocco: from Arambourg to present time.
737 *Historical Biology* **22**:186–199.
- 738 **Bardet, N., A. Houssaye, P. Vincent, X. P. Suberbiola, M. Amaghaz, E. Jourani, and S.**
739 **Meslouh.** 2015. Mosasaurids (Squamata) from the Maastrichtian phosphates of Morocco:
740 biodiversity, palaeobiogeography and palaeoecology based on tooth morphoguilds.
741 *Gondwana Research* **27**:1068–1078.
- 742 **Bardet, N., E. Gheerbrant, A. Noubhani, H. Cappetta, S. Jouve, E. Bourdon, X. P.**
743 **Suberbiola, N-E. Jalil, P. Vincent, and A. Houssaye.** 2017. Les Vertébrés des

744 phosphates crétacés-paléogènes (72,1–47,8 Ma) du Maroc. *Mémoire de la Société*
745 *géologique de France* **180**:351–452.

746 **Barrett, P. M., R. J. Butler, N. P. Edwards, and A. R. Milner.** 2008. Pterosaur distribution in
747 time and space: an atlas. Pp. 61–107 in D. W. E. Hone and E. Buffetaut, eds.

748 **Benson, R. B. J., P. Godoy, M. Bronzati, R. J Butler, and W. Gearty.** 2022. Reconstructed
749 evolutionary patterns for crocodile-line archosaurs demonstrate impact of failure to log-
750 transform body size data. *Communications Biology* **5**:1–4.

751 **Bergounioux, F. M.** 1955. Les crocodiliens fossiles des dépôts phosphatés du sud-tunisien.
752 *Comptes rendus hebdomadaires des séances de l'académie des sciences* **240**:1917–1918.

753 **Borcard, D., P. Legendre, and P. Drapeau.** 1992. Partialling out the spatial component of
754 ecological variation. *Ecology* **73**:1045–1055.

755 **Bralower, T. J.** 2008. Volcanic cause of catastrophe. *Nature* **454**:285–287.

756 **Breusch, T. S., and A. R. Pagan.** 1979. A simple test for heteroscedasticity and random
757 coefficient variation. *Econometrica* **47**:1287–1294.

758 **Brochu, C. A.** 2001. Crocodylian snouts in space and time: phylogenetic approaches toward
759 adaptive radiation. *American Zoologist* **41**:564–85.

760 **Bronzati, M., F. C. Montefeltro, and M. C. Langer.** 2015. Diversification events and the
761 effects of mass extinctions on Crocodyliformes evolutionary history. *Royal Society Open*
762 *Science* **2**:140385.

763 **Brown, W. L., and E. O. Wilson.** 1956. Character displacement. *Systematic Zoology* **5**:49–64.

764 **Buffetaut, E.** 1974. *Les crocodiliens du Sénonien Inférieur d'In Beceten (République du Niger)*.
765 Université Paris IV, Paris, France.

- 766 **Buffetaut, E.** 1978. A dyrosaurid (Crocodylia, Mesosuchia) from the upper Eocene of Burma.
767 Neues Jahrbuch für Geologie und Paläontologie. *Monatshefte* **5**:273–281.
- 768 **Buffetaut, E.** 1980. Les crocodiles paléogènes du Tilemsi (Mali): un aperçu systématique. In J.
769 Michaud, ed. *Mémoire jubilaire en hommage à R. Lavocat. Paleovertebrata* **9**(Ext.):15–
770 35.
- 771 **Buffetaut, E.** 1981. Radiation évolutive, paléoécologie et biogéographie des crocodiliens
772 mésosuchiens. *Mémoires de la Société géologique de France, nouvelle série* **142**:1–88.
- 773 **Buffetaut, E., and S. Hutt.** 1980. *Vectisuchus leptognathus*, n. g. n. sp., a slender-snouted
774 goniopholid crocodylian from the Wealden of the Isle of Wight. Neues Jahrbuch für
775 Geologie und Paläontologie. *Monatshefte* **1980**:385–390.
- 776 **Buffetaut, E., and R. Ingavat.** 1980. A new crocodylian from the Jurassic of Thailand,
777 *Sunosuchus thailandicus* n. sp. (Mesosuchia, Goniopholididae), and the
778 palaeogeographical history of South-East Asia in the Mesozoic. *Geobios* **13**:879–889.
- 779 **Buffetaut, E., and V. Suteethorn.** 2007. A sinraptorid theropod (Dinosauria: Saurischia) from
780 the Phu Kradung Formation of northeastern Thailand. *Bulletin de la Société Géologique*
781 *de France* **178**:497–502.
- 782 **Buffetaut, E., and G. Wouters.** 1979. *Atlantosuchus coupatezi*, ng. n. sp., un nouveau
783 Dyrosauride (Crocodylia, Mesosuchia) des phosphates Montiens du Maroc. *Bulletin*
784 *trimestriel de la Société Géologique de Normandie et des Amis du Museum du Havre*
785 **66**:85–90.
- 786 **Caron, M., S. Dall’Agnolo, H. Accarie, E. Barrera, E. G. Kauffman, F. Amédro, and F.**
787 **Robaszynski.** 2006. High-resolution stratigraphy of the Cenomanian–Turonian boundary

788 interval at Pueblo (USA) and wadi Bahloul (Tunisia): stable isotope and bio-events
789 correlation. *Geobios* **39**:171–200.

790 **Castanet, J., F. J. Meunier, and A. J. De Ricqlès.** 1977. L'enregistrement de la croissance
791 cyclique par le tissu osseux chez les vertébrés poïkilothermes: données comparatives et
792 essai de synthèse. *Bulletin biologique de la France et de la Belgique* **111**:183–202.

793 **Cooper, N., W. Jetz, and R. P. Freckleton.** 2010. Phylogenetic comparative approaches for
794 studying niche conservatism. *Journal of Evolutionary Biology* **23**:2529–2539.

795 **Cope, E. D.** 1866. Remarks on the remains of a gigantic extinct dinosaur from the Cretaceous
796 Greensand of New Jersey. *Proceedings of the Academy of Natural Sciences of*
797 *Philadelphia* **18**:275–279.

798 **Courtillot, V. E.** 1990. A volcanic eruption. *Scientific American* **263**:85–93.

799 **Cubo, J., M. V. A. Sena, P. Aubier, G. Houée, P. Claisse, M. G. Faure-Brac, R. Allain, R. C.**
800 **L. P. Andrade, J. M. Sayão, and G. R. Oliveira.** 2020. Were Notosuchia
801 (Pseudosuchia: Crocodylomorpha) warm-blooded? A palaeohistological analysis
802 suggests ectothermy. *Biological Journal of the Linnean Society* **131**:154–162.

803 **Daudin, F. M.** 1802. *Histoire naturelle, générale et particulière des reptiles; ouvrage faisant*
804 *suite à l'Histoire naturelle générale et particulière, composée par Leclerc de Buffon, et*
805 *rédigée par CS Sonnini.* Tome premier-huitième. Vol. 1. de l'imp. de F. Dufart.

806 **De Andrade, M. B., M. T. Young, J. B. Desojo, and S. L. Brusatte.** 2010. The evolution of
807 extreme hypercarnivory in Metriorhynchidae (Mesoeucrocodylia: Thalattosuchia) based
808 on evidence from microscopic denticle morphology. *Journal of Vertebrate Paleontology*
809 **30**:1451–1465.

810 **De Buffrénil, V., and A. Quilhac.** 2021. Bone tissue types: a brief account of currently used
811 categories. Pp. 147–190 in V. De Buffrénil, A. J. De Ricqlès, L. Zylberberg, and K.
812 Padian, eds.

813 **De Buffrénil, V., M. Laurin, and S. Jouve.** 2021. Archosauromorpha: the Crocodylomorpha.
814 Pp. 486–510 in V. De Buffrénil, A. J. De Ricqlès, L. Zylberberg, and K. Padian, eds.

815 **De Stefano, G.** 1903. Nuovi rettili degli strati a fosfato della Tunisia. *Bolletino della Societa*
816 *Geologia Italiana* **22**:51–80.

817 **De Lapparent De Broin, F.** 2002. *Elosuchus*, a new genus of crocodile from the Cretaceous of
818 the North of Africa. *Comptes Rendus Palevol* **1**:275–285.

819 **De Lapparent De Broin, F., and P. Taquet.** 1966. Découverte d'un Crocodilien nouveau dans
820 le Crétacé inférieur du Sahara. *Comptes-rendus hebdomadaires des séances de*
821 *l'académie des sciences* **262**:2326–2329.

822 **Desdevises, Y., P. Legendre, L. Azouzi, and S. Morand.** 2003. Quantifying phylogenetically
823 structured environmental variation. *Evolution* **57**:2647–2652.

824 **Dixon, P.** 2003. VEGAN, a package of R functions for community ecology. *Journal of*
825 *Vegetation Science* **14**:927–930.

826 **Drumheller, S. K., and E. W. Wilberg.** 2020. A synthetic approach for assessing the interplay
827 of form and function in the crocodyliform snout. *Zoological Journal of the Linnean*
828 *Society* **188**:507–521.

829 **Dunker, W.** 1843. Über den norddeutschen sogenannten Wälderthon und dessen
830 Versteinerungen. In *Programm der höheren Gewerbeschule in Cassel, Schulcursus von*
831 *Michaelis 1843 bis Ostern 1844*. Pp. 1–40.

- 832 **Farlow, J. O., G. R. Hurlburt, R. M. Elsey, A. R. C. Britton, and W. Langston.** 2005.
833 Femoral dimensions and body size of *Alligator mississippiensis*: estimating the size of
834 extinct mesoeucrocodylians. *Journal of Vertebrate Paleontology* **25**:354–369.
- 835 **Faure-Brac, M. G., R. Amiot, C. De Muizon, J. Cubo, and C. Lécuyer.** 2021. Combined
836 paleohistological and isotopic inferences of thermometabolism in extinct Neosuchia,
837 using *Goniopholis* and *Dyrosaurus* (Pseudosuchia: Crocodylomorpha) as case studies.
838 *Paleobiology* **48**:302–323.
- 839 **Felsenstein, J.** 1985. Phylogenies and the comparative method. *American Naturalist* **125**:1–15.
- 840 **Fischer, V., N. Bardet, R. B. J. Benson, M. S. Arkhangelsky, and M. Friedman.** 2016.
841 Extinction of fish-shaped marine reptiles associated with reduced evolutionary rates and
842 global environmental volatility. *Nature Communications* **7**:10825.
- 843 **Fontana, R. B., R. Furtado, N. Zanella, V. J. Debastiani, and S. M. Hartz.** 2021. Linking
844 ecological traits to extinction risk: analysis of a Neotropical anuran database. *Biological*
845 *Conservation* **264**:109390.
- 846 **Fortier, D., D. Perea, and C. Schultz.** 2011. Redescription and phylogenetic relationships of
847 *Meridiosaurus vallisparadisi*, a pholidosaurid from the Late Jurassic of Uruguay. In D.
848 Pol and H. C. E. Larsson, eds. *First symposium on the evolution of Crocodyliformes*.
849 *Zoological Journal of the Linnean Society* **163** (Suppl.):257–272.
- 850 **Frakes, L. A., J-L. Probst, and W. Ludwig.** 1994. Latitudinal distribution of paleotemperature
851 on land and sea from early Cretaceous to middle Miocene. *Sciences de la terre et des*
852 *planètes Comptes rendus de l'Académie des sciences* **318**:1209–1218.

853 **Fritz, S. A., and A. Purvis.** 2010. Selectivity in mammalian extinction risk and threat types: a
854 new measure of phylogenetic signal strength in binary traits. *Conservation Biology*
855 **24**:1042–1051.

856 **Godoy, P. L., and A. H. Turner.** 2020. Body size evolution in crocodylians and their extinct
857 relatives. *Encyclopedia of Life Sciences* **1**:442–452.

858 **Godoy, P. L., R. B. J. Benson, M. Bronzati, and R. J. Butler.** 2019. The multi-peak adaptive
859 landscape of crocodylomorph body size evolution. *BMC Evolutionary Biology* **19**:167.

860 **Grafen, A., and W. D. Hamilton.** 1989. The phylogenetic regression. *Philosophical*
861 *Transactions of the Royal Society of London B* **326**:119–157.

862 **Grigg, G., and D. Kirshner.** 2015. *Biology and evolution of crocodylians*. Comstock Publishing
863 Associates.

864 **Halstead, L.B.** 1975. *Sokotosuchus ianwilsoni* ng, n. sp., a new teleosaur crocodile from the
865 Upper Cretaceous of Nigeria. *Journal of Mining and Geology* **11**:101–103.

866 **Hastings, A. K.** 2012. *Early Paleogene crocodyliform evolution in the Neotropics: evidence*
867 *from northeastern Colombia*. University of Florida Press, Gainesville.

868 **Hastings, A. K., and M. Hellmund.** 2017. Evidence for prey preference partitioning in the
869 middle Eocene high-diversity crocodylian assemblage of the Geiseltal-Fossilagerstätte,
870 Germany utilizing skull shape analysis. *Geological Magazine* **154**:119–146.

871 **Hastings, A. K., J. I. Bloch, E. A. Cadena, and C. A. Jaramillo.** 2010. A new small short-
872 snouted dyrosaurid (Crocodylomorpha, Mesoeucrocodylia) from the Paleocene of
873 northeastern Colombia. *Journal of Vertebrate Paleontology* **30**:139–162.

874 **Hastings, A. K., J. I. Bloch, and C. A. Jaramillo.** 2011. A new longirostrine dyrosaurid
875 (Crocodylomorpha, Mesoeucrocodylia) from the Paleocene of north-eastern Colombia:

876 biogeographic and behavioural implications for New-World Dyrosauridae.
877 *Palaeontology* **54**:1095–1116.

878 **Hastings, A. K., J. I. Bloch, and C. A. Jaramillo.** 2015. A new blunt-snouted dyrosaurid,
879 *Anthracosuchus balrogus* gen. et sp. nov. (Crocodylomorpha, Mesoeucrocodylia), from
880 the Palaeocene of Colombia. *Historical Biology* **27**:998–1020.

881 **Herman, A. B.** 2013. Albian–Paleocene flora of the north pacific: systematic composition,
882 palaeofloristics and phytostatigraphy. *Stratigraphy and Geological Correlation* **21**:689–
883 747.

884 **Herman, A. B., and R. A. Spicer.** 2010. Mid-Cretaceous floras and climate of the Russian high
885 Arctic (Novosibirsk Islands, northern Yakutiya). *Palaeogeography, Palaeoclimatology,*
886 *Palaeoecology* **295**:409–422.

887 **Hildebrand, A. R., G. T. Penfield, D. A. Kring, M. Pilkington, Z. A. Camargo, S. B.**
888 **Jacobsen, and W. V. Boynton.** 1991. Chicxulub crater: a possible Cretaceous/Tertiary
889 boundary impact crater on the Yucatán Peninsula, Mexico. *Geology.* **19**:867–871.

890 **Hjernquist, M. B., F. Söderman, K. I. Jönsson, G. Herczeg, A. Laurila, and J. Merilä.** 2012.
891 Seasonality determines patterns of growth and age structure over a geographic gradient in
892 an ectothermic vertebrate. *Oecologia.* **170**:641–649.

893 **Hua, S., E. Buffetaut, C. Legall, and P. Rogron.** 2007. *Oceanosuchus boecensis* n. gen, n. sp.,
894 a marine pholidosaurid (Crocodylia, Mesosuchia) from the Lower Cenomanian of
895 Normandy (western France). *Bulletin de la Société Géologique de France* **178**:503–513.

896 **Hutton, J. M.** 1987. Growth and feeding ecology of the Nile crocodile *Crocodylus niloticus* at
897 Ngezi, Zimbabwe. *Journal of Animal Ecology* **56**:25–38.

- 898 **Irmis, R. B., S. J. Nesbitt, and H-D. Sues.** 2013. Early Crocodylomorpha. *In* S. J Nesbitt, J. B
899 Desojo, and R. B Irmis, eds. *Anatomy, phylogeny and palaeobiology of early archosaurs*
900 *and their kin. Geological Society of London Special Publication* **379**:275–302.
- 901 **Ives, A. R., and T. Garland Jr.** 2010. phylogenetic logistic regression for binary dependent
902 variables. *Systematic Biology* **59**:9–26.
- 903 **Jouve, S.** 2021. Differential diversification through the K-Pg boundary, and post-crisis
904 opportunism in longirostrine crocodyliforms. *Gondwana Research* **99**:110–130.
- 905 **Jouve, S., and N-E. Jalil.** 2020. Paleocene resurrection of a crocodylomorph taxon: biotic crises,
906 climatic and sea level fluctuations. *Gondwana Research* **85**:1–18.
- 907 **Jouve, S., B. Bouya, and M. Amaghazaz.** 2005a. A short-snouted dyrosaurid (Crocodyliformes,
908 Mesoeucrocodylia) from the Palaeocene of Morocco. *Palaeontology* **48**:359–369.
- 909 **Jouve, S., M. Iarochene, B. Bouya, and M. Amaghazaz.** 2005b. A new dyrosaurid
910 crocodyliform from the Paleocene of Morocco and a phylogenetic analysis of
911 Dyrosauridae. *Acta Palaeontologica Polonica* **50**:581–594.
- 912 **Jouve, S., N. Bardet, N-E. Jalil, X. P. Suberbiola, B. Bouya, and M. Amaghazaz.** 2008a. The
913 oldest African crocodylian: phylogeny, paleobiogeography, and differential survivorship
914 of marine reptiles through the Cretaceous–Tertiary boundary. *Journal of Vertebrate*
915 *Paleontology* **28**:409–421.
- 916 **Jouve, S., B. Bouya, and M. Amaghazaz.** 2008b. A long-snouted dyrosaurid (Crocodyliformes,
917 Mesoeucrocodylia) from the Paleocene of Morocco: phylogenetic and
918 palaeobiogeographic implications. *Palaeontology* **51**:281–294.

- 919 **Jouve, S., B. Mennecart, J. Douteau, and N-E. Jalil.** 2017. Biases in the study of relationships
920 between biodiversity dynamics and fluctuation of environmental conditions.
921 *Palaeontologia Electronica* **20**:1–21.
- 922 **Jouve, S., B. Khalloufi, and S. Zouhri.** 2019. Longirostrine crocodylians from the Bartonian of
923 Morocco and Paleogene climatic and sea level oscillations in the Peri-Tethys area.
924 *Journal of Vertebrate Paleontology* **39**:e1617723.
- 925 **Jouve, S., C. De Muizon, R. Cespedes-Paz, V. Sossa-Soruco, and S. Knoll.** 2021. The
926 longirostrine crocodyliforms from Bolivia and their evolution through the Cretaceous–
927 Palaeogene boundary. *Zoological Journal of the Linnean Society* **192**:475–509.
- 928 **Kauffman, E. G.** 1995. Global change leading to biodiversity crisis in a greenhouse world: the
929 Cenomanian–Turonian (Cretaceous) mass extinction. Pp. 47–71 in National Research
930 Council, eds.
- 931 **Lakin, R. J., P. M. Barrett, C. Stevenson, R. J. Thomas, and M. A Wills.** 2020. First
932 evidence for a latitudinal body mass effect in extant Crocodylia and the relationships of
933 their reproductive characters. *Biological Journal of the Linnean Society* **129**:875–887.
- 934 **Landman, N. H., R. O Johnson, M. P. Garb, L. E. Edwards, and F. T. Kyte.** 2007.
935 Cephalopods from the Cretaceous/Tertiary boundary interval on the Atlantic Coastal
936 Plain, with a description of the highest ammonite zones in North America. Part 3,
937 Manasquan River Basin, Monmouth County, New Jersey. *Bulletin of the American*
938 *Museum of Natural History* **303**:1–122.
- 939 **Laugié, M., Y. Donnadieu, J-B. Ladant, J. A. M. G, L. Bopp, and F. Raisson.** 2020.
940 Stripping back the modern to reveal the Cenomanian–Turonian climate and temperature
941 gradient underneath. *Climate of the Past* **16**:953–971.

- 942 **Laurin, M.** 2004. The evolution of body size, Cope's rule and the origin of amniotes. *Systematic*
943 *Biology* **53**:594–622.
- 944 **Mannion, P. D., R. B. J. Benson, M. T. Carrano, J. P. Tennant, J. Judd, and R. J. Butler.**
945 2015. Climate constrains the evolutionary history and biodiversity of crocodylians.
946 *Nature Communications* **6**:8438.
- 947 **Mansel-Pleydell, J. C.** 1888. Fossil reptiles of Dorset. *Proceedings of the Dorset Natural*
948 *History and Antiquarian Field Club* **9**:1–40.
- 949 **Markwick, P. J.** 1998. Crocodylian diversity in space and time: the role of climate in
950 paleoecology and its implication for understanding K/T extinctions. *Paleobiology*
951 **24**:470–497.
- 952 **Marsh, O. C.** 1870. Notice of some fossil birds from the Cretaceous and Tertiary formations of
953 the United States. *American Journal of Science* **49**(146):205–217.
- 954 **Martin, J. E., R. Amiot, C. Lécuyer, and M. J. Benton.** 2014a. Sea surface temperature
955 contributes to marine crocodylomorph evolution. *Nature Communications* **5**:4658.
- 956 **Martin, J. E., K. Lauprasert, E. Buffetaut, R. Liard, and V. Suteethorn.** 2014b. A large
957 pholidosaurid in the Phu Kradung Formation of north-eastern Thailand. *Palaeontology*
958 **57**:757–769.
- 959 **Mehl, M. G.** 1941. *Dakotasuchus kingi*, a crocodile from the Dakota of Kansas. *Denison*
960 *University Journal of Sciences and Laboratories* **36**:47–65.
- 961 **Meunier, L. M. V., and H. C. E. Larsson.** 2018. *Trematochampsia taqueti* as a *nomen dubium*
962 and the crocodyliform diversity of the Upper Cretaceous In Beceten Formation of Niger.
963 *Zoological Journal of the Linnean Society* **182**:659–680.

- 964 **Meyer, H.** 1841. *Pholidosaurus schaumburgensis*, ein saurus aus dem sandstein der Wald-
965 Formation Nord-Deutschlands. *Neues Jahrbuch für Mineralogie* **1841**:343–345.
- 966 **Mones, A.** 1980. Nuevos elementos de la Paleoherpeto fauna del Uruguay (Crocodilia y
967 Dinosauria). *Actas* **1**:265–277.
- 968 **Monnet, C.** 2009. The Cenomanian–Turonian boundary mass extinction (Late Cretaceous): new
969 insights from ammonoid biodiversity patterns of Europe, Tunisia and the Western
970 Interior (North America). *Palaeogeography, Palaeoclimatology, Palaeoecology* **282**:88–
971 104.
- 972 **Montes, L., N. Le Roy, M. Perret, V. De Buffrénil, J. Castanet, and J. Cubo.** 2007.
973 Relationships between bone growth rate, body mass and resting metabolic rate in
974 growing amniotes: a phylogenetic approach. *Biological Journal of the Linnean Society*
975 **92**:63–76.
- 976 **Mook, C. C.** 1934. A new species of *Teleorhinus* from the Benton shales. *American Museum*
977 *Novitates* **702**:1–11.
- 978 **Newton, A., and S. M. Mudge.** 2003. Temperature and salinity regimes in a shallow, mesotidal
979 lagoon, the Ria Formosa, Portugal. *Estuarine, Coastal and Shelf Science* **57**:73–85.
- 980 **Nopcsa, B. F.** 1928. The genera of reptiles. *Palaeobiologica* **1**:163–168.
- 981 **Novacek, M. J.** 1999. 100 Million years of land vertebrate evolution: the Cretaceous–Early
982 Tertiary transition. *Annals of the Missouri Botanical Garden* **86**:230–258.
- 983 **O’Brien, H. D., L. M. Lynch, K. A. Vliet, J. Brueggen, G. M. Erickson, and P. M. Gignac.**
984 2019. Crocodylian head width allometry and phylogenetic prediction of body size in
985 extinct crocodyliforms. *Integrative Organismal Biology* **1**:obz006.

- 986 **Orme, D., R. Freckleton, G. Thomas, T. Petzoldt, S. Fritz, N. Isaac, and W. Pearse.** 2013.
987 The caper package: comparative analysis of phylogenetics and evolution in R, R package
988 version **5(2):1–36.**
- 989 **Osborn, H. F.** 1904. *Teleorhinus browni*, a teleosaur in the Fort Benton. *Bulletin of the*
990 *American Museum of Natural History* **20:239–240.**
- 991 **Owen, R.** 1884. *A history of British fossil reptiles.* Cassel and Company, London.
- 992 **Peres-Neto, P. R., P. Legendre, S. Dray, and D. Borcard.** 2006. Variation partitioning of
993 species data matrices: estimation and comparison of fractions. *Ecology* **87:2614–2625.**
- 994 **Pierce, S. E., K. D. Angielczyk, and E. J. Rayfield.** 2009. Shape and mechanics in
995 thalattosuchian (Crocodylomorpha) skulls: implications for feeding behaviour and niche
996 partitioning. *Journal of Anatomy* **215:555–576.**
- 997 **Piras, P., L. Teresi, A. D. Buscalioni, and J. Cubo.** 2009. The shadow of forgotten ancestors
998 differently constrains the fate of Alligatorioidea and Crocodyloidea. *Global Ecology and*
999 *Biogeography* **18:30–40.**
- 1000 **Pouech, J., R. Amiot, C. Lécuyer, J-M. Mazin, F. Martineau, and F. Fourel.** 2014. Oxygen
1001 isotope composition of vertebrate phosphates from Cherves-de-Cognac (Berriasian,
1002 France): environmental and ecological significance. *Palaeogeography,*
1003 *Palaeoclimatology, Palaeoecology* **410:290–299.**
- 1004 **Prokoph, A., G. A. Shields, and J. Veizer.** 2008. Compilation and time-series analysis of a
1005 marine carbonate $\delta^{18}\text{O}$, $\delta^{13}\text{C}$, $^{87}\text{Sr}/^{86}\text{Sr}$ and $\delta^{34}\text{S}$ database through Earth history. *Earth-*
1006 *Science Reviews* **87:113–133.**

- 1007 **Pucéat, E., C. Lécuyer, and L. Reisberg.** 2005. Neodymium isotope evolution of NW Tethyan
1008 upper ocean waters throughout the Cretaceous. *Earth and Planetary Science Letters*
1009 **236**:705–720.
- 1010 **Puértolas-Pascual, E., A. Blanco, C. A. Brochu, and J. I. Canudo.** 2016. Review of the Late
1011 Cretaceous–early Paleogene crocodylomorphs of Europe: extinction patterns across the
1012 K-PG boundary. *Cretaceous Research* **57**:565–90.
- 1013 **Racey, A., and J. G. S. Goodall.** 2009. Palynology and stratigraphy of the Mesozoic Khorat
1014 Group red bed sequences from Thailand. *Geological Society of London Special*
1015 *Publication* **315**:69–83.
- 1016 **R Core Team.** 2013. *R: a language and environment for statistical computing*. R Foundation for
1017 Statistical Computing, Vienna, Austria.
- 1018 **Robertson, D. S., W. M. Lewis, P. M. Sheehan, and O. B. Toon.** 2013. K-Pg extinction
1019 patterns in marine and freshwater environments: the impact winter model. *Journal of*
1020 *Geophysical Research: Biogeosciences* **118**:1006–1014.
- 1021 **Roxo, M. G. O.** 1929. *Pequenos guias da collecção de paleontologia do Museu Nacional*
1022 *(Reptis). II-Crocodilianos*. Mendocça, Machado & Co., Rio de Janeiro.
- 1023 **Sachs, S., M. T. Young, P. Abel, and H. Mallison.** 2021. A new species of *Cricosaurus*
1024 (Thalattosuchia, Metriorhynchidae) based upon a remarkably well-preserved skeleton
1025 from the Upper Jurassic of Germany. *Palaeontologia Electronica*.
1026 <https://doi.org/10.26879/928>.
- 1027 **Sakamoto, M., G. T. Lloyd, and M. J. Benton.** 2010. Phylogenetically structured variance in
1028 felid bite force: the role of phylogeny in the evolution of biting performance. *Journal of*
1029 *Evolutionary Biology* **23**:463–478.

- 1030 **Salih, K. O., D. C. Evans, R. Bussert, N. Klein, and J. Müller.** 2022. *Brachiosuchus*
1031 *kababishensis*, a new long-snouted dyrosaurid (Mesoeucrocodylia) from the Late
1032 Cretaceous of north central Sudan. *Historical Biology* **34**:821–840.
- 1033 **Salisbury, S. W., and D. Naish.** 2011. Crocodylians. Pp. 305–369 in D. J. Batten, ed.
- 1034 **Schoene, B., M. P. Eddy, K. M. Samperton, C. B. Keller, G. Keller, T. Adatte, and S. F. R.**
1035 **Khadr.** 2019. U-Pb constraints on pulsed eruption of the Deccan Traps across the end-
1036 Cretaceous mass extinction. *Science* **363**:862–866.
- 1037 **Scotese, C. R., H. Song, B. J. W. Mills, and D. G. Van Der Meer.** 2021. Phanerozoic
1038 paleotemperatures: the earth’s changing climate during the last 540 million years. *Earth-*
1039 *Science Reviews* **215**:103503.
- 1040 **Scott, B. R., and P. S. L. Anderson.** 2023. Examining competition during the
1041 agnathan/gnathostome transition using distance-based morphometrics. *Paleobiology*
1042 **49**:313–28.
- 1043 **Shapiro, S. S., and M. B. Wilk.** 1965. An analysis of variance test for normality (complete
1044 samples). *Biometrika* **52**:591–611.
- 1045 **Shiller, T. A., H. G. Porras-Muzquiz, and T. M. Lehman.** 2016. *Sabinosuchus coahuilensis*, a
1046 new dyrosaurid crocodyliform from the Escondido Formation (Maastrichtian) of
1047 Coahuila, Mexico. *Journal of Vertebrate Paleontology* **36**:e1222586.
- 1048 **Soul, L. C., and D. F. Wright.** 2021. *Phylogenetic comparative methods: a user’s guide for*
1049 *paleontologists*. Elements of Paleontology. Cambridge University Press, New York.
- 1050 **Sprain, C. J., P. R. Renne, L. Vanderkluyzen, K. Pande, S. Self, and T. Mittal.** 2019. The
1051 eruptive tempo of Deccan volcanism in relation to the Cretaceous–Paleogene boundary.
1052 *Science* **363**:866–870.

- 1053 **Stockdale, M. T., and M. J. Benton.** 2021. Environmental drivers of body size evolution in
1054 crocodile-line archosaurs. *Communications Biology* **4**:1–11.
- 1055 **Stubbs, T. L., S. E. Pierce, A. Elsler, P. S. L. Anderson, E. J. Rayfield, and M. J. Benton.**
1056 2021. Ecological opportunity and the rise and fall of crocodylomorph evolutionary
1057 innovation. *Proceedings of the Royal Society of London B* **288**:20210069.
- 1058 **Toljagić, O., and R. J. Butler.** 2013. Triassic–Jurassic mass extinction as trigger for the
1059 Mesozoic radiation of crocodylomorphs. *Biology Letters* **9**:20130095.
- 1060 **Troxell, E. L.** 1925. *Hyposaurus*, a marine crocodylian. *American Journal of Science* **9**:489–514.
- 1061 **Tung Ho, L. S., and C. Ané.** 2014. A linear-time algorithm for Gaussian and non-Gaussian trait
1062 evolution models. *Systematic Biology* **63**:397–408.
- 1063 **Turgeon, S. C., and R. A. Creaser.** 2008. Cretaceous oceanic anoxic event 2 triggered by a
1064 massive magmatic episode. *Nature* **454**:323–326.
- 1065 **Vandermark, D., J. A. Tarduno, and D. B. Brinkman.** 2007. A fossil champsosaur population
1066 from the high Arctic: implications for Late Cretaceous paleotemperatures.
1067 *Palaeogeography, Palaeoclimatology, Palaeoecology* **248**:49–59.
- 1068 **Van Valkenburgh, B., X. Wang, and J. Damuth.** 2004. Cope’s rule, hypercarnivory, and
1069 extinction in North American canids. *Science* **306**:101–104.
- 1070 **Vérard, C., C. Hochard, P. O. Baumgartner, G. M. Stampfli, and M. Liu.** 2015. 3D
1071 palaeogeographic reconstructions of the Phanerozoic versus sea-level and Sr-ratio
1072 variations. *Journal of Palaeogeography* **4**:64–84.
- 1073 **Wan, X., P. B. Wignall, and W. Zhao.** 2003. The Cenomanian–Turonian extinction and
1074 oceanic anoxic event: evidence from southern Tibet. *Palaeogeography,*
1075 *Palaeoclimatology, Palaeoecology* **199**:283–298.

1076 **Wang, M., and G. T. Lloyd.** 2016. Rates of morphological evolution are heterogeneous in Early
1077 Cretaceous birds. *Proceedings of the Royal Society of London B* **283**:20160214.

1078 **Watkins, D. K., and J. M. Self-Trail.** 2005. Calcareous nannofossil evidence for the existence
1079 of the Gulf Stream during the late Maastrichtian. *Paleoceanography*. **20**:PA3006.

1080 **Wiest L., I. Buynevich, D. Grandstaff, Z. Maza Jr, and K. Lacovara.** 2016. Ichnological
1081 evidence for endobenthic response to the K-PG event, New Jersey, U.S.A. *Palaios*
1082 **31**:231–241.

1083 **Wilberg, E. W., A. H. Turner, and C. A. Brochu.** 2019. Evolutionary structure and timing of
1084 major habitat shifts in Crocodylomorpha. *Scientific Reports* **9**:514.

1085 **Wilke, T., T. Hauffe, E. Jovanovska, A. Cvetkoska, T. Donders, K. Ekschmitt, A. Francke,**
1086 **et al.** 2020. Deep drilling reveals massive shifts in evolutionary dynamics after formation
1087 of ancient ecosystem. *Science Advances* **6**:eabb2943.

1088 **Yessoufou, K., B. H. Daru, and T. J. Davies.** 2012. Phylogenetic patterns of extinction risk in
1089 the Eastern Arc ecosystems, an African biodiversity hotspot. *PLoS ONE* **7**:e47082.

1090 **Young, M. T., M. A. Bell, M. B. De Andrade, and S. L. Brusatte.** 2011. Body size estimation
1091 and evolution in metriorhynchid crocodylomorphs: implications for species
1092 diversification and niche partitioning. *Zoological Journal of the Linnean Society*
1093 **163**:1199–1216.

1094 **Zhang, L., W. W. Hay, C. Wang, and X. Gu.** 2019. The evolution of latitudinal temperature
1095 gradients from the latest Cretaceous through the Present. *Earth-Science Reviews*
1096 **189**:147–158.

1097 **Zittel, K.** 1902. In K. Zittel and C. R. Eastmann, eds. **2**:215.

1098

1099 **Figure 1.** Supertree of Tethysuchia, the topology shown here is Jouve 1. The green spot indicates
1100 the Pholidosauridae; the red spot, Dyrosauroidae; the orange spot, Dyrosauridae; the yellow spot,
1101 Phosphatosaurinae; and the black spot, Hyposaurinae. The alternative topologies can be observed
1102 in Supplementary File 2.

1103 **Figure 2.** Representation of variation partitioning for a dependent variable, the gray rectangle
1104 represents all of the variation of the dependent variable. Four different partitions are proposed:
1105 partition A corresponds to the strictly ecological impact on variation, partition B corresponds to
1106 the strictly phylogenetic impact on variation, partition C corresponds to the common impact of
1107 phylogeny and ecology (phylogenetic niche conservatism), and partition D corresponds to the
1108 unexplained part of variation.

1109 **Figure 3.** Phylogenetic generalized least squares (PGLS) curve for tethysuchians (blue),
1110 pholidosaurids (green), and dyrosauroids (red). The circles correspond to Pholidosauridae
1111 species, and the triangles correspond to Dyrosauroidae species.

1112 **Figure 4.** Distribution map of tethysuchians from the (A) pre- and (B) post-OAE 2 (second
1113 Oceanic Anoxic Event) faunas. The red polygon shows the repartition without *Sabinosuchus*
1114 *coahuilensis* and *Hyposaurus natator*. Map generated by the Paleobiology Database.

1115

1116 **Table 1.** Results from the *D*-statistic analysis for second Oceanic Anoxic Event (OAE 2) and
1117 Cretaceous/Paleogene (K/Pg) crisis. The first topology is the same as in Fig. 1. The second
1118 topology shows *Dakotasuchus kingi* in a clade including *Pholidosaurus chevres*, *Pholidosaurus*
1119 *purbeckensis*, and *Pholidosaurus schaumburgensis*. The third topology shows *Vectisuchus*
1120 *leptognathus* as a pholidosaurid in a clade with *Elosuchus*. The fourth topology shows *V.*

1121 *leptognathus* as a pholidosaurid in a clade with *Sarcosuchus* and *Chalawan thailandicus*. These
1122 alternative topologies may be observed in Supplementary File 2.

1123 **Table 2.** Results from the phylogenetic logistic regression (PLR) and generalized linear model
1124 (GLM) analyses; significant p -values are lower than 0.05. The first topology is the same as in
1125 Fig. 1. The remaining topologies are in the same order as in Table 1.

1126 **Table 3.** Results from the phylogenetic generalized least squares (PGLS), generalized least
1127 squares (GLS), and linear models (LM) analyses, significant p -values are lower than 0.05. The
1128 first topology is the same as in Fig. 1. The remaining topologies are in the same order as in Table
1129 1.

1130 **Table 4.** comparison of corrected Akaike information criterion (AICc) between a
1131 paleotemperature-influenced model and a null model for the phylogenetic generalized least
1132 squares (PGLS), generalized least squares (GLS), and linear models (LM) analyses. The
1133 topologies are in the same order as in Table 1.

1134 **Table 5.** Results from the variation partitioning analyses, adjusted R^2 is noted along with p -
1135 values, if possible, within parentheses.